

October 15, 2025

From:

Nathaniel Byars, Lonquist & Co. LLC

Sergey Samsonov, PhD, InSAR Corporation

**Re: Combined Monthly Surface Deformation Report – September 2025
Sulphur Mines Salt Dome, Louisiana**

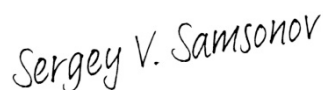
Please find attached the combined monthly deformation report for the Sulphur Mines dome, which includes results from the precision tiltmeters and GNSS stations for the September monitoring period and the cumulative InSAR results as of the end of the month.

Status of a deformation alert plan. We continue testing a draft deformation alert system that reports daily tiltmeter activity in relation to the full statistical history of the network. Alert thresholds will be set and adjusted to prioritize long-duration signals observed at multiple monitoring sites over anomalous or short-duration tilt signals associated with precipitation, shallow deformation, or mechanical activities near individual sites. We plan to integrate tiltmeter deformation alert levels with real-time monitoring data from Sulphur Mines, which include the Cavern 7 pressure and microseismic monitoring. GNSS and InSAR data will also be used for validation.

Sincerely,



Nathaniel Byars
Principal Engineer
Lonquist & Co. LLC



Sergey Samsonov, PhD
InSAR Corporation

Attachment List

- A. Tiltmeter/GNSS Data Report - September 2025
- B. TSX-A InSAR report - September 29, 2025
- C. TSX/PAZ InSAR report - September 29, 2025
- D. Vertical & East-West 2D InSAR report - September 29, 2025

ATTACHMENT A

Tiltmeter/GNSS Data Report - September 2025

October 15, 2025

Sergey Samsonov, PhD, InSAR Corporation
 Nathaniel Byars, Lonquist & Co. LLC

Re: Tiltmeter/GNSS Data Evaluation – September 2025, Sulphur Mines Salt Dome, Louisiana

The tiltmeter/GNSS network, which includes twenty tiltmeters and five GNSS stations, has been operational since June 1, 2024. It was installed and is currently being operated by Halliburton’s Pinnacle Group. Please refer to Figure 1 for the map of the tiltmeter and GNSS stations. Station coordinates are provided in Appendix 3.

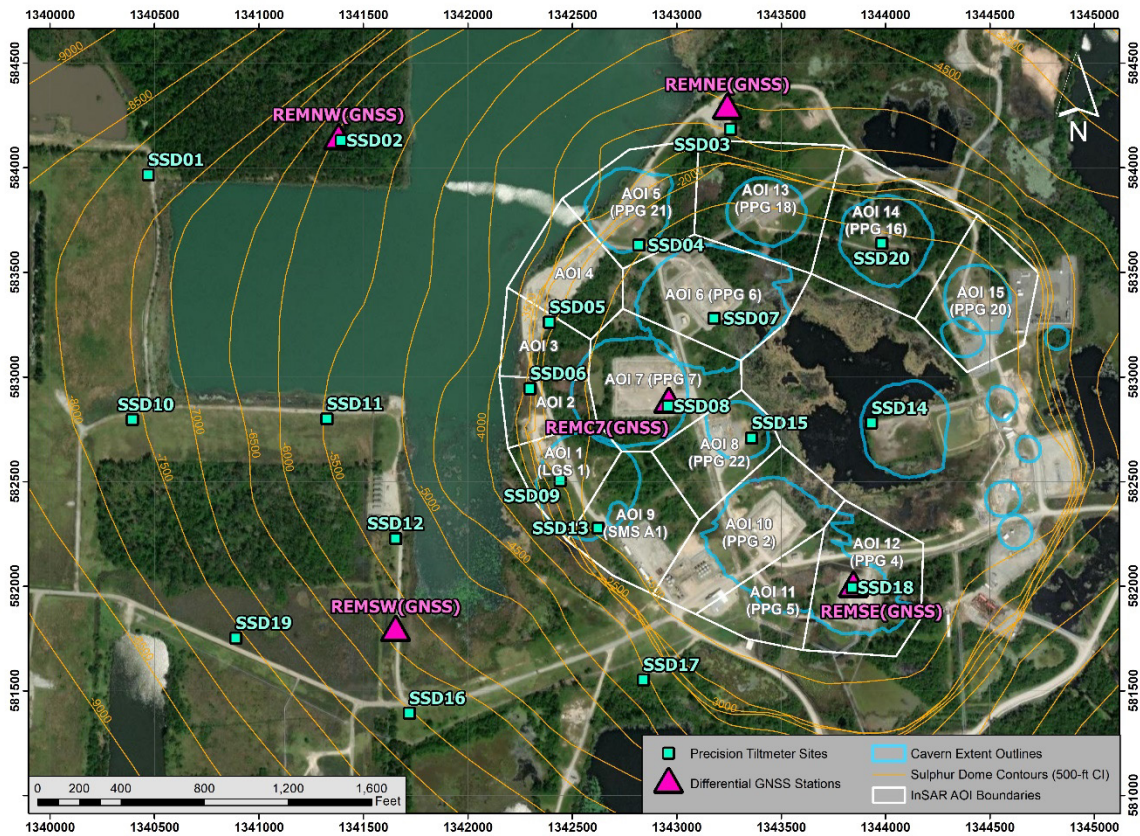


Figure 1. Map of the tiltmeter and GNSS network installed at Sulphur Mines dome. The cyan squares indicate the tiltmeter site locations. The GNSS stations are shown by pink triangles. The InSAR AOI boundaries are shown for reference. The surface projection of the various salt caverns is indicated by blue lines. The salt dome contours are in light orange. The backdrop is an aerial photograph of the Sulphur Mines salt dome.

Introduction

This report describes tiltmeter and GNSS measurements from the Sulphur Mines Salt Dome collected in September 2025.

For each tiltmeter station, the report provides:

- Raw measurements of east and north tilt components with outliers removed by filtering (measured in microradians) at the four-minute temporal resolution and their linear trends.
- Detrended east and north tilt components at four-minute temporal resolution.
- Daily ranges of east and north tilt components.
- Daily precipitation amount (measured in inches).
- Daily tilt direction distribution diagram, along with the direction to Cavern 7 and the direction of the linear trend.

For each GNSS station, the report provides:

- Daily averages of the east, north, and vertical deformation (measured in inches) and their linear trends estimated in the global reference frame.
- Deformation rates (measured in inches per year) estimated in the local reference frame. Deformation rates in a local reference frame are computed by subtracting the tectonic plate deformation rate, common to all sites, from the measurements taken in the global reference frame.

Summary of tiltmeter observations

The tiltmeter network operated without interruption throughout September. No signals related to anomalous activity in Cavern 7 were detected during this reporting period. Appendix 1 includes plots for each tiltmeter station.

SSD17 showed a consistent eastward tilt in its east-component throughout most of September. In the north-component, the tilt was dominantly northward in the first half of the month, reversing to southward in the second half (see Figure 2).

Figure 3 presents the tilt signals recorded by the SSD17 tiltmeter during July-September 2025, alongside annulus and tubing pressure data from the wellhead of Cavern 4. The data suggest that changes in tilt may have followed pressure variations in Caverns 2, 4, and 5, indicating a possible delayed response. The total tilt magnitude recorded by SSD17 was approximately 200 microradians, smaller than values previously observed by other instruments over similar time spans. Nevertheless, this marks the first potential instance of a tilt response linked to pressure variations within a cavern. However, the current

dataset is insufficient to confirm this hypothesis, particularly given the absence of similar anomalies in the records from other tiltmeters.

Several precipitation events disrupted the established tilt trends over multiple days. The region is known for substantial rainfall during the summer months, which has notably influenced recent tiltmeter data. During these events, we closely monitored tilt directions at all stations and found no consistent indication of tilt toward Cavern 7. Figure 4 shows the tilt signals recorded by the SSD15 tiltmeter. On September 24, this instrument registered nearly 100 microradians of tilt, interrupting the prior trend at least through the end of September. We believe that coinciding precipitation events on September 23-24 are responsible for this signal in SSD15. However, even larger precipitation events in the past did not produce similarly strong responses. One possible explanation is that rainfall measurements from the remote weather station, located 2.4 miles to the southwest, may not accurately reflect the actual precipitation at the tiltmeter site, and localized rainfall on those dates could have been more intense.

Multiple tiltmeters recorded changes in tilt direction at irregular intervals that cannot be fully explained or attributed solely to precipitation events. For instance, Figure 5 shows an abrupt change in the tilt trend recorded by SSD11 beginning on September 21, while Figure 6 displays a similar change in SSD19 starting on September 30. Since these anomalies were observed only at individual stations, they are most likely associated with local influences, possibly shallow subsurface features or nearby mechanical activities. We suspect that ongoing levee construction may have contributed to some of these unexplained tilt signals.

The tilt data is manually reviewed daily using a 7-day rolling window. This process helps identify any changes in trends that are consistently observed at multiple tiltmeter sites over at least a few days. During the reported period, the tiltmeter data did not show any consistent ground movement patterns that would indicate deep-sourced deformation or any immediate concerns regarding Cavern 7.

SSD17: Analyzed range: 2024-06-01 – 2025-10-07 | Plotted range: 2025-09-01 – 2025-09-30 (CTZ)

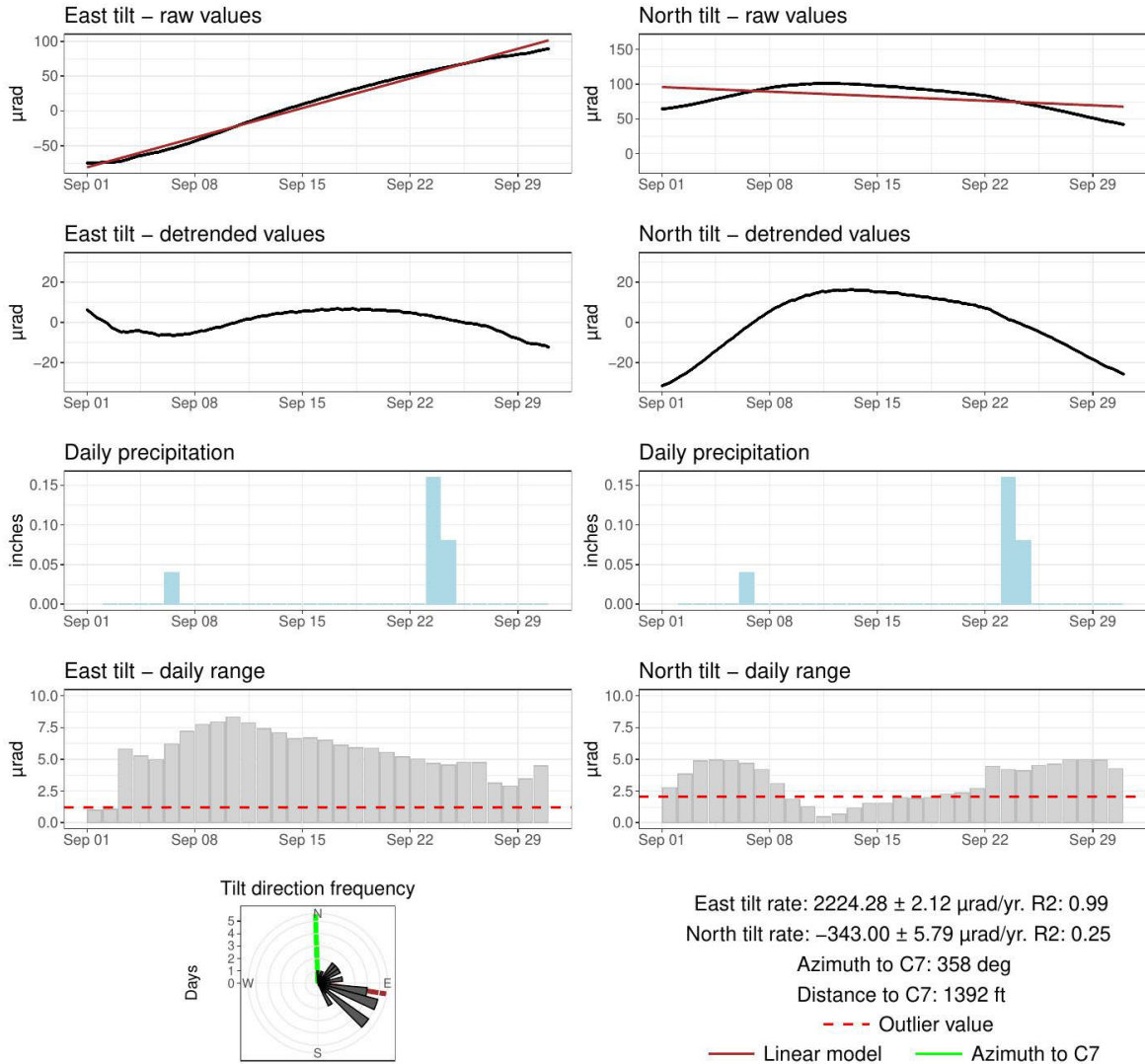


Figure 2. Charts of the tilt signals observed by the SSD17 tiltmeter over the current monthly reporting period. Note large daily tilt ranges in the east component and reversing trend in the north component.

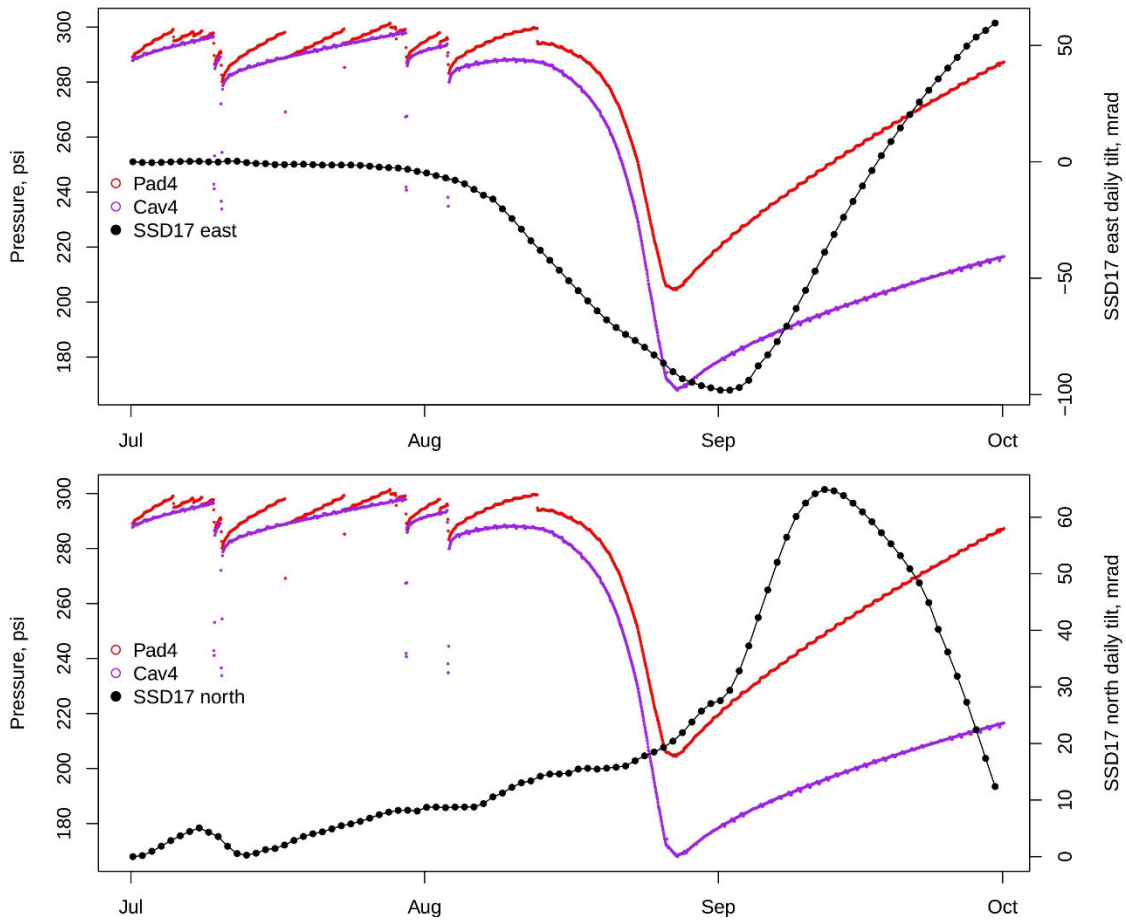


Figure 3. Tilt signals recorded by the SSD17 tiltmeter during the July–September 2025 period, plotted alongside annulus (pad) and tubing pressure data from Cavern 4. The top panel shows east-component tilt with pressure, while the bottom panel shows north-component tilt with the same pressure records.

SSD15: Analyzed range: 2024-06-01 – 2025-10-07 | Plotted range: 2025-09-01 – 2025-09-30 (CTZ)

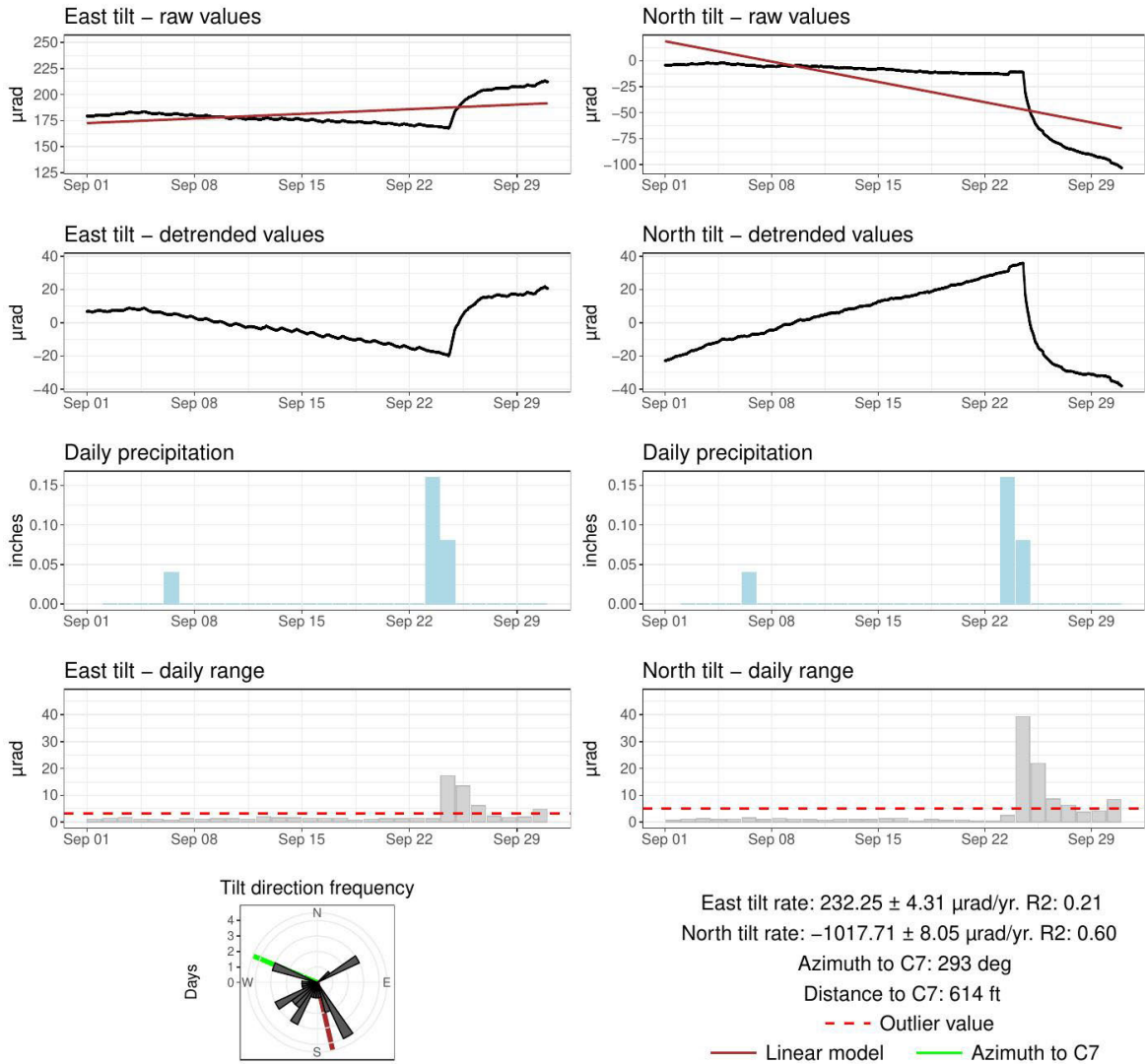


Figure 4. Charts of the tilt signals observed by the SSD15 tiltmeter over the current monthly reporting period. Note large daily tilt ranges in the east and north components following a precipitation event.

SSD11: Analyzed range: 2024-06-01 – 2025-10-07 | Plotted range: 2025-09-01 – 2025-09-30 (CTZ)

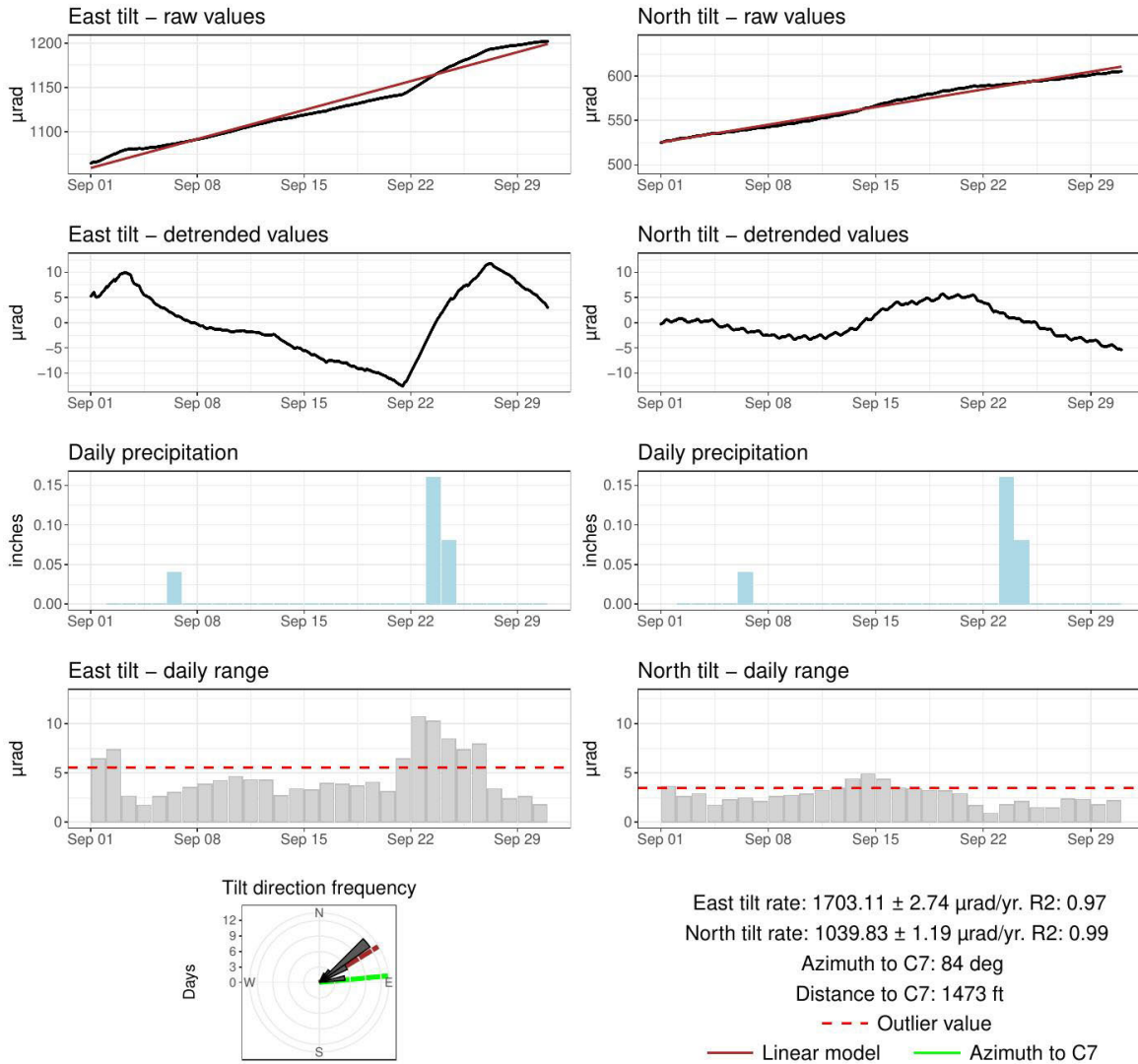


Figure 5. Charts of the tilt signals observed by the SSD11 tiltmeter over the current monthly reporting period. Note the abrupt change on September 21 and large daily tilt ranges in the east component.

SSD19: Analyzed range: 2024-06-01 – 2025-10-07 | Plotted range: 2025-09-01 – 2025-09-30 (CTZ)

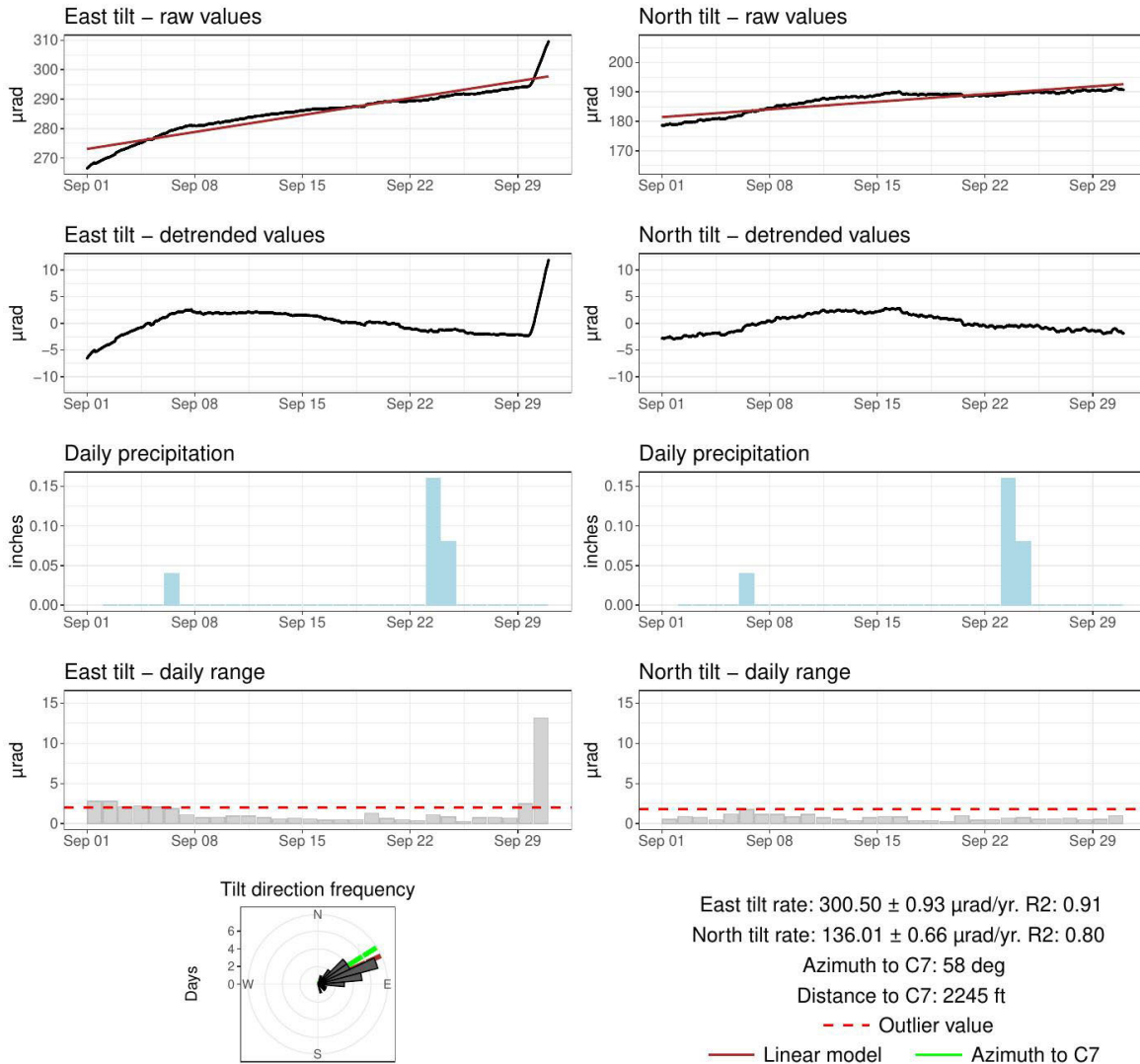


Figure 6. Charts of the tilt signals observed by the SSD19 tiltmeter over the current monthly reporting period. Note the abrupt increase in daily tilt range on September 30 in the east component.

Summary of GNSS observations

The GNSS network operated continuously and without interruption throughout September. Appendix 2 presents plots for each GNSS station. We calculated the annualized three-dimensional deformation rates (east, north, and vertical) at each site within a local reference frame by subtracting a constant tectonic rate, common to all sites, from measurements in the global reference frame. Daily measurements from September support an ongoing deformation trend, primarily characterized by horizontal motion

directed toward Central Lake, accompanied by subsidence. Notably, the subsidence rate increases closer to Central Lake.

In previous reports, we identified non-linear behavior in both the east and vertical components of the REMNE GNSS station. Specifically, the east component showed westward acceleration, while the vertical component indicated a decreasing subsidence rate, potentially transitioning to slow uplift. During September, this signal did not visibly progress and may have stabilized.

Analysis Maps

Three maps have been created to visually summarize the results of the current analysis. These maps are displayed below and are also included in Appendix 3.

- Figure 7 is a vector map illustrating the direction and magnitude of the tilt and deformation rates identified at each tiltmeter (during the current reporting period) and each GNSS station (from July 22, 2024, to the end of the current reporting period).
- Figure 8 presents rose diagrams showing the daily tilt direction frequency for each tiltmeter, covering the entire data history from June 2024 to the present.
- Figure 9 details the daily tilt direction frequency for the current monthly reporting period.

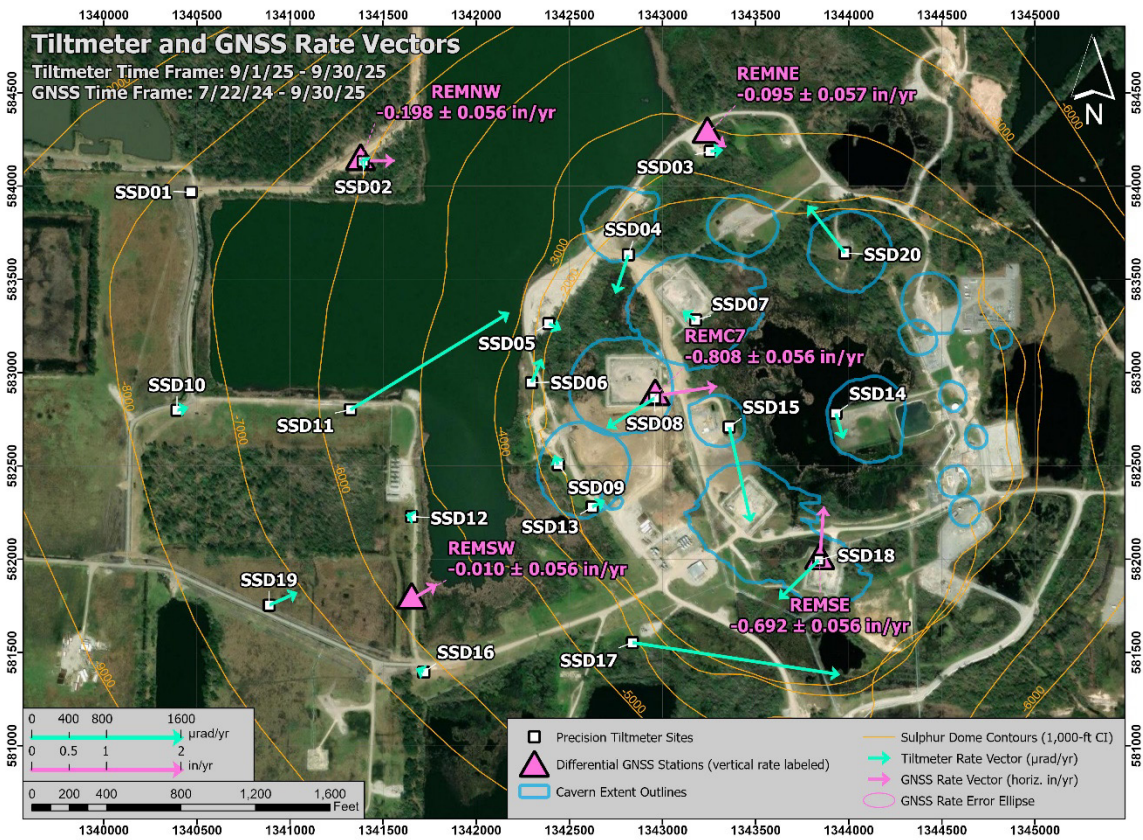


Figure 7. Map of deformation rate vectors for the tiltmeters and GNSS stations over their respective evaluated time frames. The tiltmeter vectors are shown in cyan and scaled by their respective values in units of microradians per year. The GNSS vectors and their corresponding error ellipses (derived from east and north rate errors) are shown in pink representing inches of horizontal movement per year. The GNSS stations are additionally labeled with the vertical motion rate and corresponding error value.

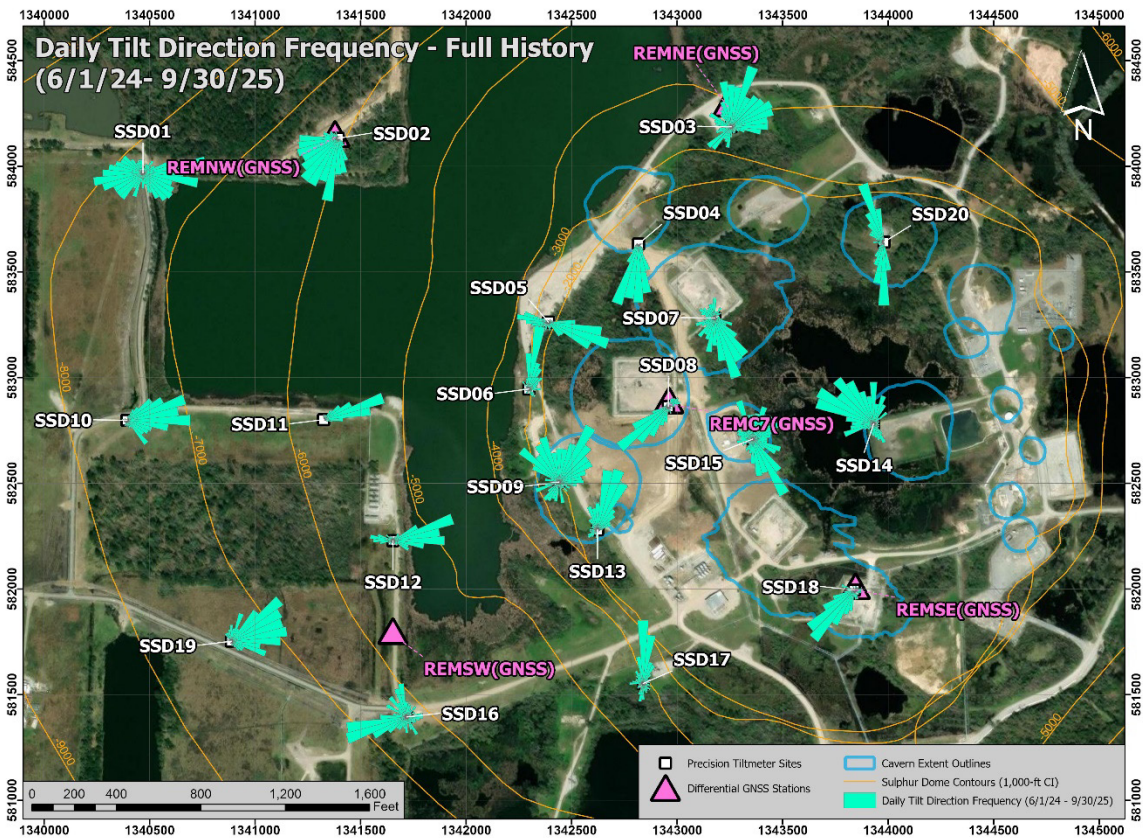


Figure 8. Map of daily tilt direction distribution for each tiltmeter for the full data history beginning in June 2024. Rose diagrams indicate the number of days that tilt was oriented along specific azimuths (bin size is 10°).

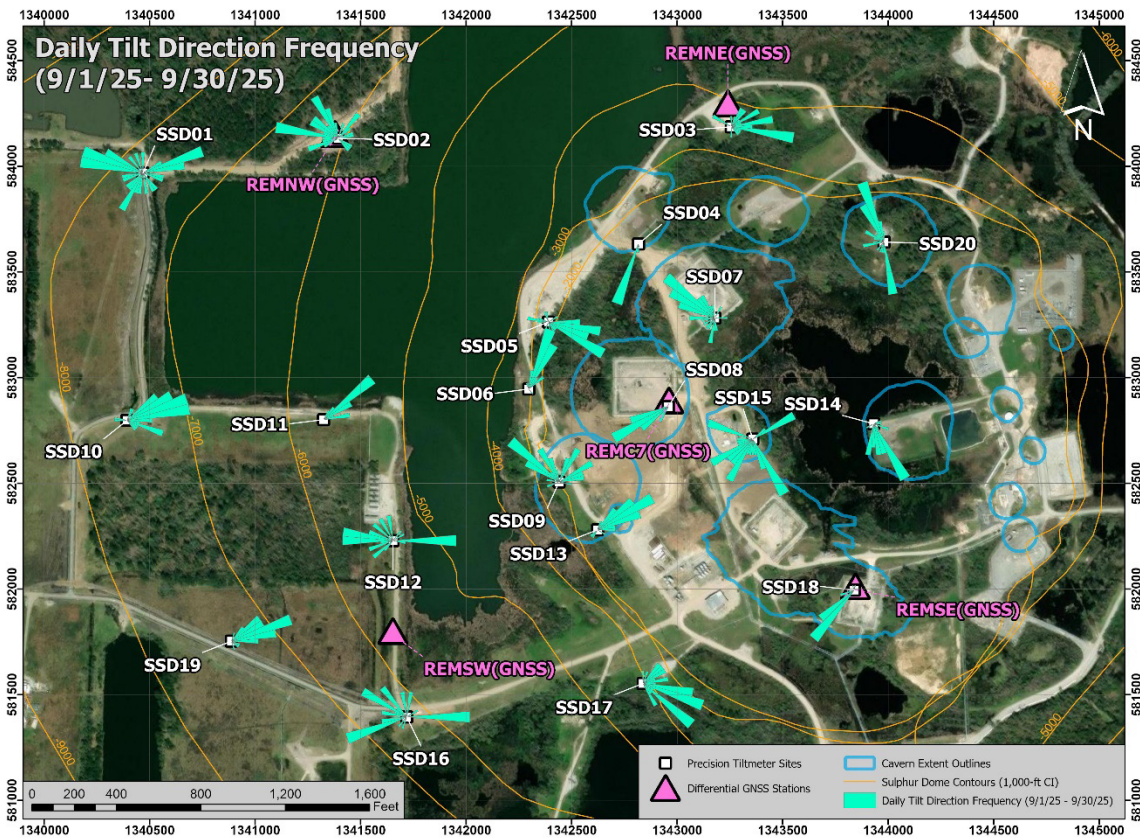


Figure 9. Map of daily tilt direction distribution for each tiltmeter for the current monthly reporting period. Rose diagrams indicate the number of days that tilt was oriented along specific azimuths (bin size is 10°).

Deformation Alert System Update

We continue testing a draft deformation alert system that incorporates the magnitude of daily tiltmeter readings using non-Gaussian statistics across the full tiltmeter network. This allows for the appropriate interpretation of long-duration tilt observations and helps bypass the effects of short-duration anomalous tilt signals associated with precipitation and mechanical activities near the monitoring sites. We plan to evaluate the tilt alert system until we are confident it will give reliable results. In addition, we will use this ongoing analysis to set and adjust the alert triggering thresholds and refine the appropriate response actions due to a change in the alert status.

Our theoretical deformation (Mogi) modelling (discussed in the deformation monitoring plan dated December 22, 2023) indicates that deep deformation associated with potential changes in volume at Cavern 7 (located at a depth of approximately 2,500 to 3,160 feet) is expected to impact the entire tiltmeter array. If the deformation moves upward from Cavern 7, we anticipate that the corresponding tiltmeter response will be concentrated at the stations nearest the cavern, and the tilt magnitude will increase. In contrast, local,

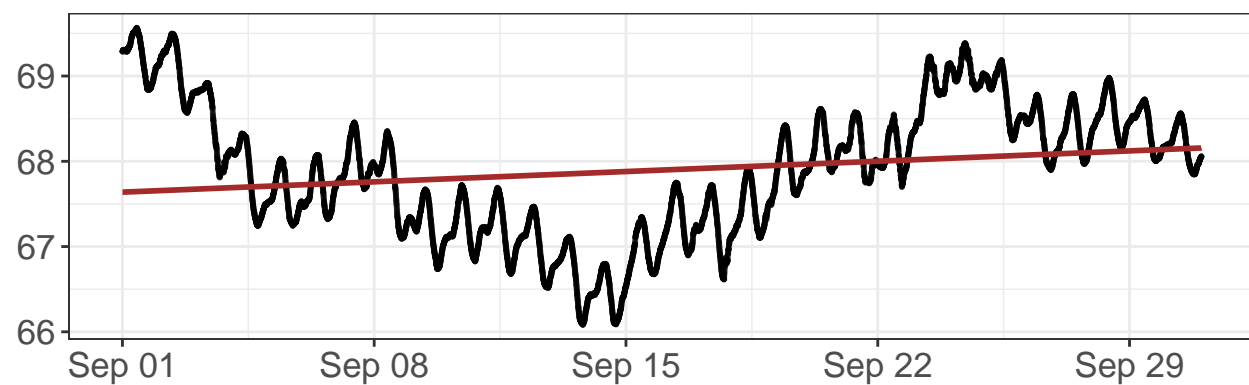
shallow deformation, such as movement in the caprock, is likely to affect only the nearby tiltmeters.

We anticipate that short-term deformation alert levels will be evaluated with the other real-time monitoring observations currently active at Sulphur Mines, which include the Cavern 7 pressure and microseismic monitoring. Additionally, long-term trends from GNSS and InSAR, which typically become available with some delay, will also be necessary for ongoing alert assessments.

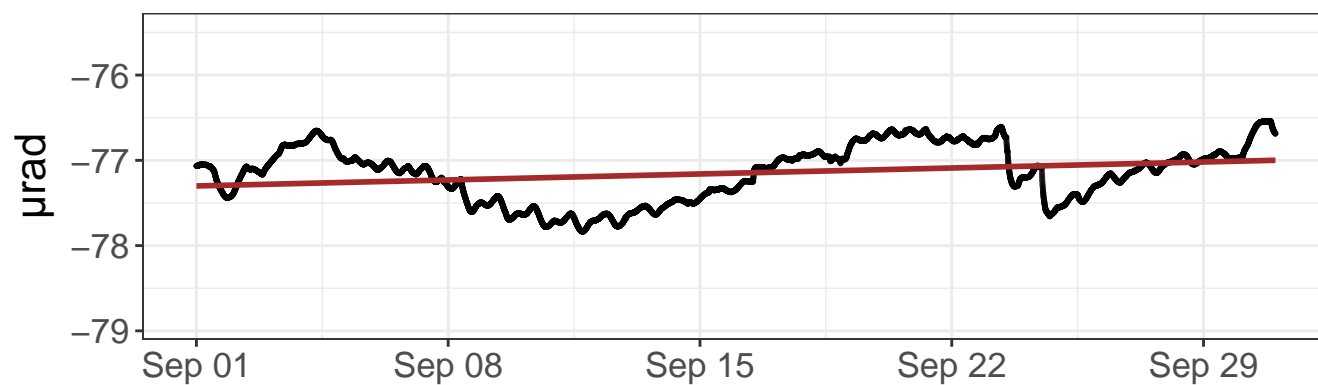
APPENDIX 1

Tiltmeter Data Plots

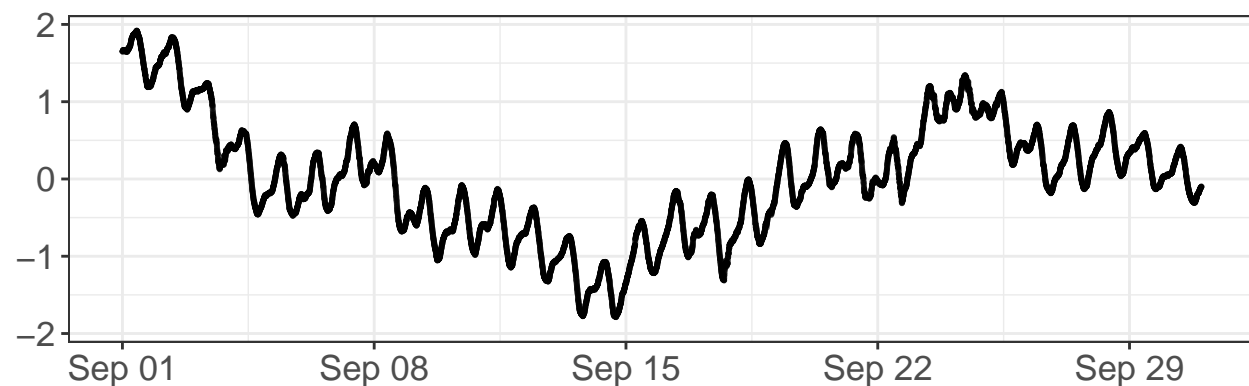
East tilt – raw values



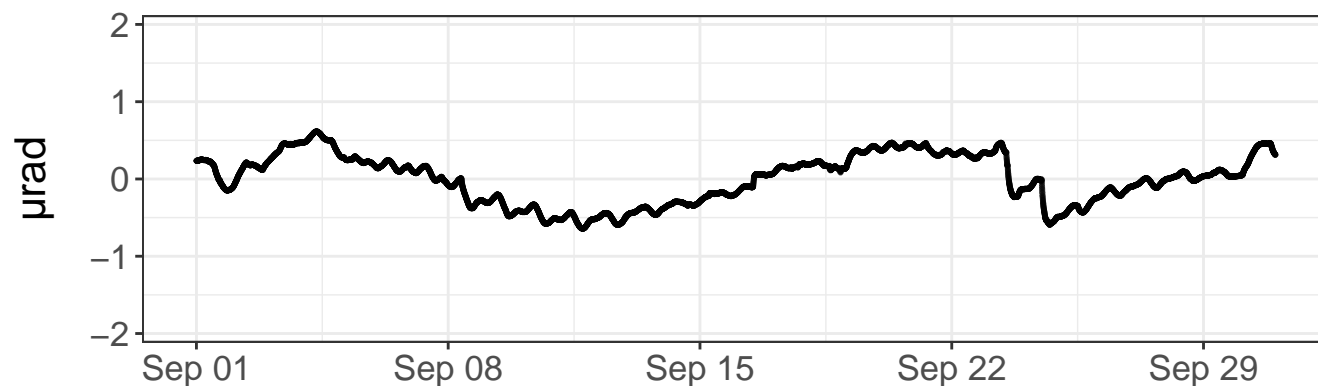
North tilt – raw values



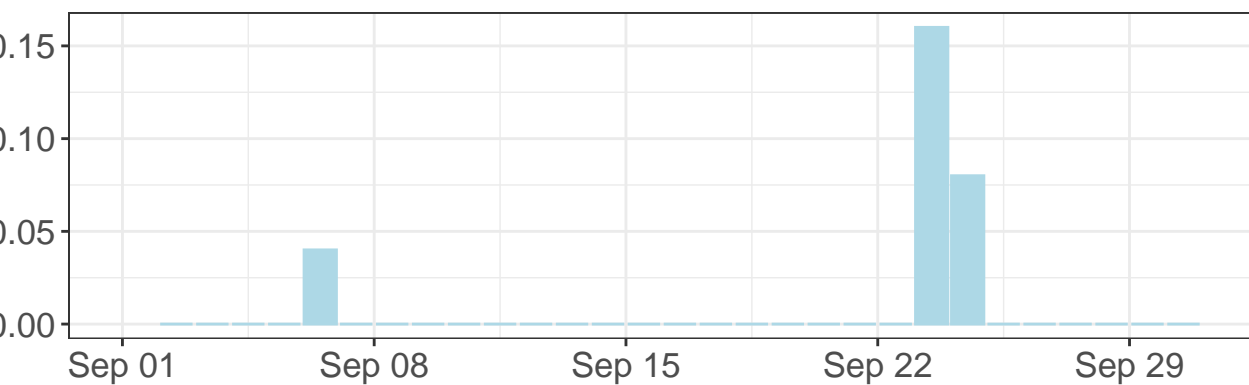
East tilt – detrended values



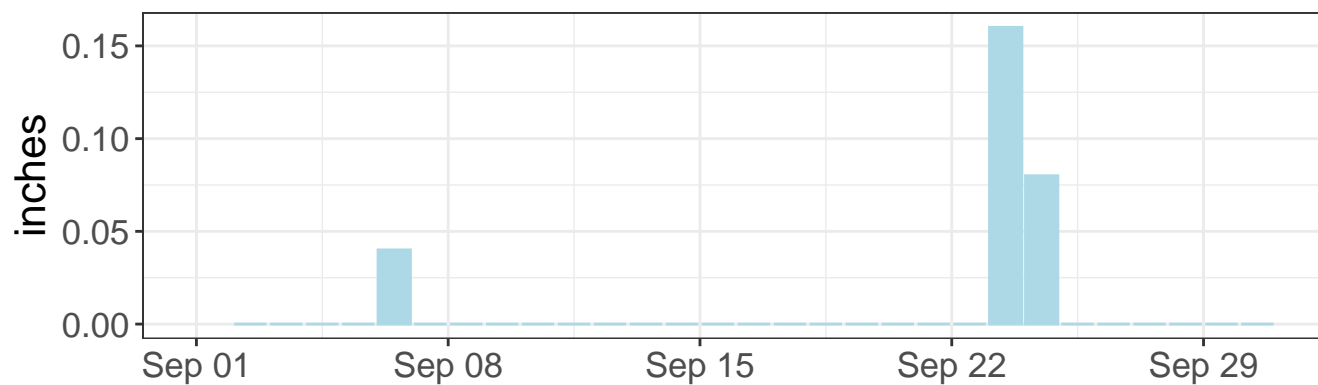
North tilt – detrended values



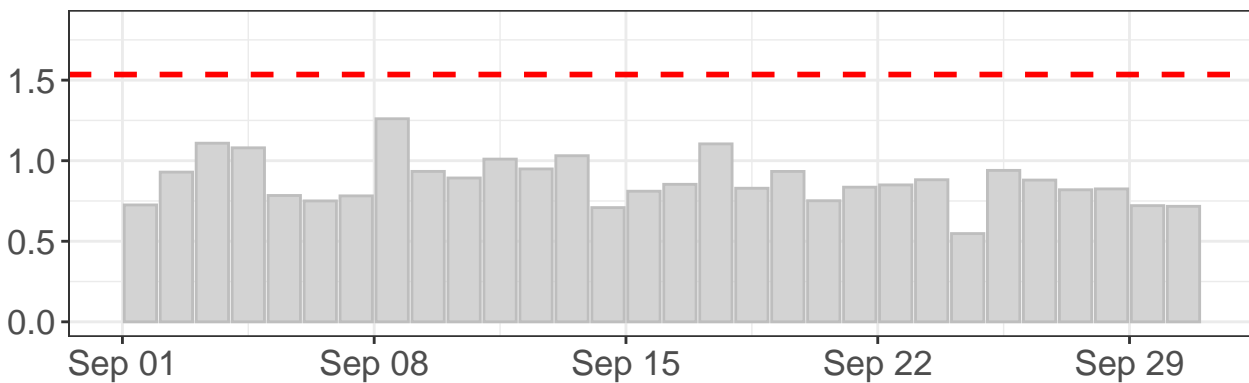
Daily precipitation



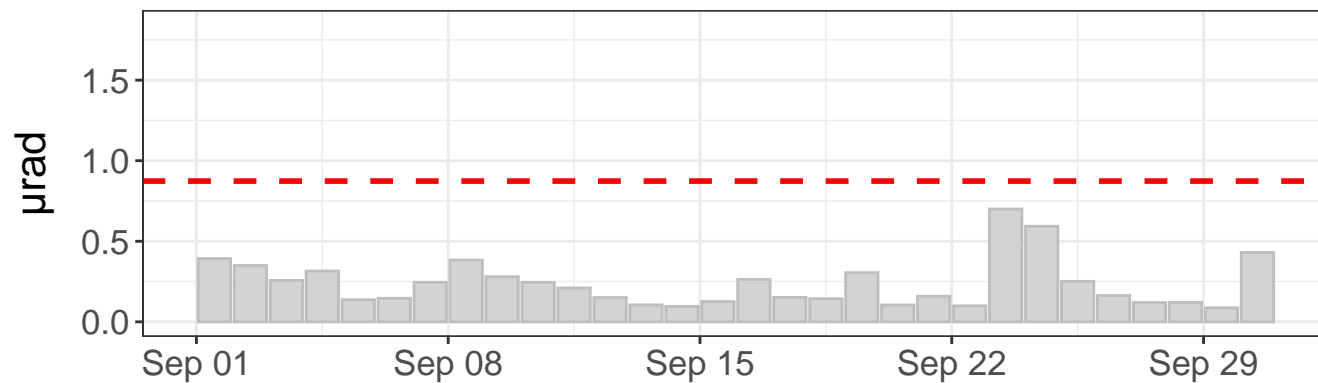
Daily precipitation



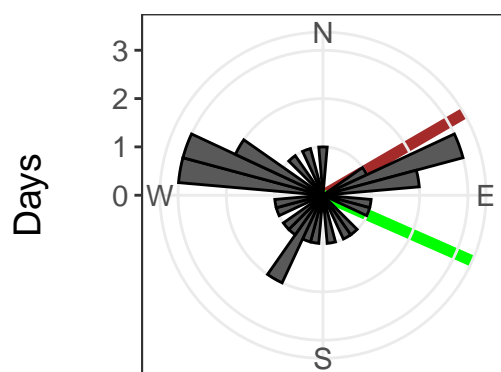
East tilt – daily range



North tilt – daily range



Tilt direction frequency



East tilt rate: $6.31 \pm 0.31 \mu\text{rad/yr}$. R^2 : 0.04

North tilt rate: $3.66 \pm 0.13 \mu\text{rad/yr}$. R^2 : 0.07

Azimuth to C7: 114 deg

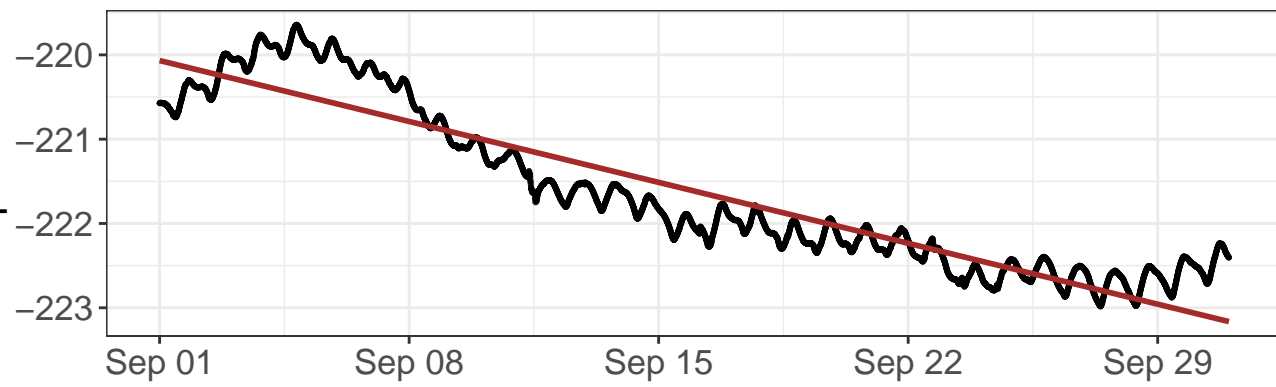
Distance to C7: 2538 ft

--- Outlier value

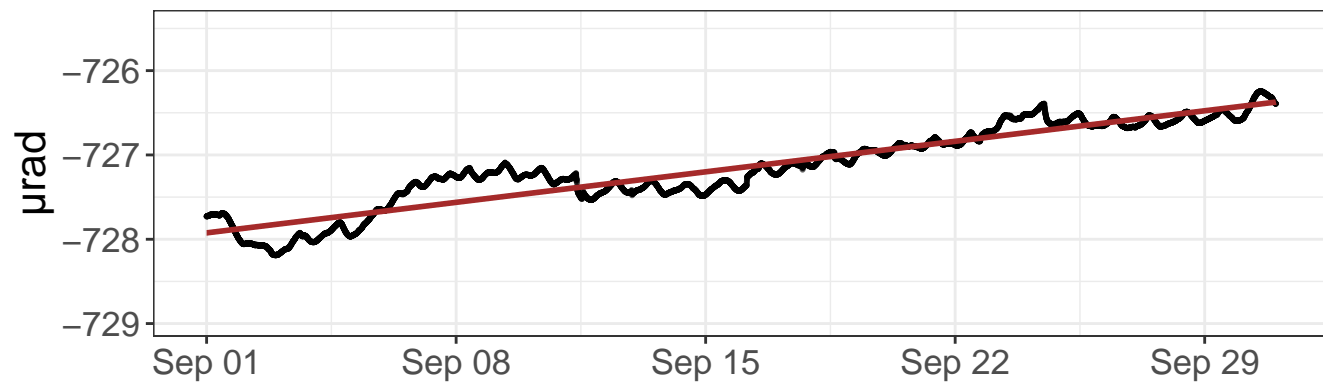
— Linear model

— Azimuth to C7

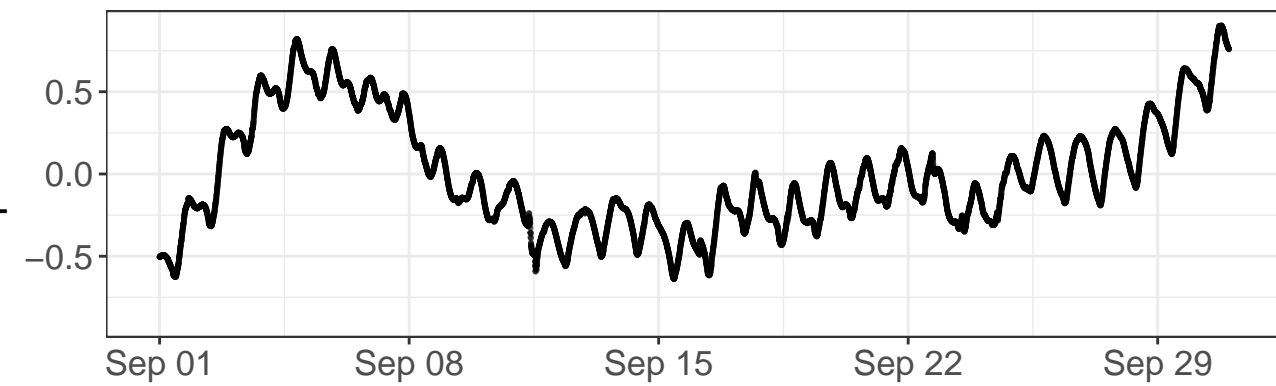
East tilt – raw values



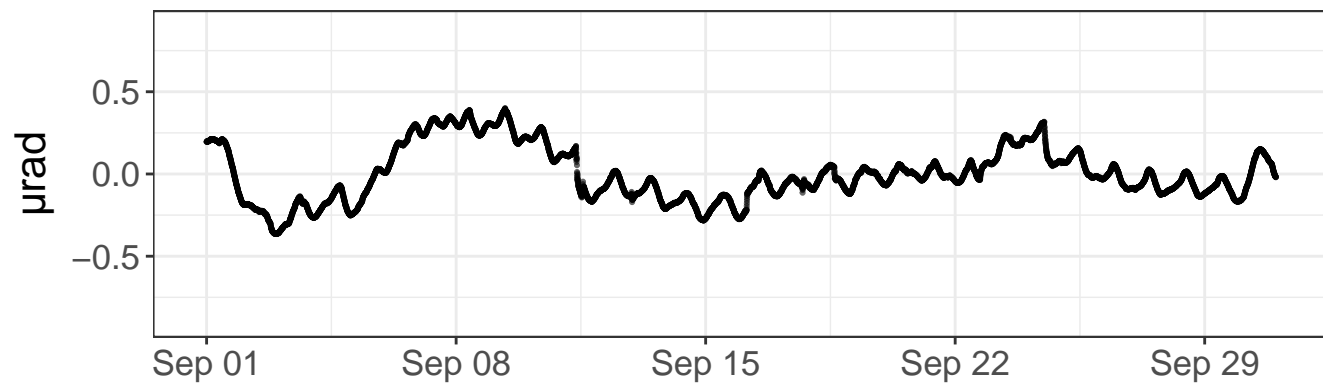
North tilt – raw values



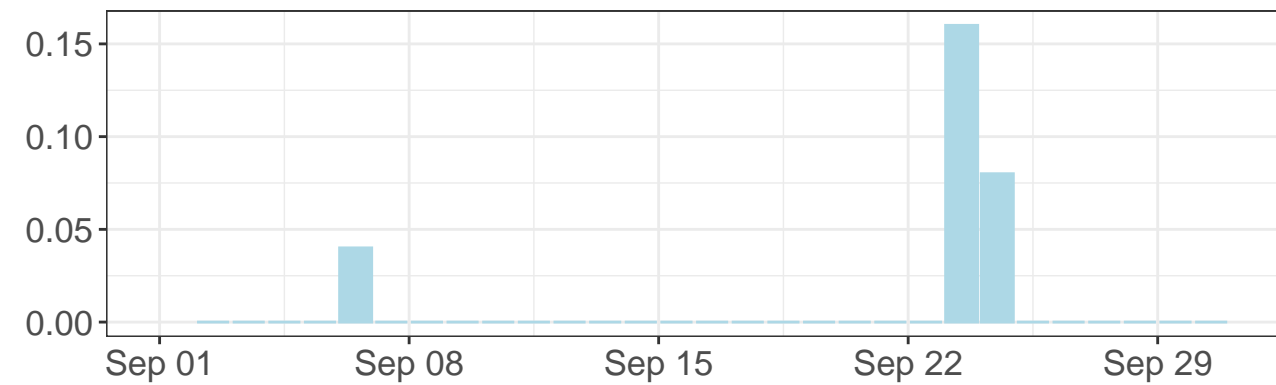
East tilt – detrended values



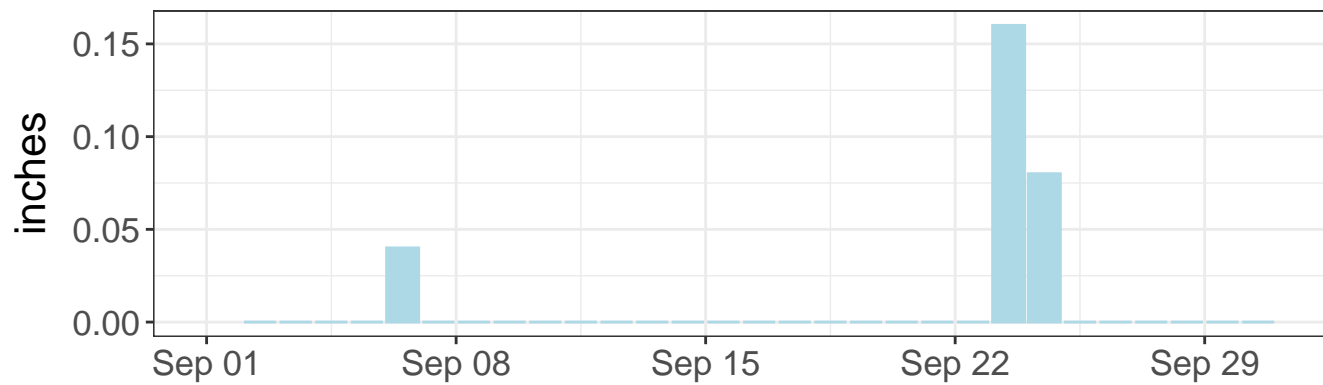
North tilt – detrended values



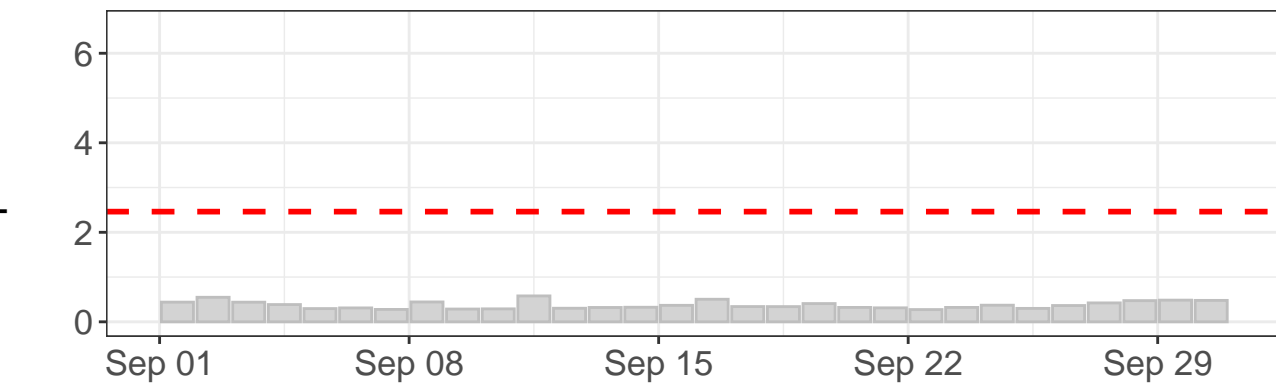
Daily precipitation



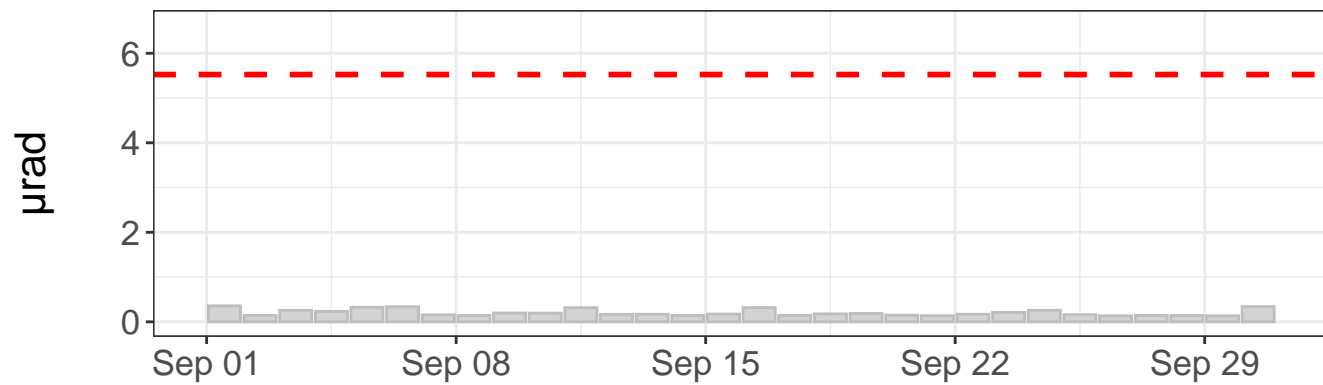
Daily precipitation



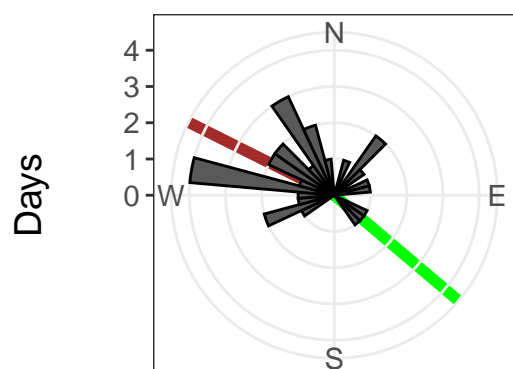
East tilt – daily range



North tilt – daily range



Tilt direction frequency



East tilt rate: $-37.67 \pm 0.14 \mu\text{rad}/\text{yr}$. $R^2: 0.87$

North tilt rate: $18.88 \pm 0.07 \mu\text{rad}/\text{yr}$. $R^2: 0.88$

Azimuth to C7: 130 deg

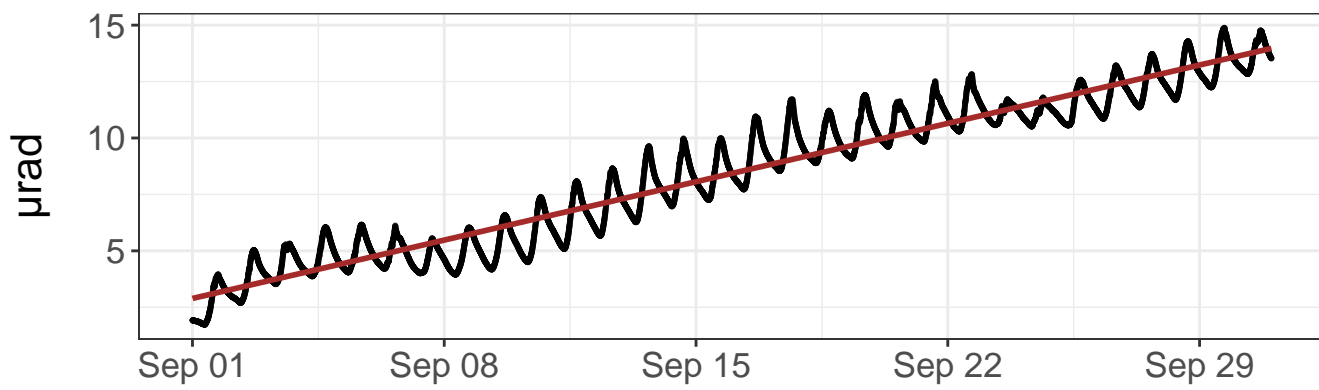
Distance to C7: 1834 ft

--- Outlier value

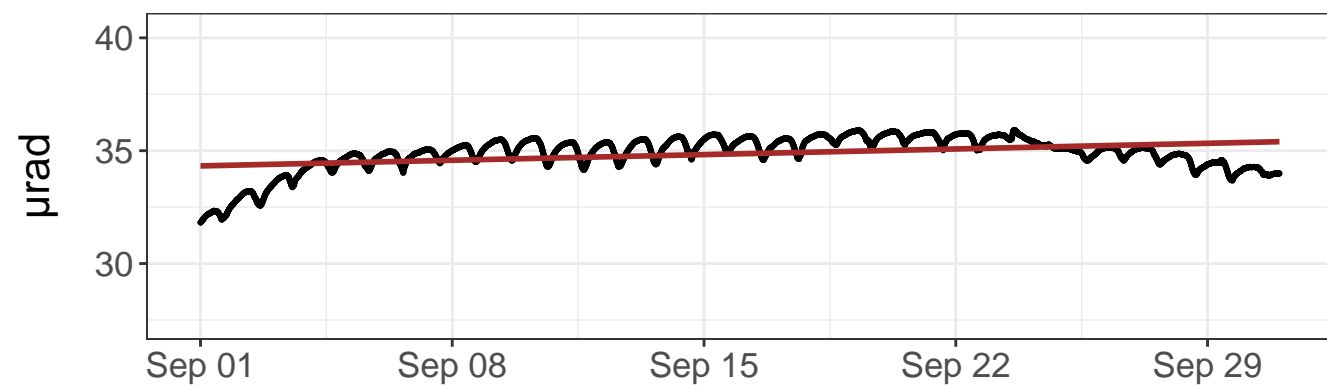
— Linear model

— Azimuth to C7

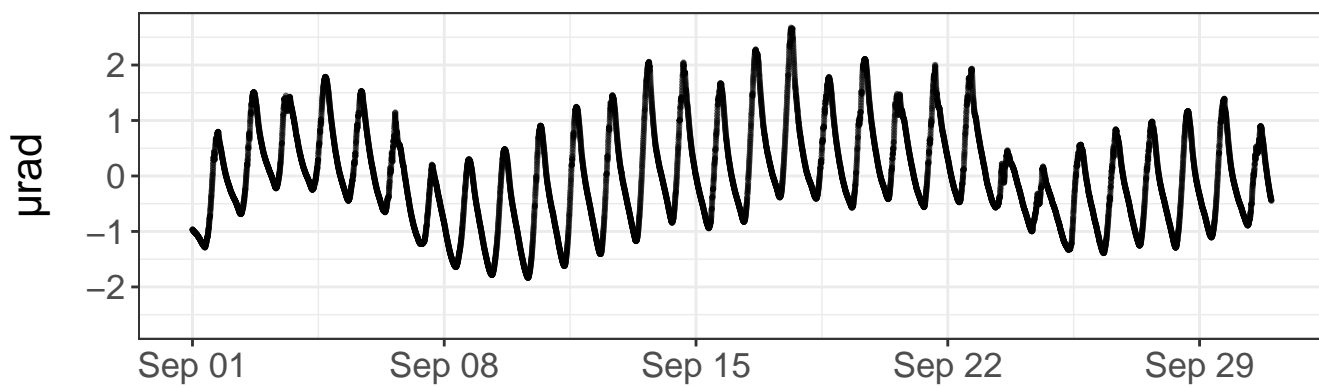
East tilt – raw values



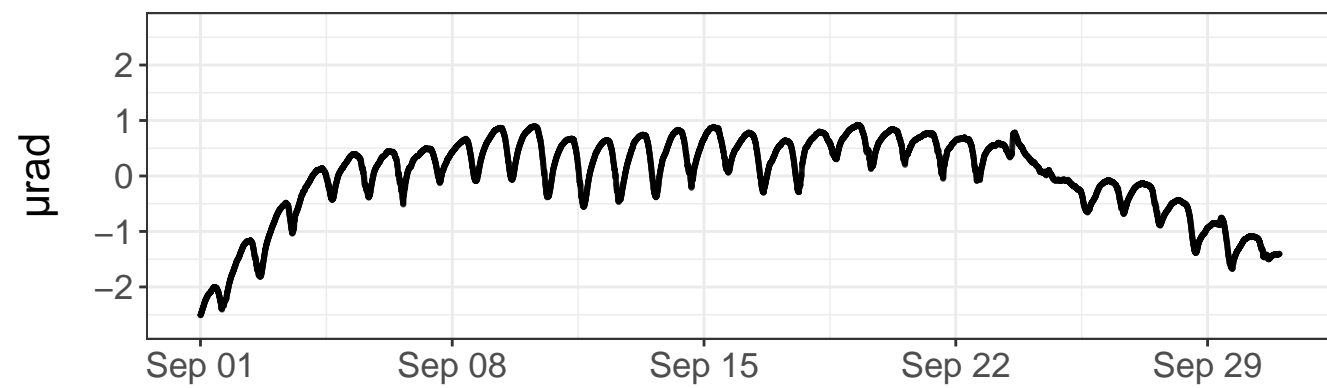
North tilt – raw values



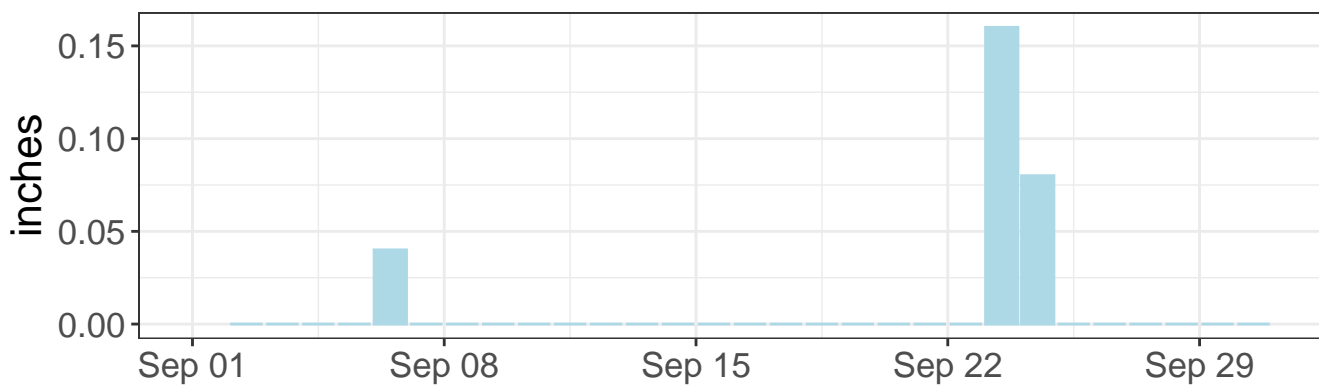
East tilt – detrended values



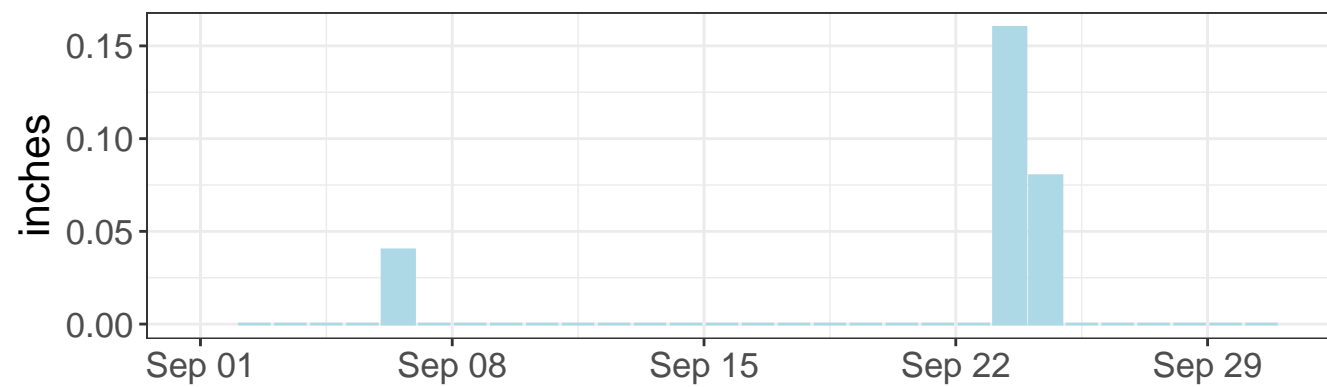
North tilt – detrended values



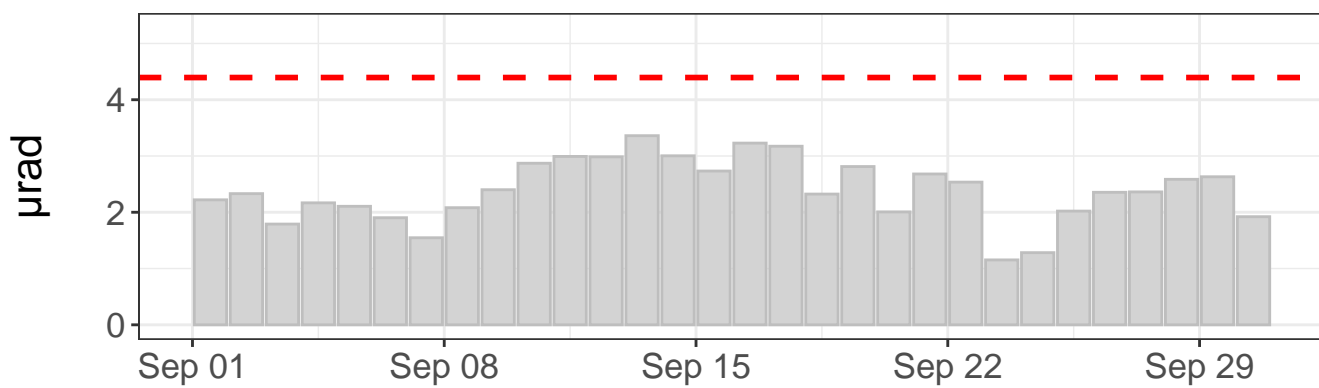
Daily precipitation



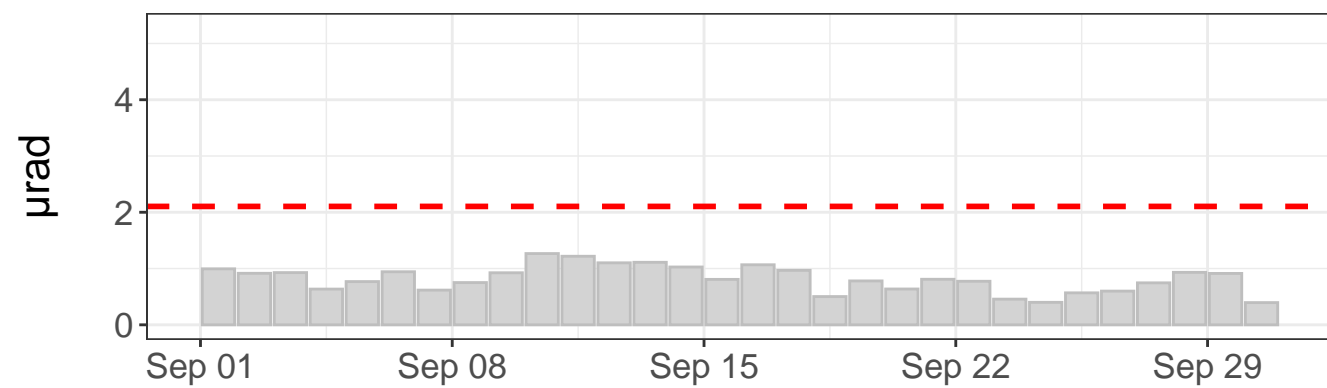
Daily precipitation



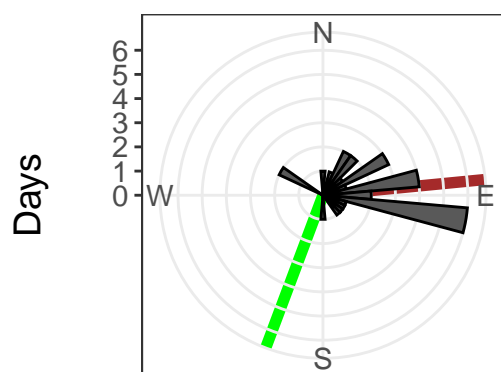
East tilt – daily range



North tilt – daily range



Tilt direction frequency



East tilt rate: $134.80 \pm 0.35 \mu\text{rad/yr}$. $R^2: 0.93$

North tilt rate: $13.06 \pm 0.30 \mu\text{rad/yr}$. $R^2: 0.15$

Azimuth to C7: 201 deg

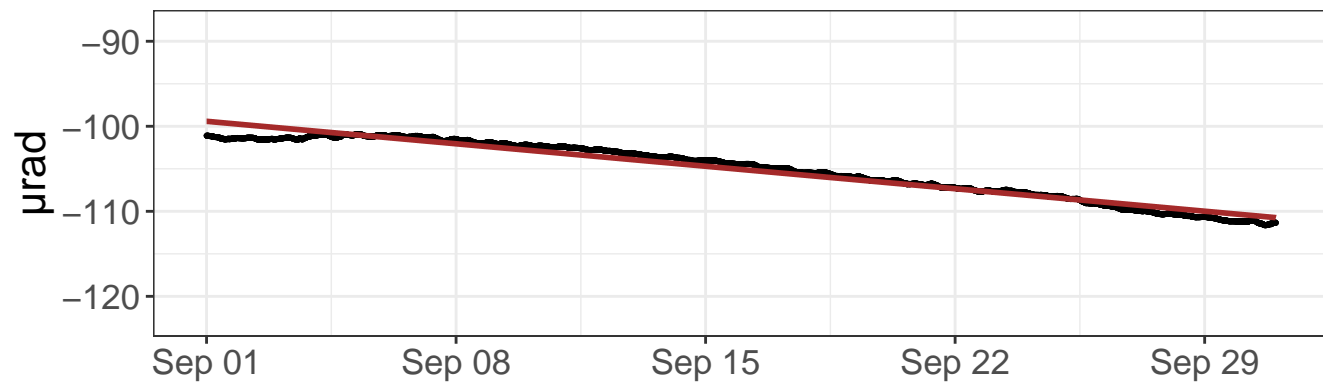
Distance to C7: 1326 ft

--- Outlier value

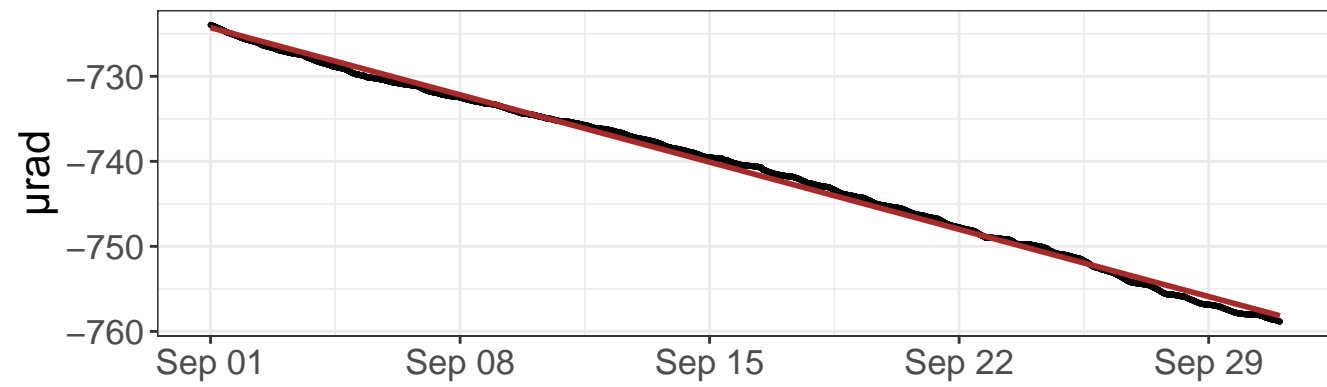
— Linear model

— Azimuth to C7

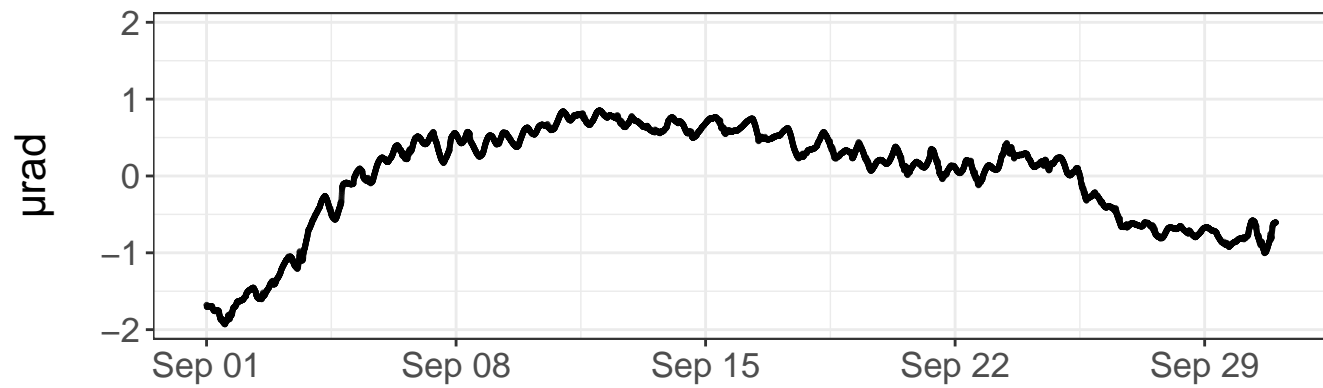
East tilt – raw values



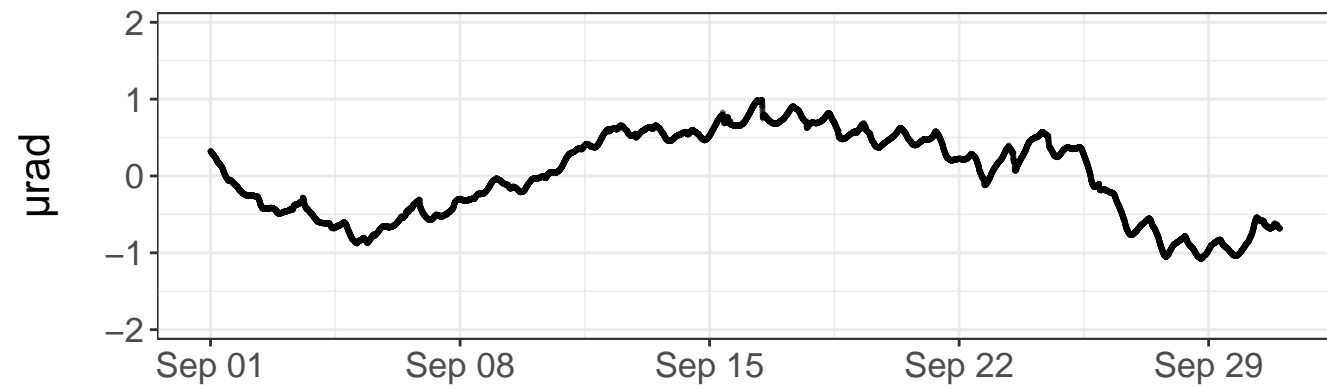
North tilt – raw values



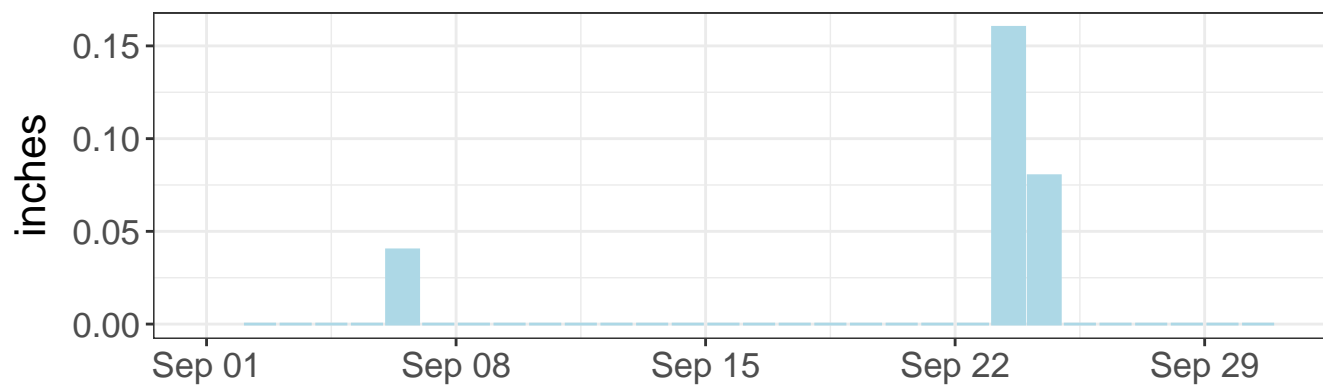
East tilt – detrended values



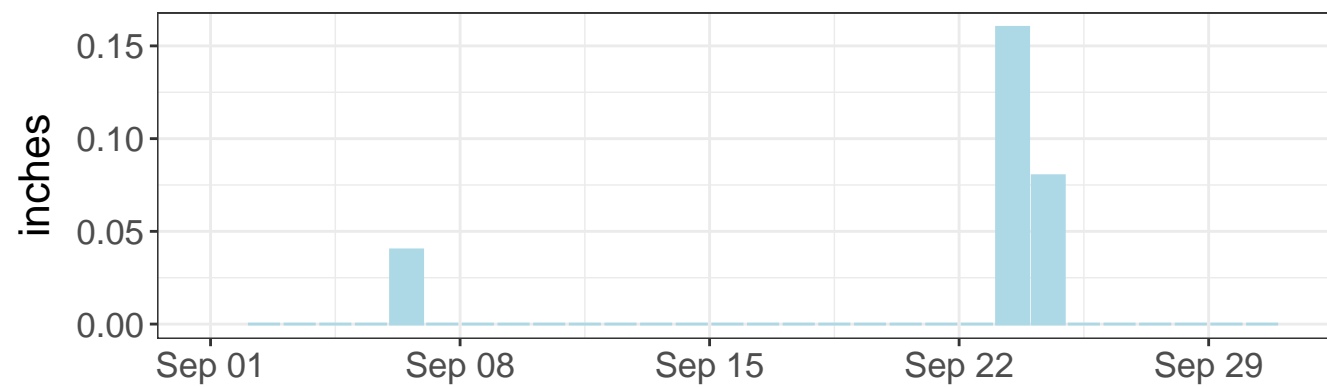
North tilt – detrended values



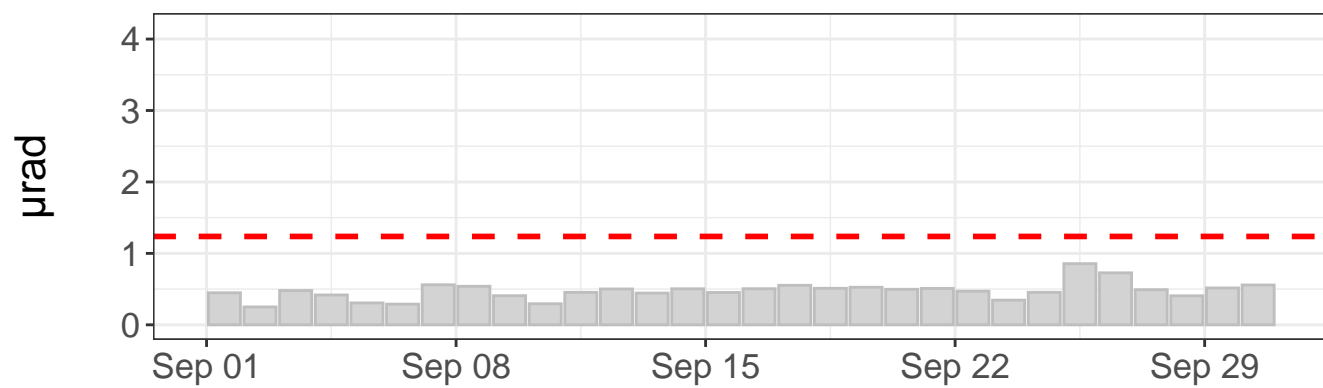
Daily precipitation



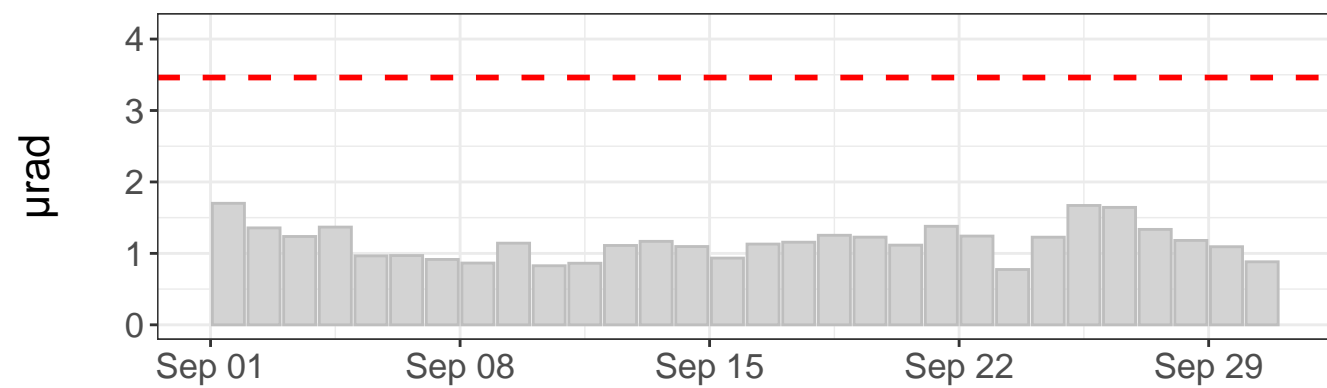
Daily precipitation



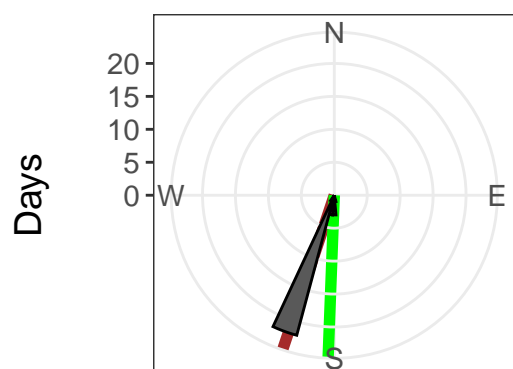
East tilt – daily range



North tilt – daily range



Tilt direction frequency



East tilt rate: $-137.84 \pm 0.27 \mu\text{rad}/\text{yr}$. R2: 0.96

North tilt rate: $-412.37 \pm 0.23 \mu\text{rad}/\text{yr}$. R2: 1.00

Azimuth to C7: 182 deg

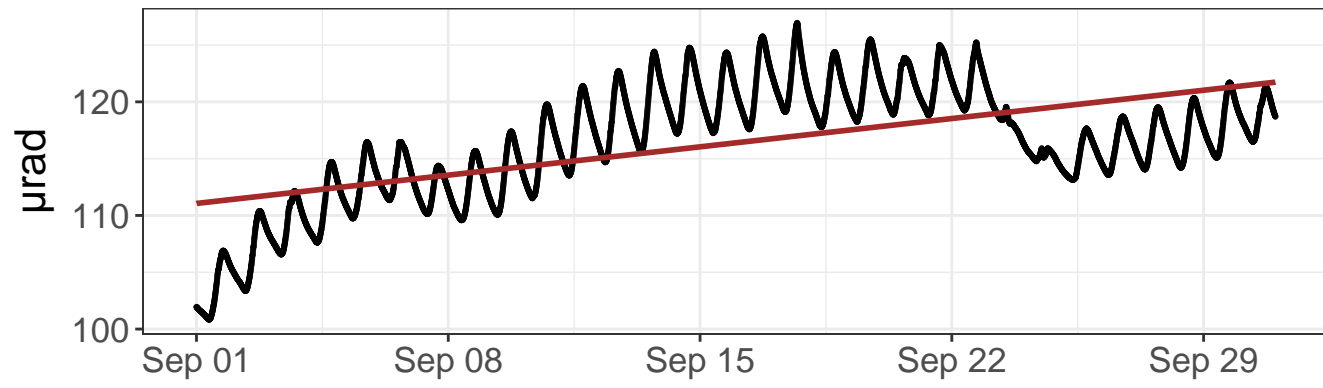
Distance to C7: 688 ft

--- Outlier value

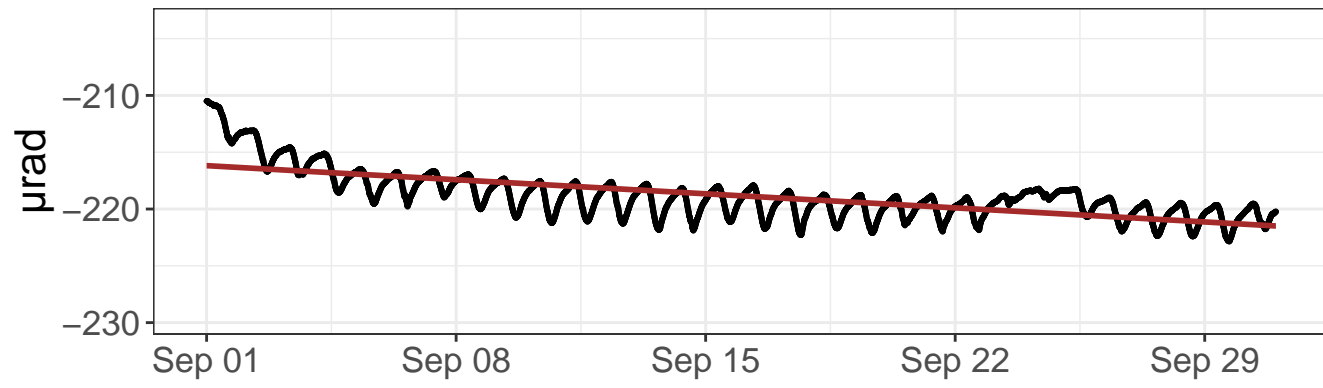
— Linear model

— Azimuth to C7

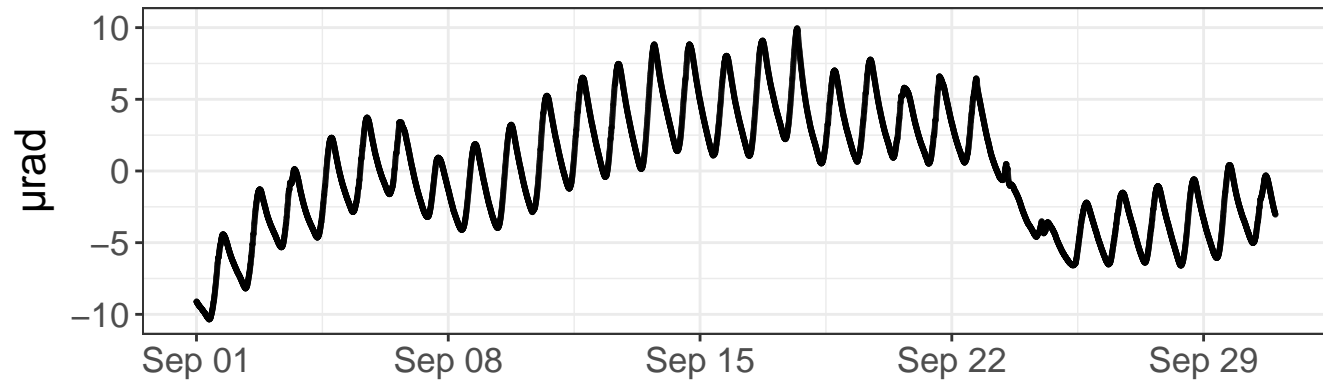
East tilt – raw values



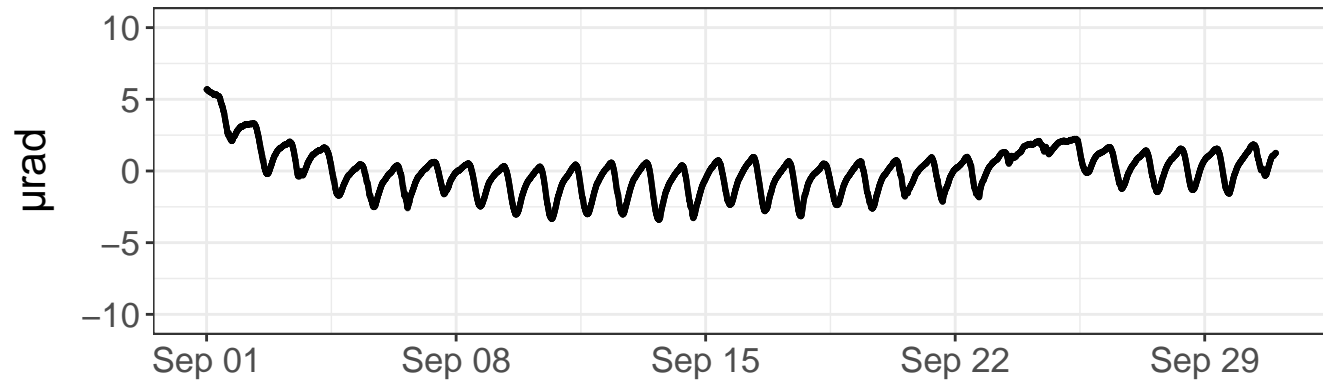
North tilt – raw values



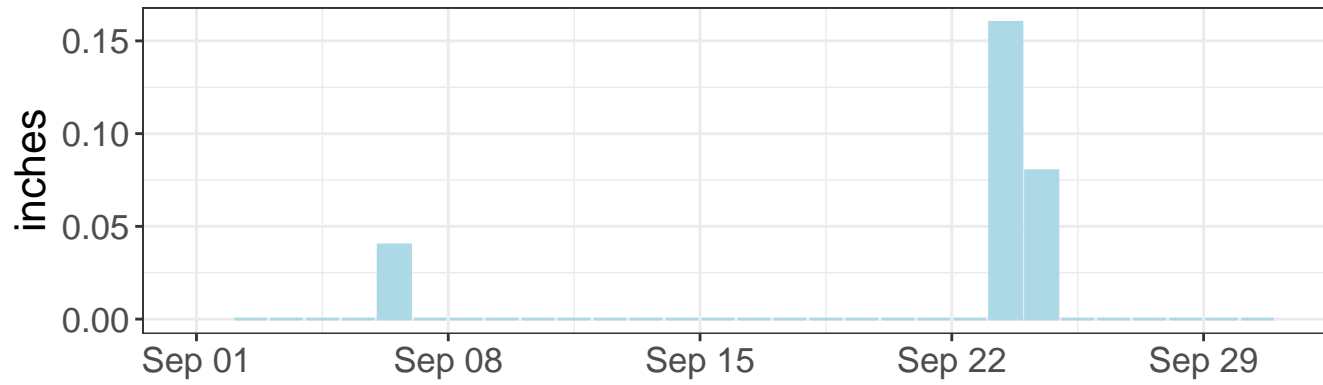
East tilt – detrended values



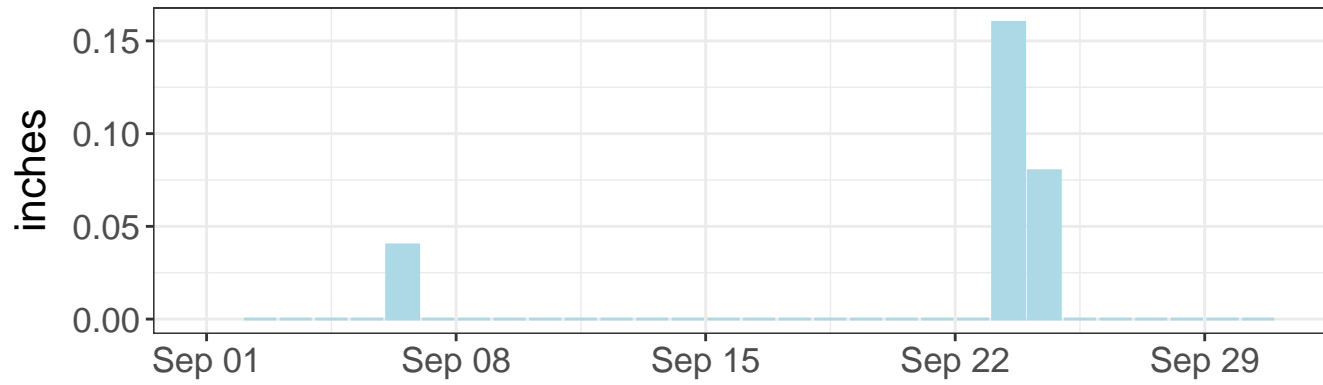
North tilt – detrended values



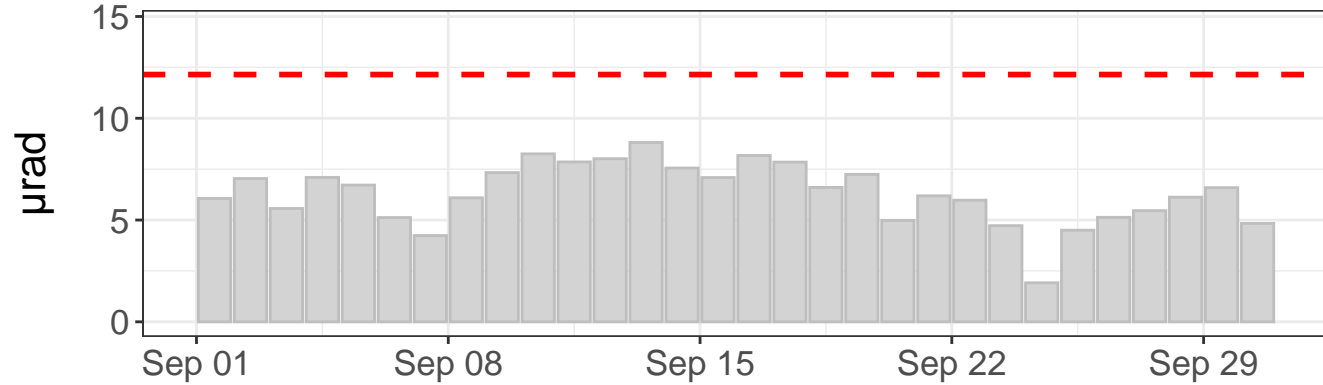
Daily precipitation



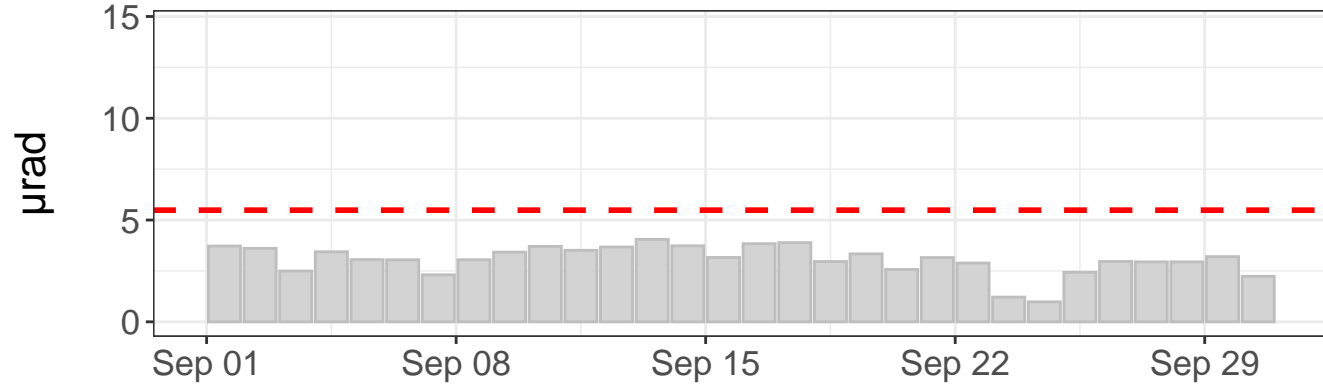
Daily precipitation



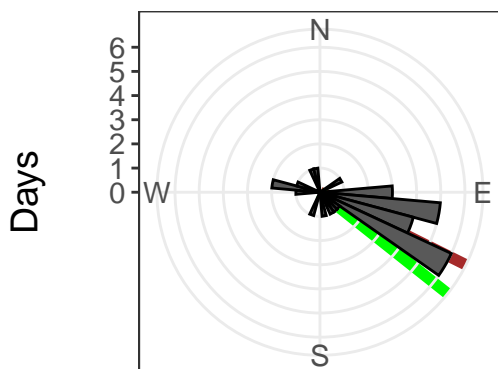
East tilt – daily range



North tilt – daily range



Tilt direction frequency



East tilt rate: $129.91 \pm 1.69 \mu\text{rad/yr}$. R^2 : 0.35

North tilt rate: $-64.60 \pm 0.61 \mu\text{rad/yr}$. R^2 : 0.51

Azimuth to C7: 128 deg

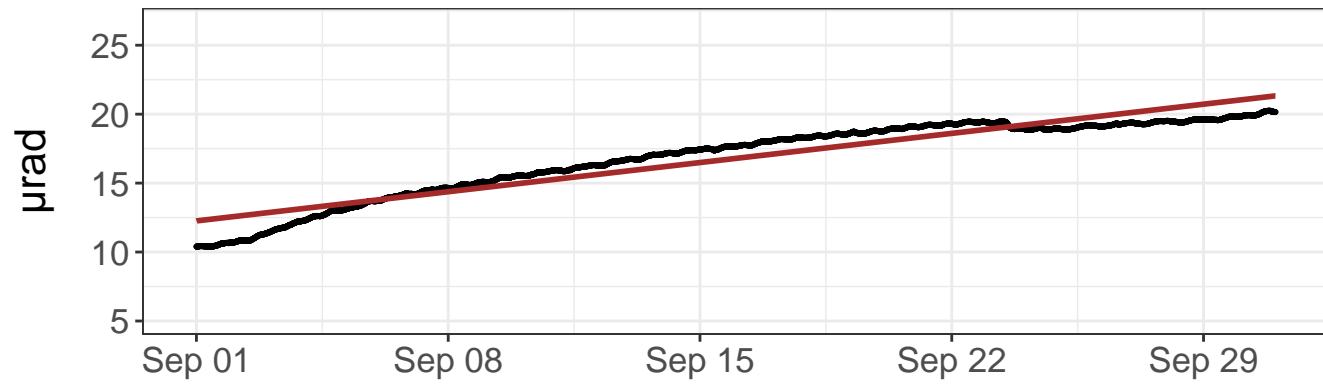
Distance to C7: 512 ft

- - - Outlier value

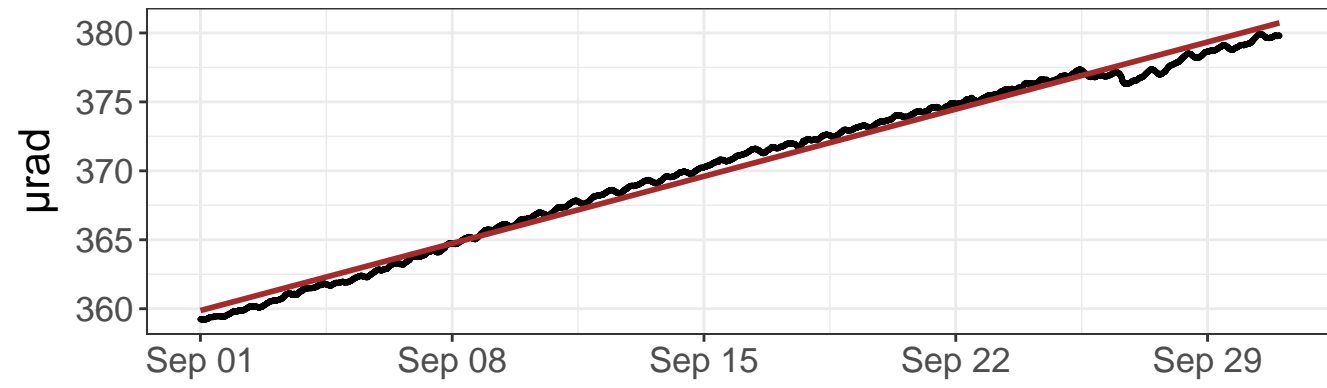
— Linear model

— Azimuth to C7

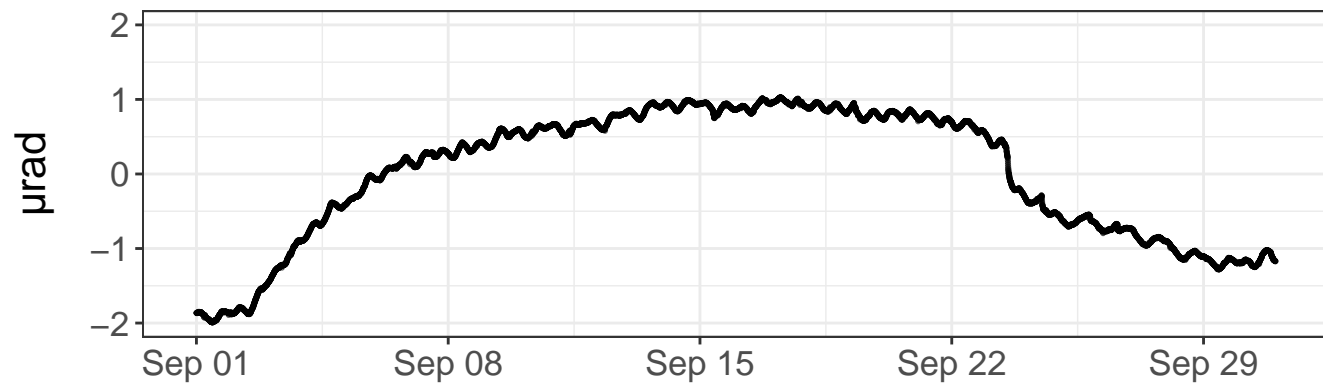
East tilt – raw values



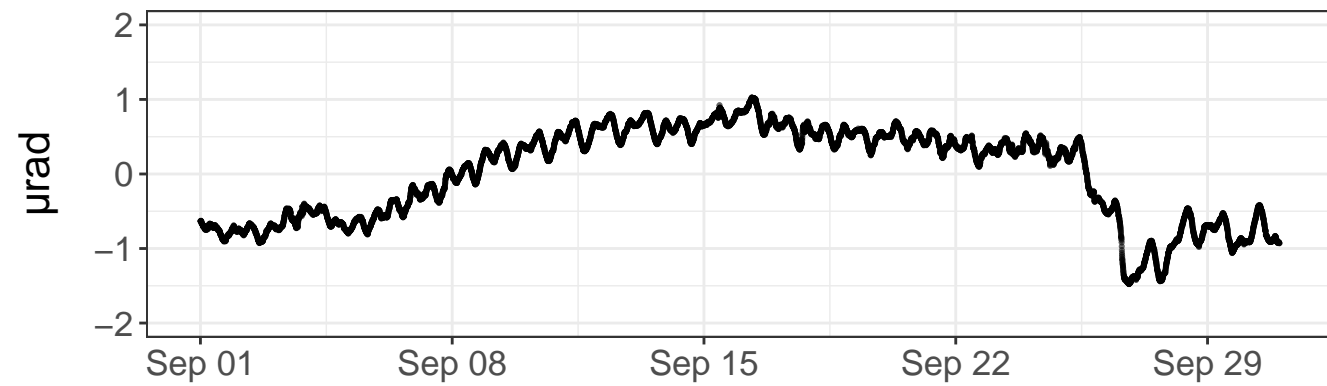
North tilt – raw values



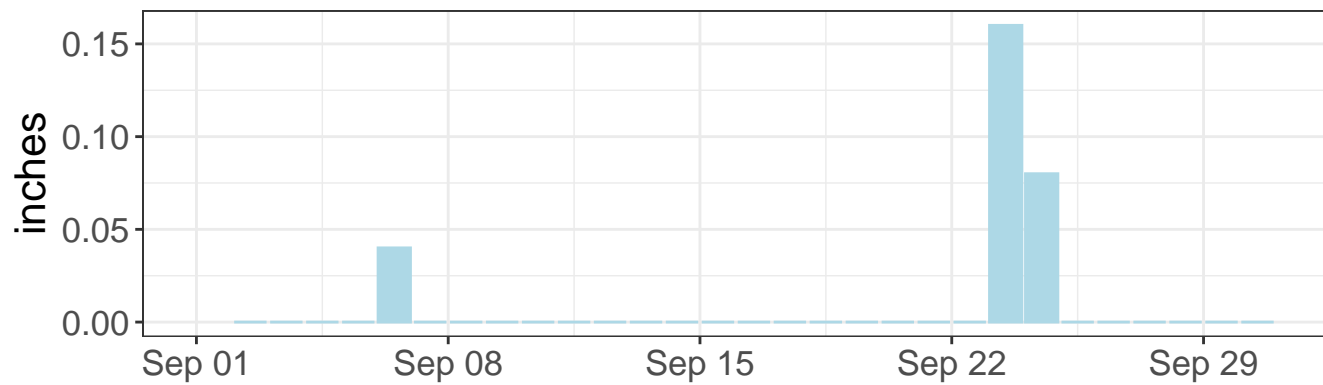
East tilt – detrended values



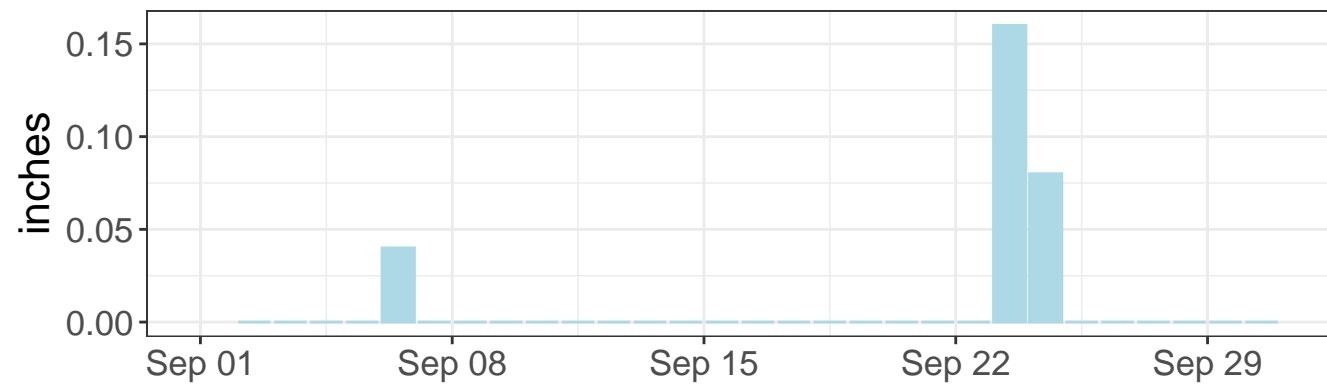
North tilt – detrended values



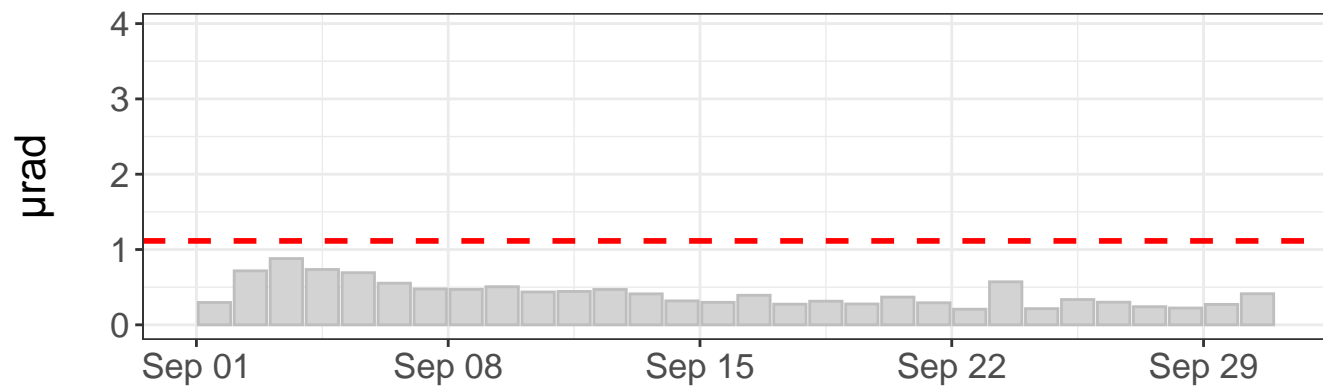
Daily precipitation



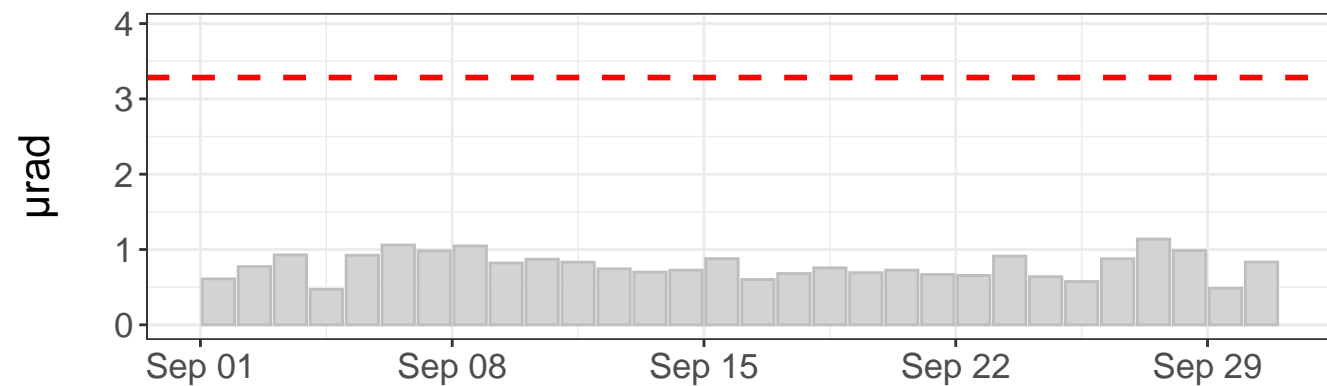
Daily precipitation



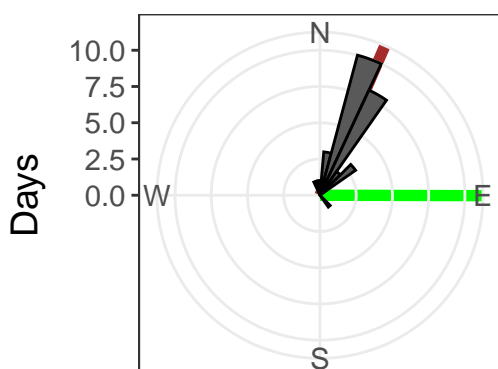
East tilt – daily range



North tilt – daily range



Tilt direction frequency



East tilt rate: $110.34 \pm 0.36 \mu\text{rad/yr}$. $R^2: 0.90$

North tilt rate: $253.84 \pm 0.25 \mu\text{rad/yr}$. $R^2: 0.99$

Azimuth to C7: 90 deg

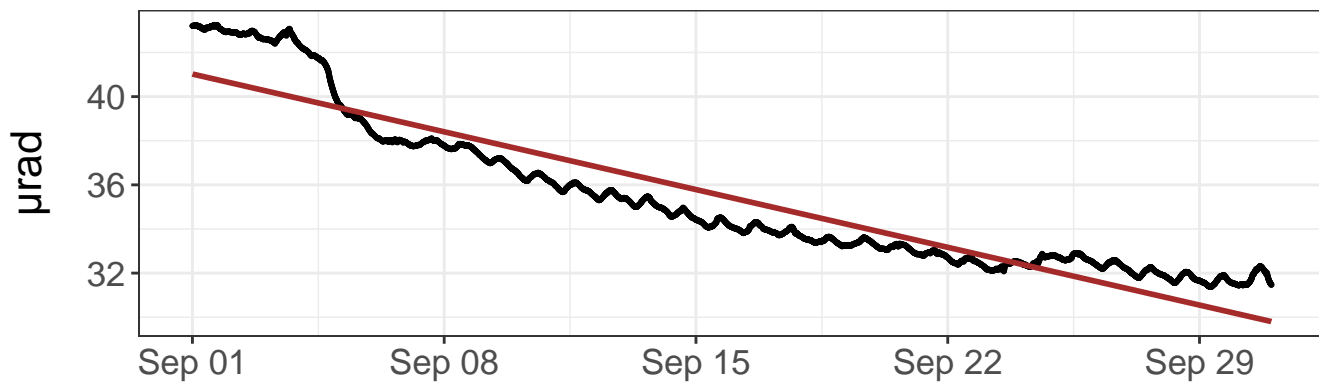
Distance to C7: 494 ft

--- Outlier value

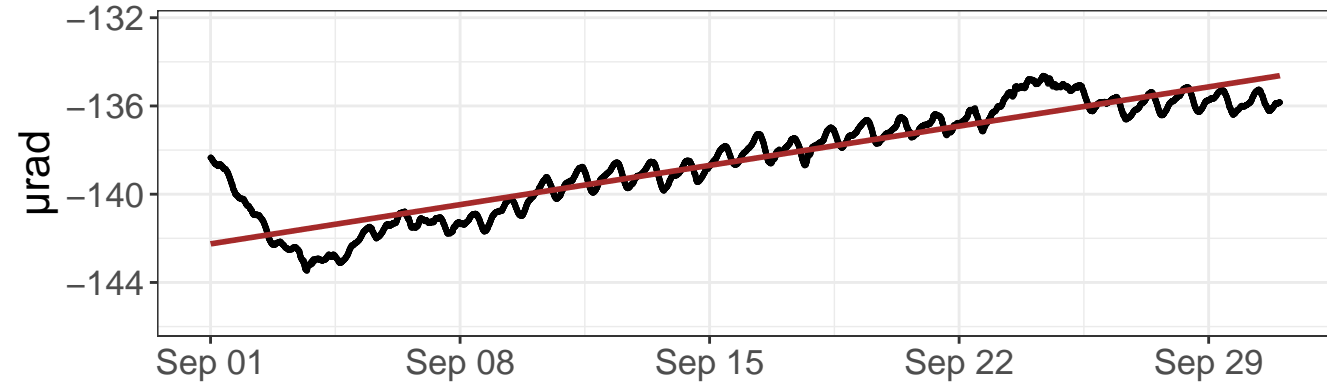
— Linear model

— Azimuth to C7

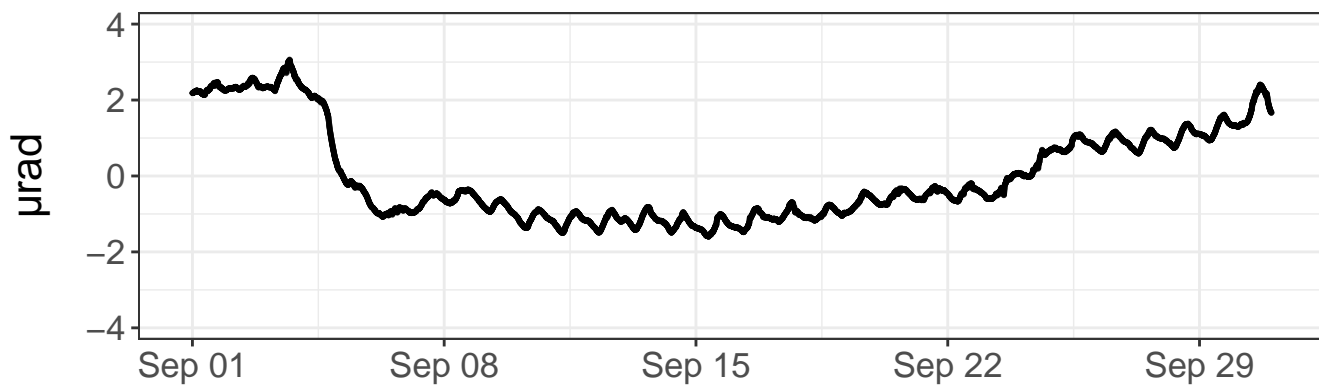
East tilt – raw values



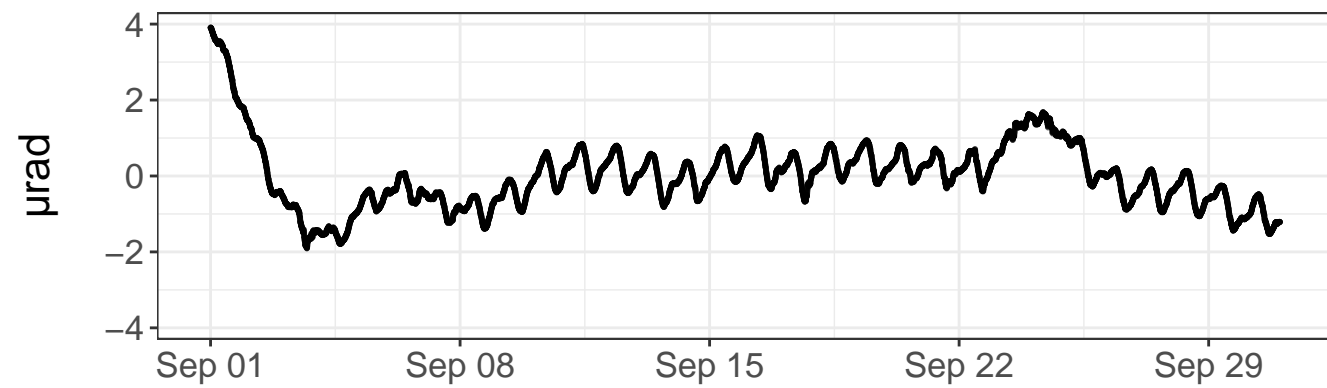
North tilt – raw values



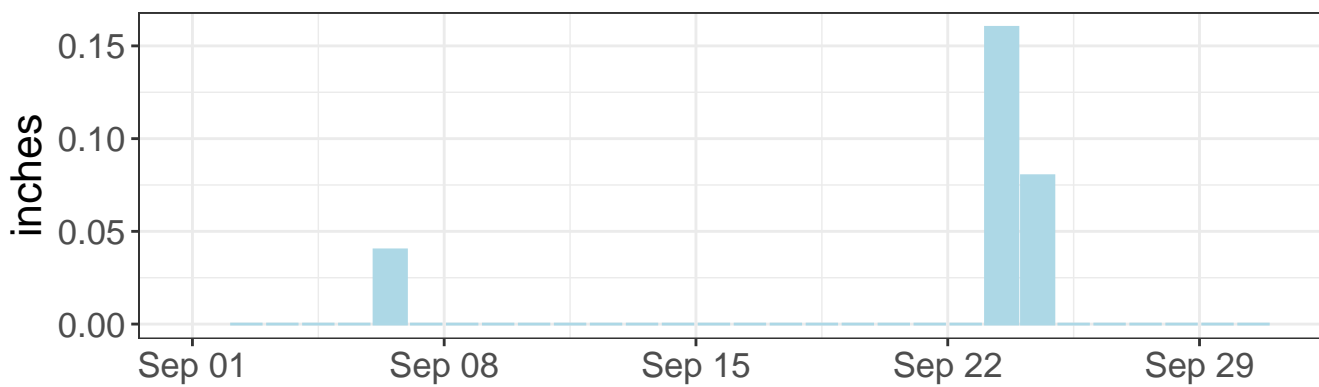
East tilt – detrended values



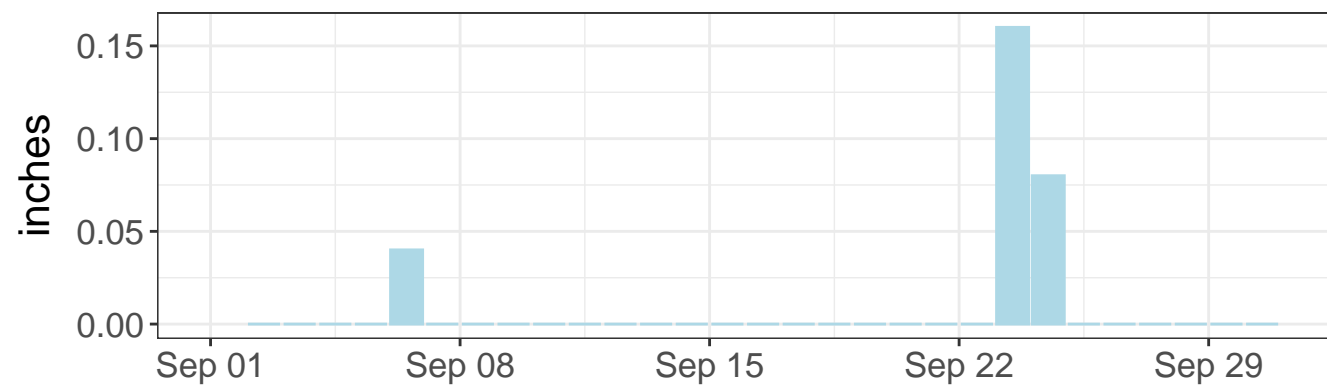
North tilt – detrended values



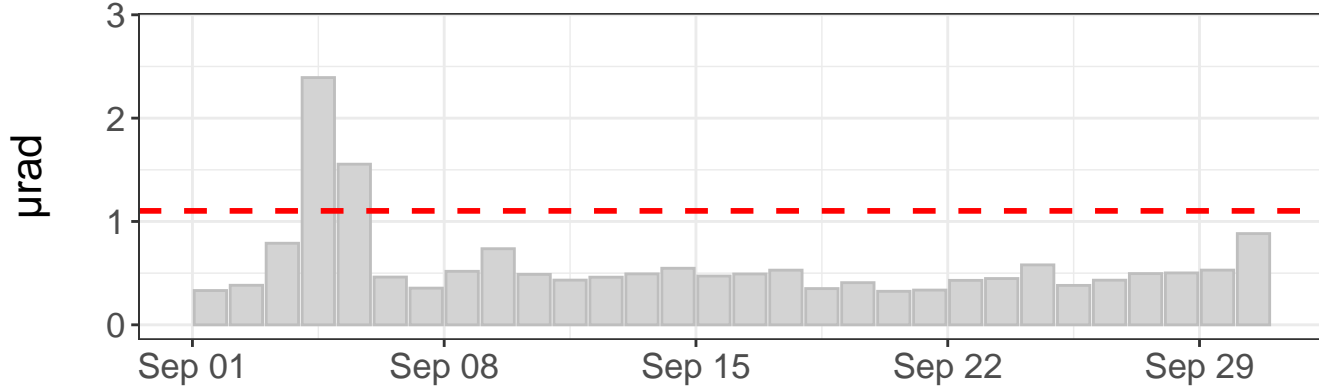
Daily precipitation



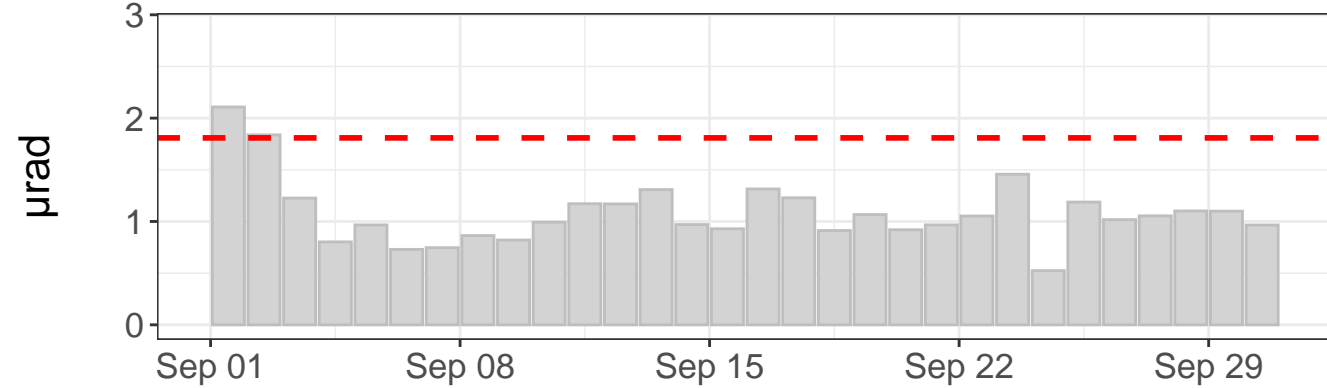
Daily precipitation



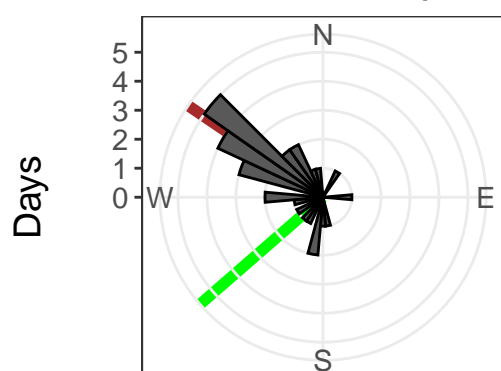
East tilt – daily range



North tilt – daily range



Tilt direction frequency



East tilt rate: $-136.52 \pm 0.50 \mu\text{rad}/\text{yr}$. $R^2: 0.87$

North tilt rate: $92.77 \pm 0.36 \mu\text{rad}/\text{yr}$. $R^2: 0.86$

Azimuth to C7: 229 deg

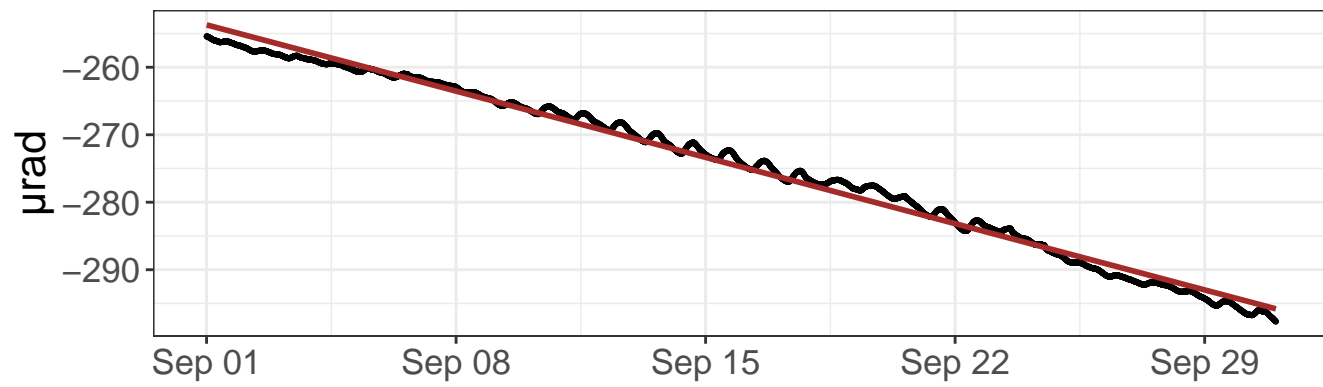
Distance to C7: 513 ft

- - - Outlier value

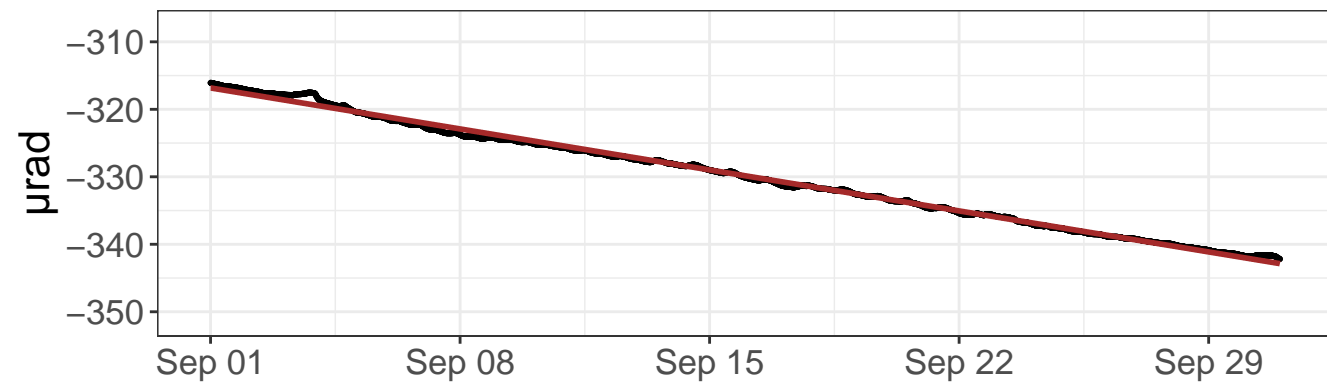
— Linear model

— Azimuth to C7

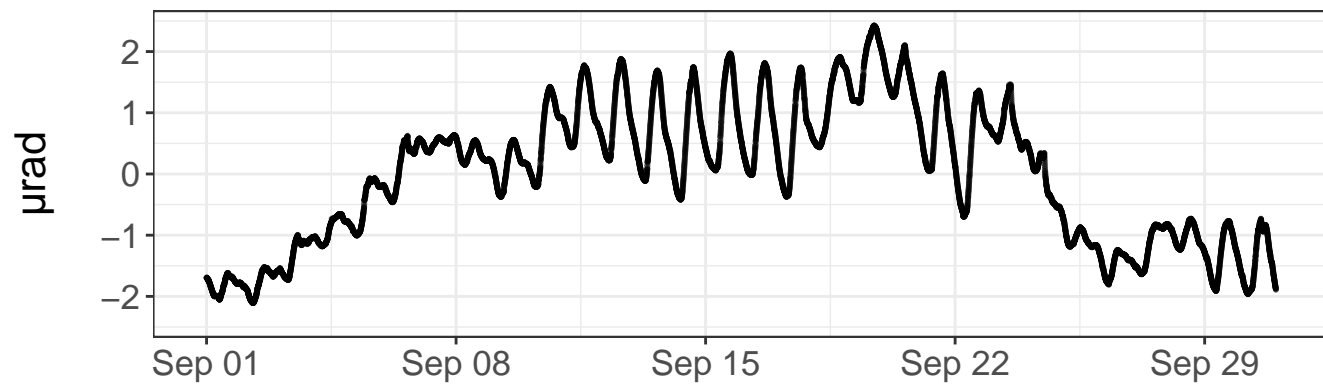
East tilt – raw values



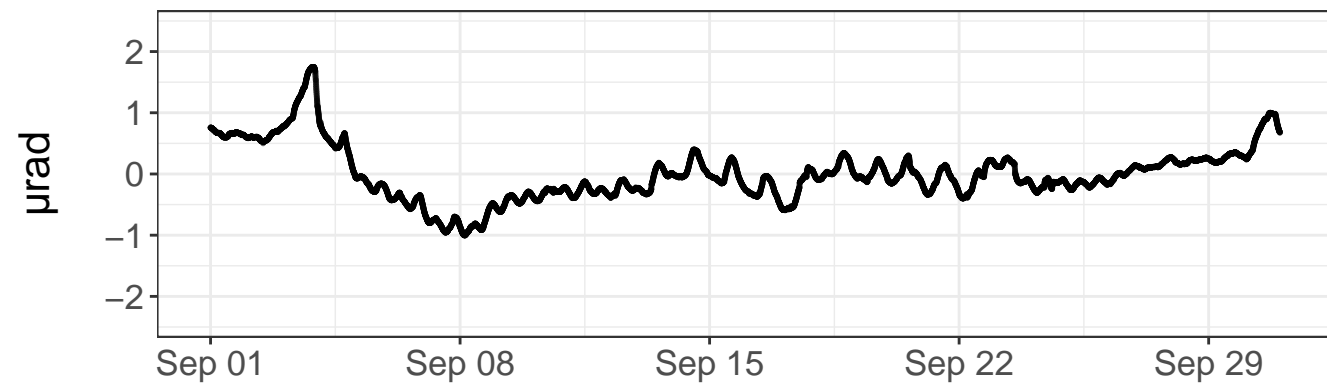
North tilt – raw values



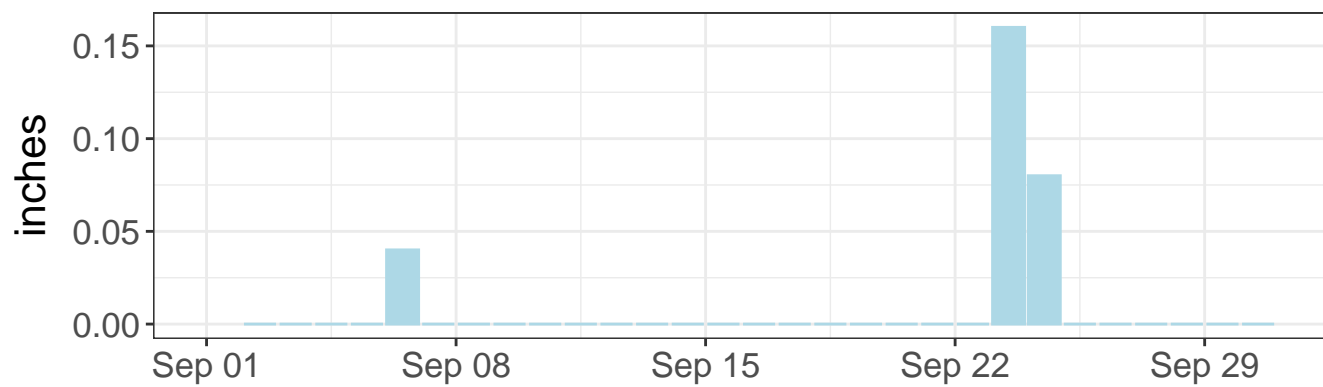
East tilt – detrended values



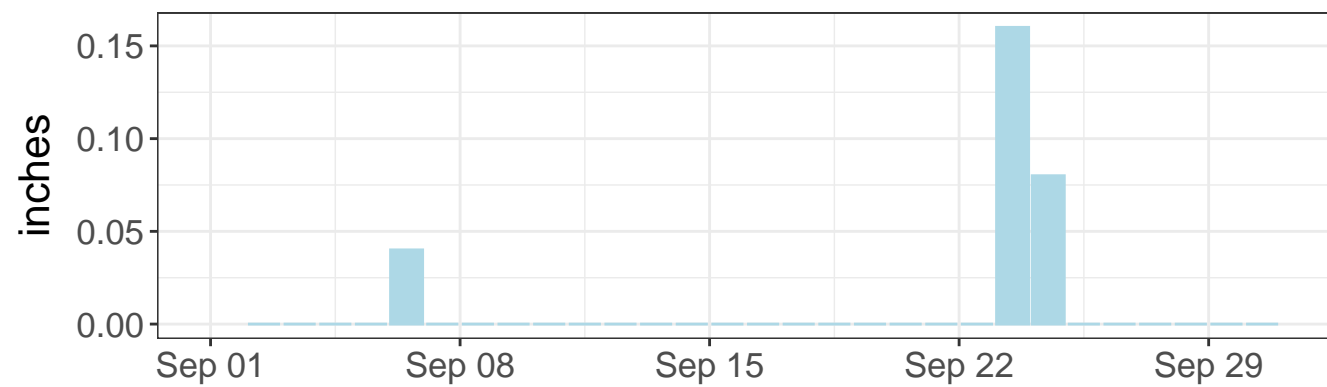
North tilt – detrended values



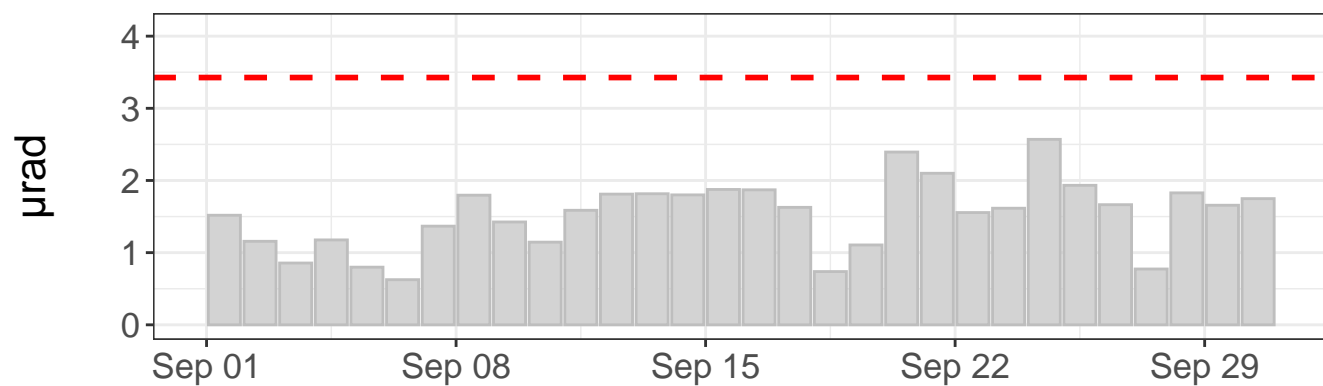
Daily precipitation



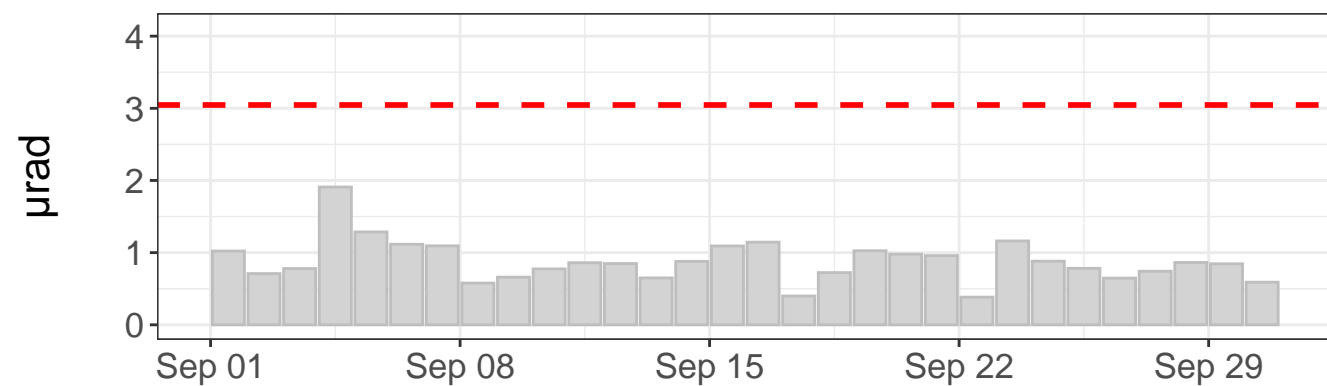
Daily precipitation



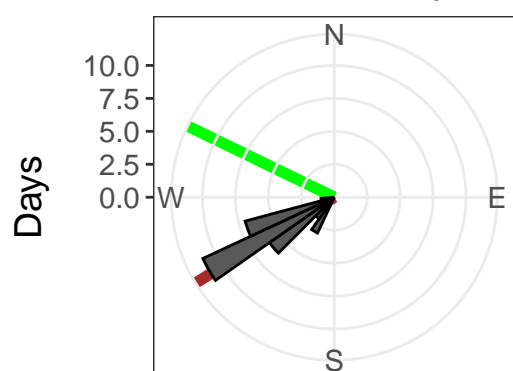
East tilt – daily range



North tilt – daily range



Tilt direction frequency



East tilt rate: $-512.00 \pm 0.46 \mu\text{rad}/\text{yr}$. R2: 0.99

North tilt rate: $-316.76 \pm 0.18 \mu\text{rad}/\text{yr}$. R2: 1.00

Azimuth to C7: 296 deg

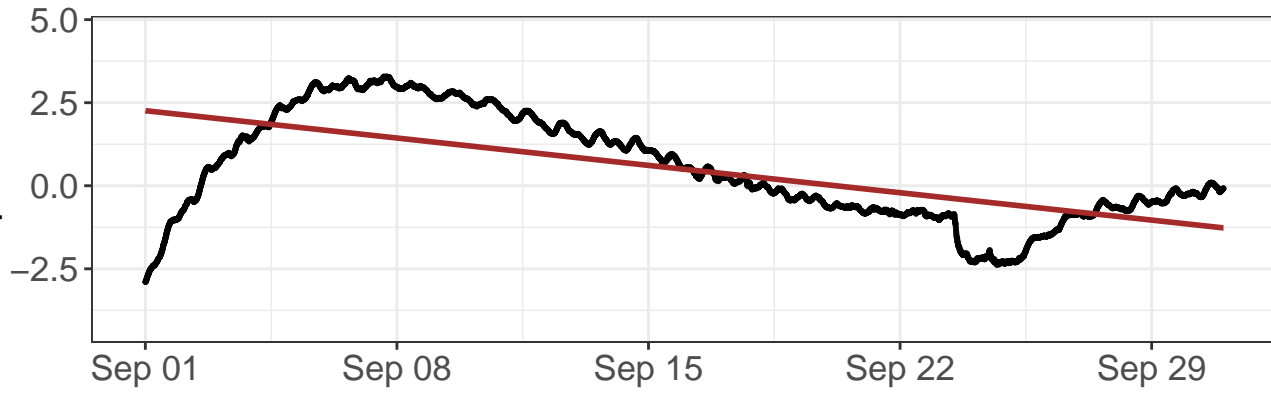
Distance to C7: 186 ft

--- Outlier value

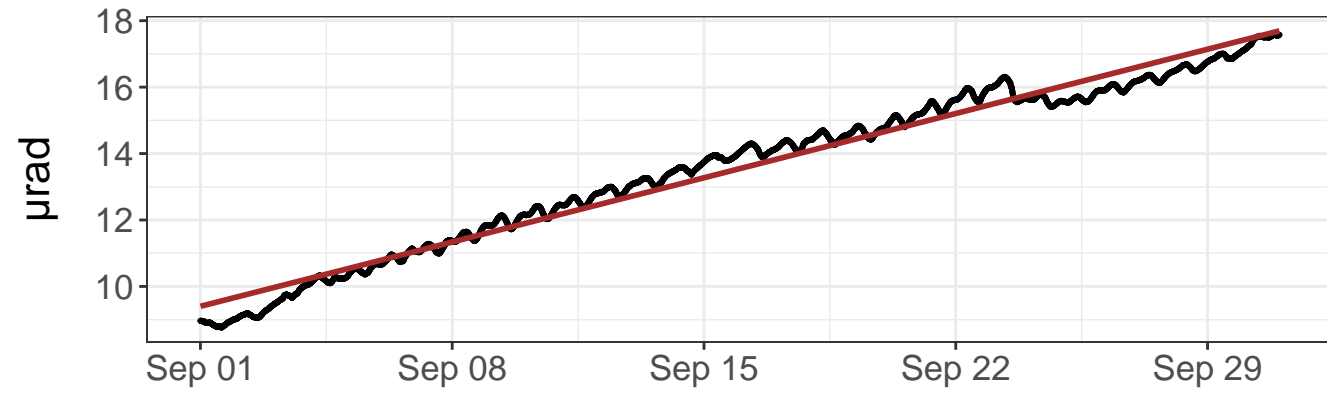
— Linear model

— Azimuth to C7

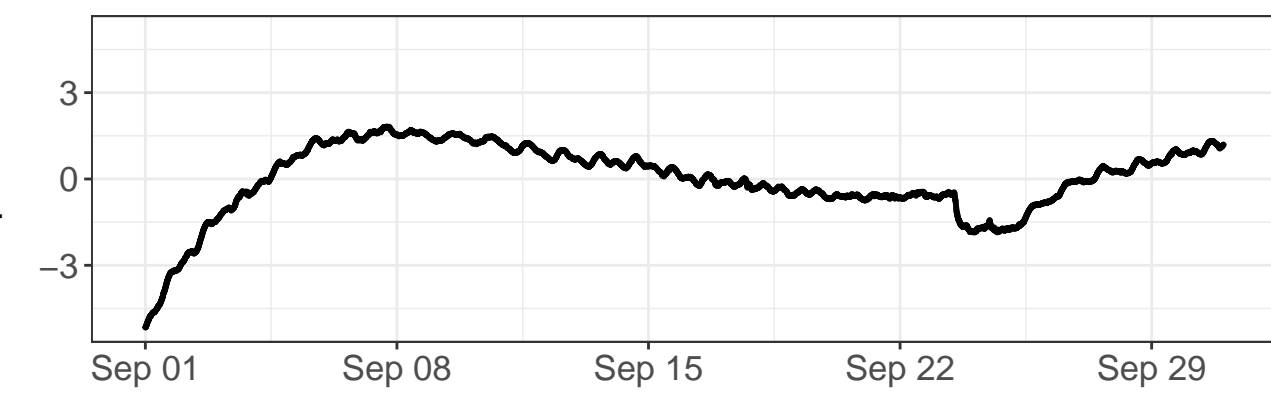
East tilt – raw values



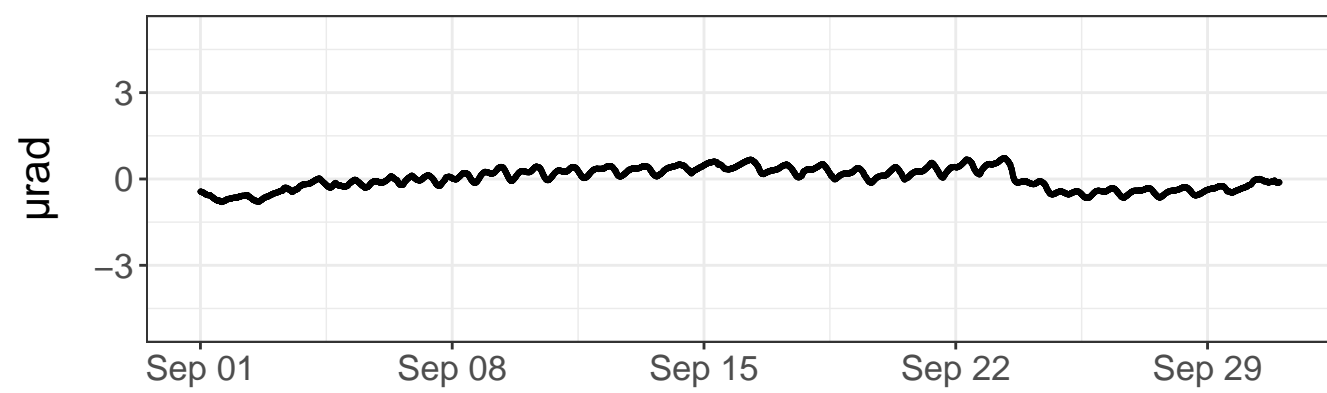
North tilt – raw values



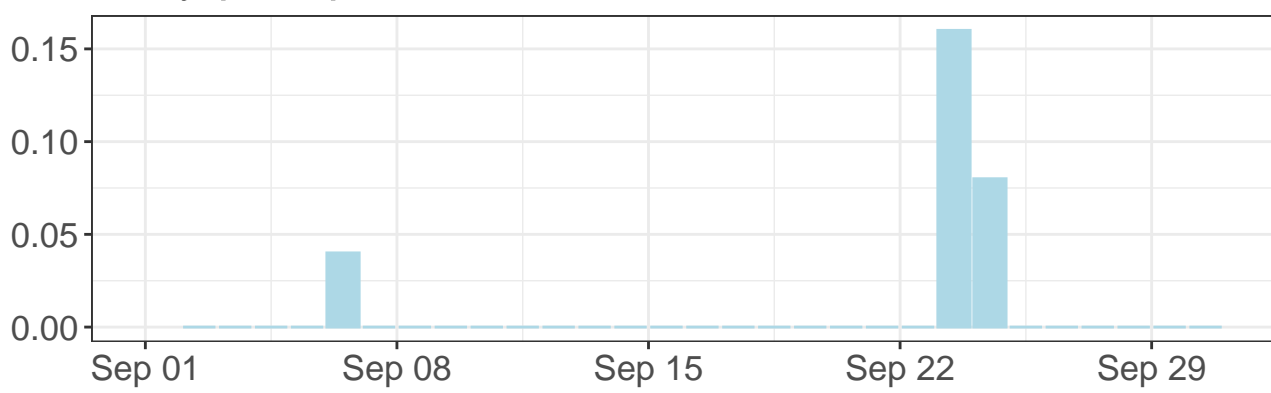
East tilt – detrended values



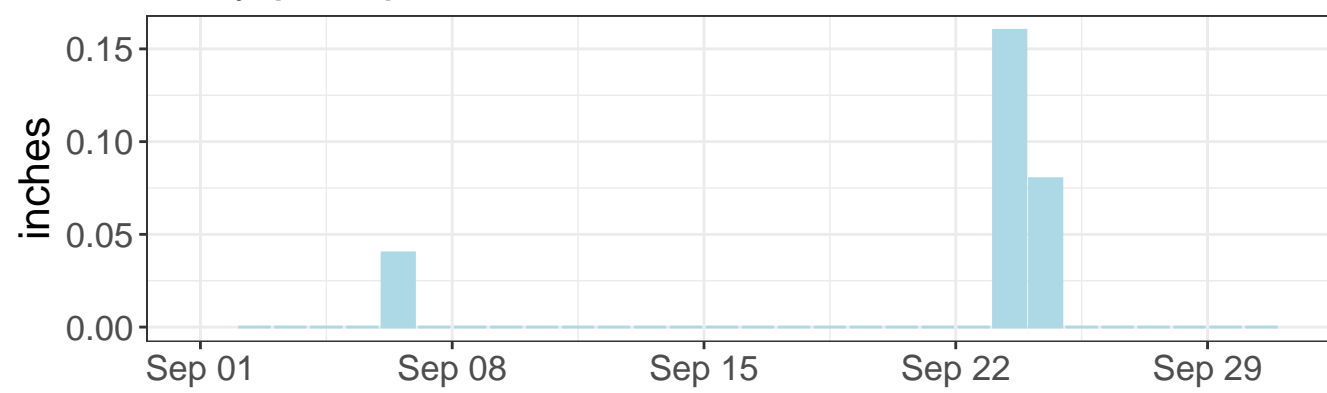
North tilt – detrended values



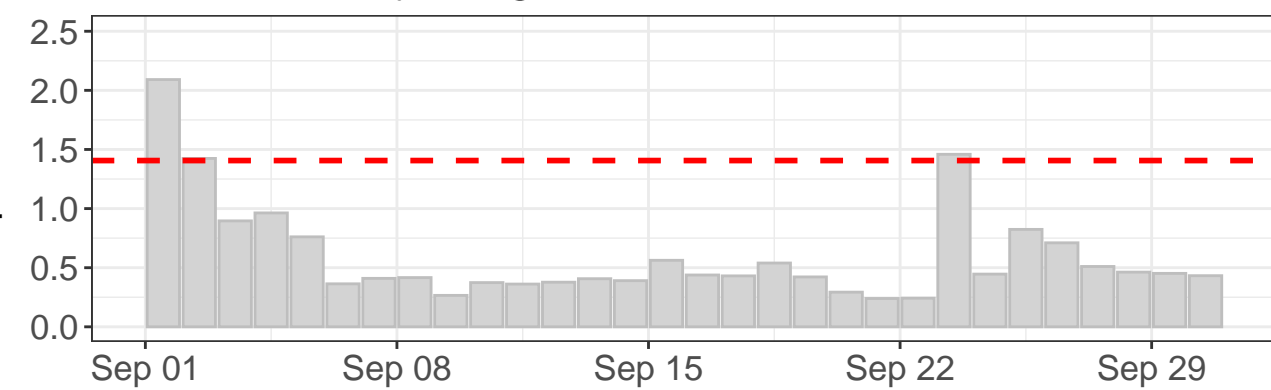
Daily precipitation



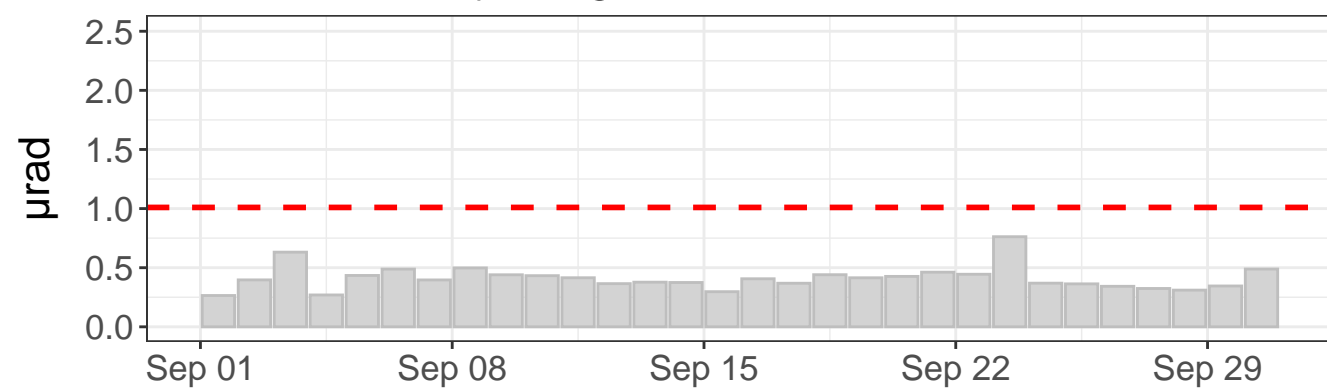
Daily precipitation



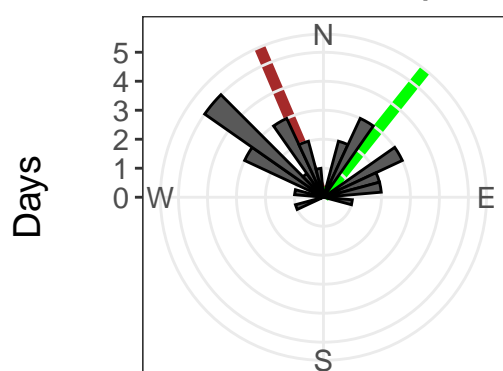
East tilt – daily range



North tilt – daily range



Tilt direction frequency



East tilt rate: -42.93 ± 0.51 $\mu\text{rad}/\text{yr}$. R^2 : 0.40

North tilt rate: 100.87 ± 0.15 $\mu\text{rad}/\text{yr}$. R^2 : 0.98

Azimuth to C7: 39 deg

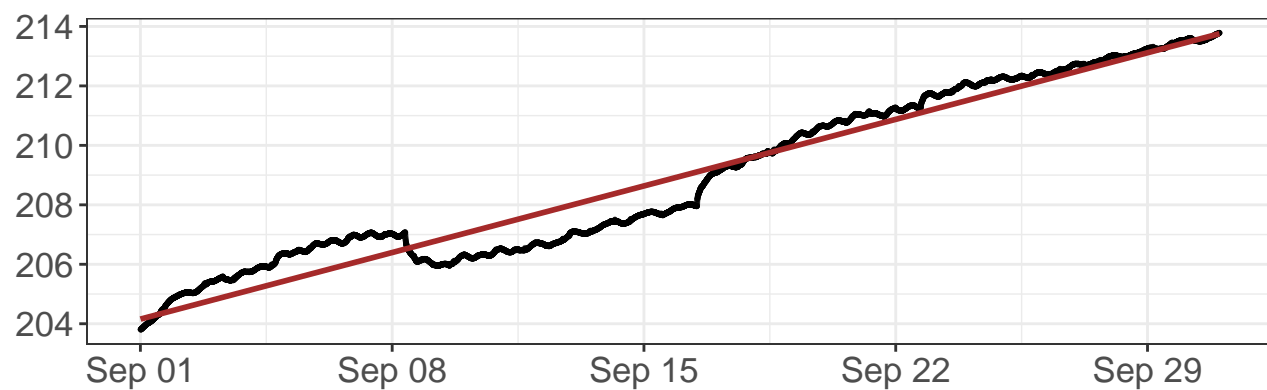
Distance to C7: 561 ft

--- Outlier value

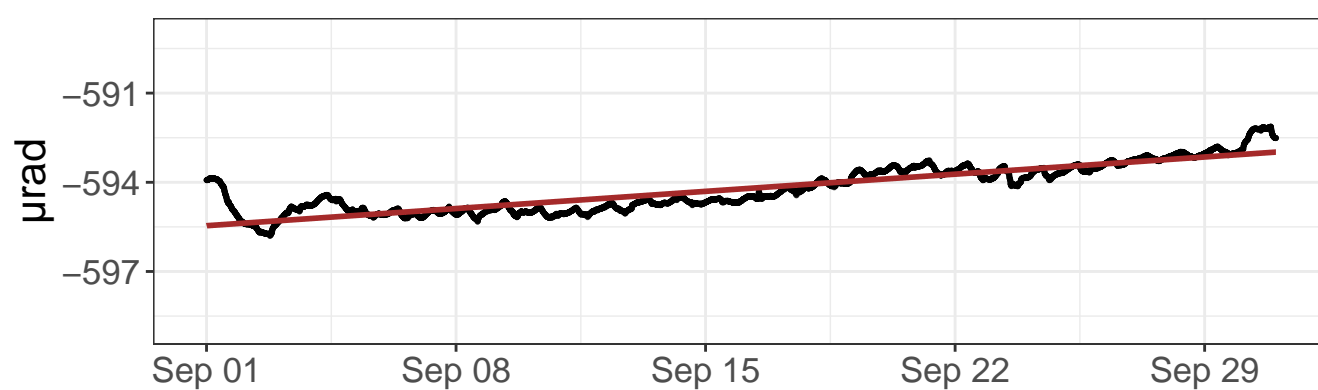
— Linear model

— Azimuth to C7

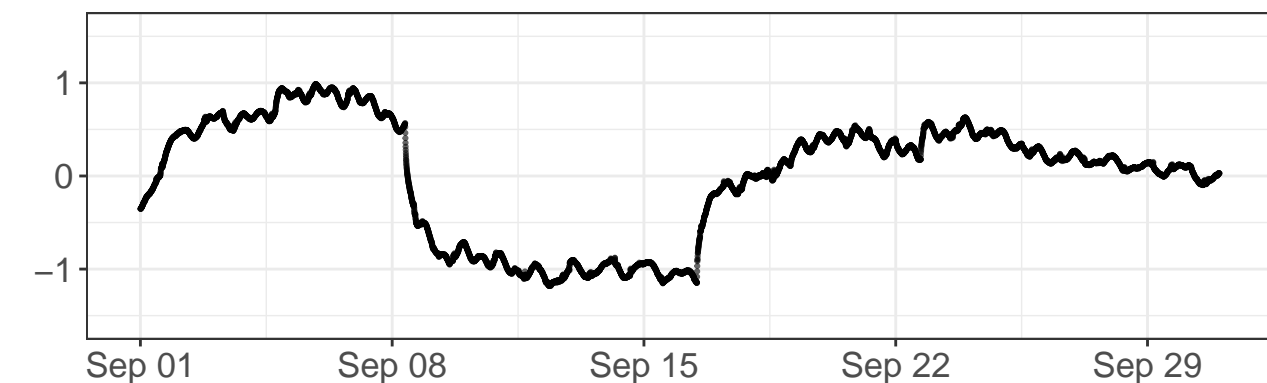
East tilt – raw values



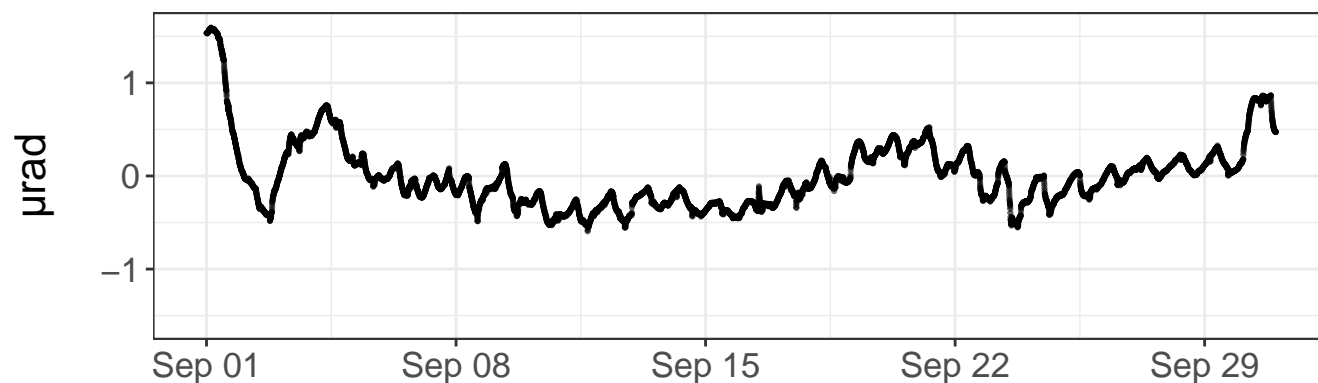
North tilt – raw values



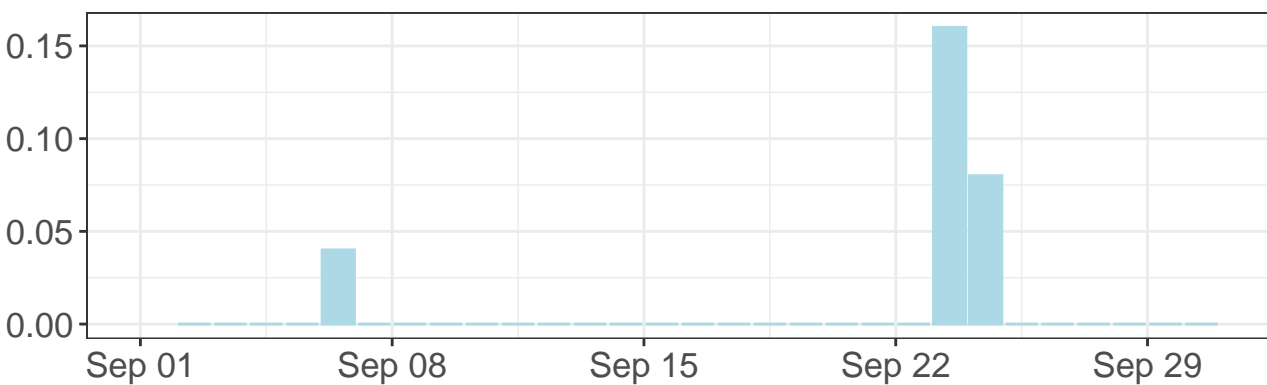
East tilt – detrended values



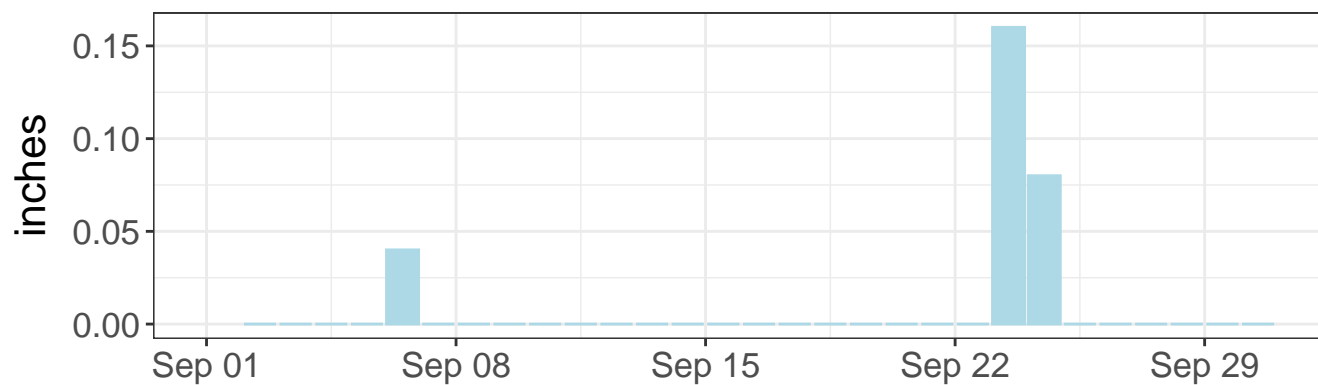
North tilt – detrended values



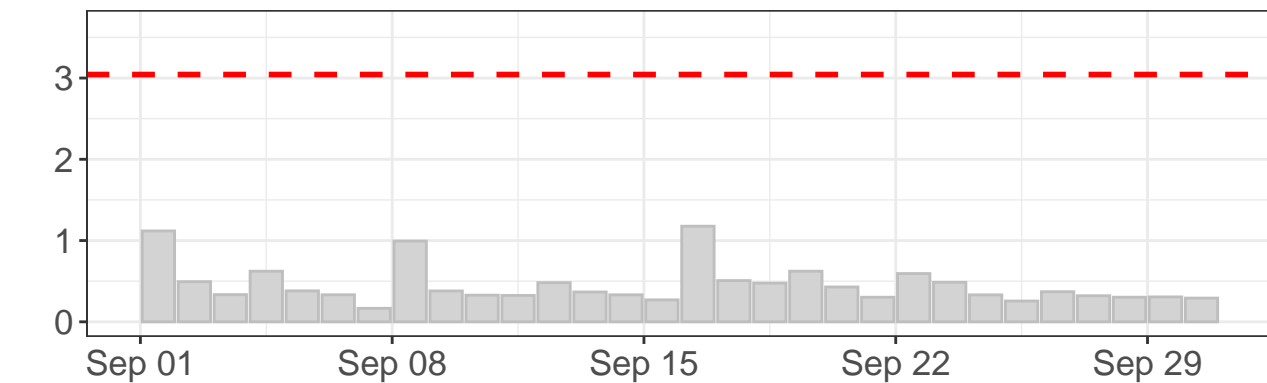
Daily precipitation



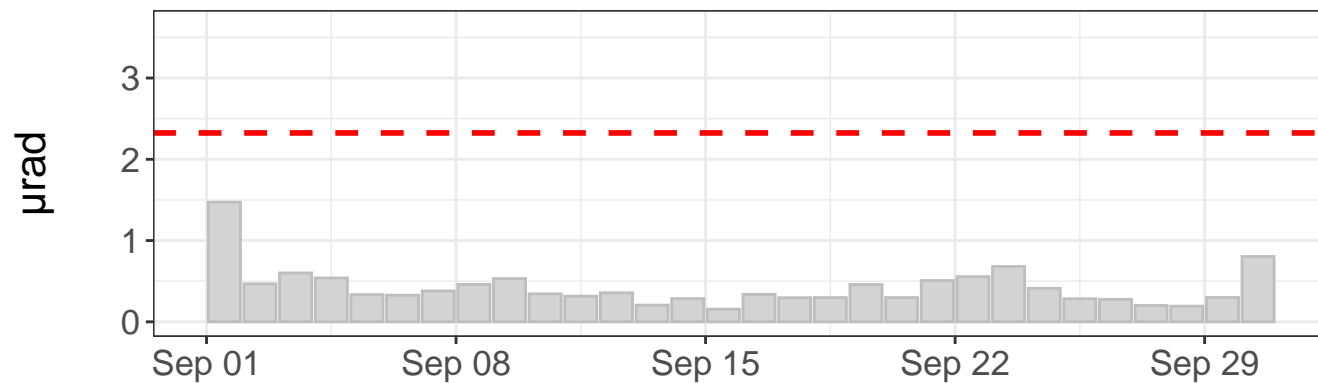
Daily precipitation



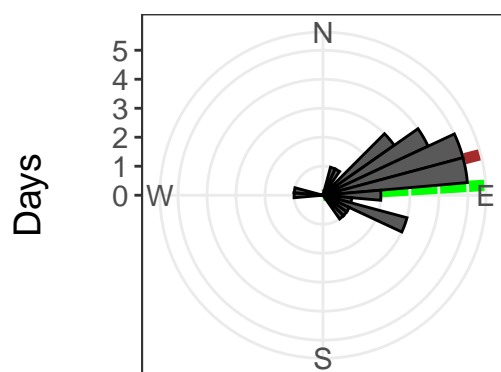
East tilt – daily range



North tilt – daily range



Tilt direction frequency



East tilt rate: $116.79 \pm 0.26 \mu\text{rad/yr}$. $R^2: 0.95$

North tilt rate: $30.13 \pm 0.14 \mu\text{rad/yr}$. $R^2: 0.80$

Azimuth to C7: 87 deg

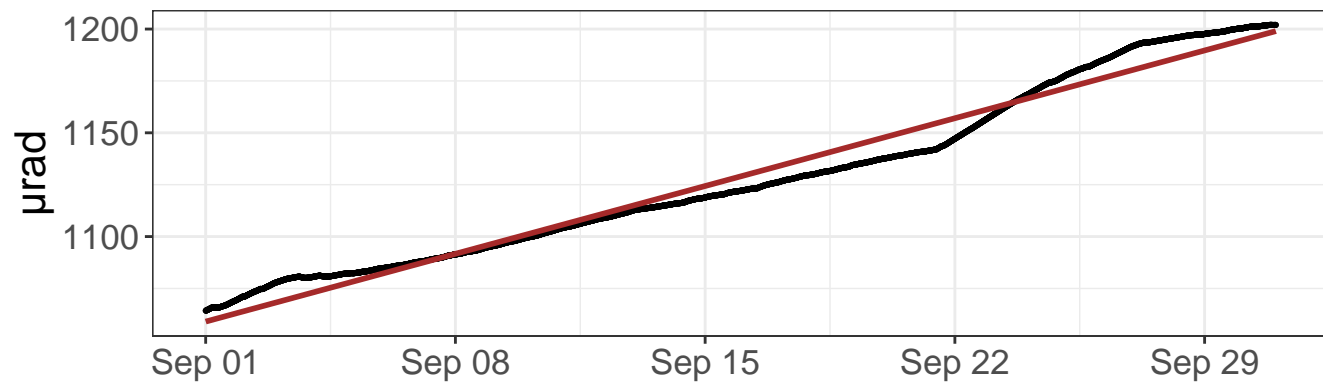
Distance to C7: 2402 ft

--- Outlier value

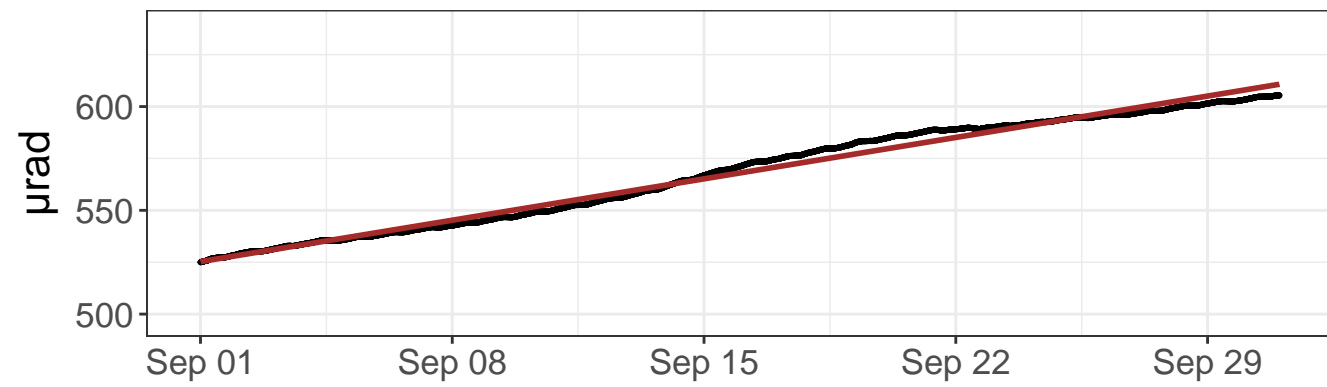
— Linear model

— Azimuth to C7

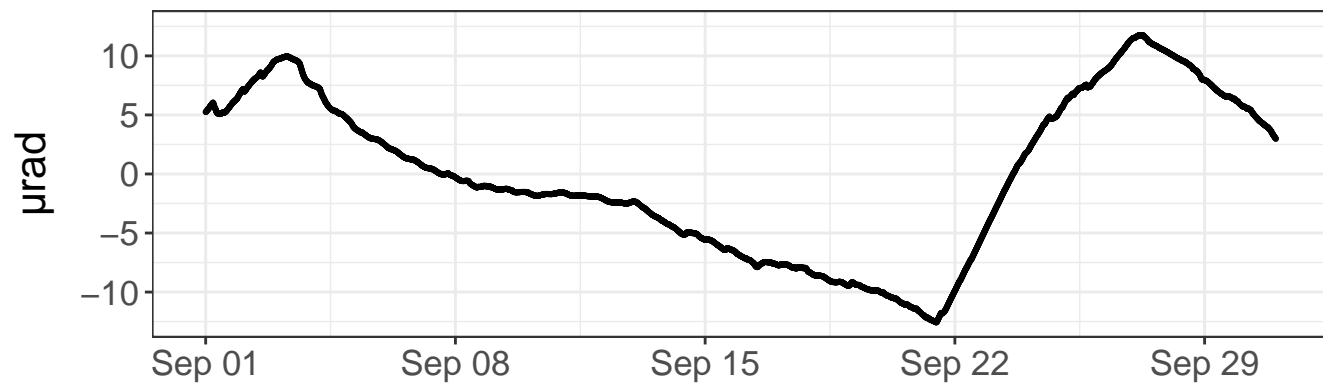
East tilt – raw values



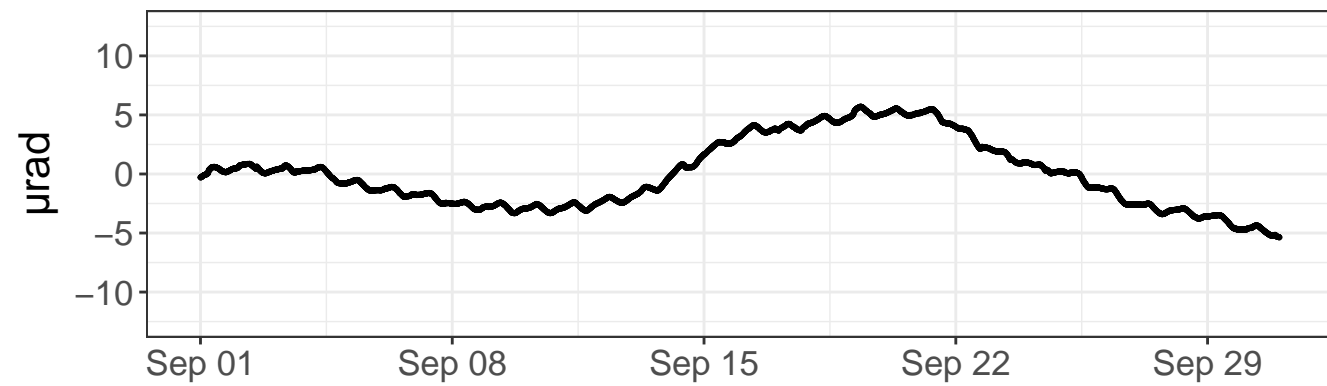
North tilt – raw values



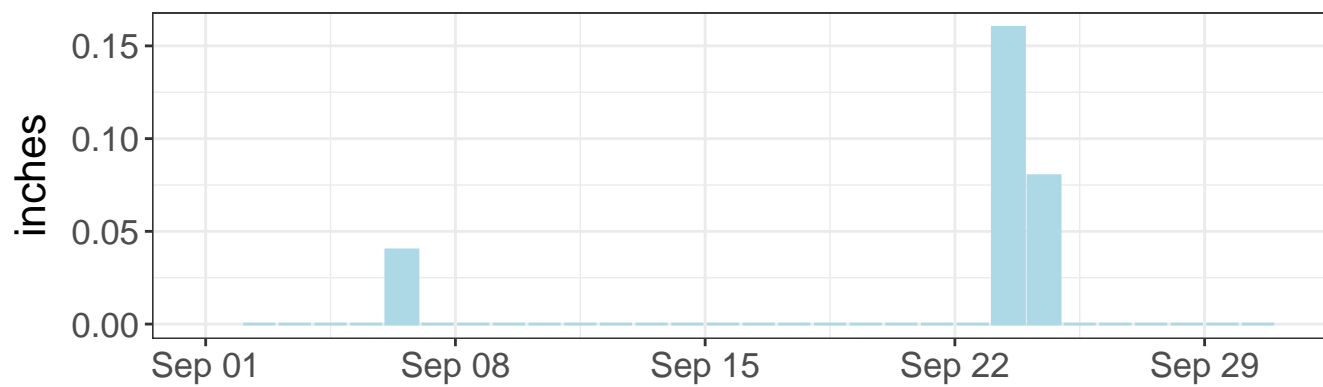
East tilt – detrended values



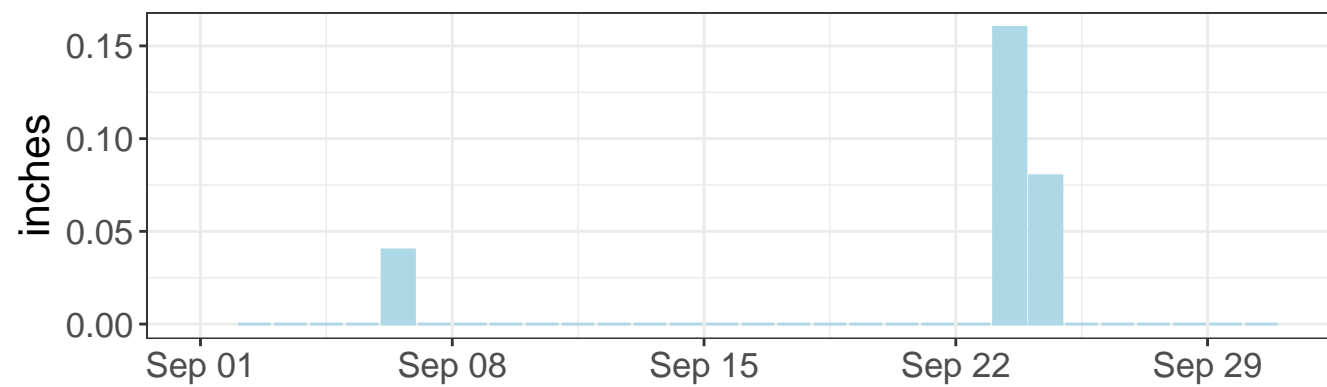
North tilt – detrended values



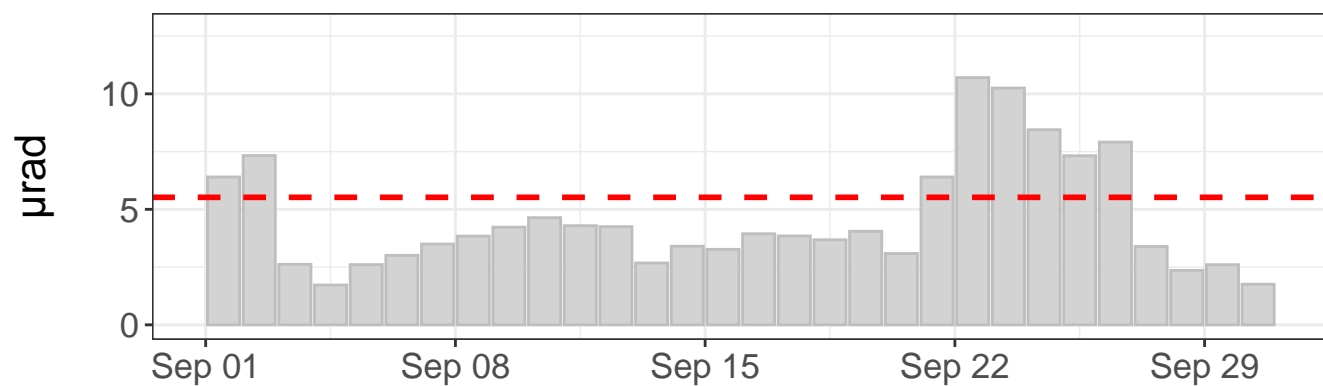
Daily precipitation



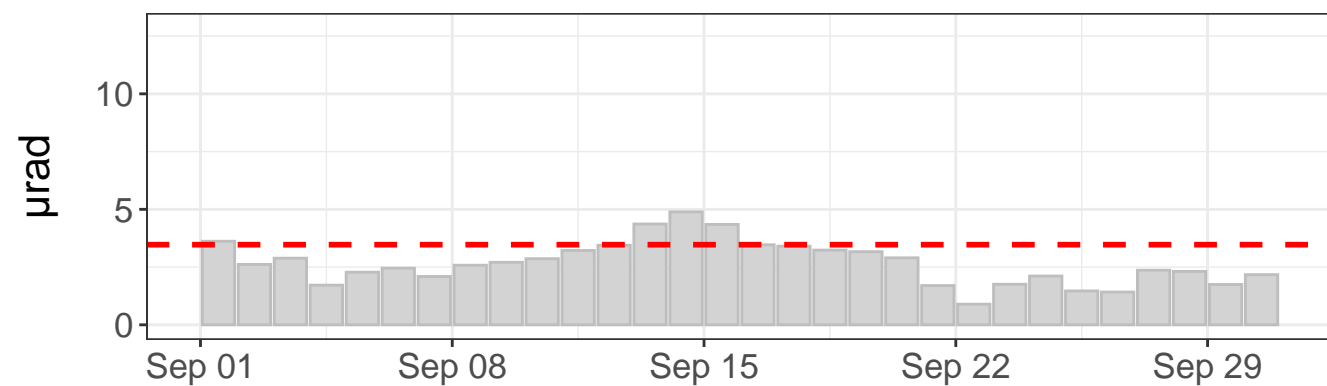
Daily precipitation



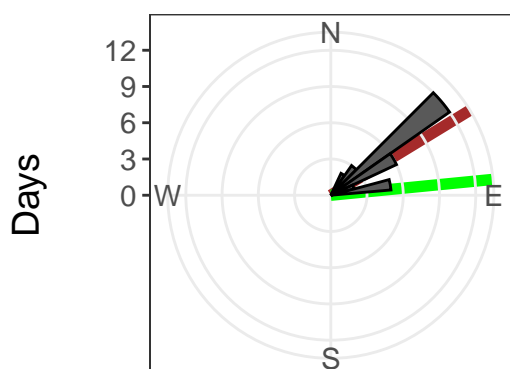
East tilt – daily range



North tilt – daily range



Tilt direction frequency



East tilt rate: $1703.11 \pm 2.74 \mu\text{rad}/\text{yr}$. $R^2: 0.97$

North tilt rate: $1039.83 \pm 1.19 \mu\text{rad}/\text{yr}$. $R^2: 0.99$

Azimuth to C7: 84 deg

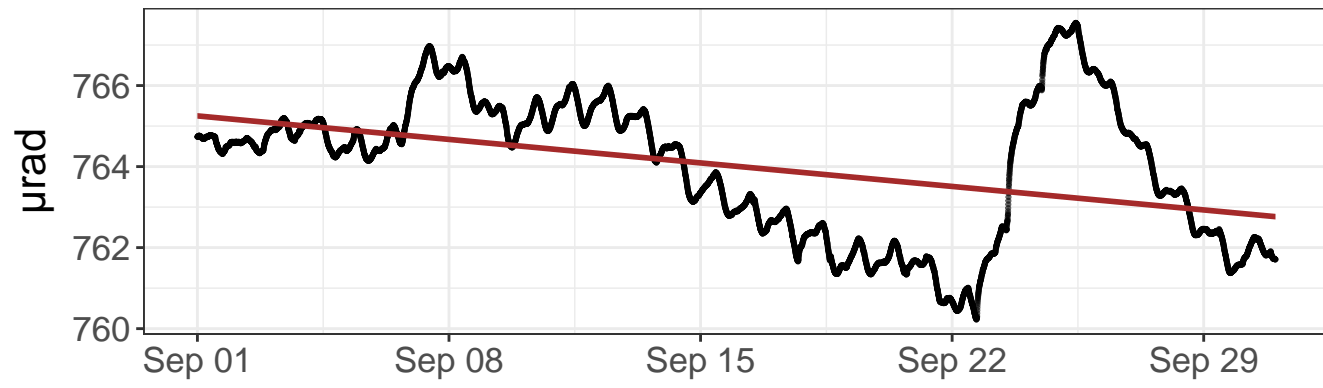
Distance to C7: 1473 ft

--- Outlier value

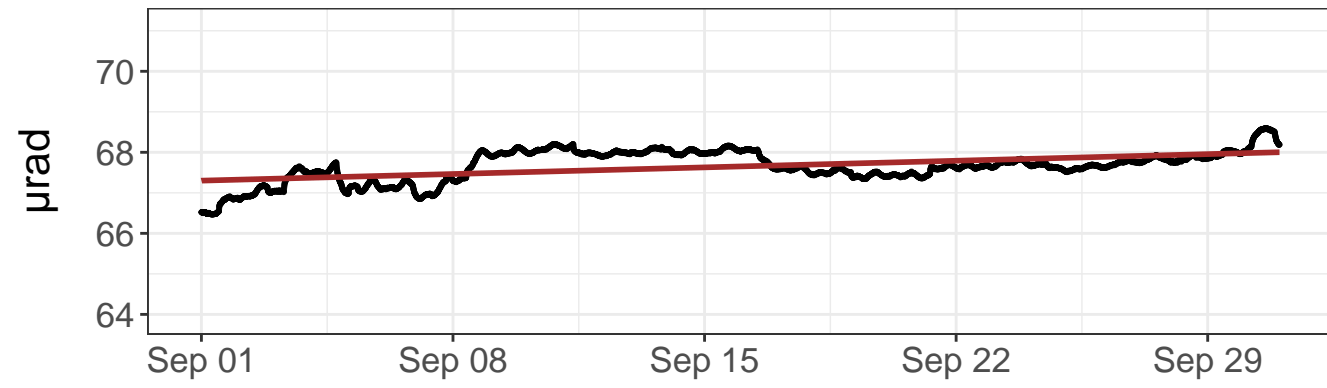
— Linear model

— Azimuth to C7

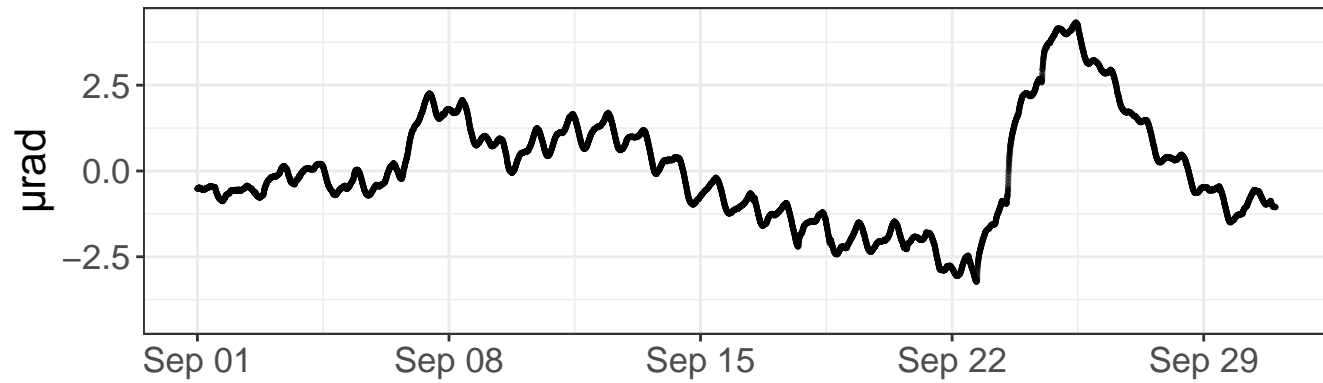
East tilt – raw values



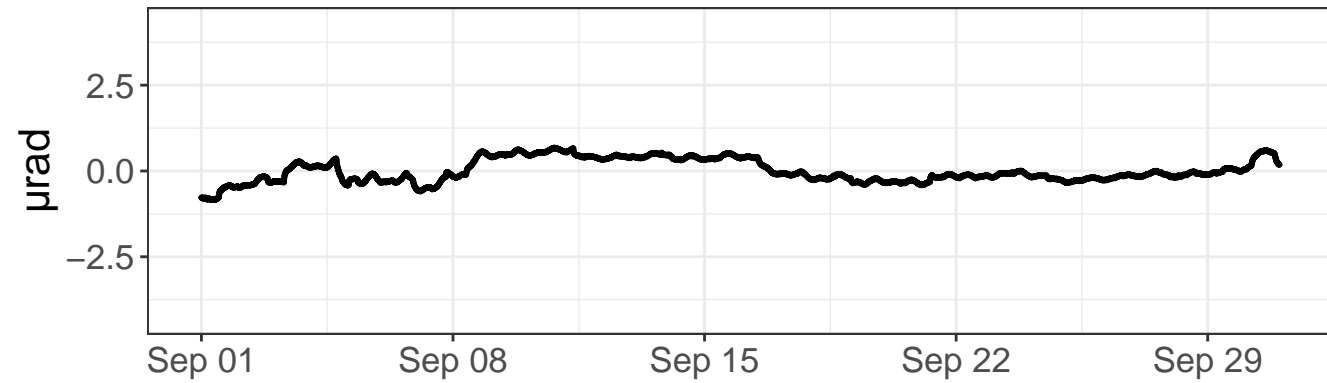
North tilt – raw values



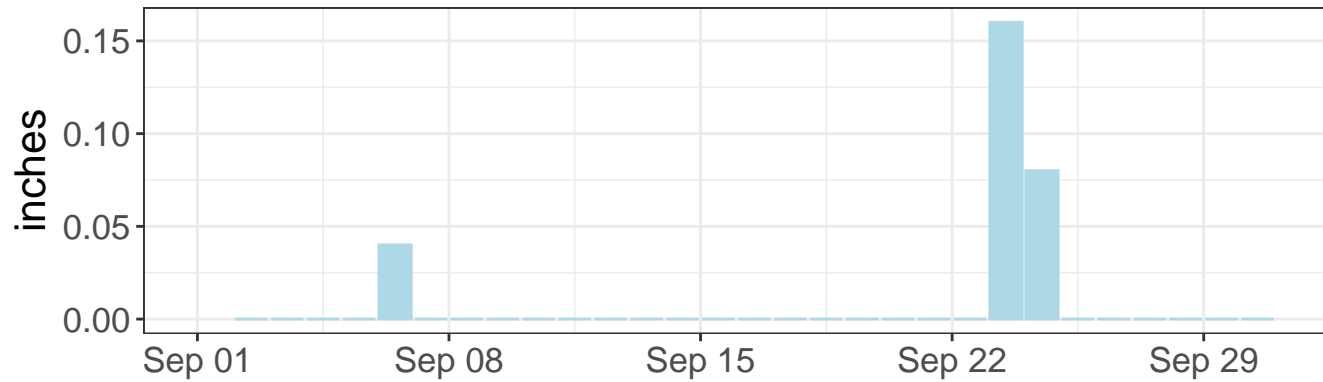
East tilt – detrended values



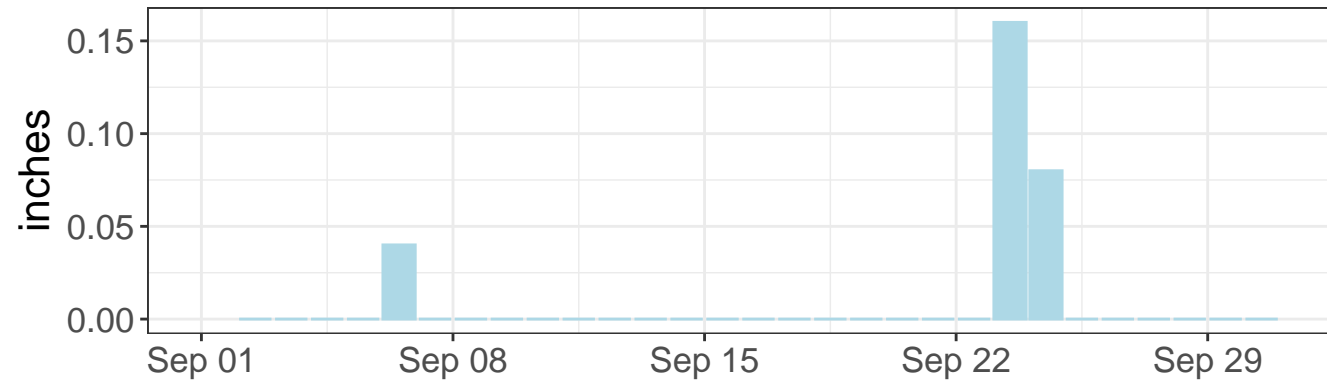
North tilt – detrended values



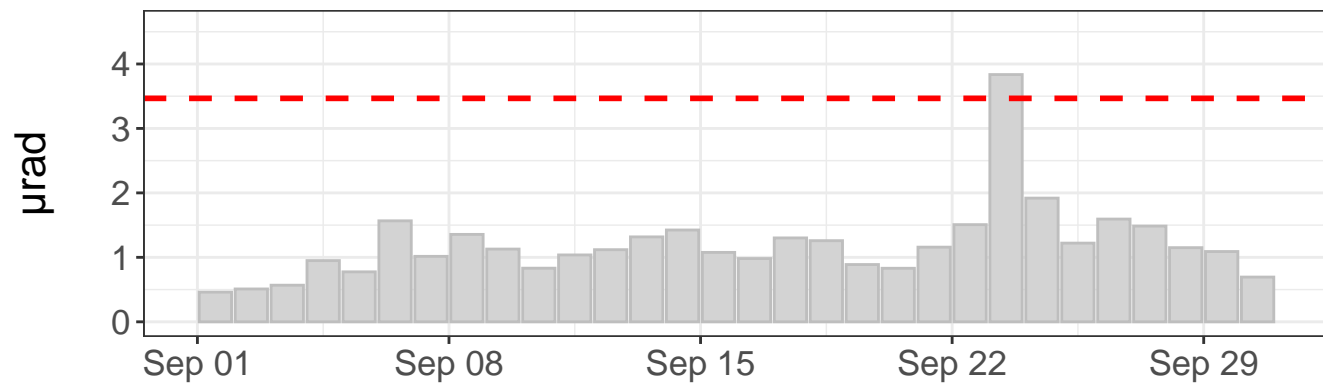
Daily precipitation



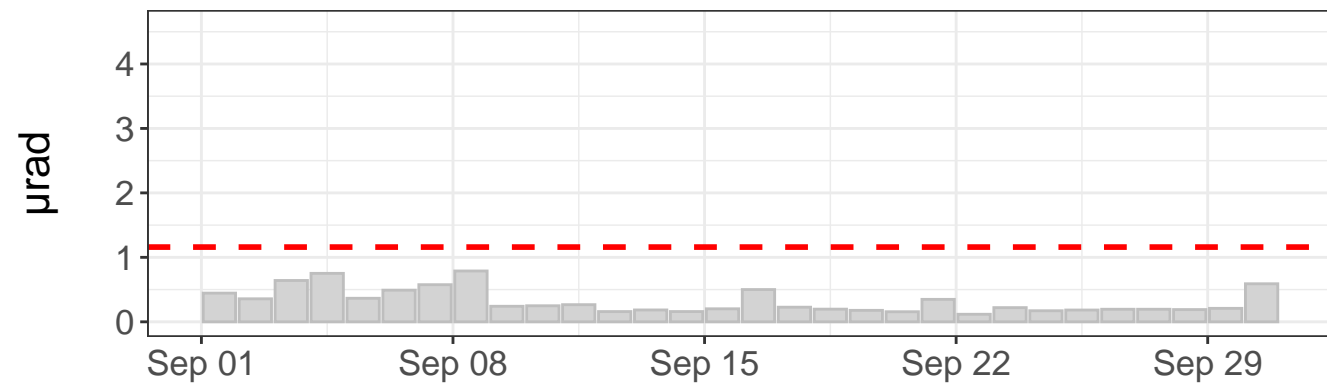
Daily precipitation



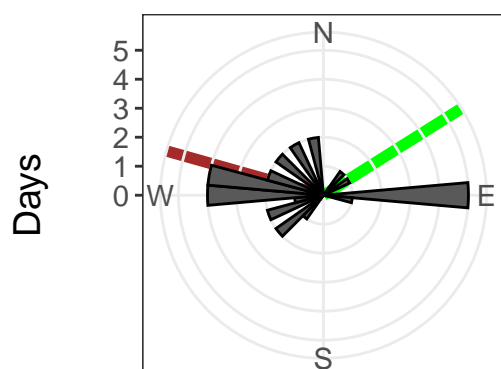
East tilt – daily range



North tilt – daily range



Tilt direction frequency



East tilt rate: $-30.26 \pm 0.64 \mu\text{rad}/\text{yr}$. R^2 : 0.17

North tilt rate: $8.53 \pm 0.14 \mu\text{rad}/\text{yr}$. R^2 : 0.27

Azimuth to C7: 58 deg

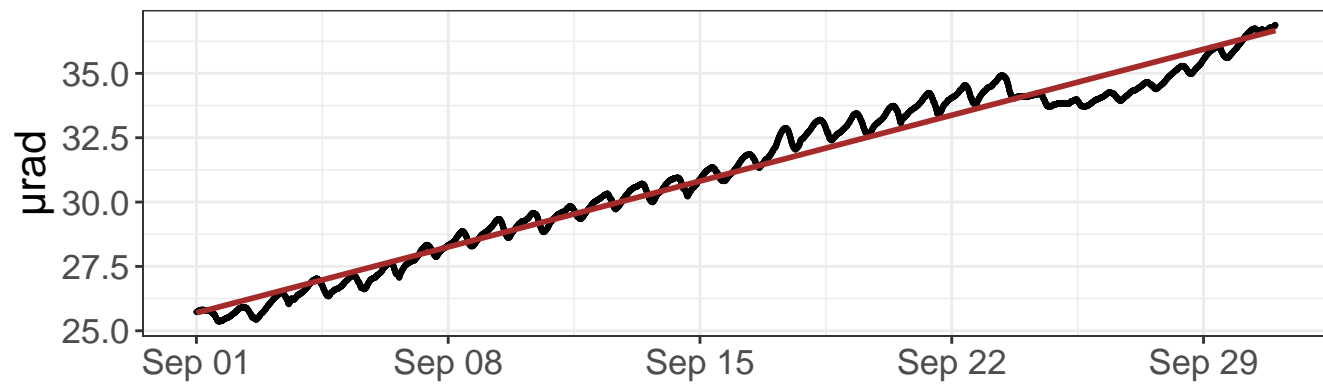
Distance to C7: 1344 ft

--- Outlier value

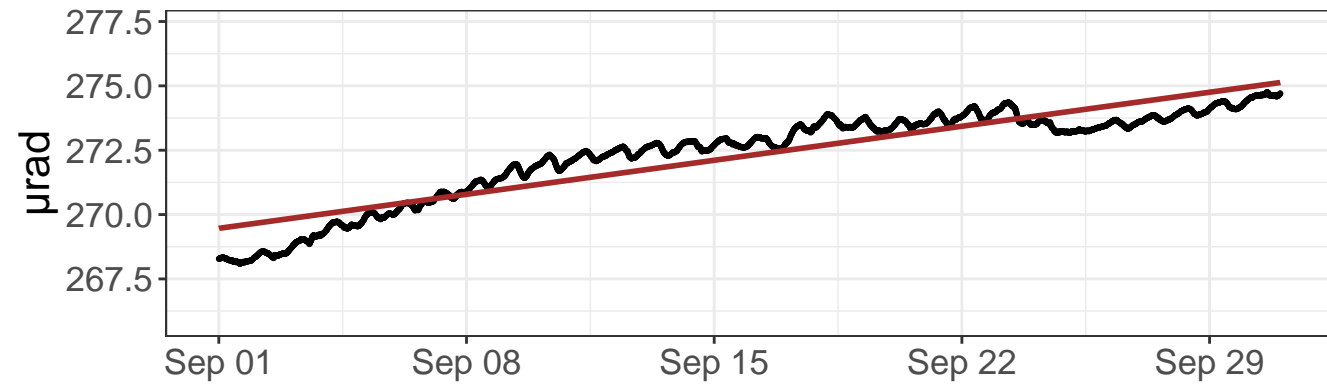
— Linear model

— Azimuth to C7

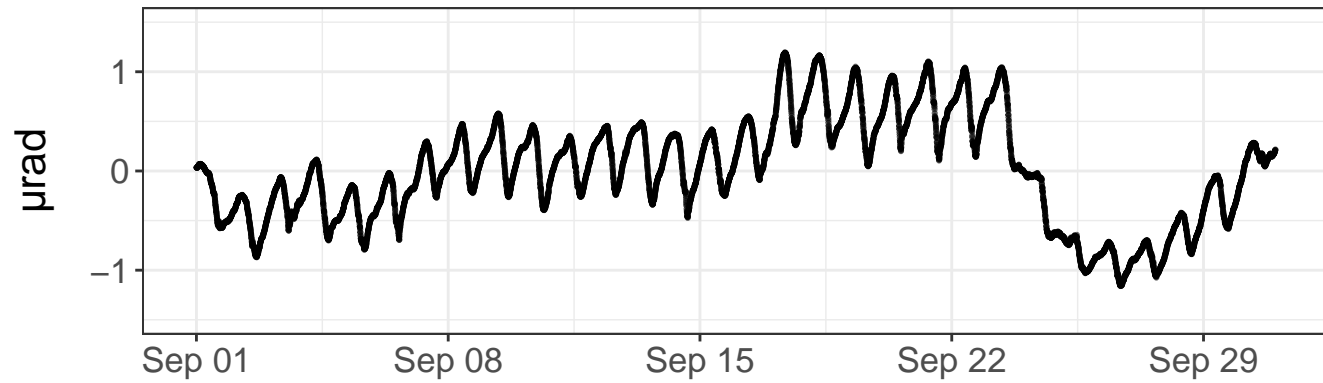
East tilt – raw values



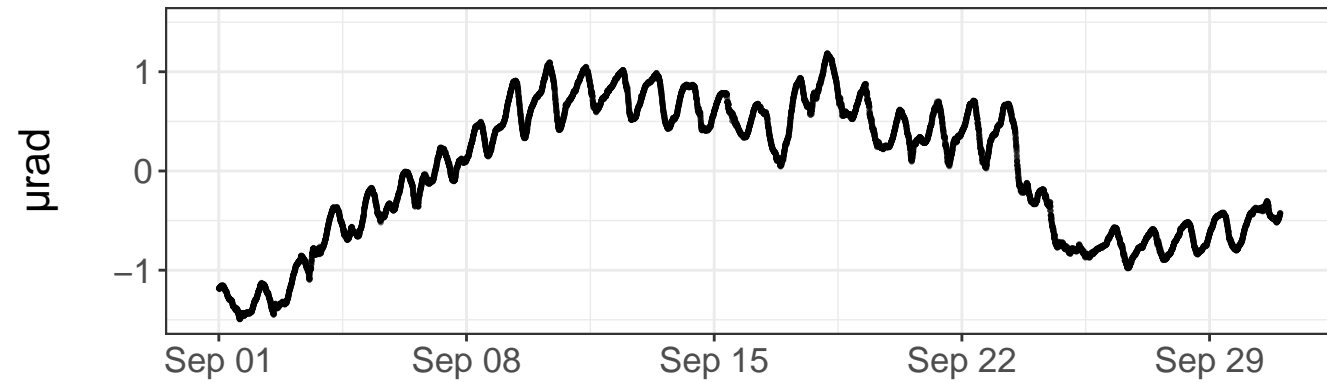
North tilt – raw values



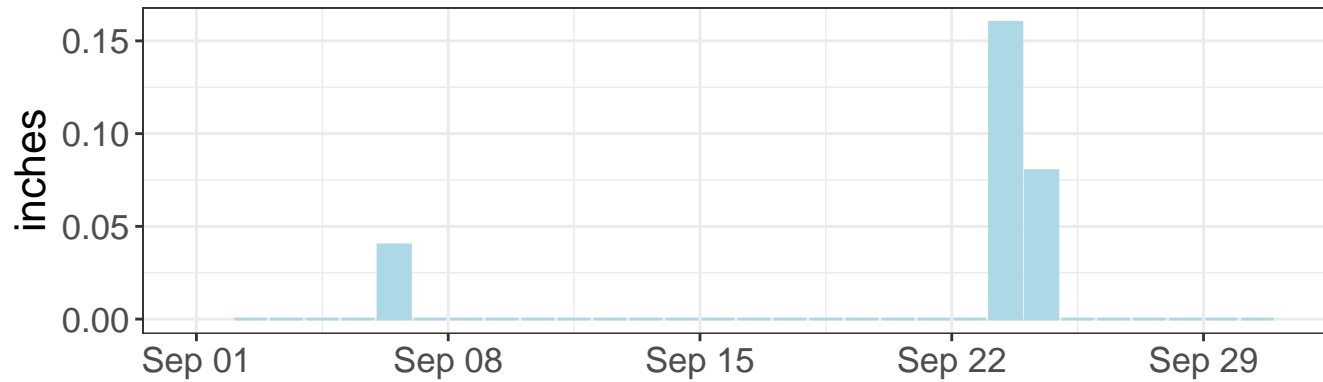
East tilt – detrended values



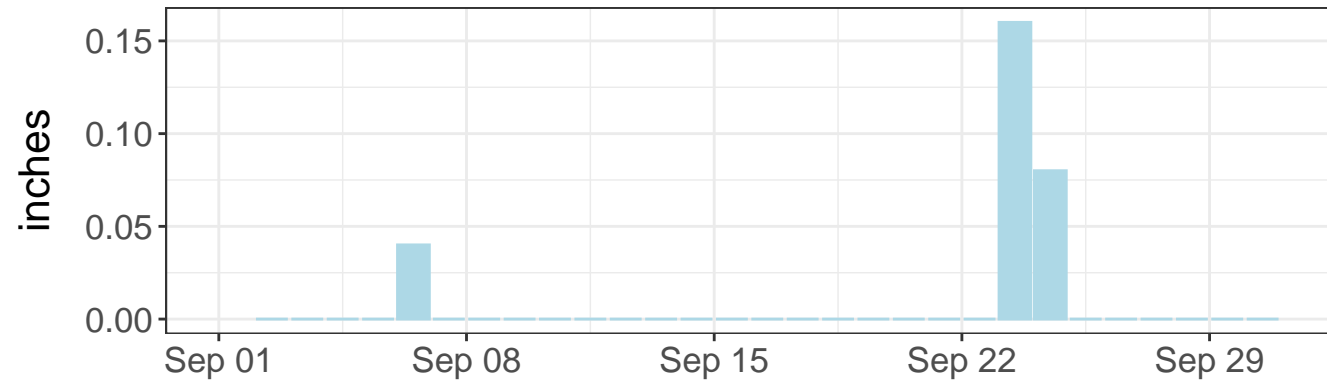
North tilt – detrended values



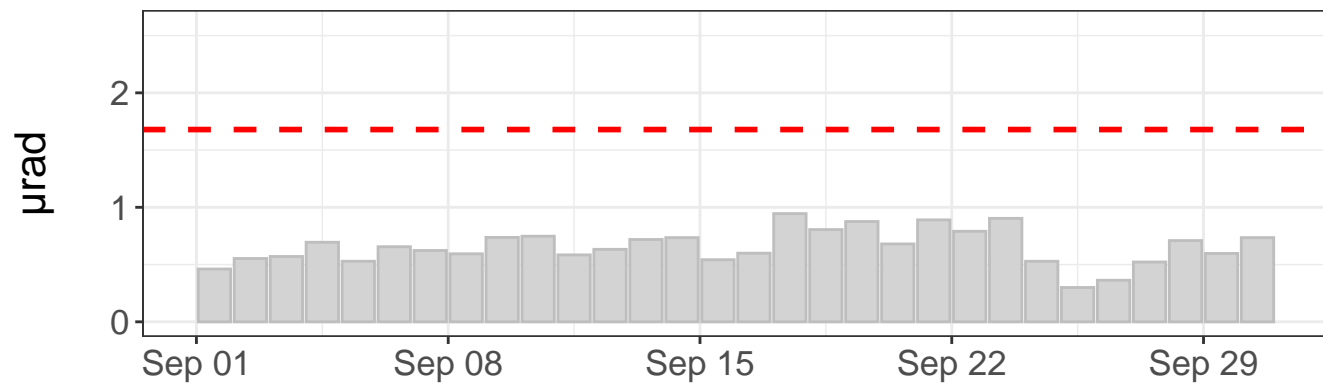
Daily precipitation



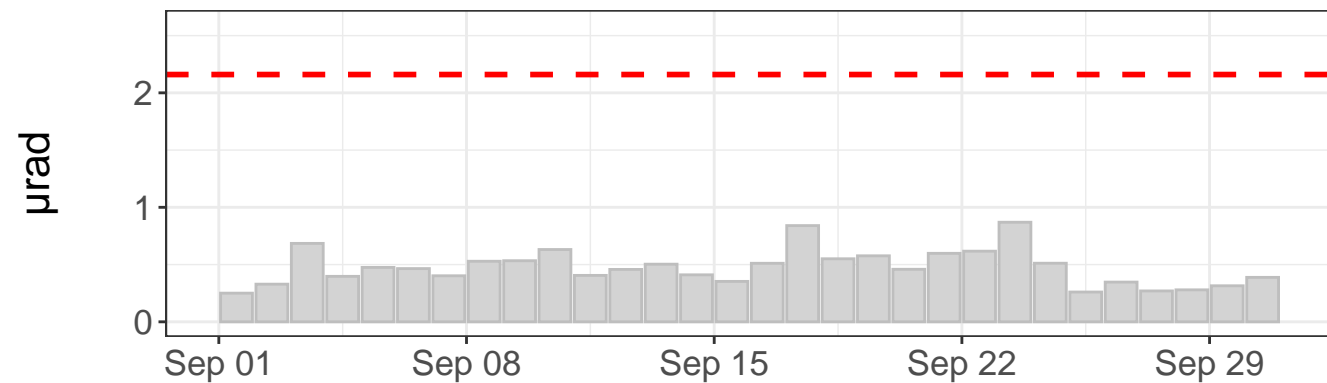
Daily precipitation



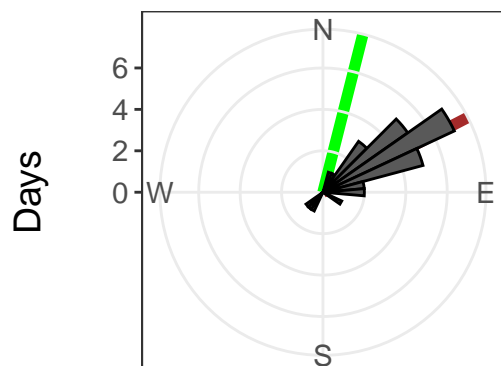
East tilt – daily range



North tilt – daily range



Tilt direction frequency



East tilt rate: $133.50 \pm 0.21 \mu\text{rad}/\text{yr}$. R^2 : 0.97

North tilt rate: $68.92 \pm 0.28 \mu\text{rad}/\text{yr}$. R^2 : 0.85

Azimuth to C7: 14 deg

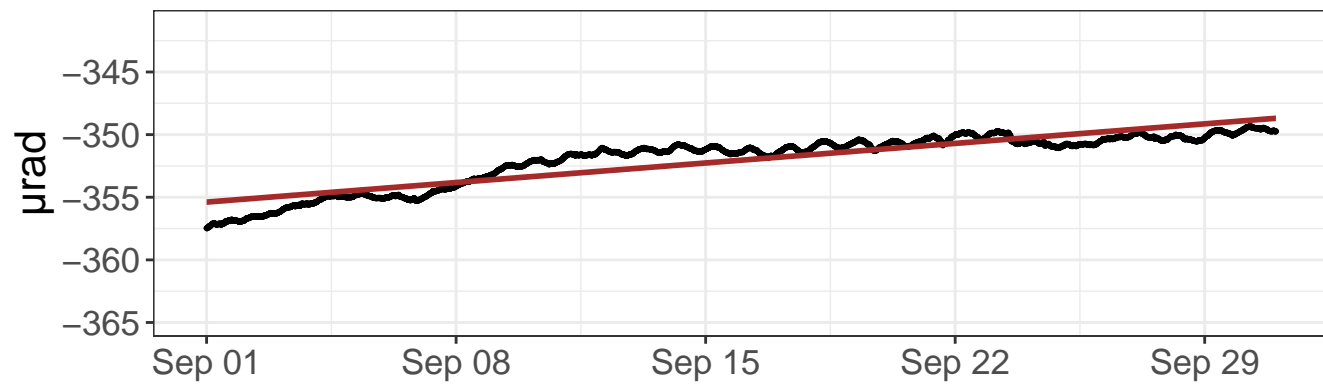
Distance to C7: 686 ft

- - - Outlier value

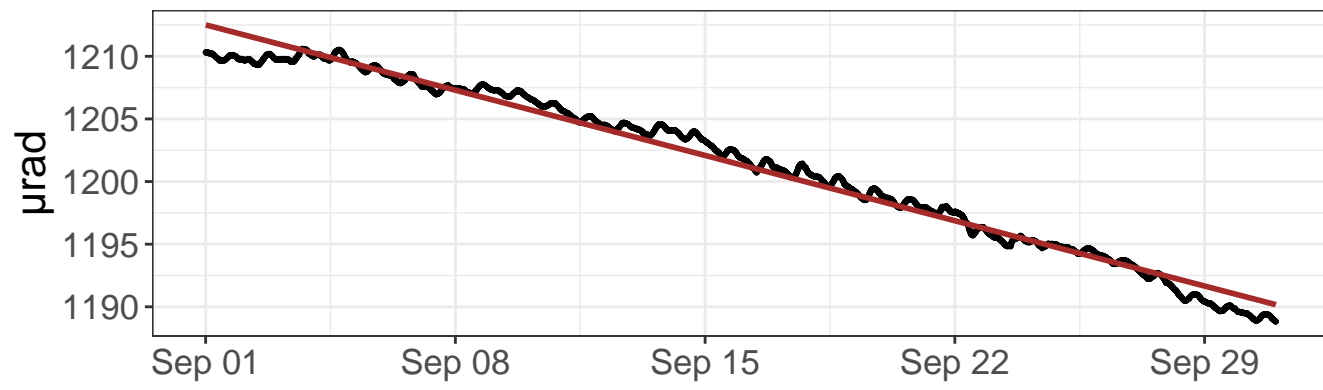
— Linear model

— Azimuth to C7

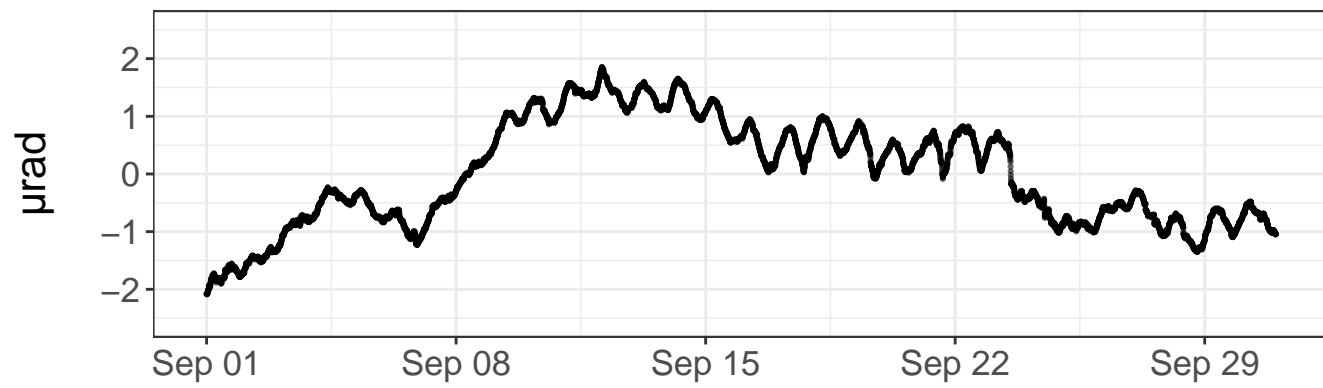
East tilt – raw values



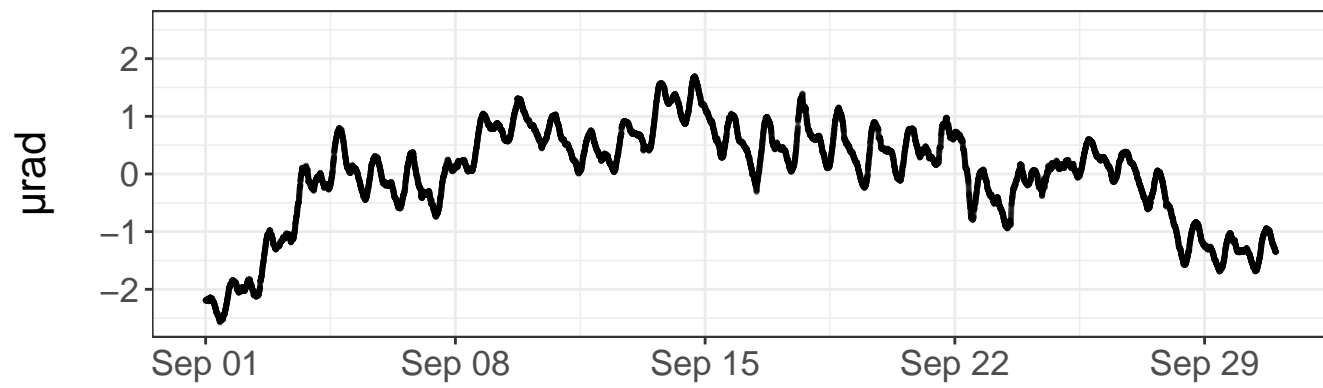
North tilt – raw values



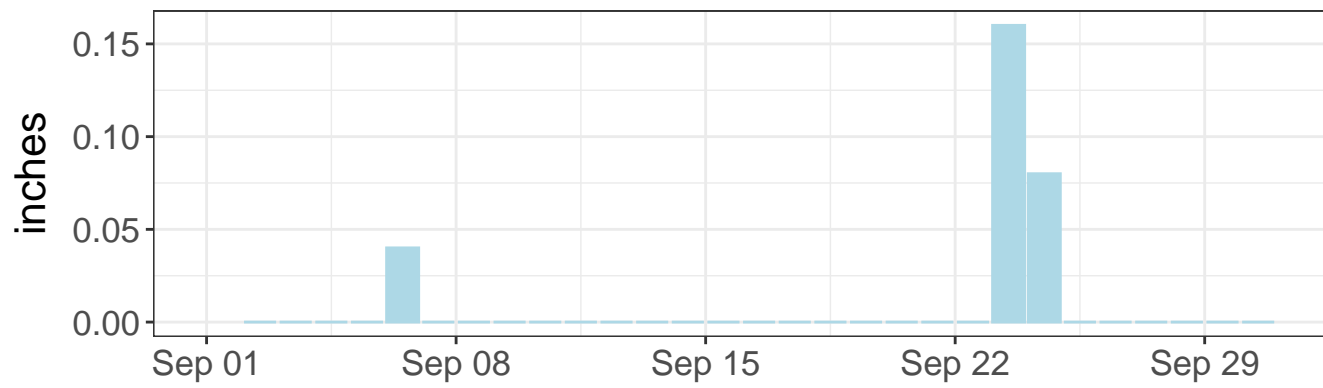
East tilt – detrended values



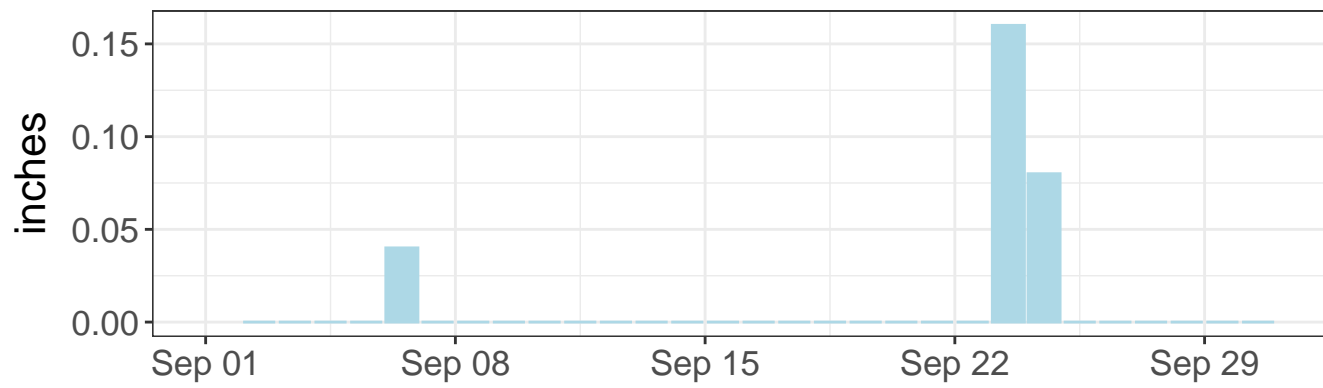
North tilt – detrended values



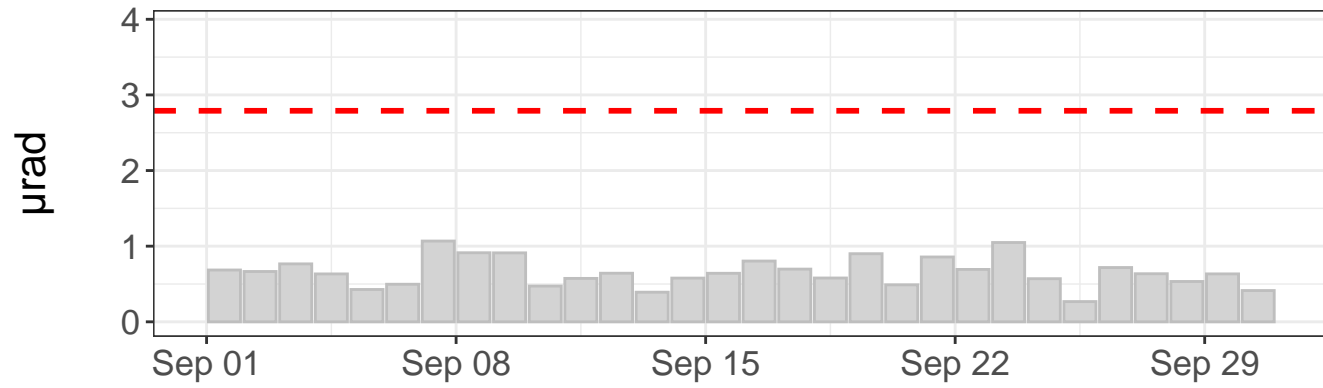
Daily precipitation



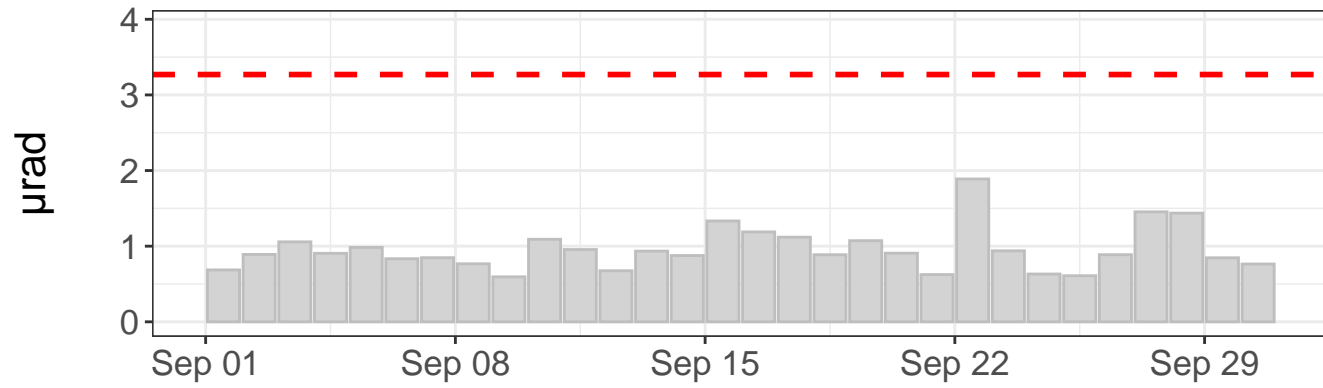
Daily precipitation



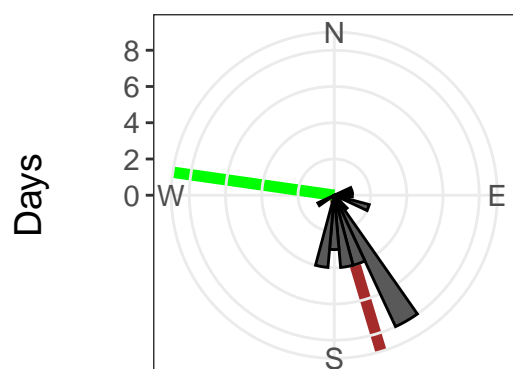
East tilt – daily range



North tilt – daily range

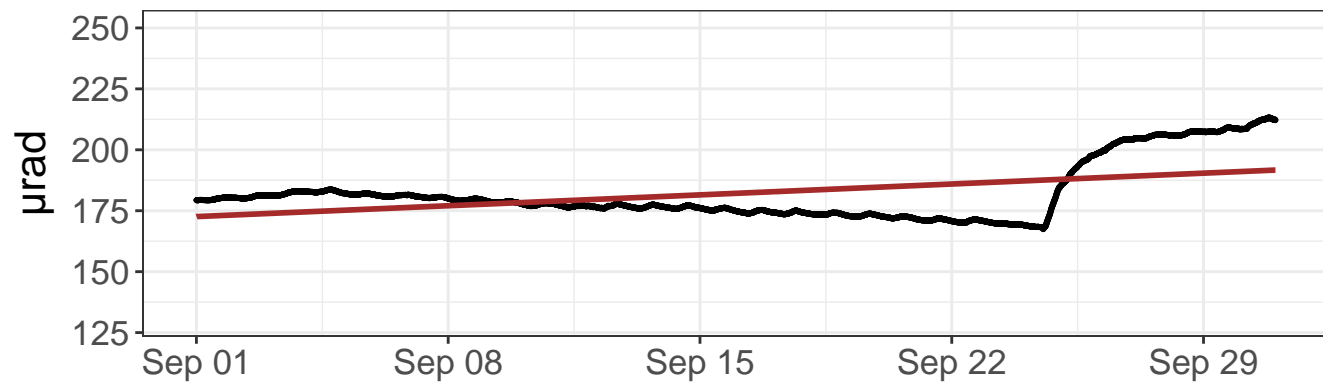


Tilt direction frequency

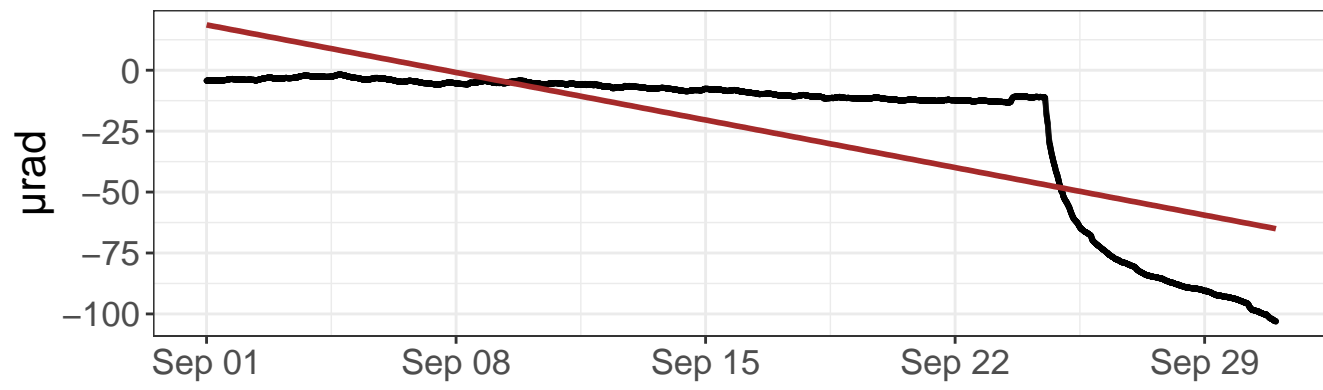


East tilt rate: $81.43 \pm 0.37 \mu\text{rad}/\text{yr}$. $R^2: 0.82$
 North tilt rate: $-271.81 \pm 0.35 \mu\text{rad}/\text{yr}$. $R^2: 0.98$
 Azimuth to C7: 278 deg
 Distance to C7: 1151 ft
 - - - Outlier value
 — Linear model — Azimuth to C7

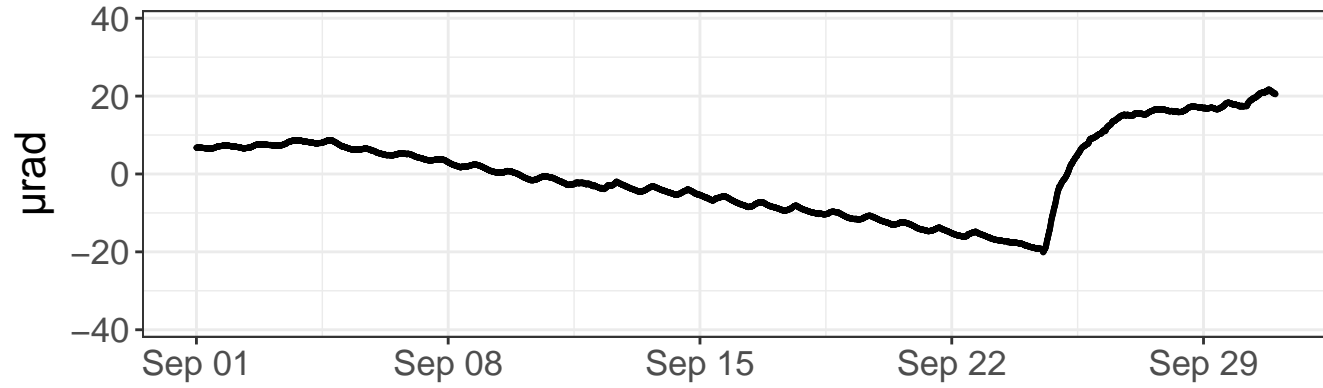
East tilt – raw values



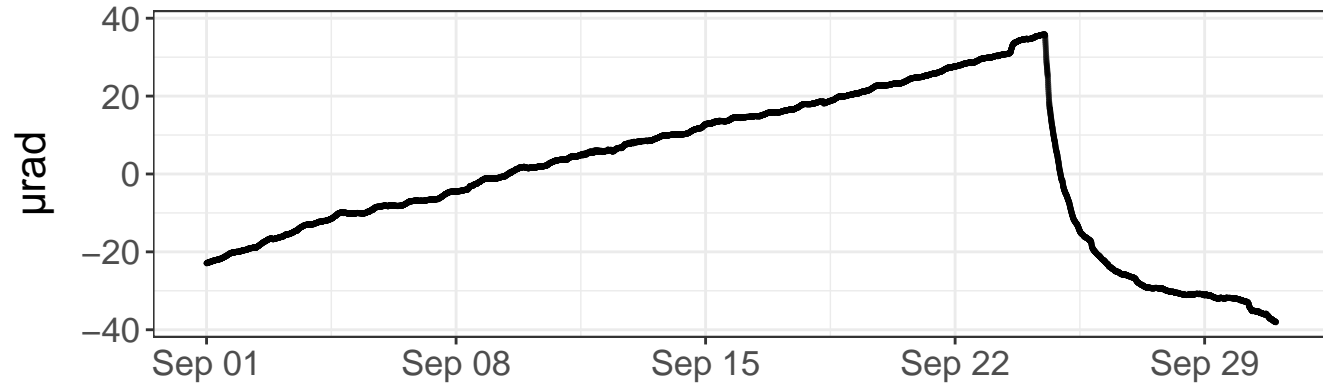
North tilt – raw values



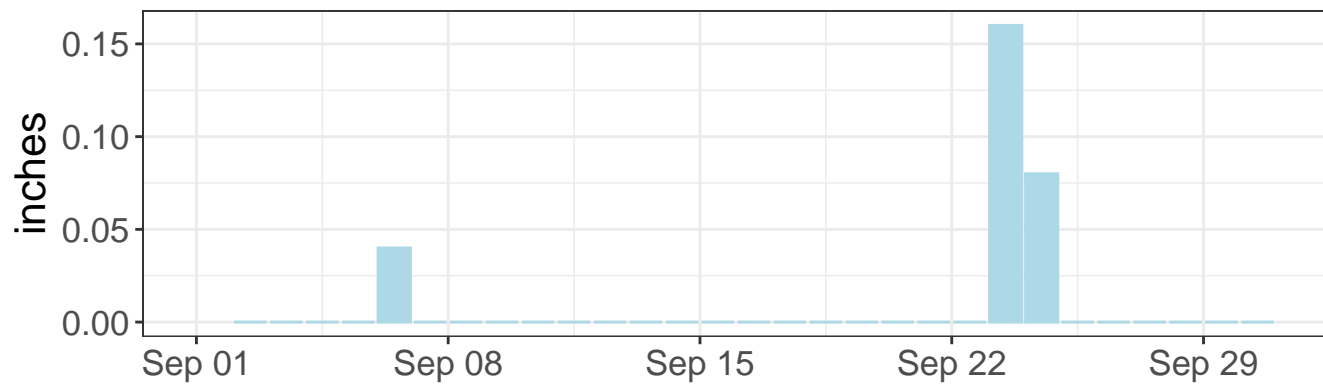
East tilt – detrended values



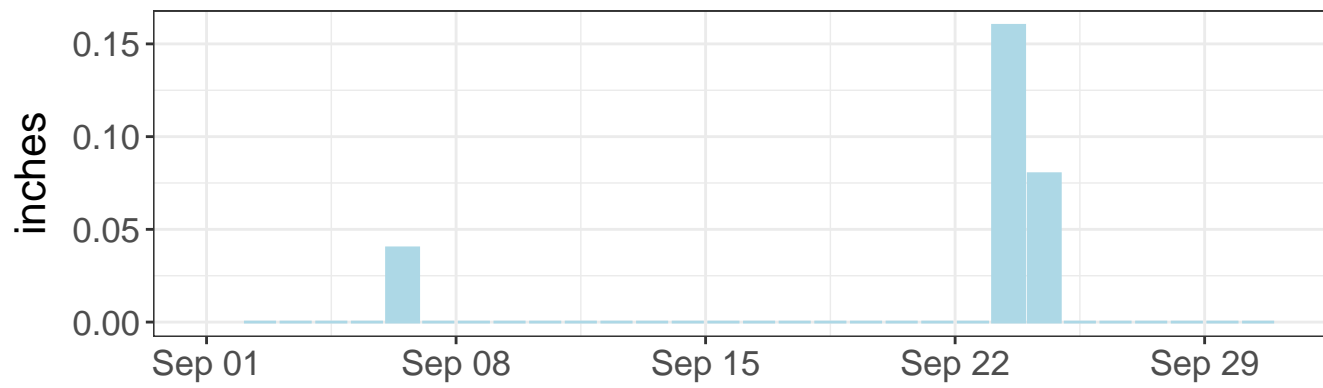
North tilt – detrended values



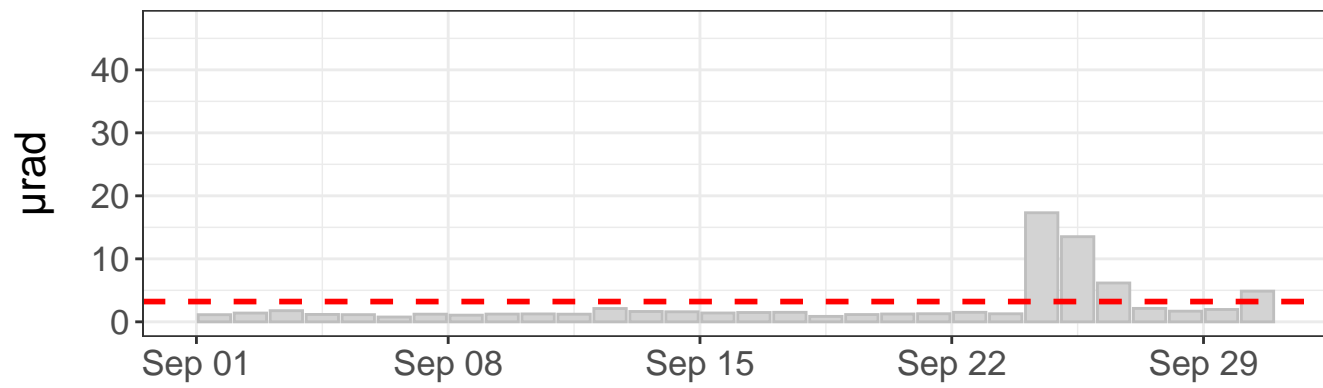
Daily precipitation



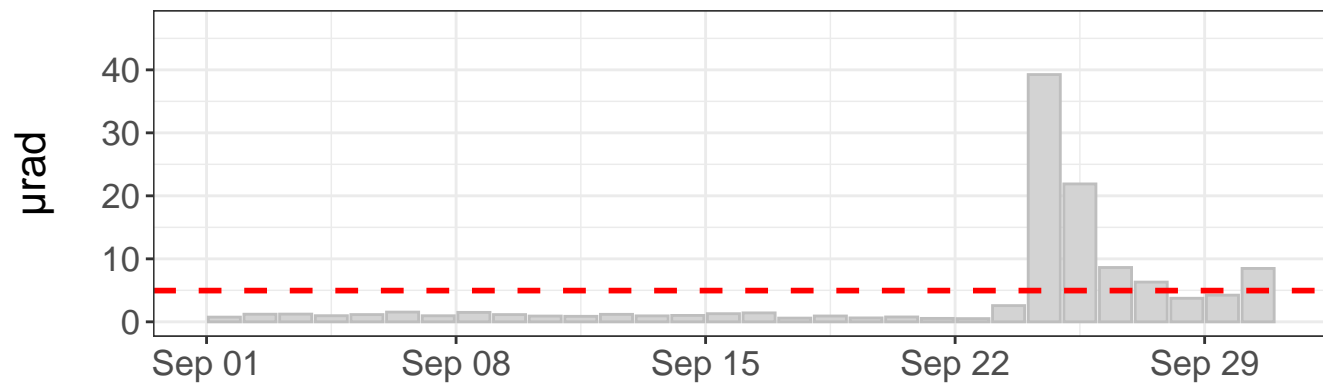
Daily precipitation



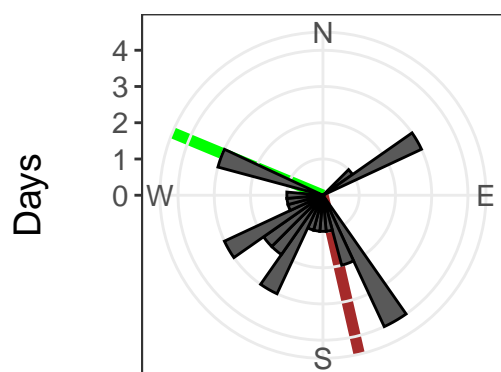
East tilt – daily range



North tilt – daily range

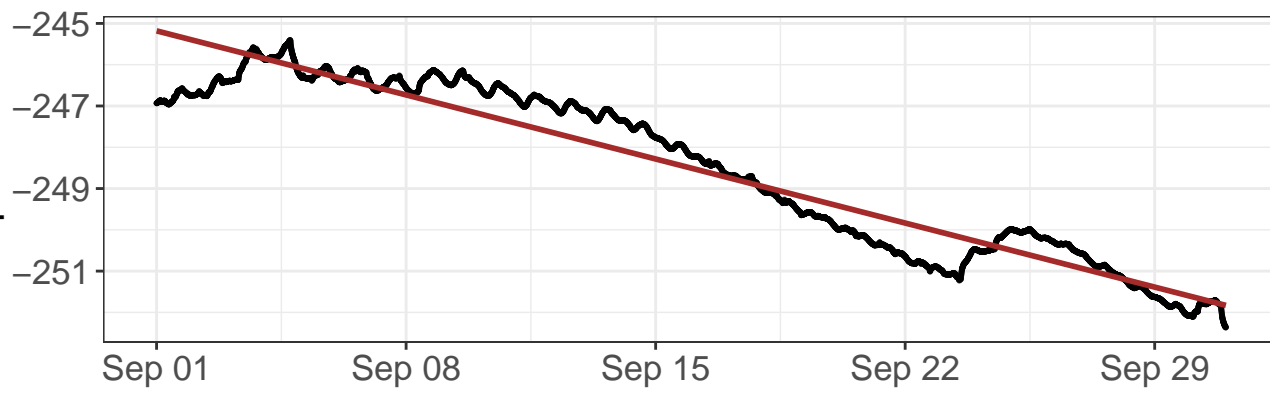


Tilt direction frequency

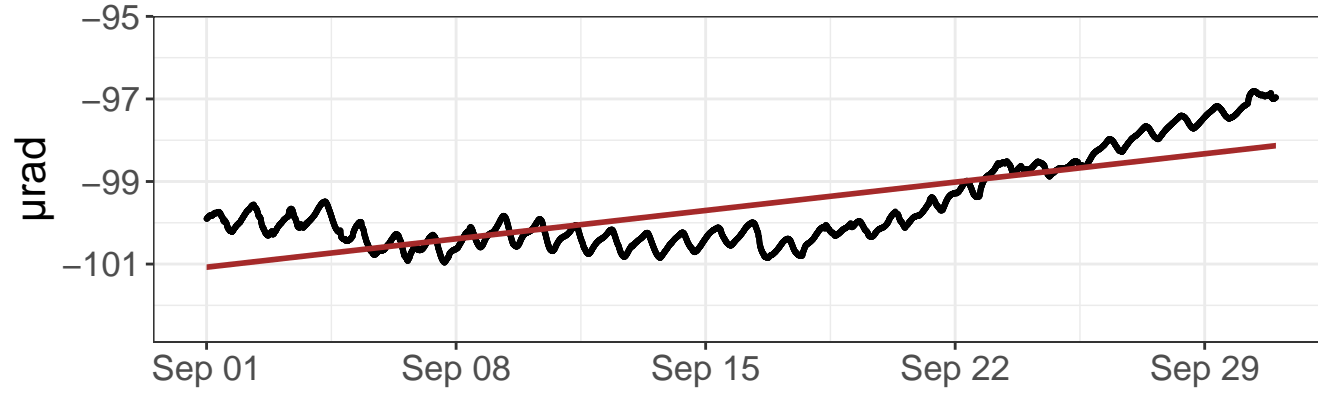


East tilt rate: $232.25 \pm 4.31 \mu\text{rad/yr}$. $R^2: 0.21$
 North tilt rate: $-1017.71 \pm 8.05 \mu\text{rad/yr}$. $R^2: 0.60$
 Azimuth to C7: 293 deg
 Distance to C7: 614 ft
 - - - Outlier value
 — Linear model — Azimuth to C7

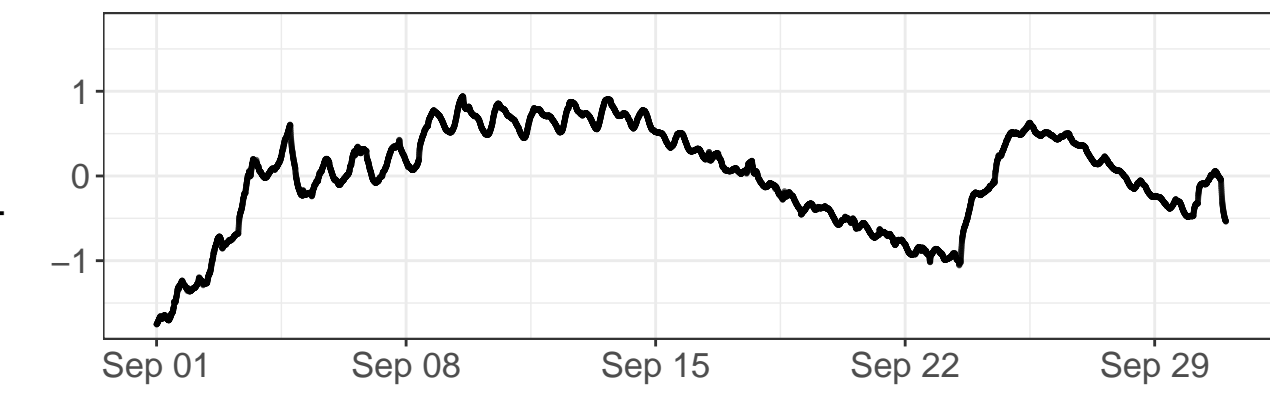
East tilt – raw values



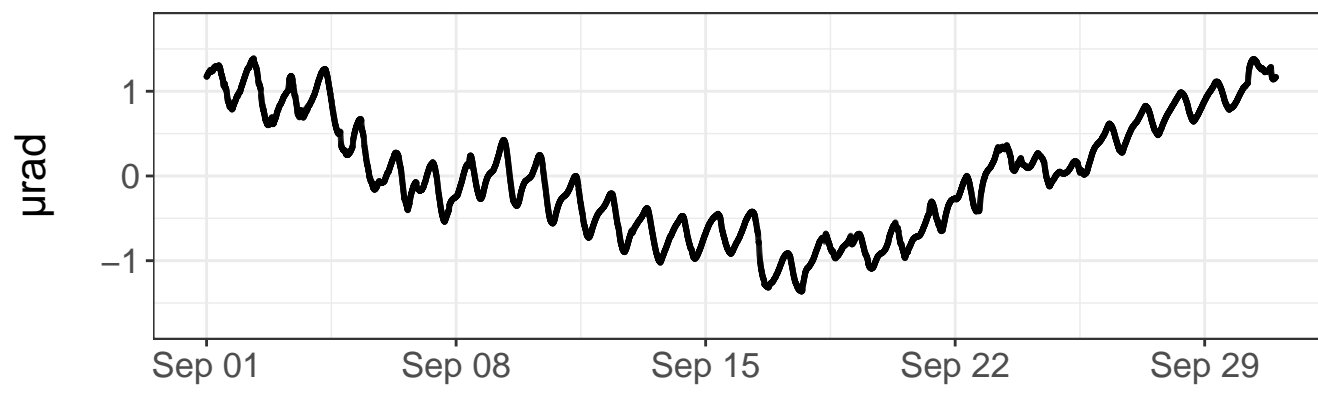
North tilt – raw values



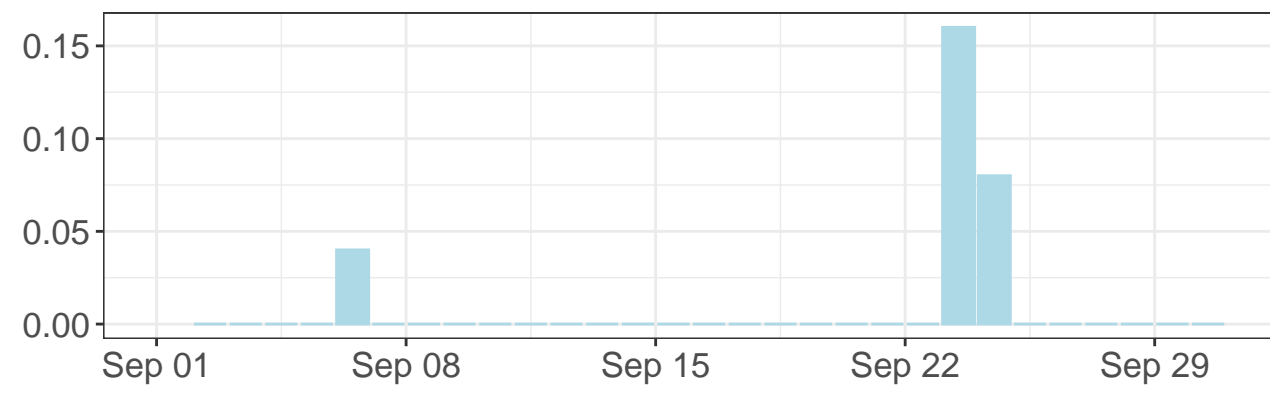
East tilt – detrended values



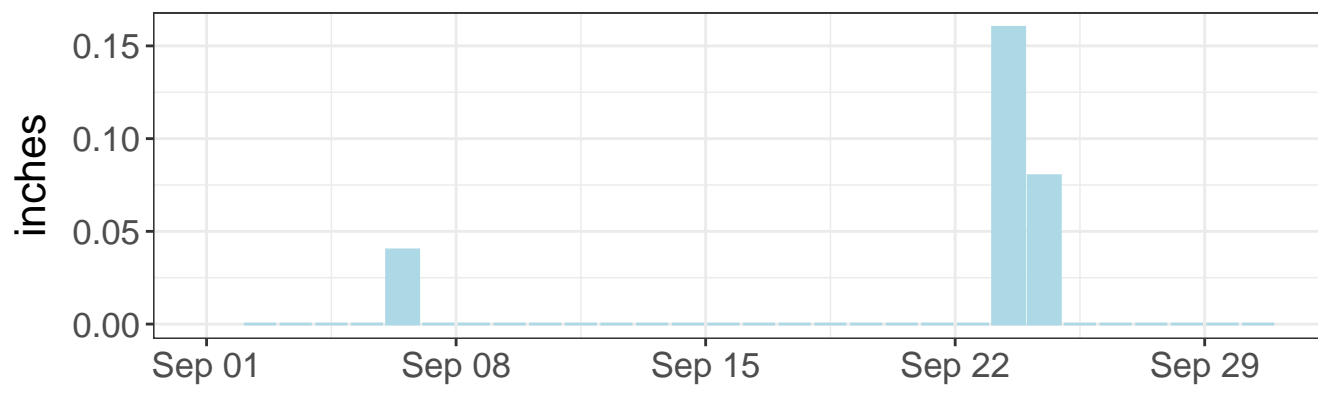
North tilt – detrended values



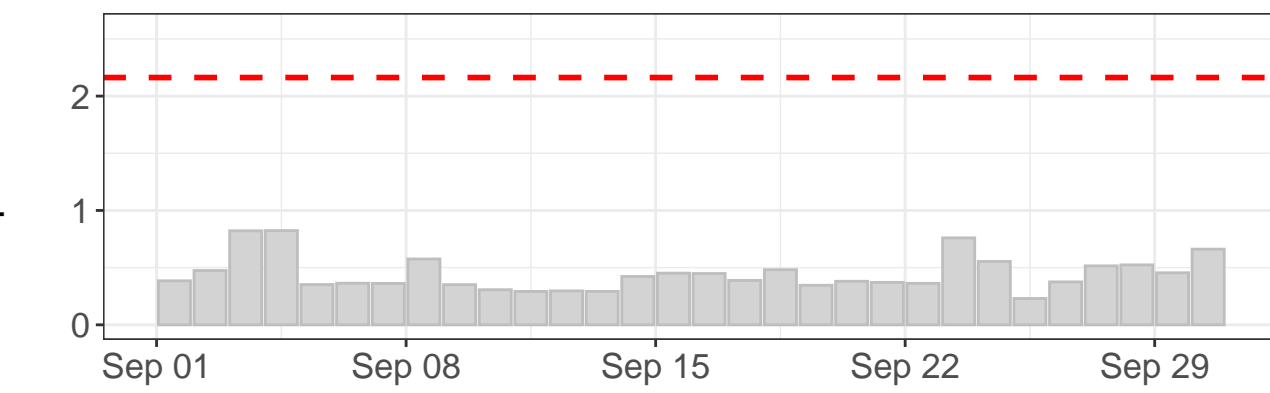
Daily precipitation



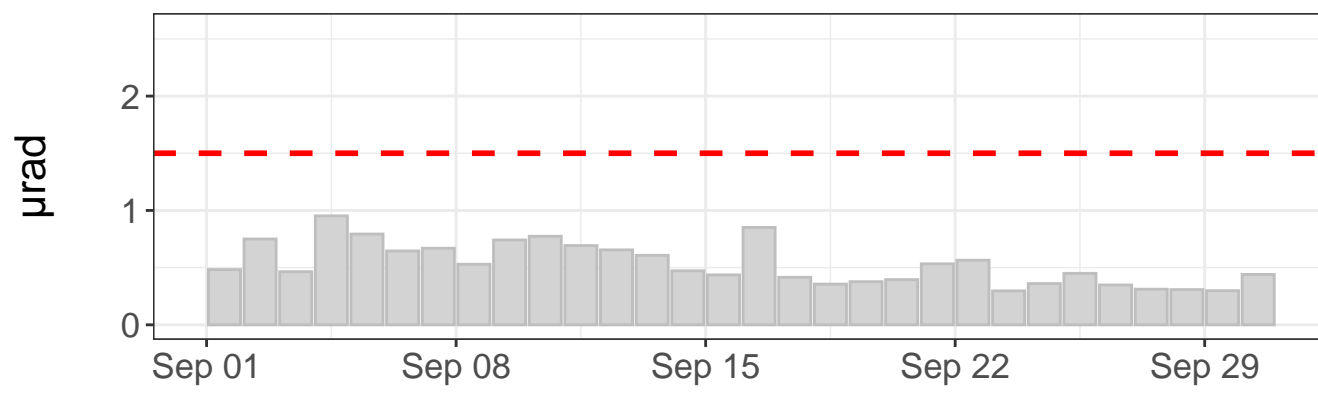
Daily precipitation



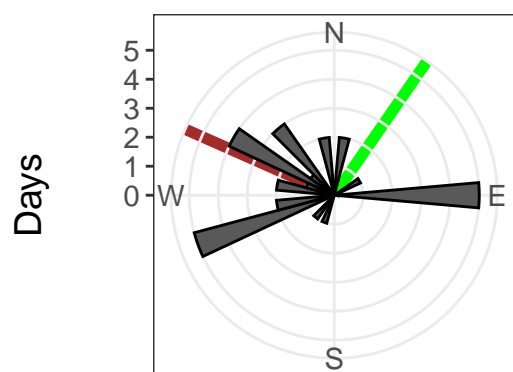
East tilt – daily range



North tilt – daily range



Tilt direction frequency



East tilt rate: $-80.92 \pm 0.24 \mu\text{rad/yr}$. $R^2: 0.91$

North tilt rate: $35.82 \pm 0.28 \mu\text{rad/yr}$. $R^2: 0.60$

Azimuth to C7: 35 deg

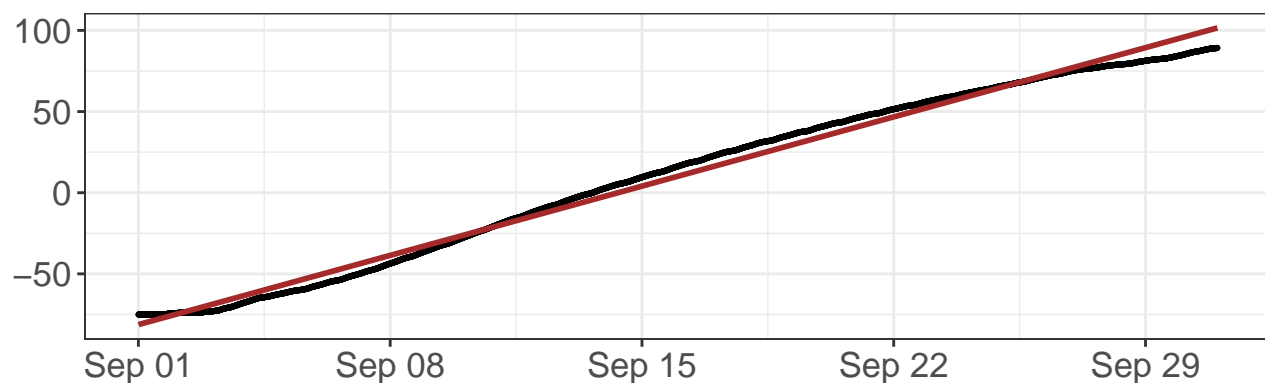
Distance to C7: 1885 ft

- - - Outlier value

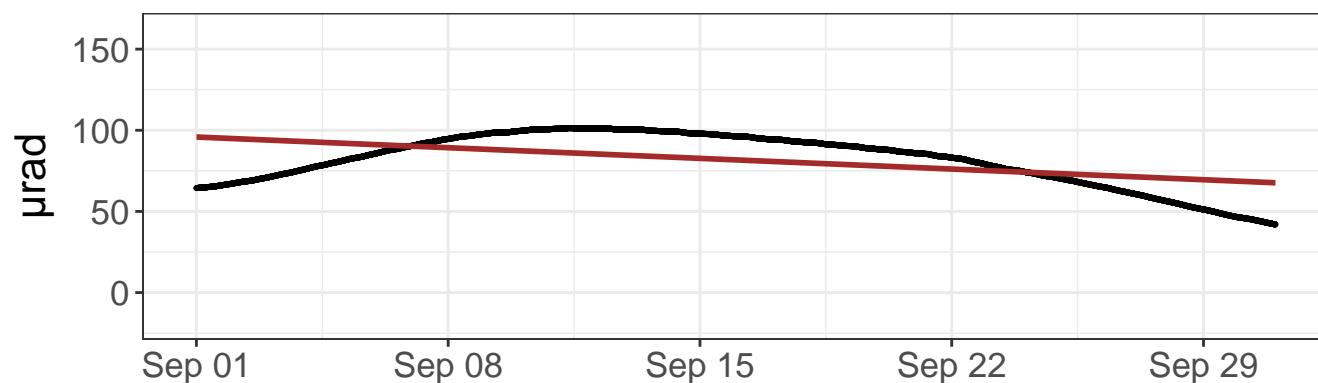
— Linear model

— Azimuth to C7

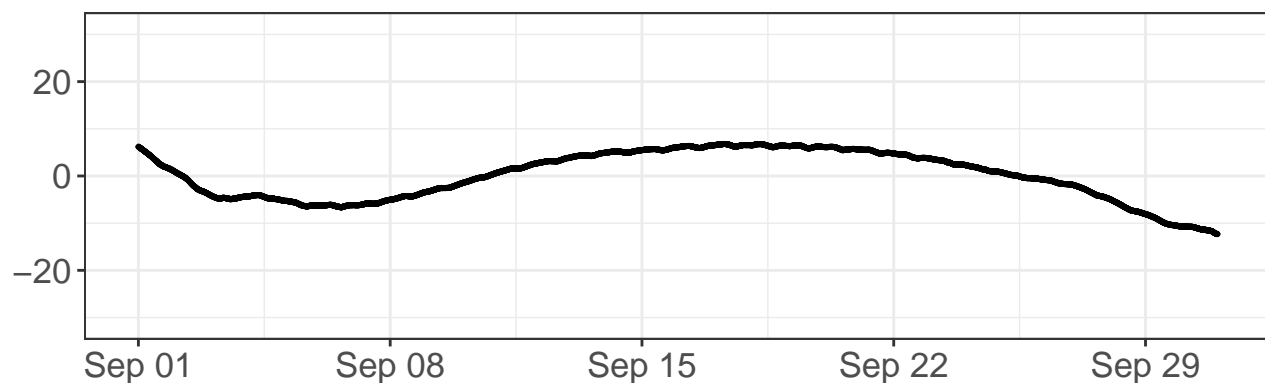
East tilt – raw values



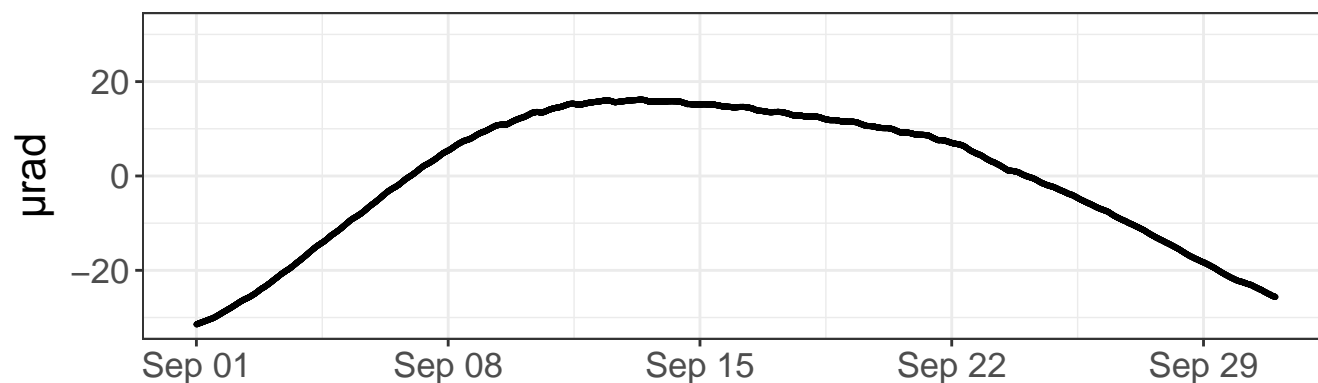
North tilt – raw values



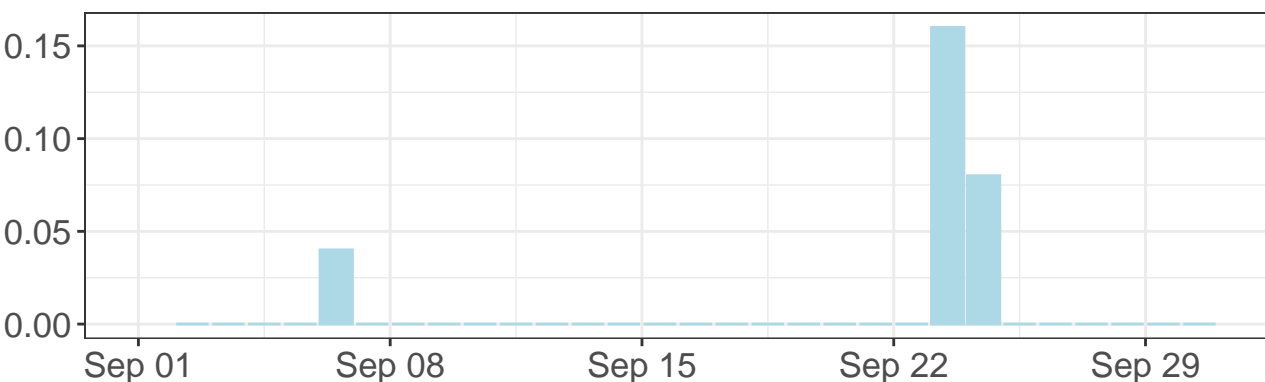
East tilt – detrended values



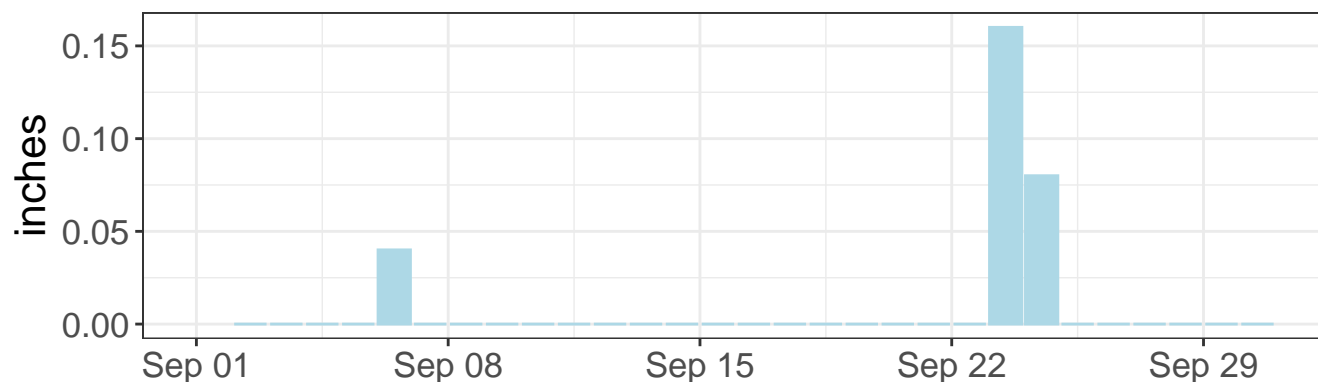
North tilt – detrended values



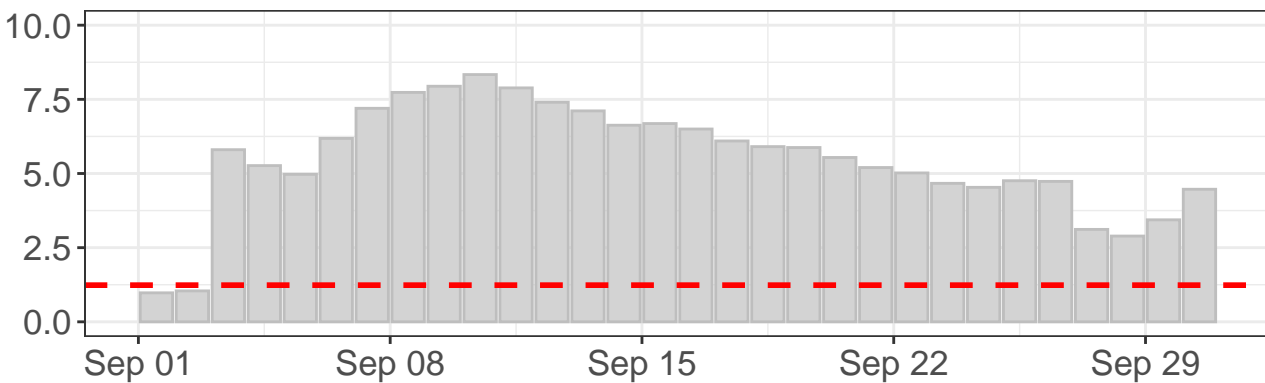
Daily precipitation



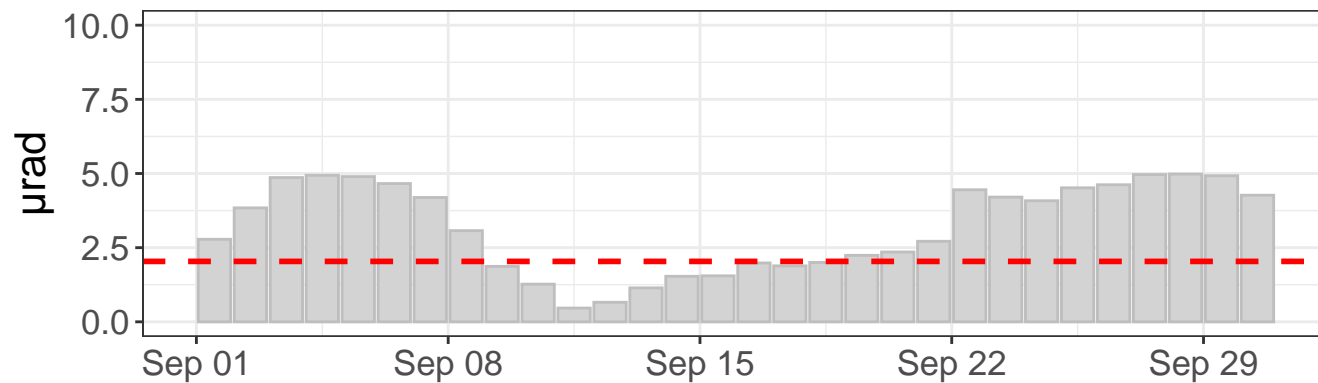
Daily precipitation



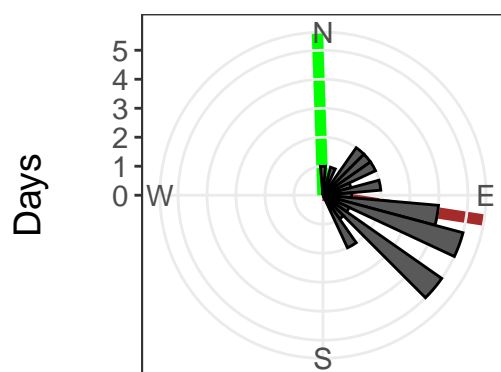
East tilt – daily range



North tilt – daily range



Tilt direction frequency



East tilt rate: $2224.28 \pm 2.12 \mu\text{rad}/\text{yr}$. R^2 : 0.99

North tilt rate: $-343.00 \pm 5.79 \mu\text{rad}/\text{yr}$. R^2 : 0.25

Azimuth to C7: 358 deg

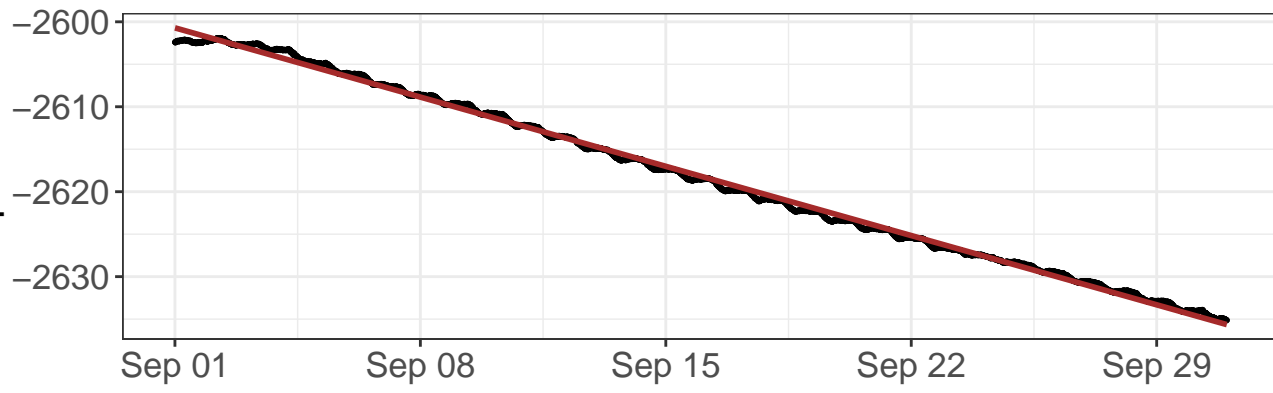
Distance to C7: 1392 ft

--- Outlier value

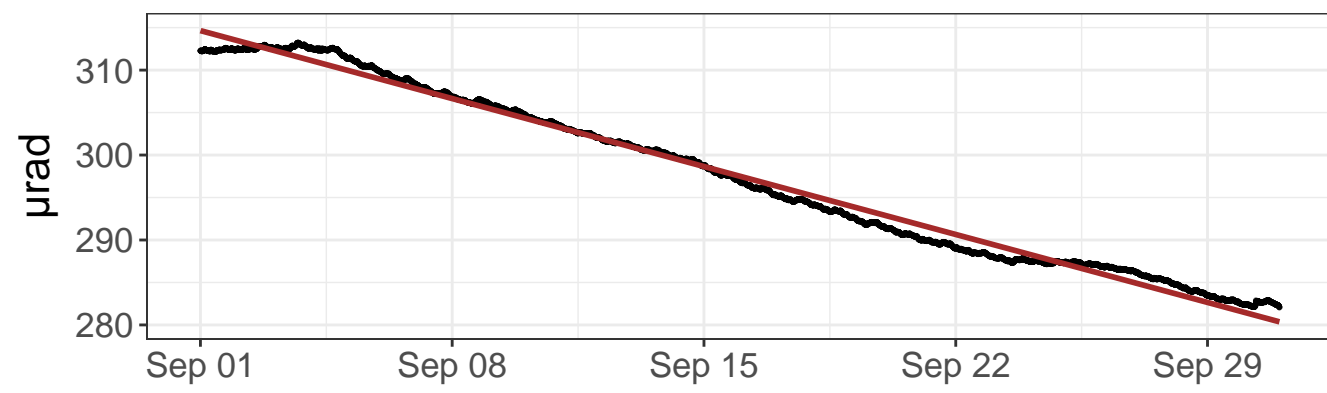
— Linear model

— Azimuth to C7

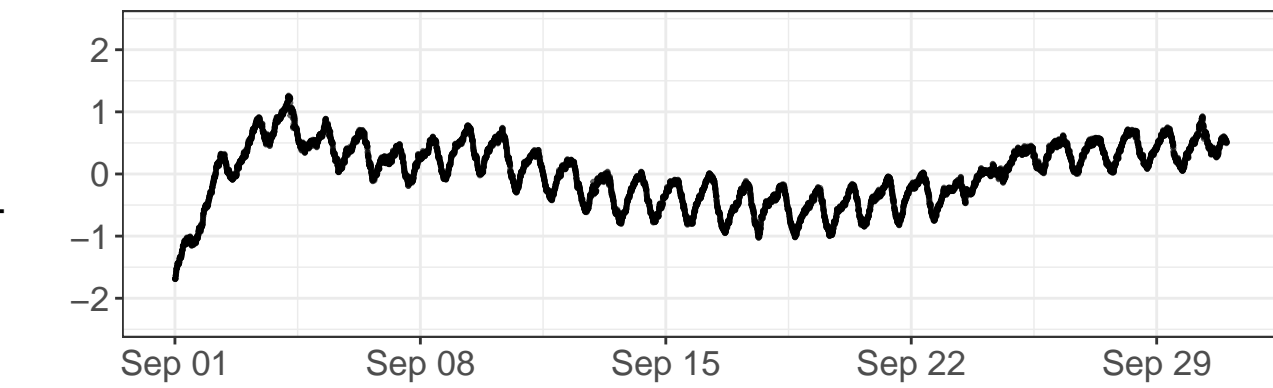
East tilt – raw values



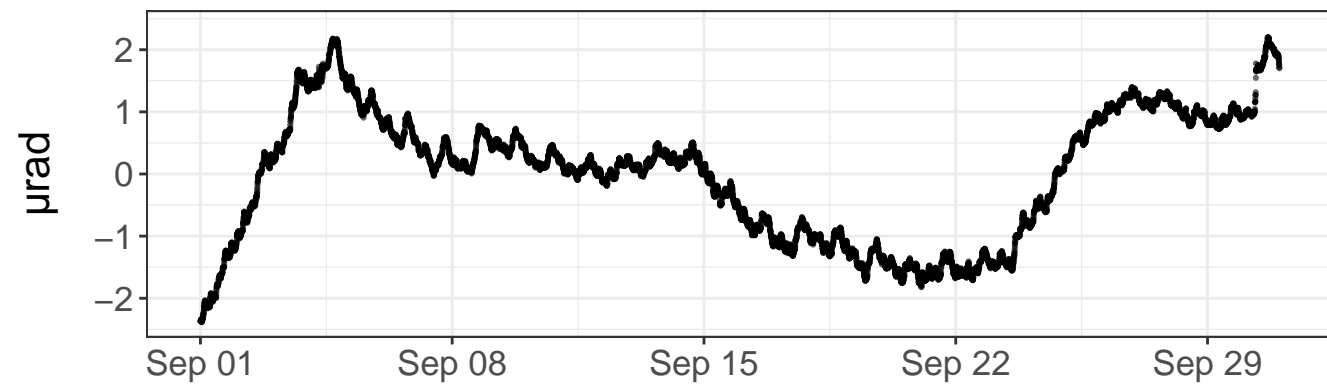
North tilt – raw values



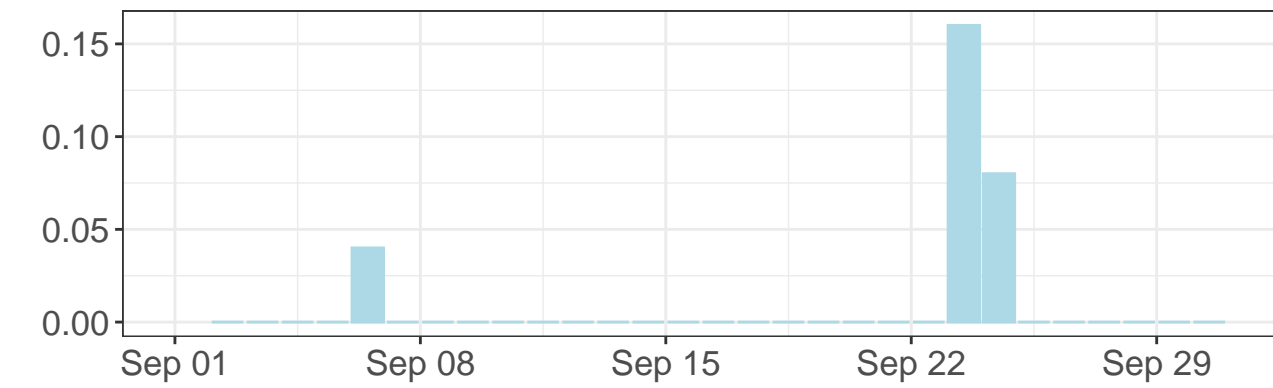
East tilt – detrended values



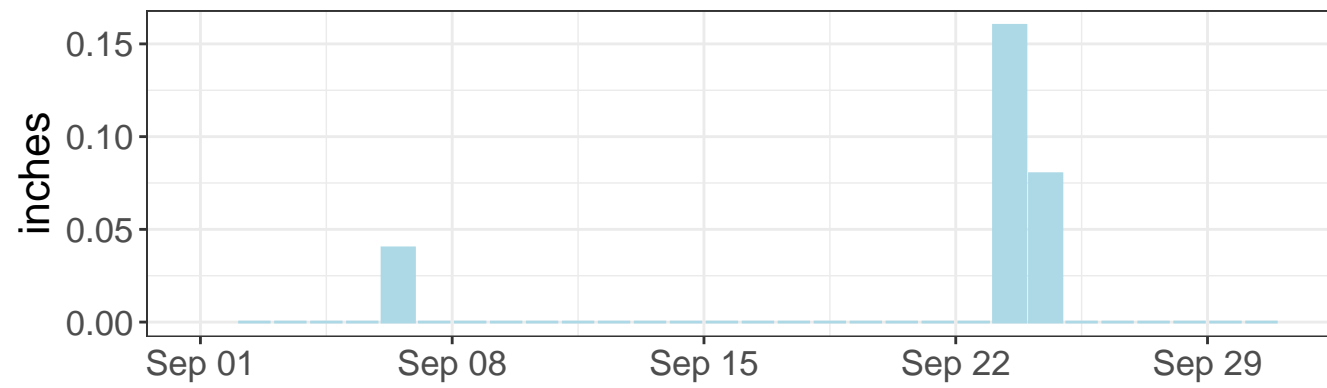
North tilt – detrended values



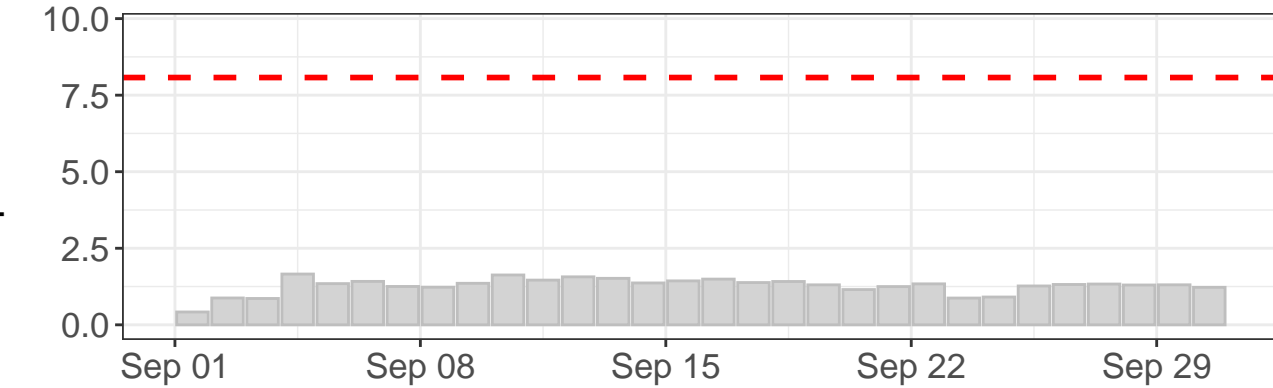
Daily precipitation



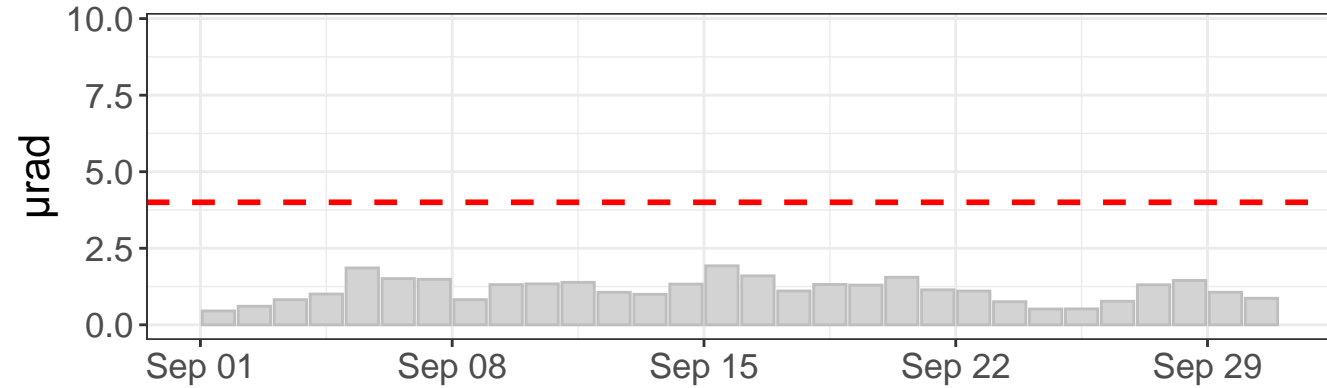
Daily precipitation



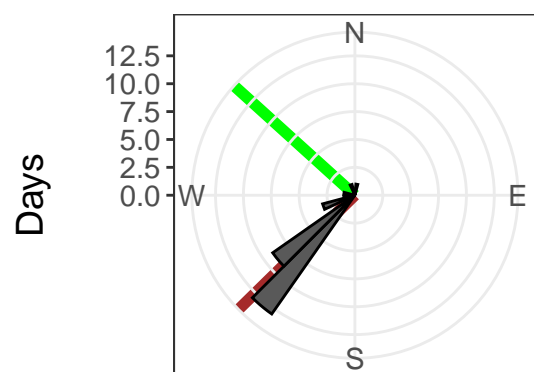
East tilt – daily range



North tilt – daily range



Tilt direction frequency



East tilt rate: $-425.02 \pm 0.20 \mu\text{rad}/\text{yr}$. R2: 1.00

North tilt rate: $-417.11 \pm 0.42 \mu\text{rad}/\text{yr}$. R2: 0.99

Azimuth to C7: 312 deg

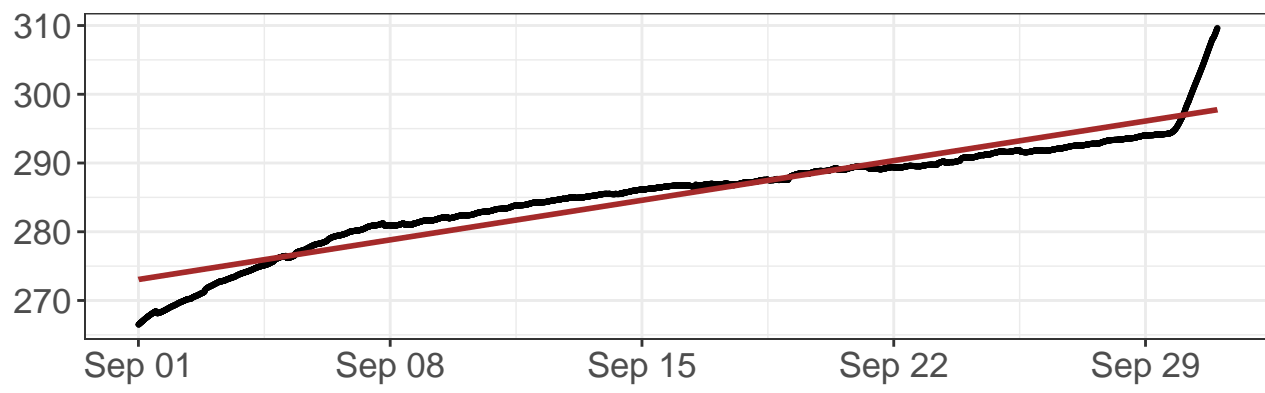
Distance to C7: 1415 ft

--- Outlier value

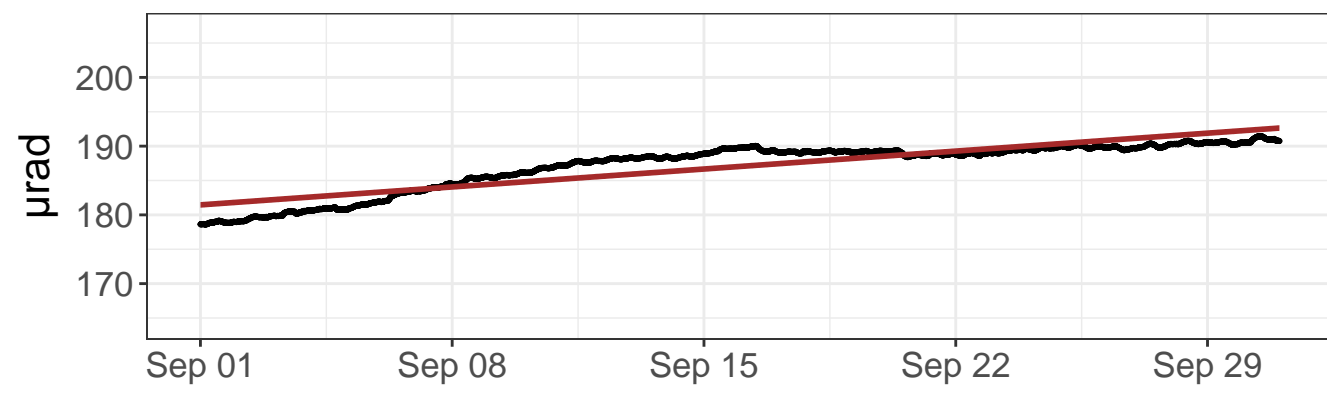
— Linear model

— Azimuth to C7

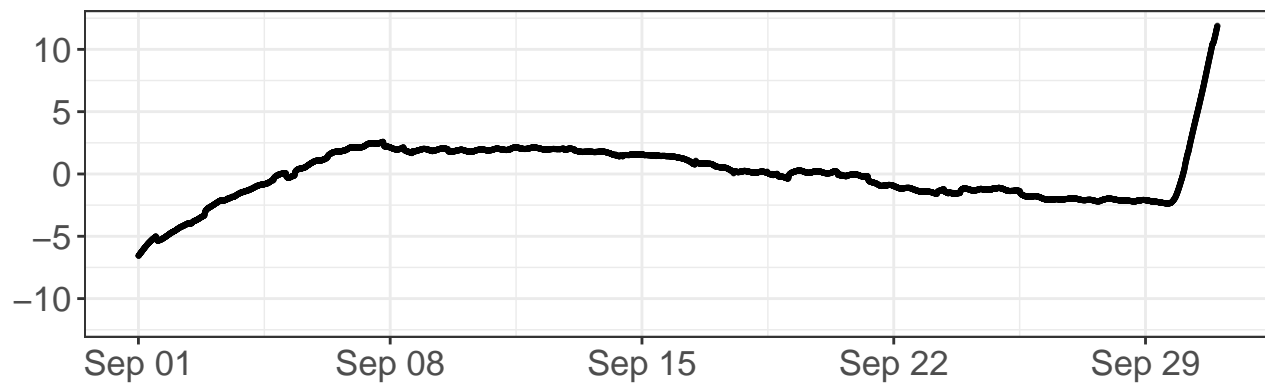
East tilt – raw values



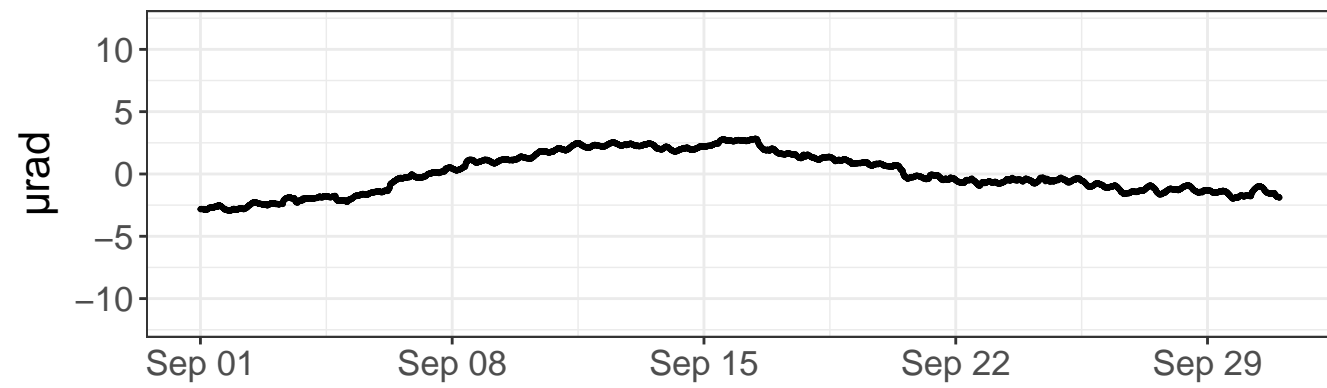
North tilt – raw values



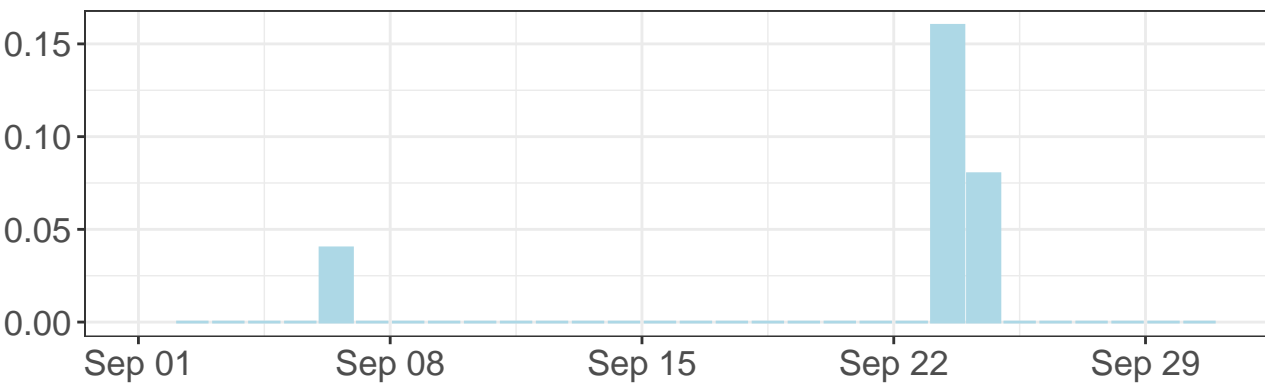
East tilt – detrended values



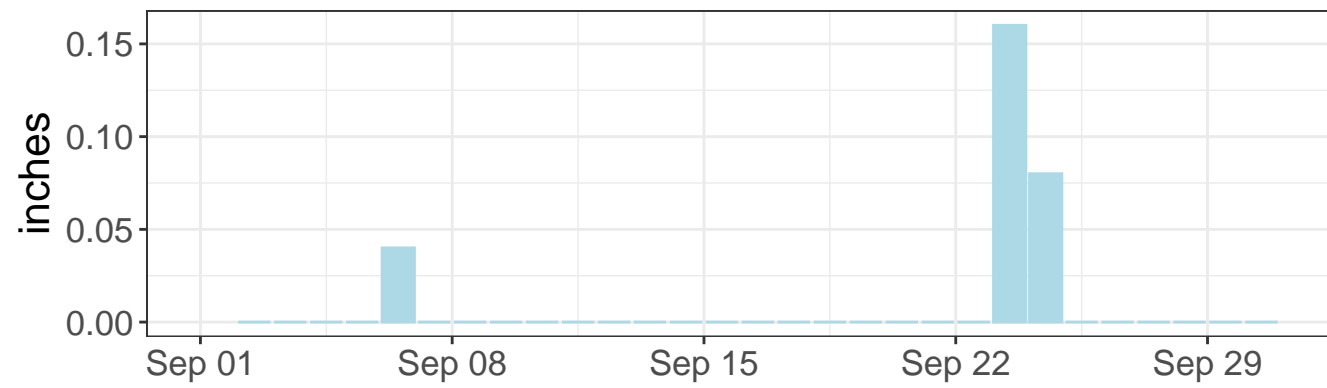
North tilt – detrended values



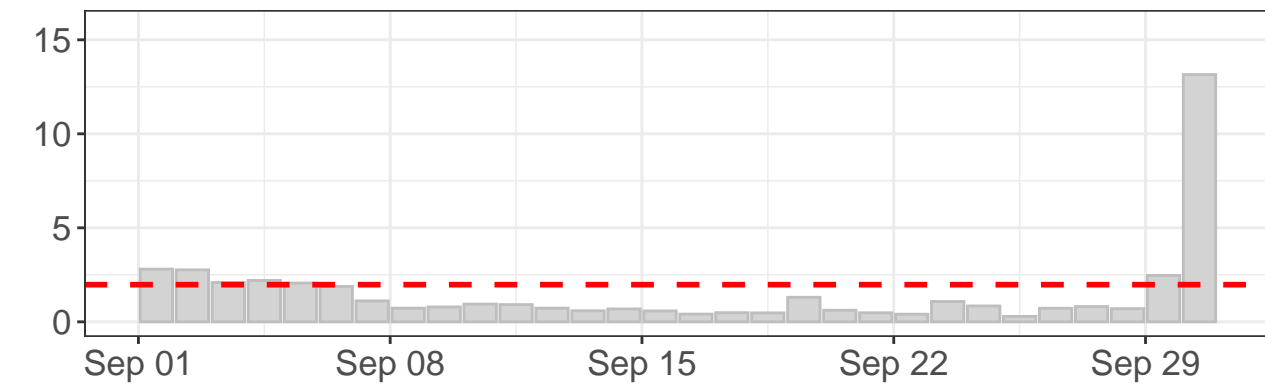
Daily precipitation



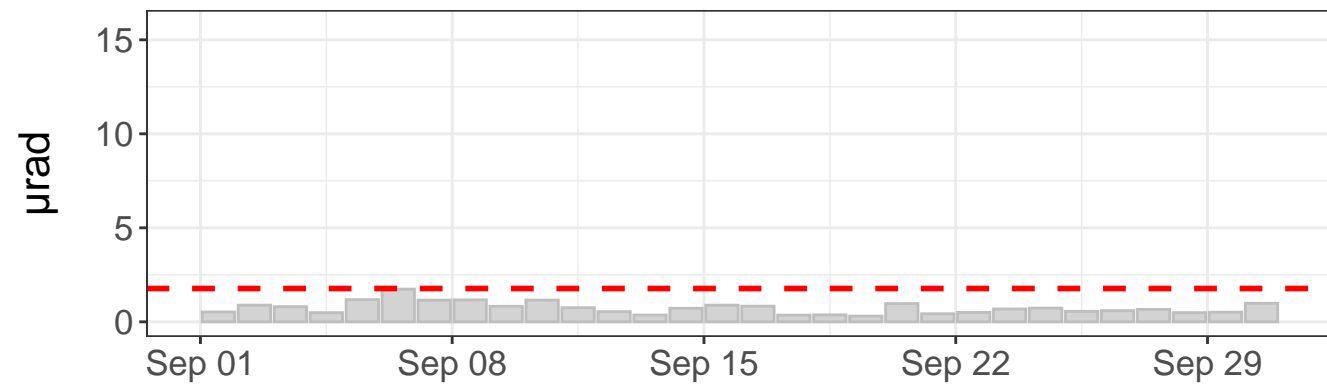
Daily precipitation



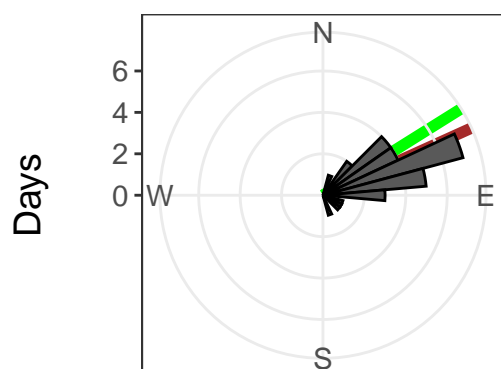
East tilt – daily range



North tilt – daily range



Tilt direction frequency



East tilt rate: 300.50 ± 0.93 $\mu\text{rad}/\text{yr}$. R^2 : 0.91

North tilt rate: 136.01 ± 0.66 $\mu\text{rad}/\text{yr}$. R^2 : 0.80

Azimuth to C7: 58 deg

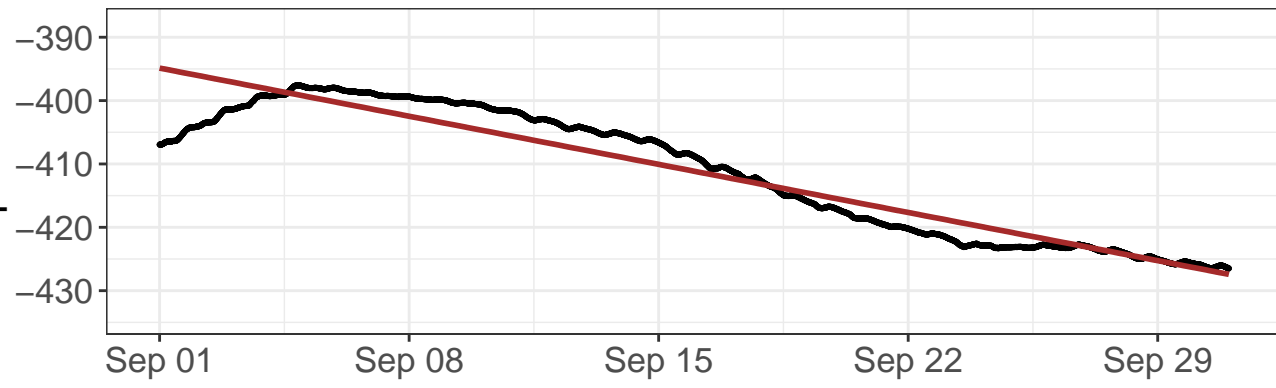
Distance to C7: 2245 ft

--- Outlier value

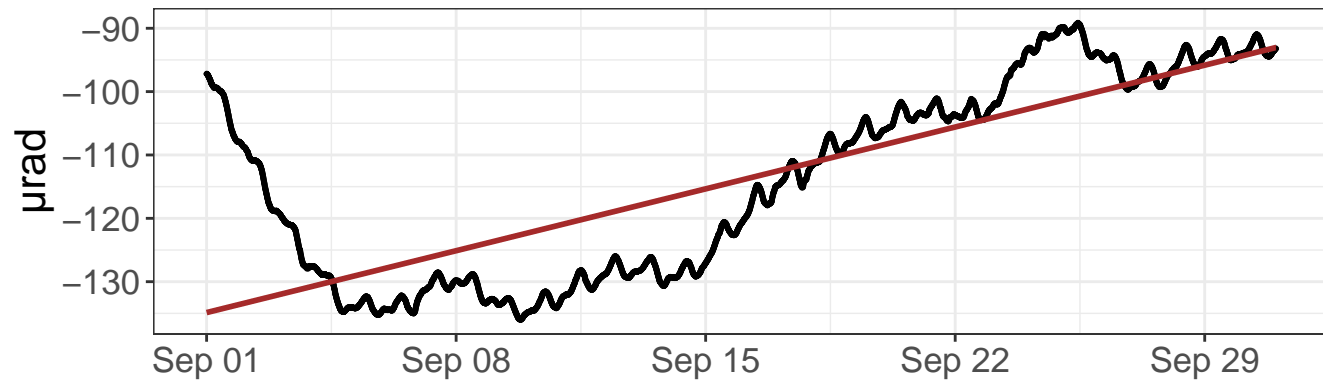
— Linear model

— Azimuth to C7

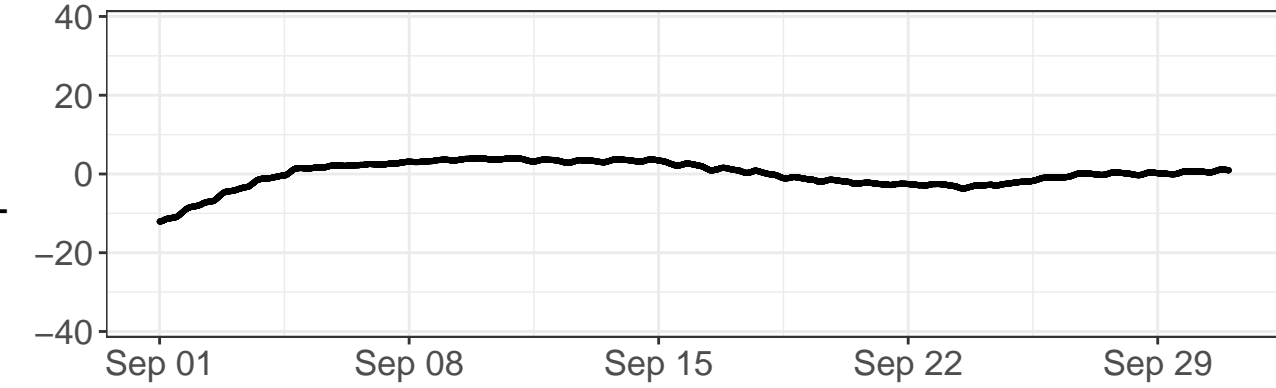
East tilt – raw values



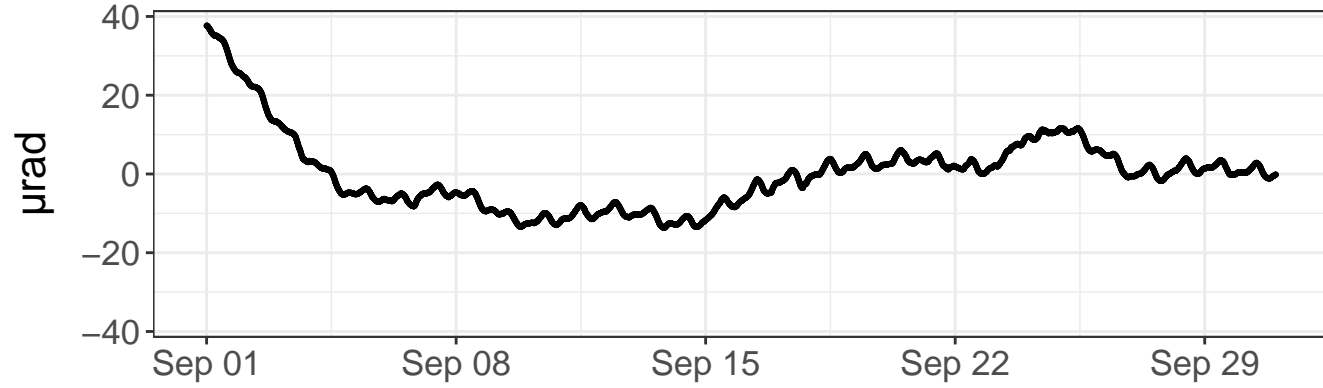
North tilt – raw values



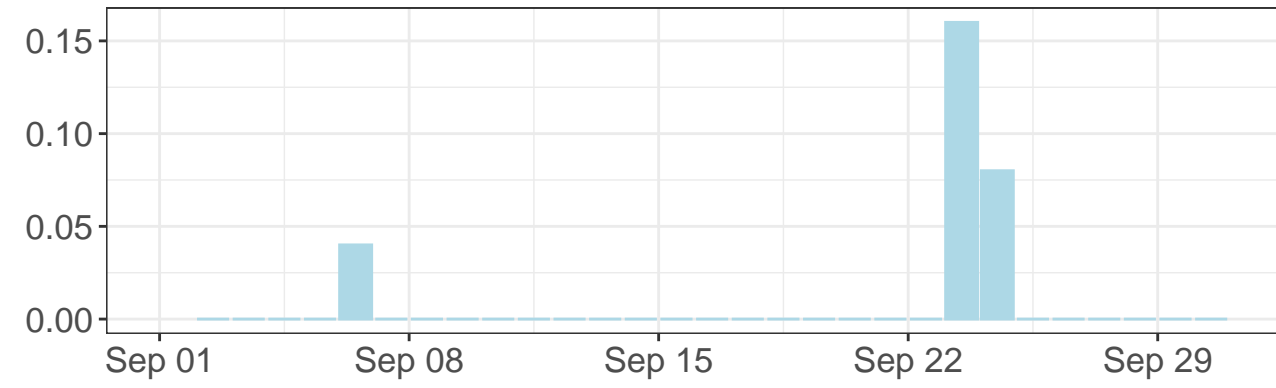
East tilt – detrended values



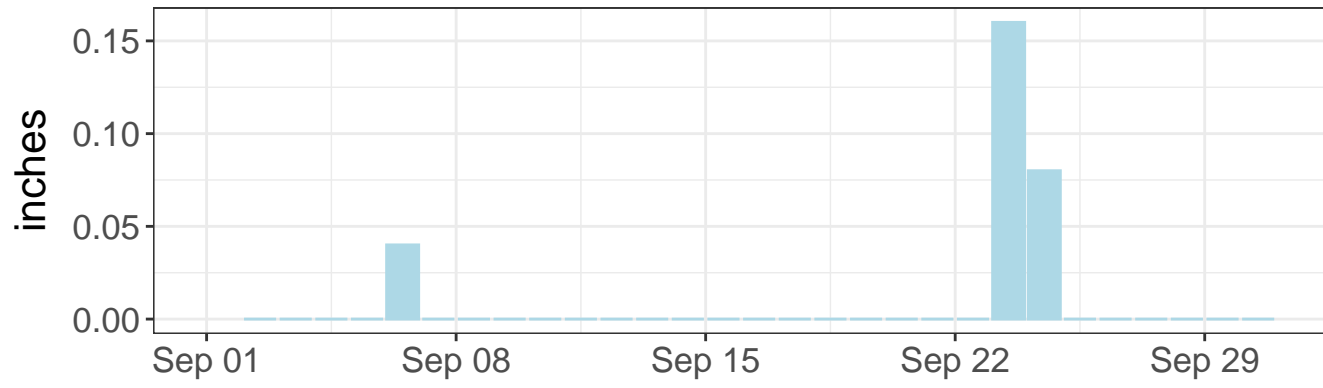
North tilt – detrended values



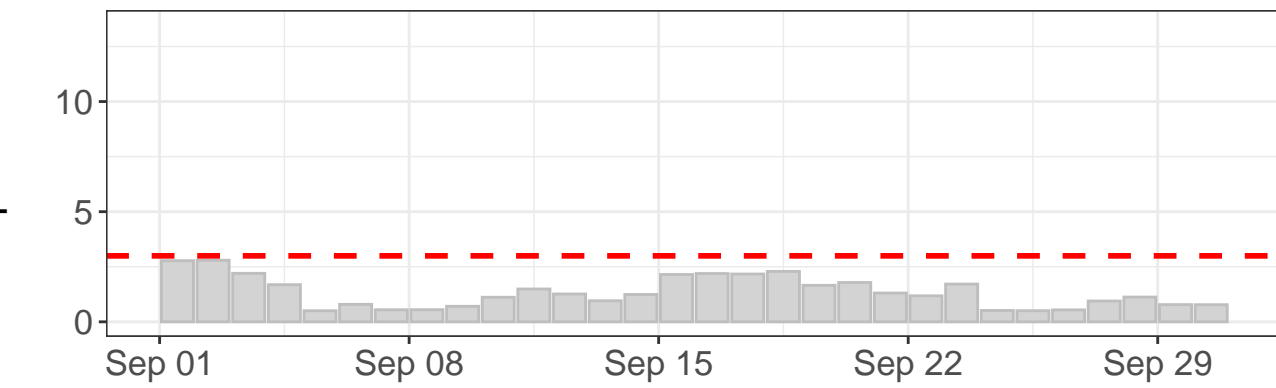
Daily precipitation



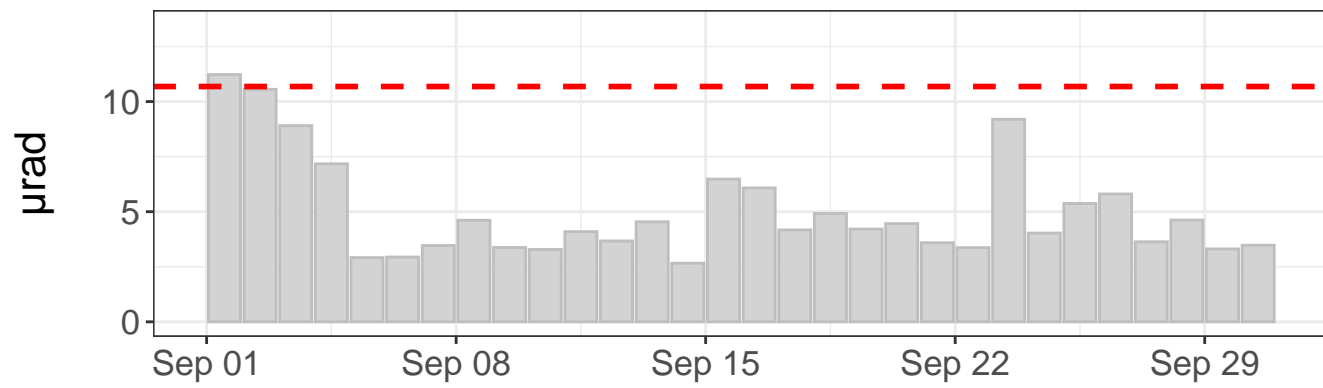
Daily precipitation



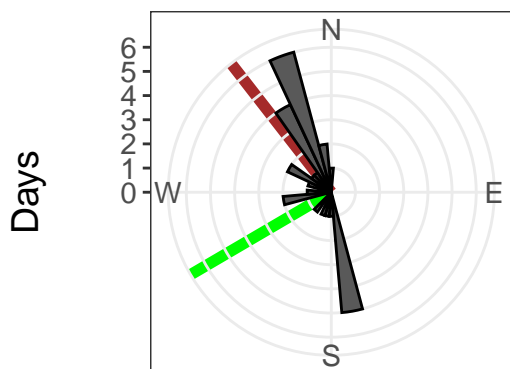
East tilt – daily range



North tilt – daily range



Tilt direction frequency



East tilt rate: $-396.11 \pm 1.31 \mu\text{rad}/\text{yr}$. R^2 : 0.89

North tilt rate: $509.02 \pm 3.89 \mu\text{rad}/\text{yr}$. R^2 : 0.61

Azimuth to C7: 240 deg

Distance to C7: 1378 ft

- - - Outlier value

— Linear model

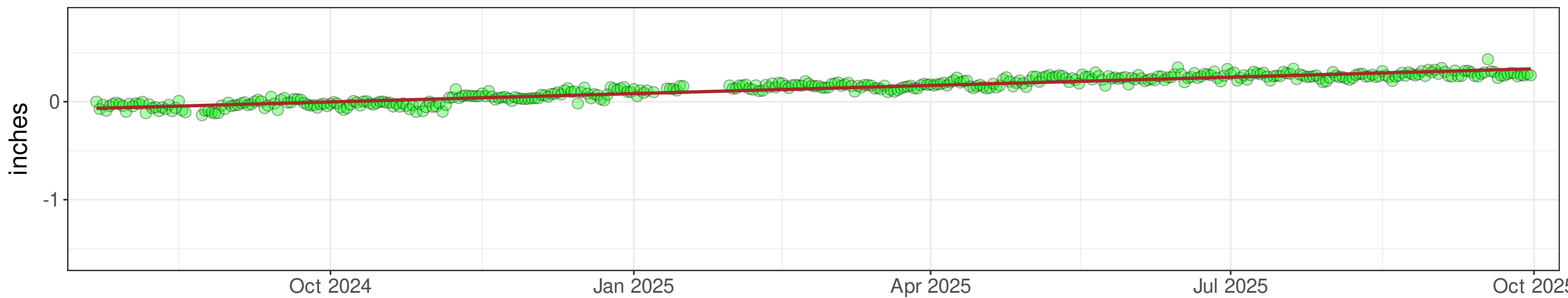
— Azimuth to C7

APPENDIX 2

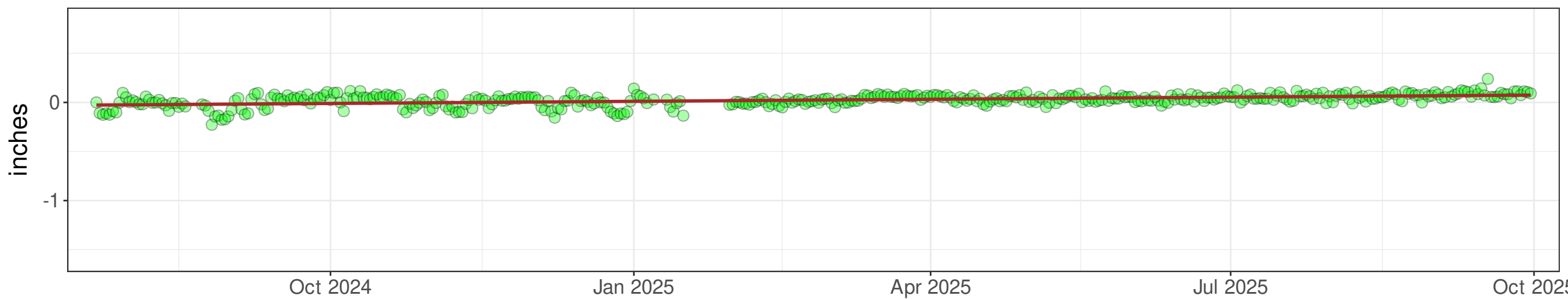
GNSS Data Plots

REMC7: Plotted range: 2024-07-22 - 2025-09-30 (CTZ)

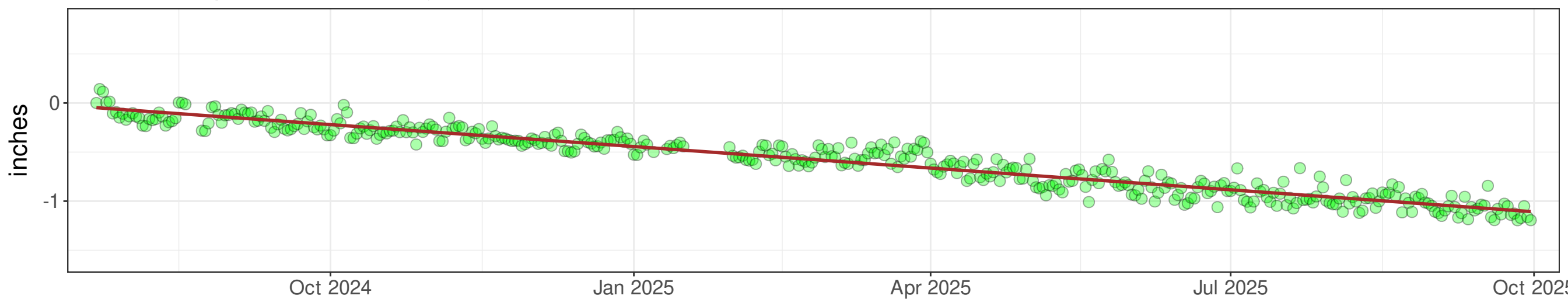
East displacement - daily values



North displacement - daily values



Vertical displacement - daily values



Local east rate: 0.821 ± 0.019 inches/year, R2: 0.89

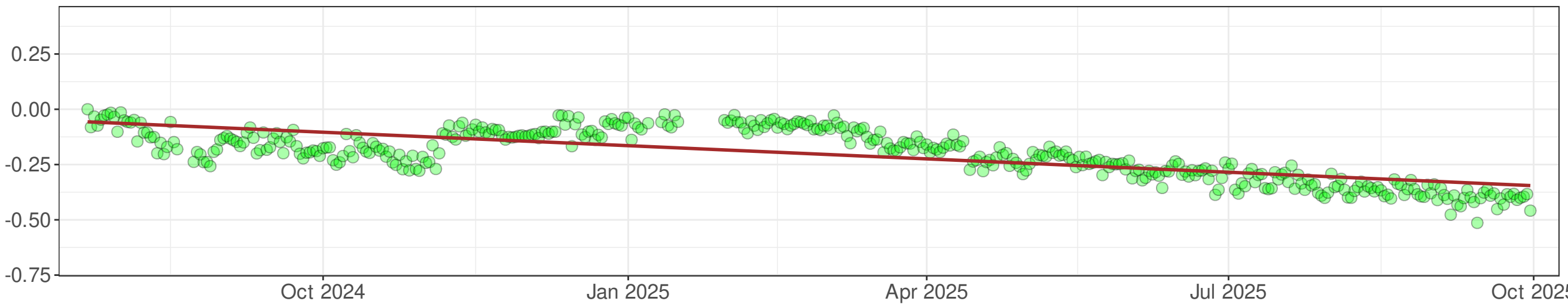
Local north rate: 0.127 ± 0.019 inches/year, R2: 0.25

Local vertical rate: -0.809 ± 0.057 inches/year, R2: 0.93

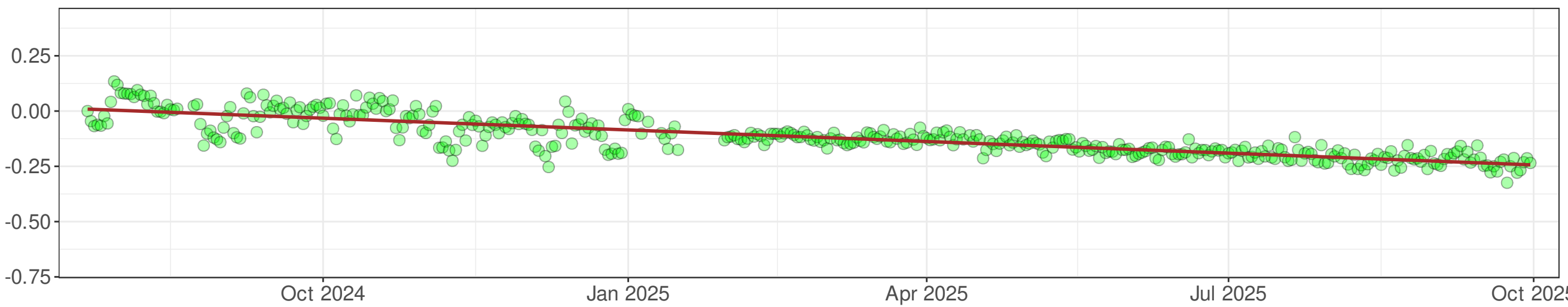
— Linear model

Local rate values have been calculated by removing the regional tectonic plate rates from the raw data displayed in the charts.

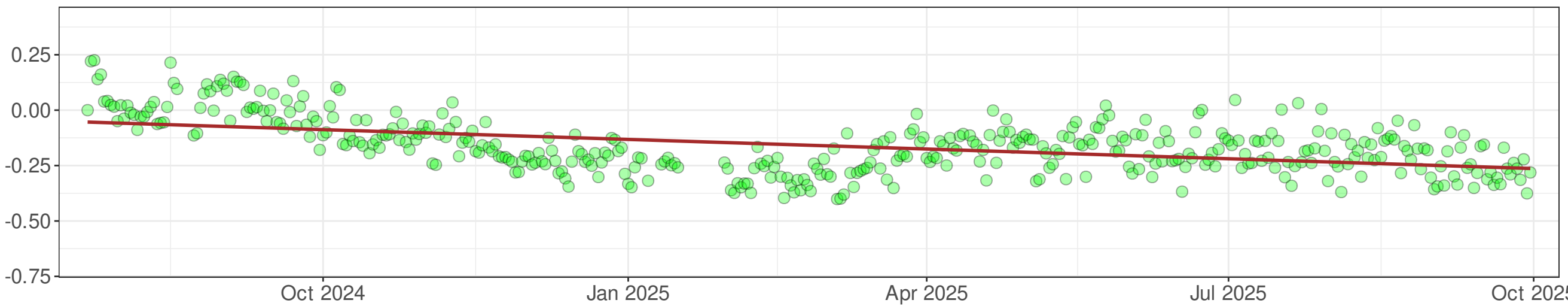
East displacement - daily values



North displacement - daily values



Vertical displacement - daily values



Local east rate: 0.240 ± 0.021 inches/year, R2: 0.55

Local north rate: -0.170 ± 0.019 inches/year, R2: 0.71

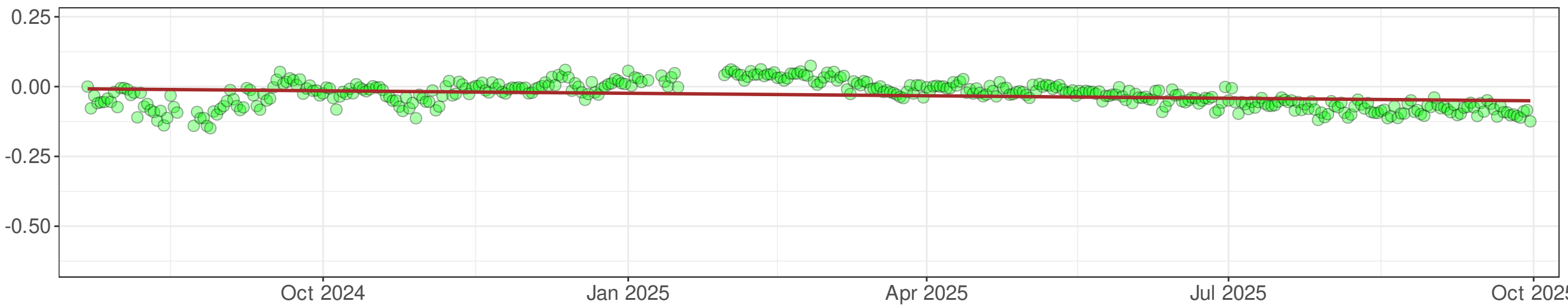
Local vertical rate: -0.096 ± 0.057 inches/year, R2: 0.25

— Linear model

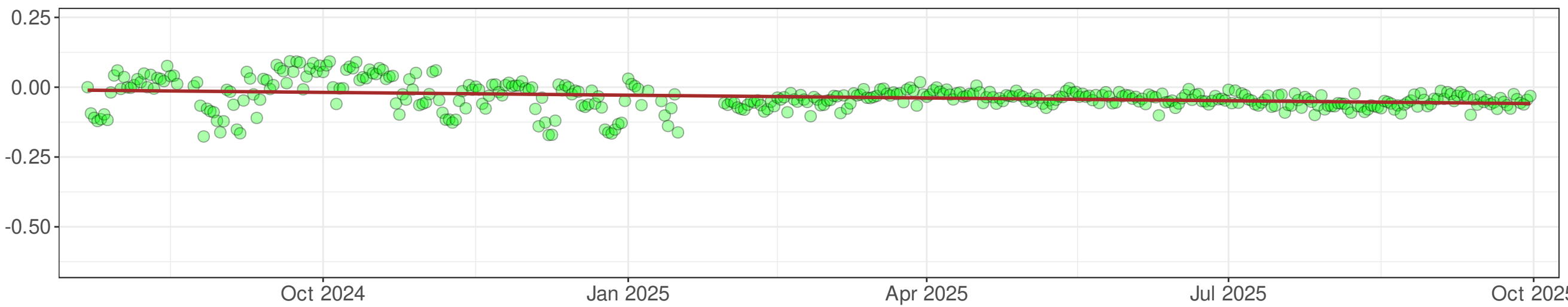
Local rate values have been calculated by removing the regional tectonic plate rates from the raw data displayed in the charts.

REMNW: Plotted range: 2024-07-22 - 2025-09-30 (CTZ)

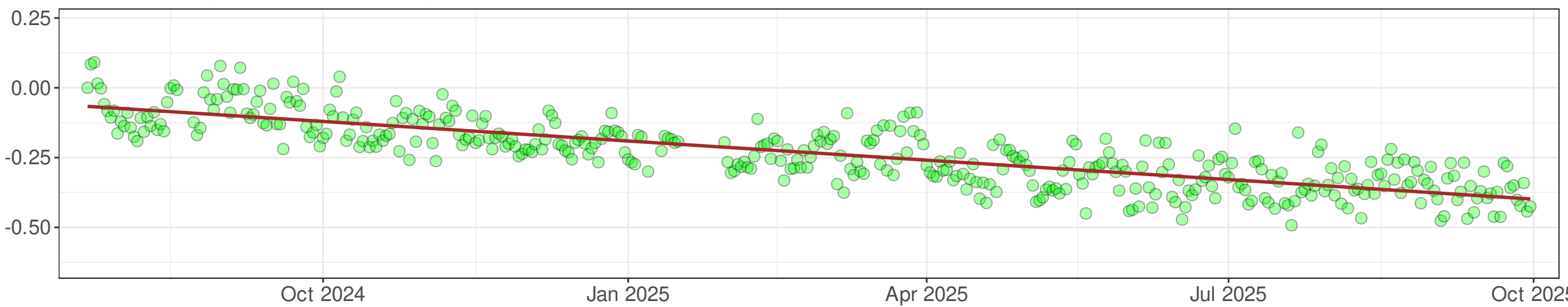
East displacement - daily values



North displacement - daily values



Vertical displacement - daily values



Local east rate: 0.447 ± 0.020 inches/year, R2: 0.08

Local north rate: 0.002 ± 0.019 inches/year, R2: 0.08

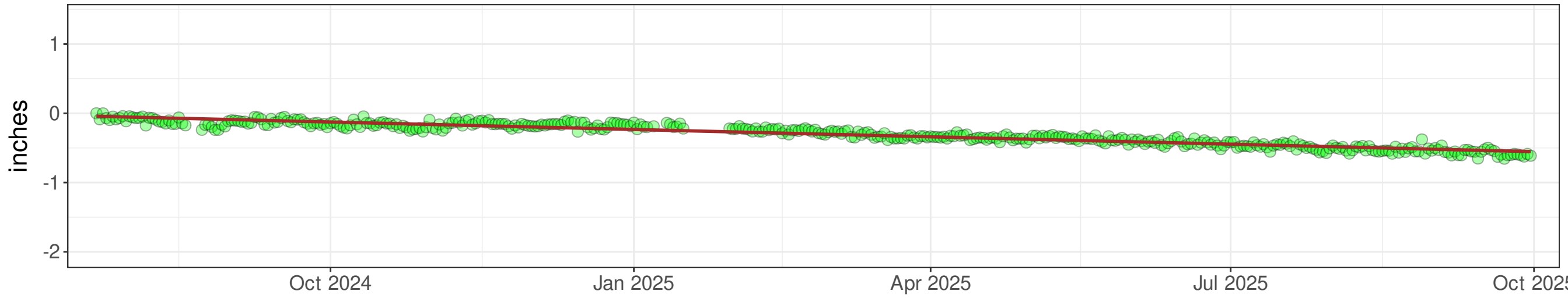
Local vertical rate: -0.198 ± 0.056 inches/year, R2: 0.67

— Linear model

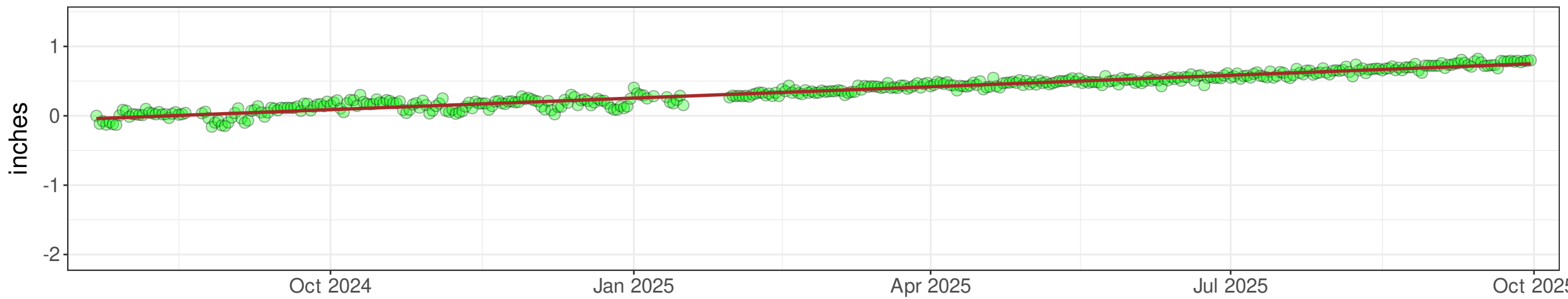
Local rate values have been calculated by removing the regional tectonic plate rates from the raw data displayed in the charts.

REMSE: Plotted range: 2024-07-22 - 2025-09-30 (CTZ)

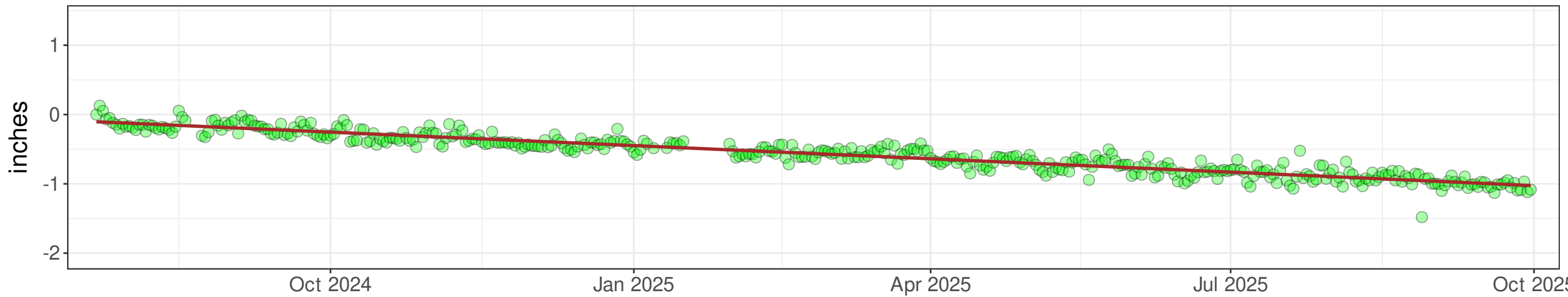
East displacement - daily values



North displacement - daily values



Vertical displacement - daily values



Local east rate: 0.054 ± 0.020 inches/year, R2: 0.90

Local north rate: 0.706 ± 0.019 inches/year, R2: 0.94

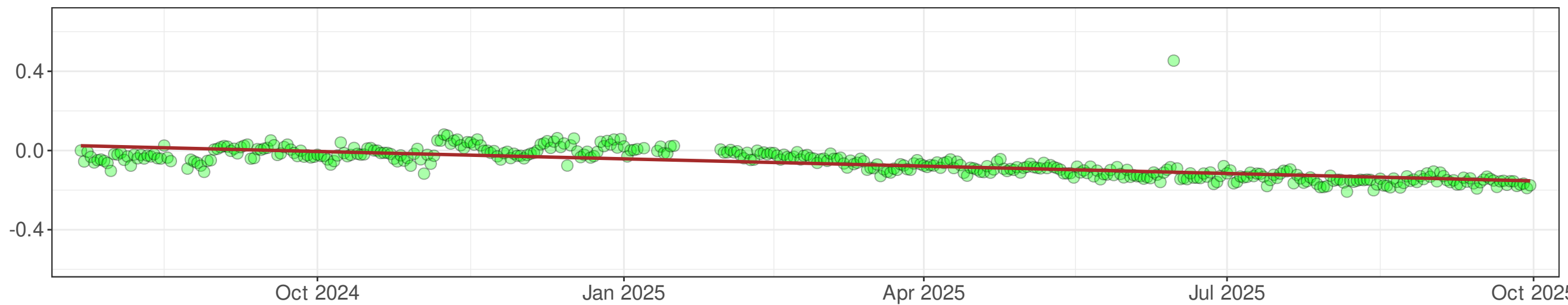
Local vertical rate: -0.692 ± 0.057 inches/year, R2: 0.90

— Linear model

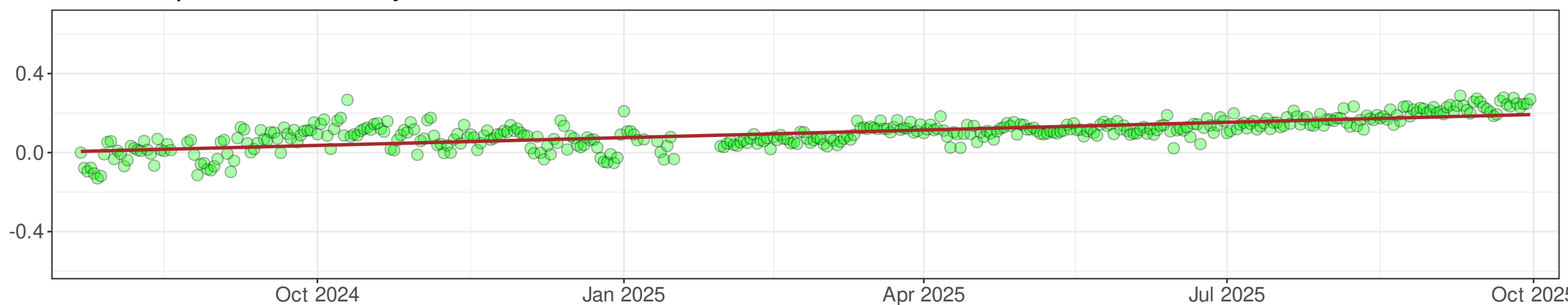
Local rate values have been calculated by removing the regional tectonic plate rates from the raw data displayed in the charts.

REMSW: Plotted range: 2024-07-22 - 2025-09-30 (CTZ)

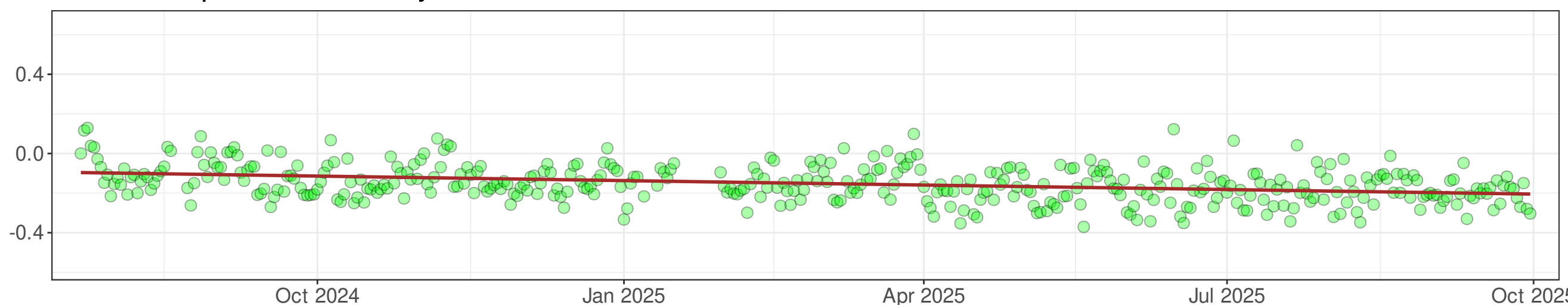
East displacement - daily values



North displacement - daily values



Vertical displacement - daily values



Local east rate: 0.334 ± 0.020 inches/year, R2: 0.55

Local north rate: 0.198 ± 0.019 inches/year, R2: 0.52

Local vertical rate: -0.011 ± 0.057 inches/year, R2: 0.12

— Linear model

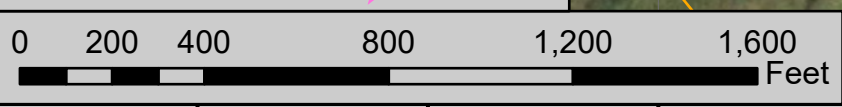
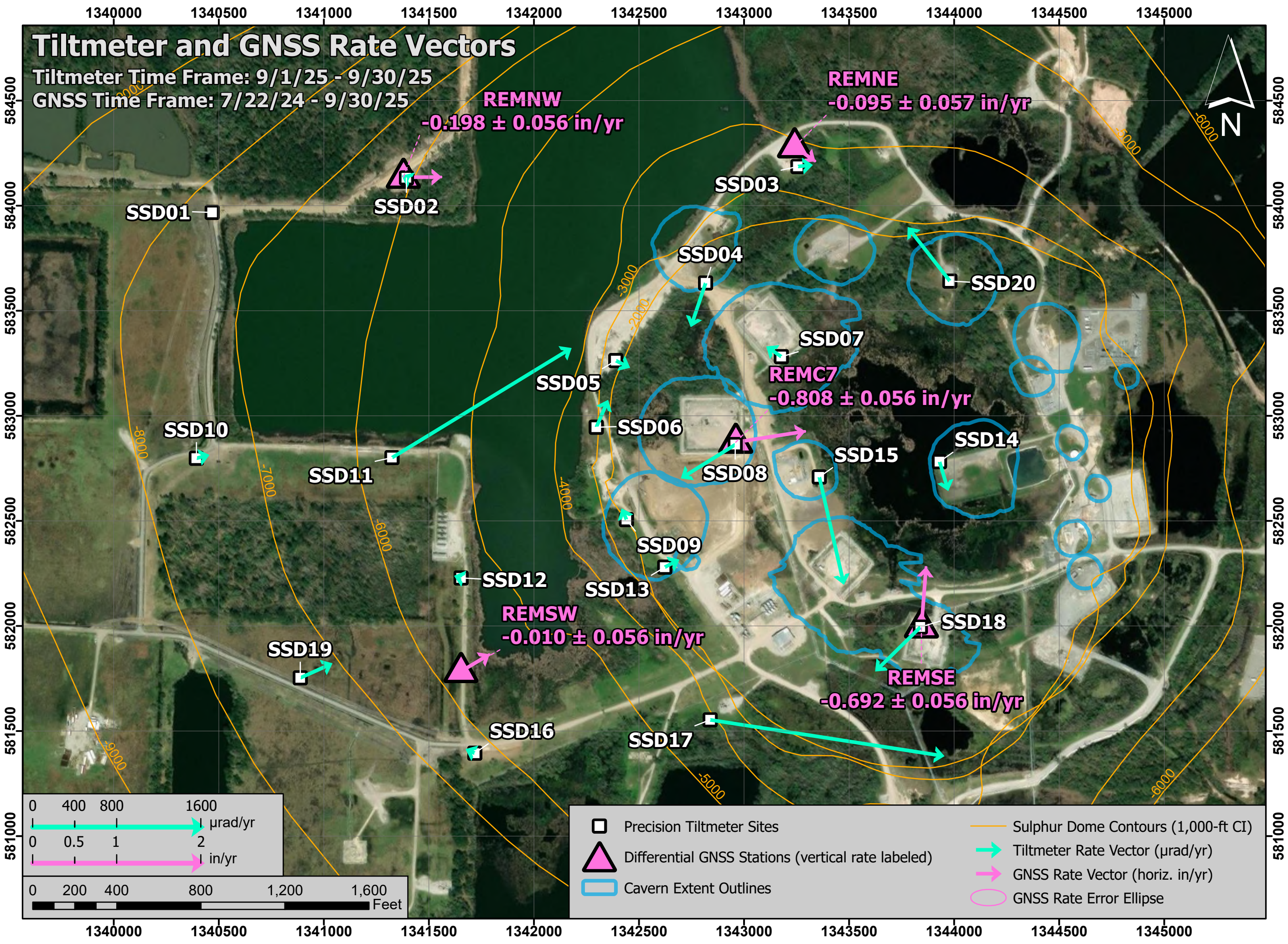
Local rate values have been calculated by removing the regional tectonic plate rates from the raw data displayed in the charts.

APPENDIX 3

Analysis Maps

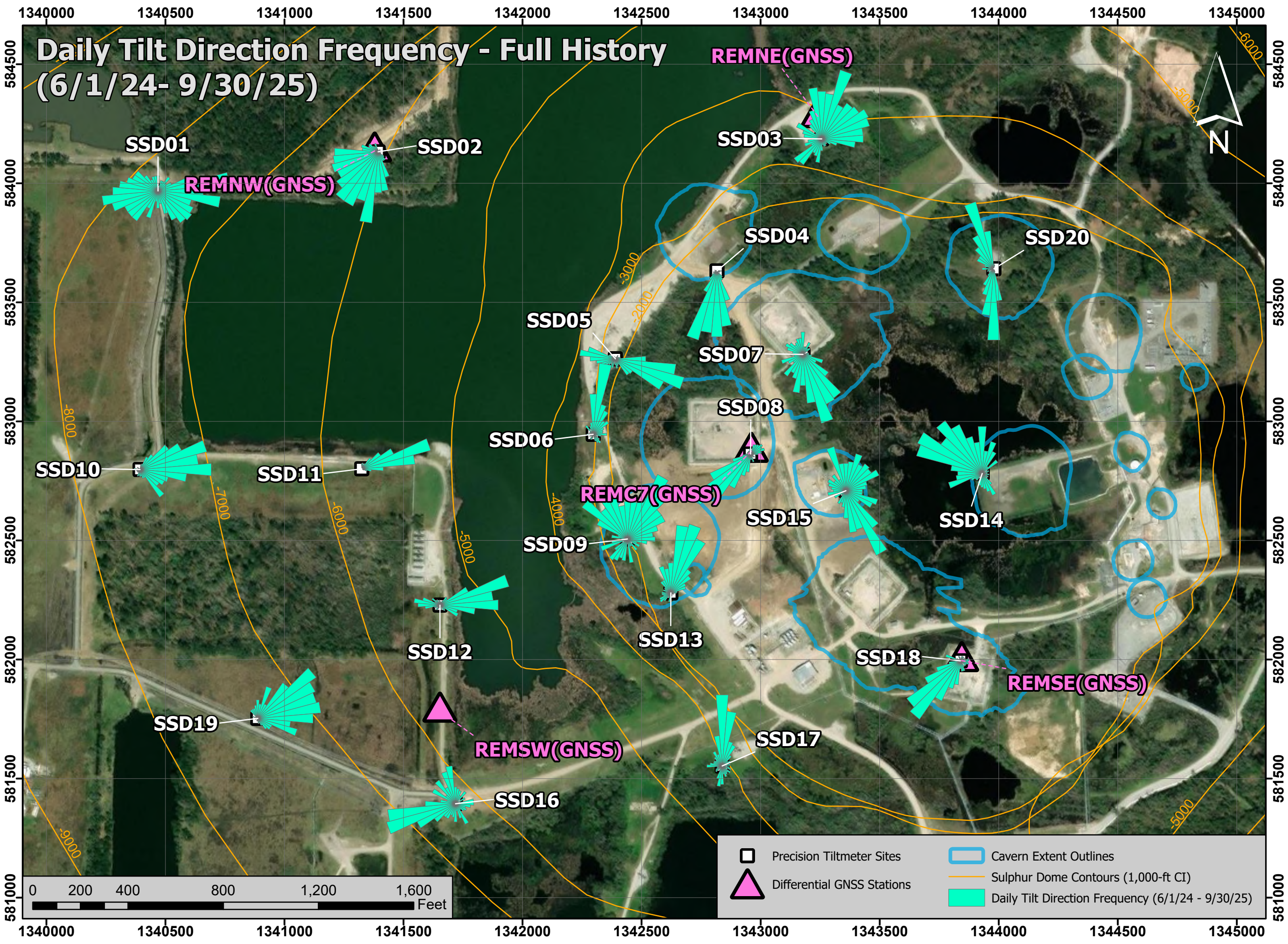
Tiltmeter and GNSS Rate Vectors






Tiltmeter Time Frame: 9/1/25 - 9/30/25
GNSS Time Frame: 7/22/24 - 9/30/25



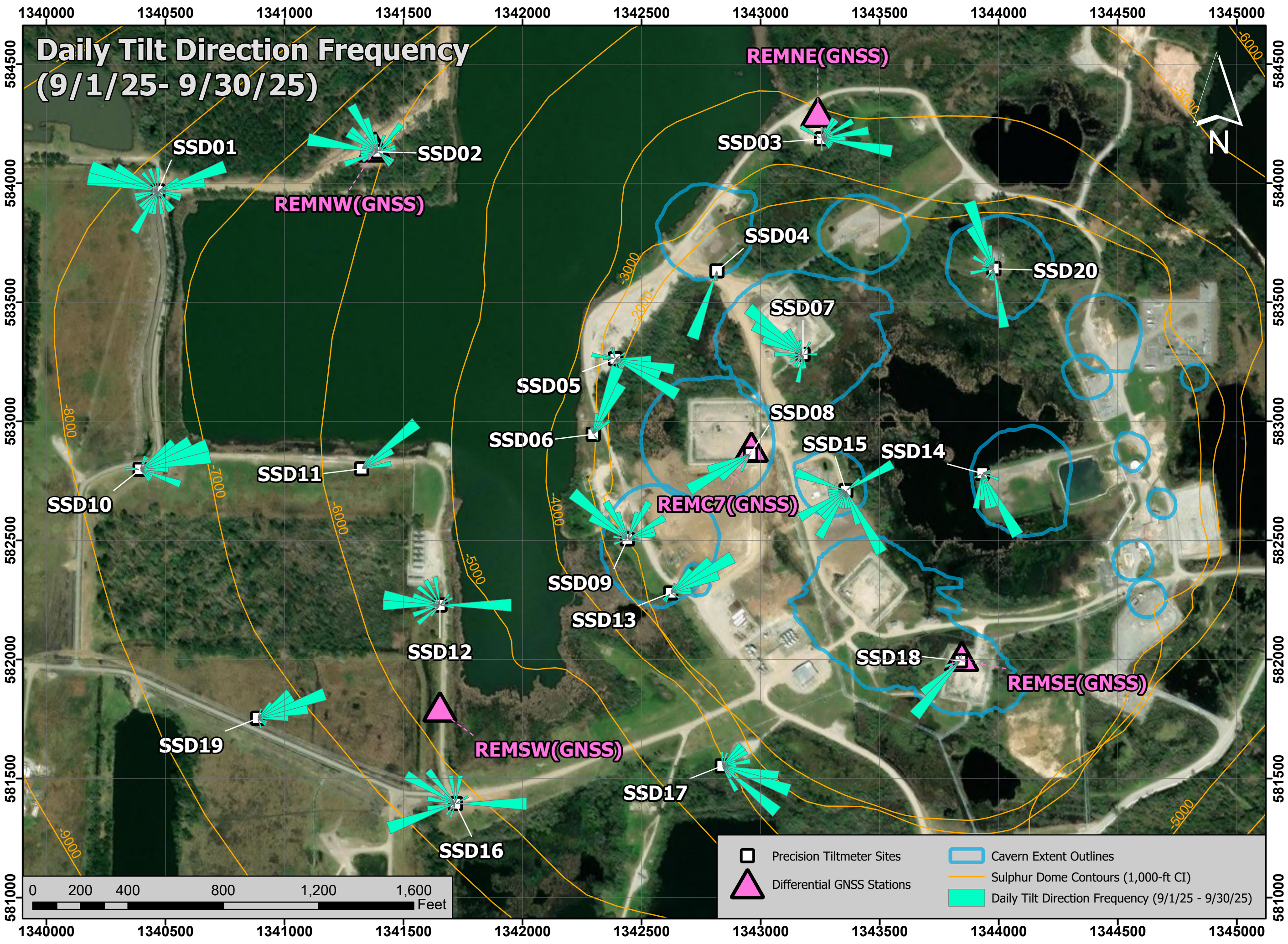
- Precision Tiltmeter Sites
- △ Differential GNSS Stations (vertical rate labeled)
- Cavern Extent Outlines
- Sulphur Dome Contours (1,000-ft CI)
- Tiltmeter Rate Vector ($\mu\text{rad/yr}$)
- GNSS Rate Vector (horiz. in/yr)
- GNSS Rate Error Ellipse

Daily Tilt Direction Frequency - Full History (6/1/24- 9/30/25)



	Precision Tiltmeter Sites		Cavern Extent Outlines
	Differential GNSS Stations		Sulphur Dome Contours (1,000-ft CI)
			Daily Tilt Direction Frequency (6/1/24 - 9/30/25)

Daily Tilt Direction Frequency (9/1/25- 9/30/25)



Location of GNSS and Tiltmeter Stations

Sulphur Mines Salt Dome

(Coordinate Datum: WGS 84)

Differential GNSS Stations		
Name	Latitude	Longitude
REMC7	30.253327	-93.414588
REMNE	30.257206	-93.413782
REMNW	30.256713	-93.419670
REMSE	30.250953	-93.411739
REMSW	30.250263	-93.418668
Off-dome Reference Station	30.257750	-93.426649

Precision Tiltmeter Sites		
Name	Latitude	Longitude
SSD01	30.256207	-93.422543
SSD02	30.256705	-93.419624
SSD03	30.256947	-93.413727
SSD04	30.255402	-93.415087
SSD05	30.254365	-93.416418
SSD06	30.253489	-93.416695
SSD07	30.254456	-93.413924
SSD08	30.253295	-93.414595
SSD09	30.252288	-93.416215
SSD10	30.252987	-93.422714
SSD11	30.253043	-93.419765
SSD12	30.251485	-93.418691
SSD13	30.251674	-93.415624
SSD14	30.253120	-93.411511
SSD15	30.252891	-93.413320
SSD16	30.249195	-93.418437
SSD17	30.249687	-93.414899
SSD18	30.250951	-93.411754
SSD19	30.250140	-93.421087
SSD20	30.255485	-93.411405

ATTACHMENT B

TSX-A InSAR report - September 29, 2025



TSX-A Satellite Update

Continuous InSAR Monitoring of
Ground Displacement At Westlake
Caverns and Western Dome Flank

Sulphur Mines Salt Dome

Prepared for:
Westlake Chemical

Prepared by:
Lonquist Field Service, LLC
8591 United Plaza Blvd., Suite 280
Baton Rouge, LA 70809

Dataset
Satellite Source
TerraSAR-X - Ascending
Most Recent Image Date
Monday, September 29, 2025

Analysis Report Date:
October 15, 2025

Dataset Information	
Satellite Source	TerraSAR-X - Ascending
Revisit Frequency	11 days
Most Recent Image Date	Monday, September 29, 2025
Dataset Image Count	81
Dataset Time Range	February 4, 2023 - September 29, 2025
Dataset Length	2.65 Years
Satellite Line-of-Sight (LOS)	44° West of Vertical (Viewing site from the West)

Analysis Methodology

Time Series Charts
Trend lines were calculated for the averaged displacement values within each AOI. Both a nonlinear (quadratic) and linear regression were applied to each AOI point group to identify rates of change in LOS displacement. These trends are displayed in the Time Series section of this report.

Contour Maps
A nonlinear (quadratic) and linear trend was also calculated for each individual measurement point across the analysis region. Nonlinear trend values for each point were used to generate Velocity and Acceleration contour maps to convey the spatial distribution of the calculated movement. The linear trend values for each point (which lack an acceleration component) were used to generate an additional Velocity contour map. Maps depicting the individual data points colored by these trend values are also included in the last section of the report.

Negative velocity values indicate subsidence or eastward movement and positive velocity indicates uplift or westward movement. Negative acceleration values indicate increasing rates of subsidence, increasing eastward movement, or slowing westward movement and positive acceleration values indicate slowing rates of subsidence, slowing eastward movement, or increasing westward movement.

Observations

To-date there have been no acute deviations from established subsidence trends in the areas investigated.

The time series charts show broadly consistent near-linear trends among the analysis AOIs. Acceleration values for the quadratic (non-linear) trend fit are negative in all AOIs (increasing negative displacement rates) but minor overall. A slight seasonal fluctuation may be evident in some of the charts, but with less prominence than in the TSX/PAZ data.

The contour maps show the greatest negative displacement centered around the western central portion of the dome where the combination of subsidence and eastern horizontal movement (toward dome center) are expected to produce the greatest rate of movement away from the satellite's line of sight from the west.



Date Signed: October 15, 2025
Austin, Texas

Nathaniel L. Byars, P.E.
Principal Engineer
Louisiana License No. 40697

InSAR Data Sources

InSAR Data

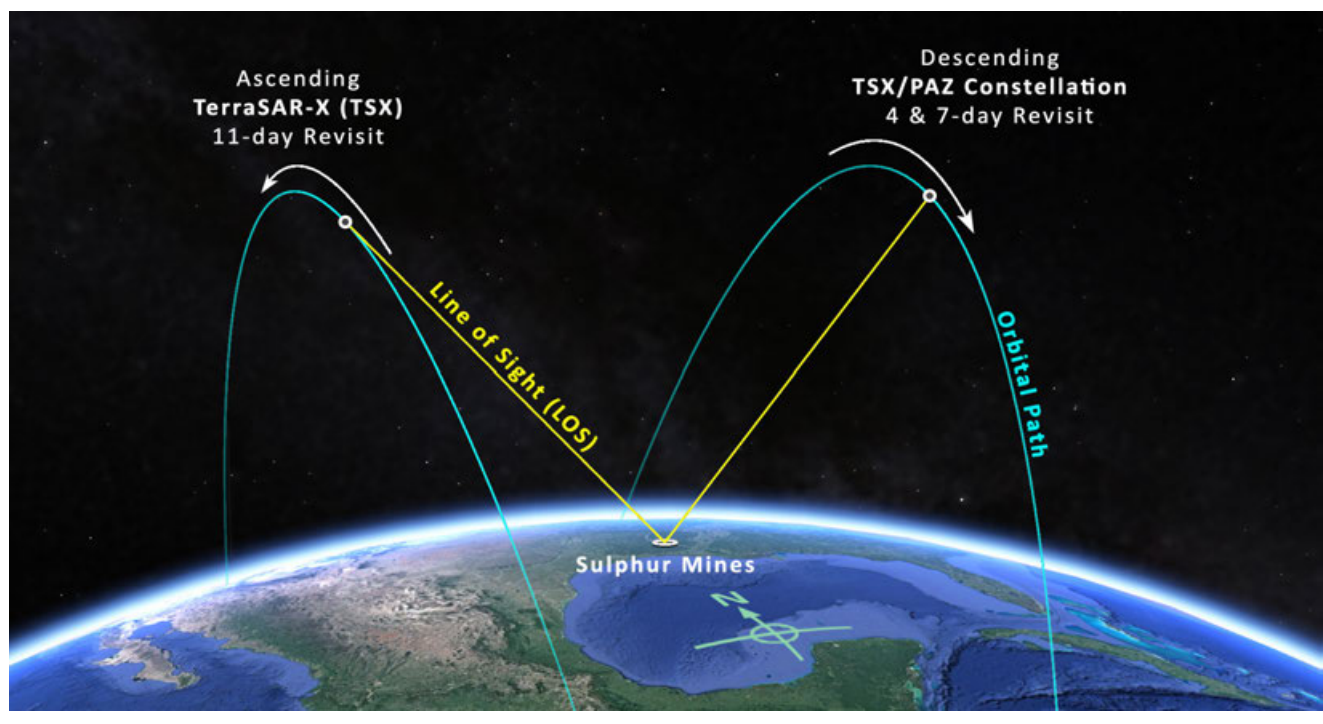
Interferometric Synthetic Aperture Radar (InSAR) is the most well established method to continually evaluate small, normally undetectable, ground movement over a large area. Radar imagery collected via satellites over successive orbital passes is used to identify and define measurement points on the ground. Objects or ground features providing a stable reflection of radar energy such as buildings, roads, and infrastructure produce the highest quality measurement points. InSAR analysis identifies the change in distance between the satellite and each measurement point over time relative to a stable reference point within the imaged area.

Satellite Sources

Two InSAR datasets are being used to evaluate subsidence over the Sulphur Mines Salt Dome. These datasets provide Line-of-Sight (LOS) displacement measurements from both ascending and descending orbits. An ascending orbit denotes the satellite's longitudinal course from south to north as it passes over the site, while a descending orbit denotes the satellite is moving from north to south.

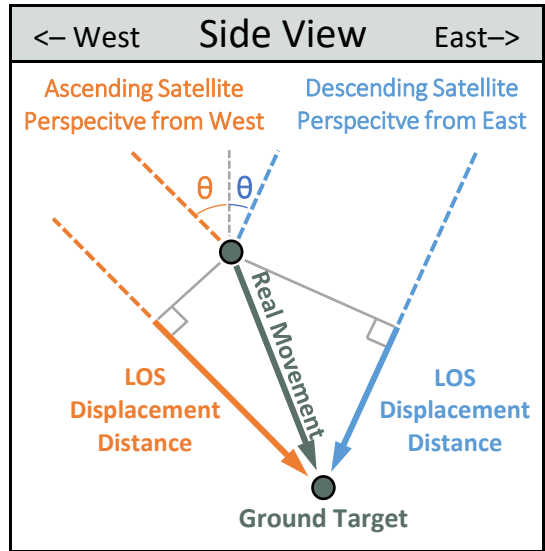
The first dataset comes from the high-resolution TerraSAR-X satellite on an ascending orbit track ("TSX-A") that captures data from the west of the site on an 11-day frequency. The second comes from a pair of high-resolution satellites that include the TerraSAR-X satellite and the PAZ satellite ("TSX/PAZ Constellation") which share the same descending orbit track and capture data from east of the site, each with an 11-day frequency. Their orbits are offset with the PAZ satellite passing over the site 4 days after the TSX satellite. Prior to May 2024, the ascending data was captured from a low-resolution Sentinel-1 satellite at a similar viewing angle to the TSX orbit. The transition to the ascending TSX track was made to increase data accuracy and measurement point density once a suitable data history had been gathered for trend analysis. The image below depicts the orbital paths of the current satellites in relation to the Sulphur Mines Salt Dome.

Satellite Orbital Diagram



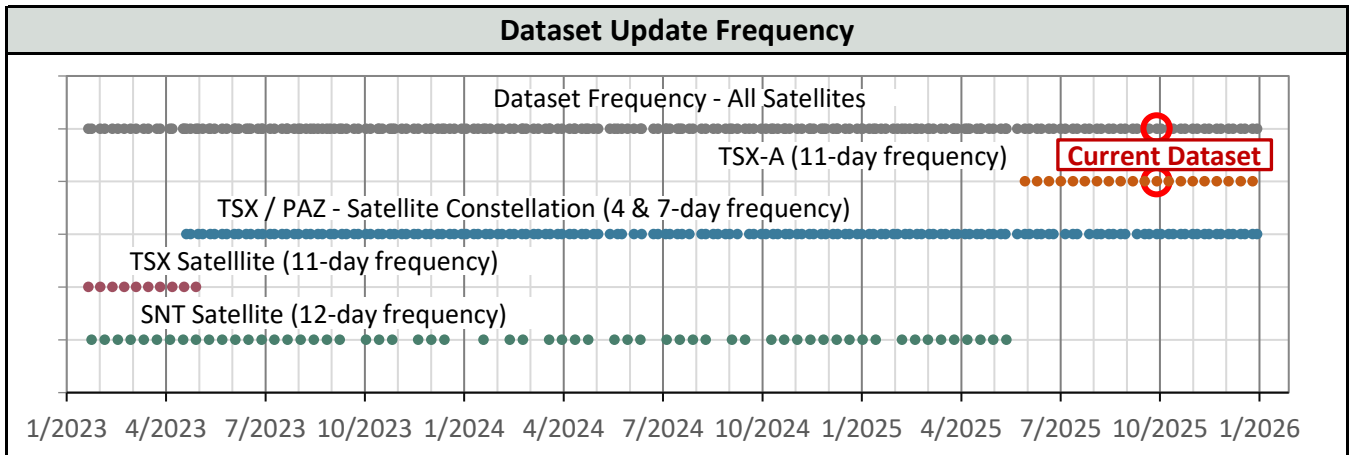
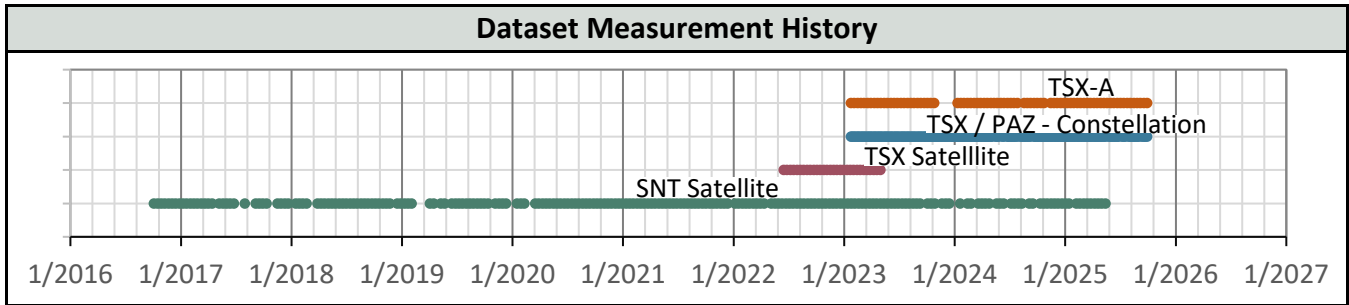
InSAR Line-of-Site (LOS) Data

LOS displacement measurements refer to a change in distance between the satellite sensor and the ground target. Measurement positions on the west side of the Sulphur Dome are known to be experiencing some eastward movement toward the dome center due to the geometry of the subsidence basin. The InSAR satellites view the site from eastward and westward positions so LOS measurements are understood to convey a movement distance that is not purely vertical. The diagram to the right illustrates the geometric relationship between the theoretical Real movement of a ground target and LOS displacement measurements from two different satellite viewing directions.

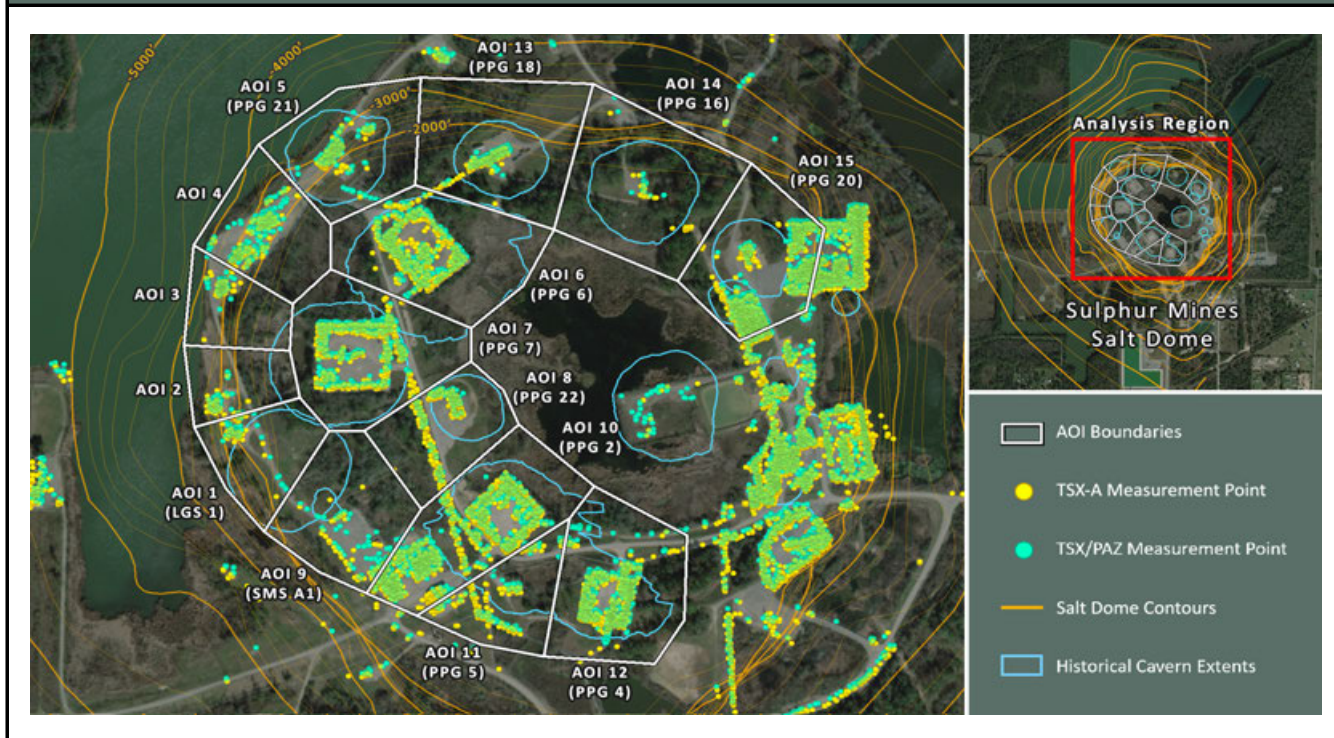


Satellite Properties & Image Frequency

Satellite and Data Properties	SNT	TSX-A	TSX/PAZ Constellation
Band (Wavelength)	C-band (2.32 in)	X-band (1.22 in)	X-band (1.22 in)
Track	T136	T52	T67 & T120
Pixel resolution	65 x 16 ft	3 x 3 ft	3 x 3 ft
Revisit frequency	12 days	11 days	4 & 7 days
Orbit (LOS Angle, θ)	Ascending (42°)	Ascending (44°)	Descending (37°)
Data Start Date	10/4/2016	2/4/2023	1/24/2023
Measurement error range	± 0.20 in	± 0.06 in	± 0.07 in



AOI Boundaries & InSAR Measurement Points

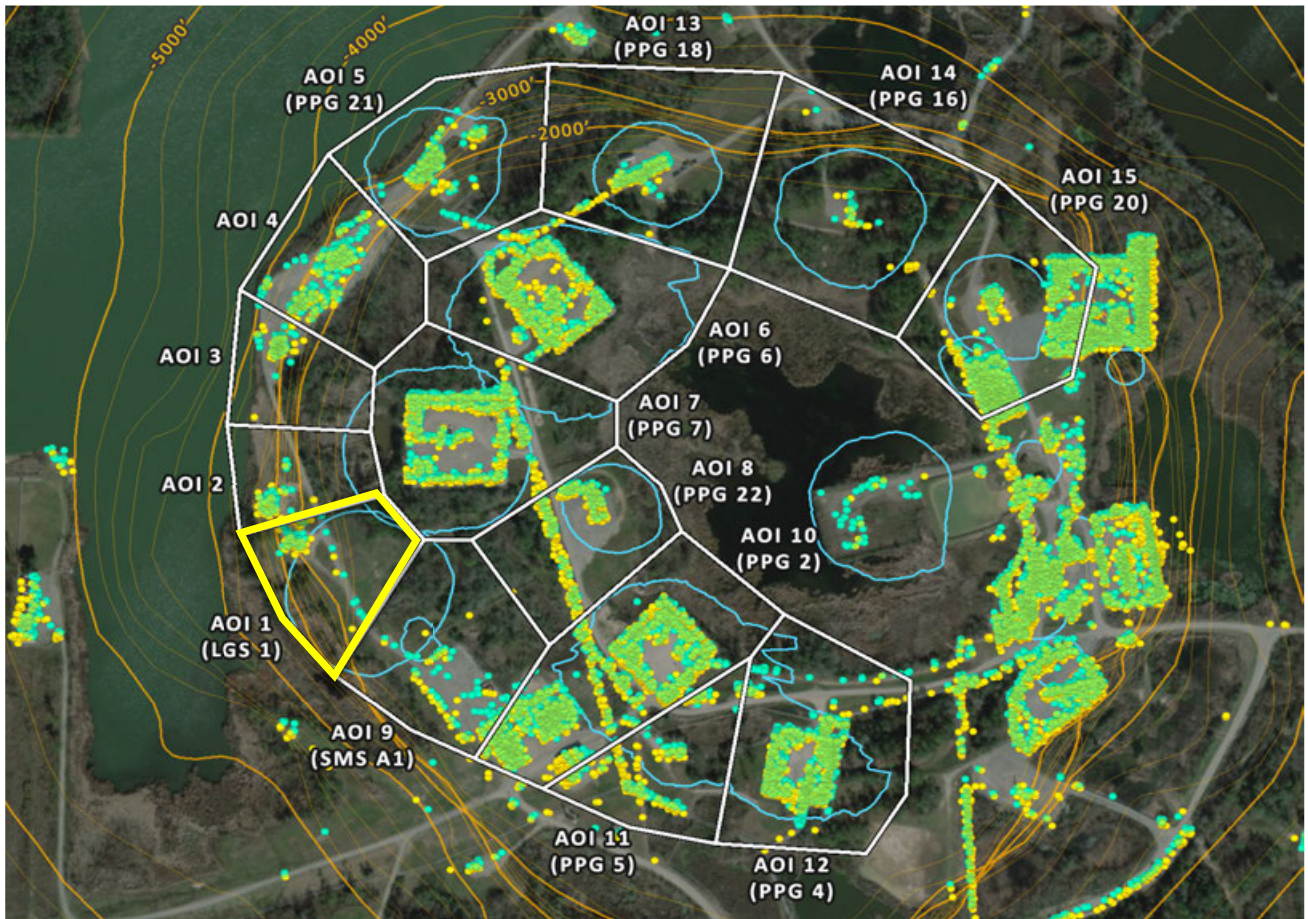


Subsidence Monitoring Areas of Interest (AOIs)

To visually convey and evaluate trend consistency for the displacement time series of each ground target, measurement points were grouped and their displacement values were averaged. The point groups are referred to as Areas of Interest (AOIs) in this analysis and their boundaries are depicted on the above map. The below table lists the trend values calculated in each AOI for the dataset evaluated in this report.

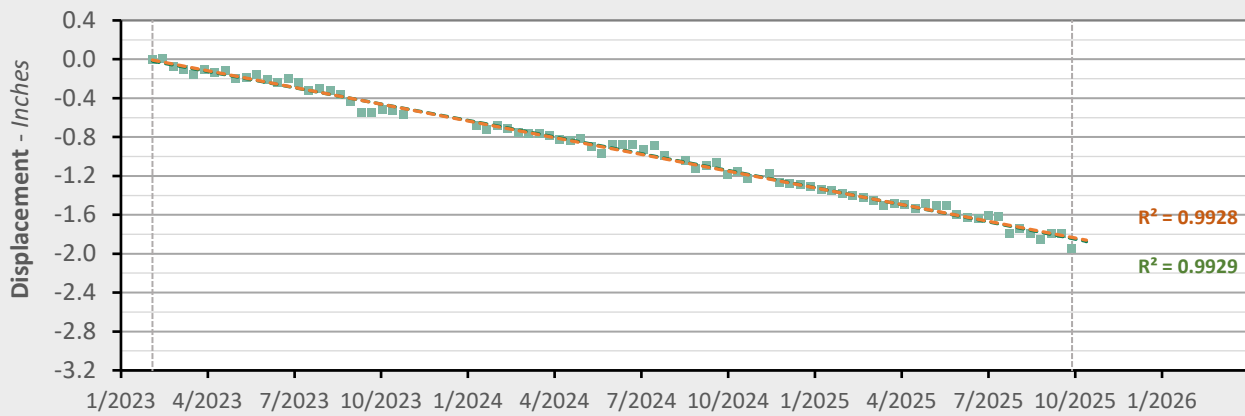
AOI Name	TSX-A (9/29/2025)	LOS Velocity (in/yr)		LOS Acceleration (in/yr ²)	
	Point Count	Nonlinear	Linear	Nonlinear	Linear
AOI 1 (LGS 1)	51	-0.72	-0.69	-0.02	0.00
AOI 2	39	-0.72	-0.69	-0.02	0.00
AOI 3	55	-0.67	-0.60	-0.05	0.00
AOI 4	124	-0.66	-0.61	-0.03	0.00
AOI 5 (PPG 21)	111	-0.61	-0.54	-0.05	0.00
AOI 6 (PPG 6)	408	-0.98	-0.84	-0.10	0.00
AOI 7 (PPG 7)	371	-1.15	-1.00	-0.11	0.00
AOI 8 (PPG 22)	188	-1.24	-1.13	-0.09	0.00
AOI 9 (SMS A1)	50	-0.80	-0.77	-0.02	0.00
AOI 10 (PPG 2)	813	-1.07	-0.93	-0.10	0.00
AOI 11 (PPG 5)	154	-0.94	-0.79	-0.11	0.00
AOI 12 (PPG 4)	326	-0.73	-0.65	-0.06	0.00
AOI 13 (PPG 18)	93	-0.69	-0.63	-0.05	0.00
AOI 14 (PPG 16)	22	-0.49	-0.38	-0.09	0.00
AOI 15 (PPG 20)	526	-0.32	-0.23	-0.07	0.00

AOI 1 (LGS 1) - Location Map

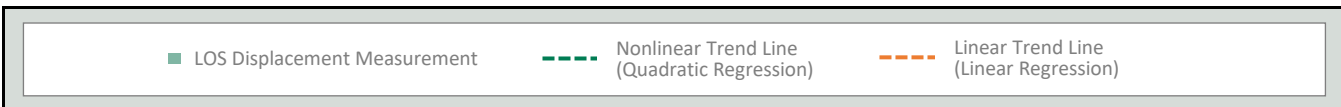


AOI 1 (LGS 1) - Displacement Time Series

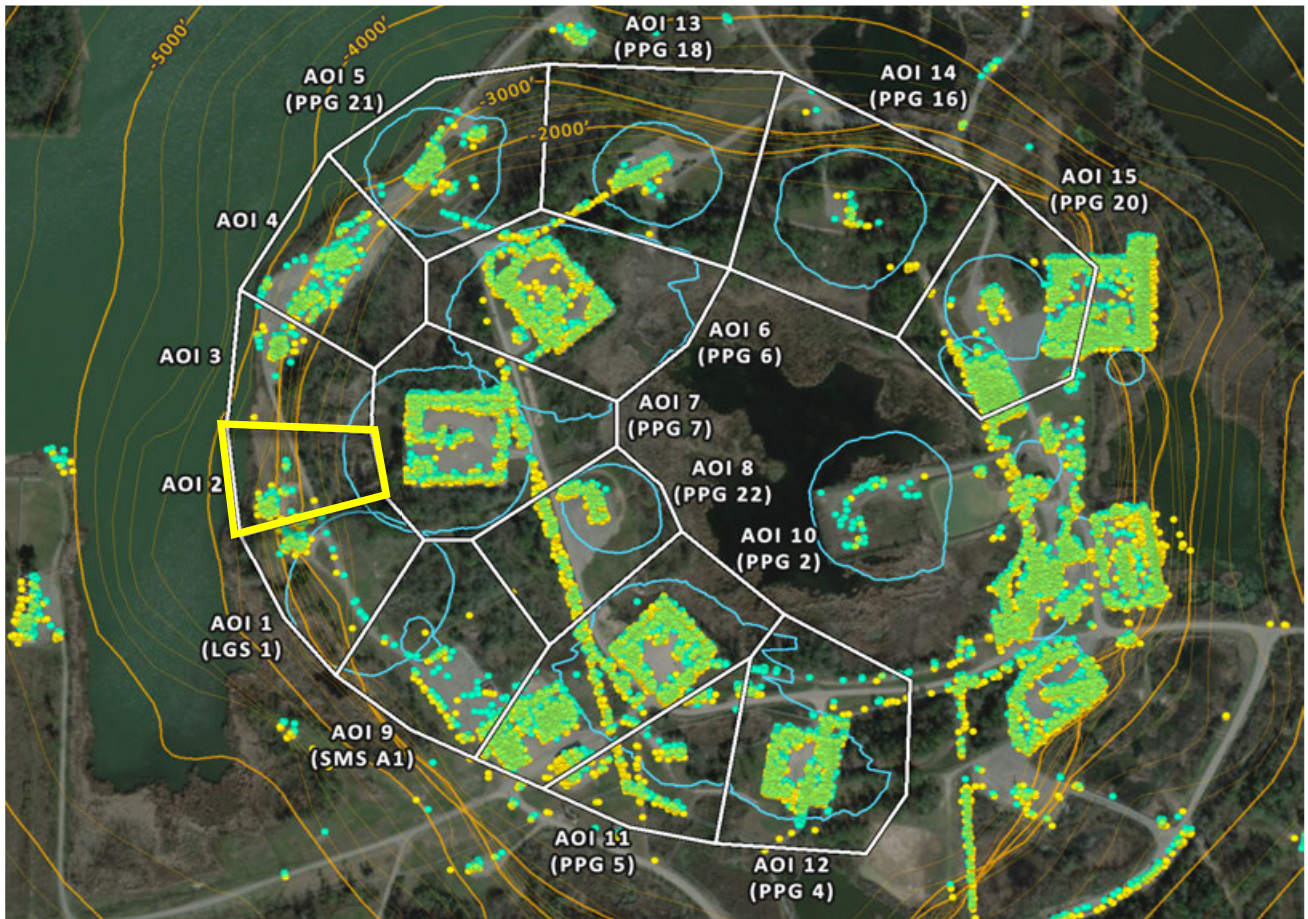
TSX-A (9/29/2025) Point Count: 51



	Nonlinear Trend	Linear Trend
Velocity:	-0.72 in/yr	-0.69 in/yr
Acceleration:	-0.02 in/yr ²	0.00 in/yr ²

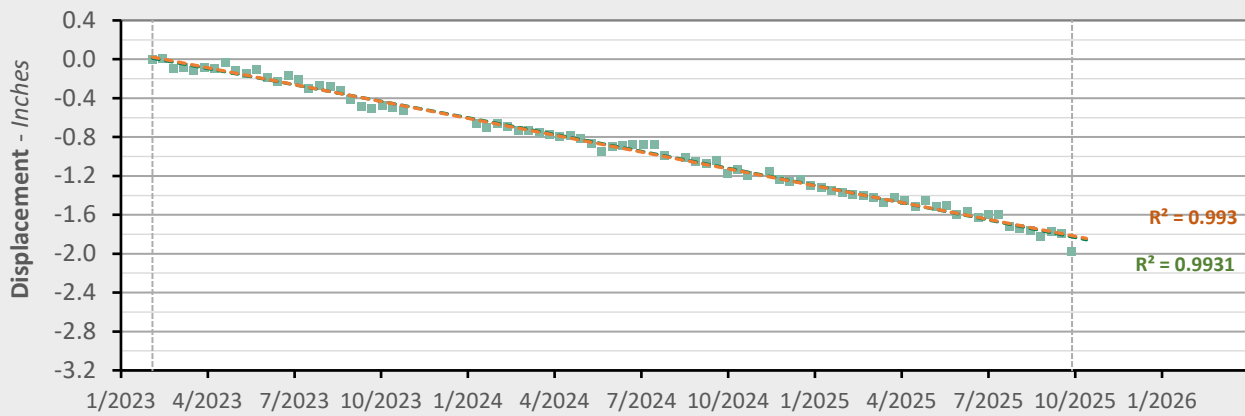


AOI 2 - Location Map

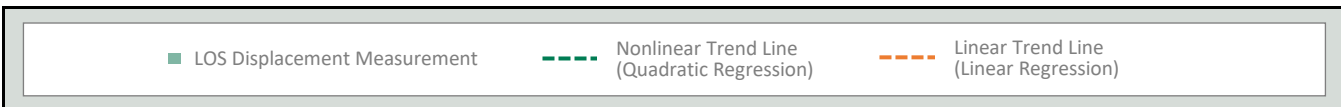


AOI 2 - Displacement Time Series

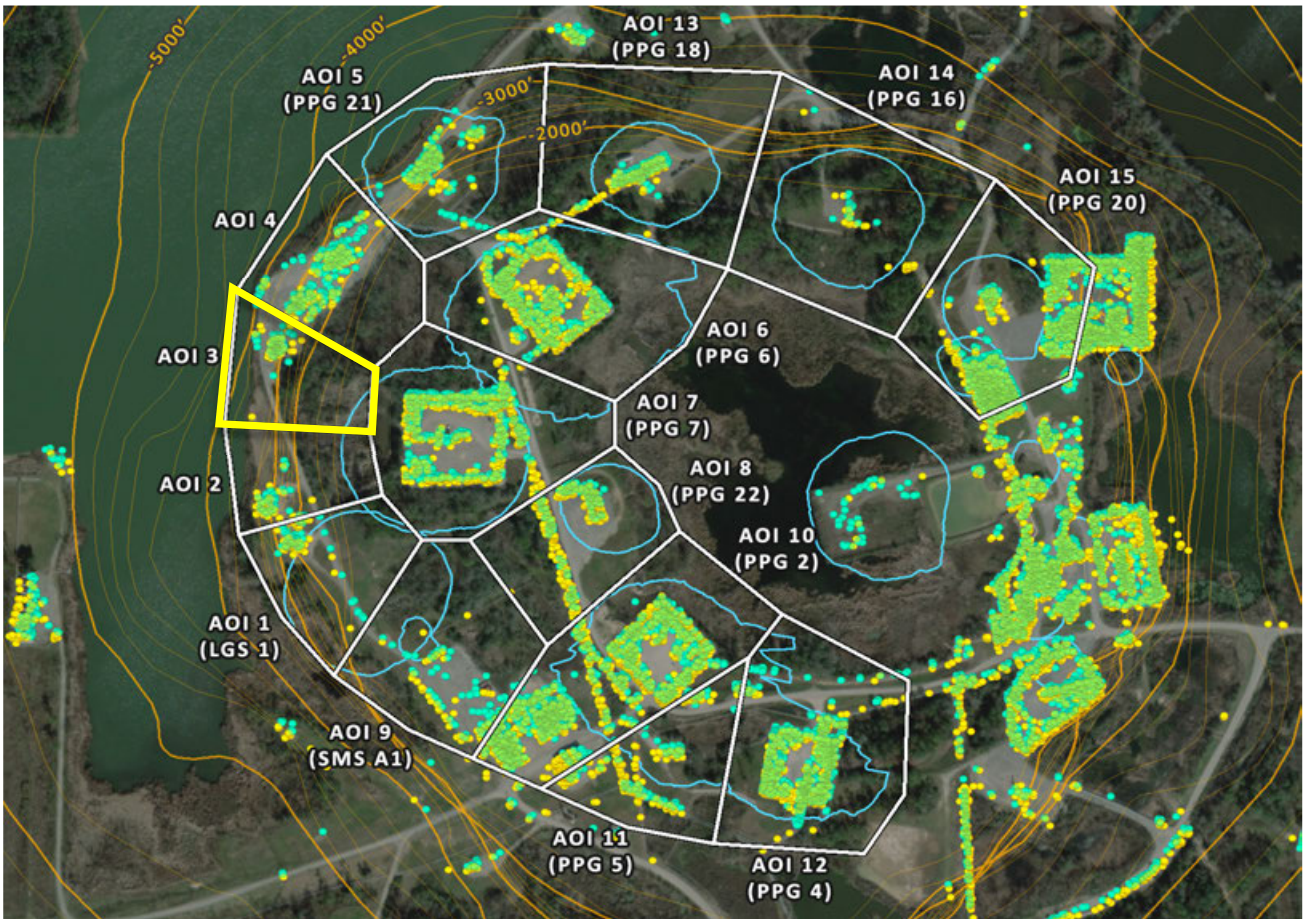
TSX-A (9/29/2025) Point Count: 39



	Nonlinear Trend	Linear Trend
Velocity:	-0.72 in/yr	-0.69 in/yr
Acceleration:	-0.02 in/yr ²	0.00 in/yr ²

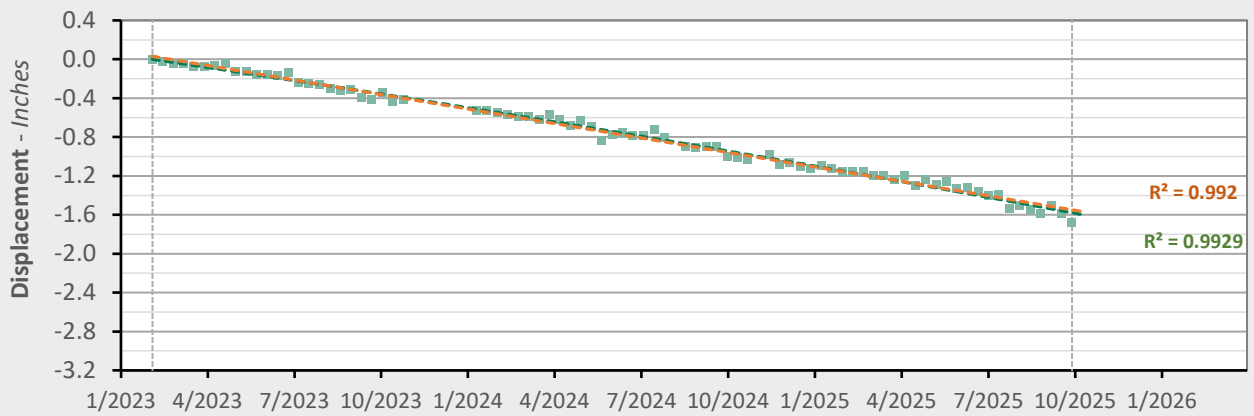


AOI 3 - Location Map

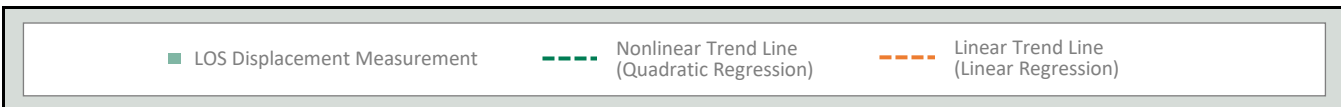


AOI 3 - Displacement Time Series

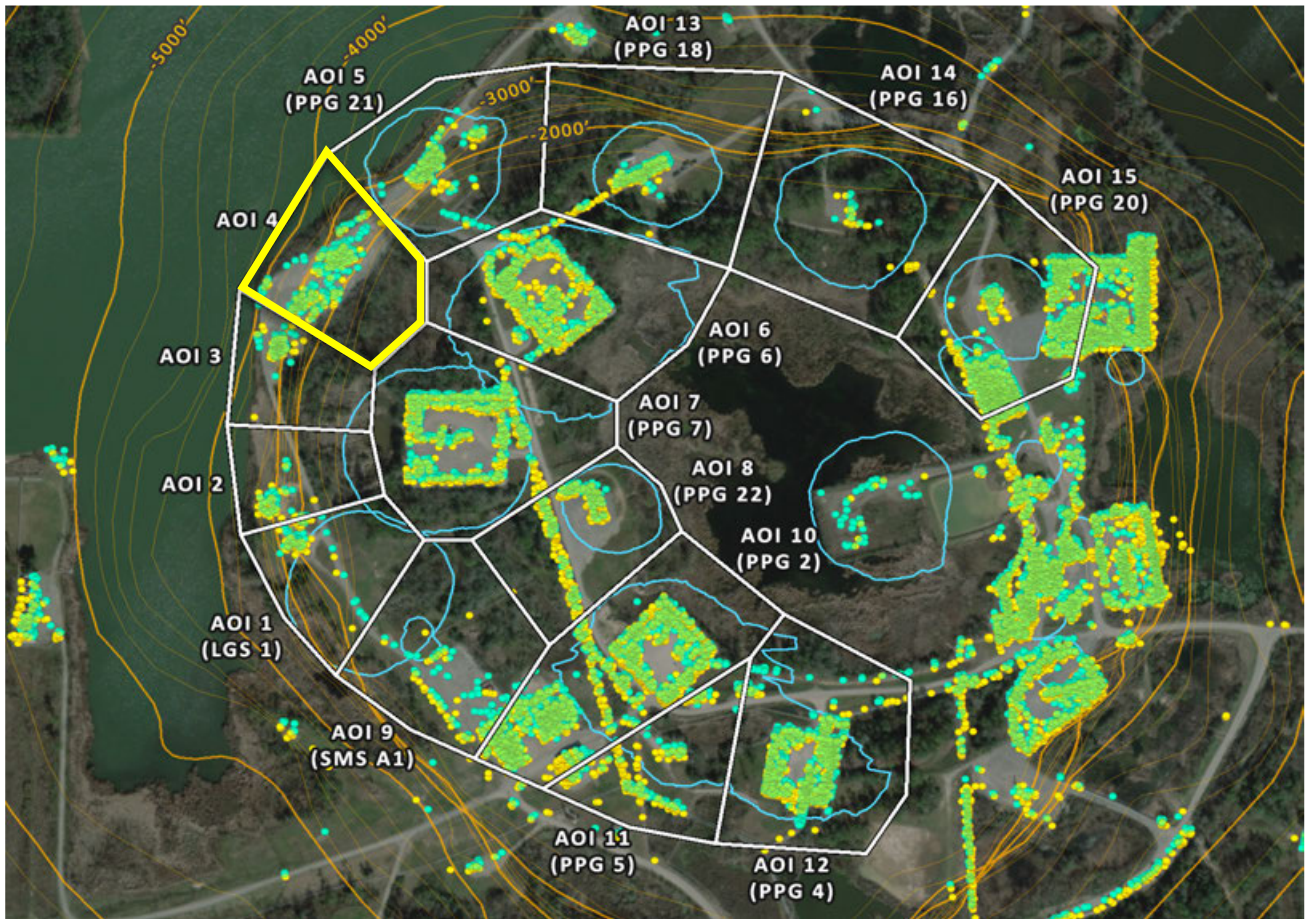
TSX-A (9/29/2025) Point Count: 55



	Nonlinear Trend	Linear Trend
Velocity:	-0.67 in/yr	-0.60 in/yr
Acceleration:	-0.05 in/yr ²	0.00 in/yr ²

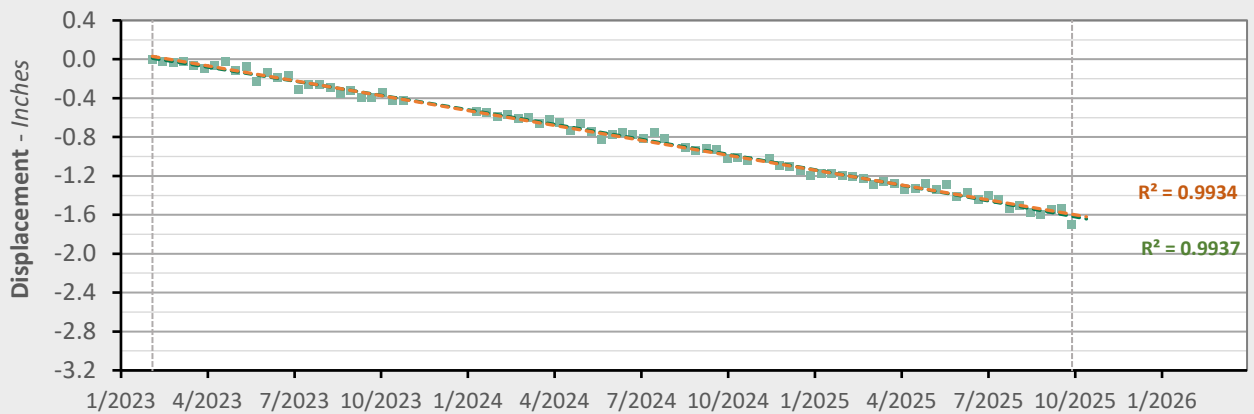


AOI 4 - Location Map

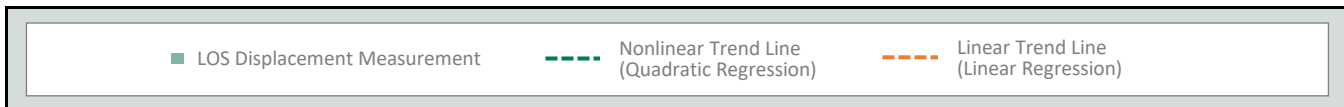


AOI 4 - Displacement Time Series

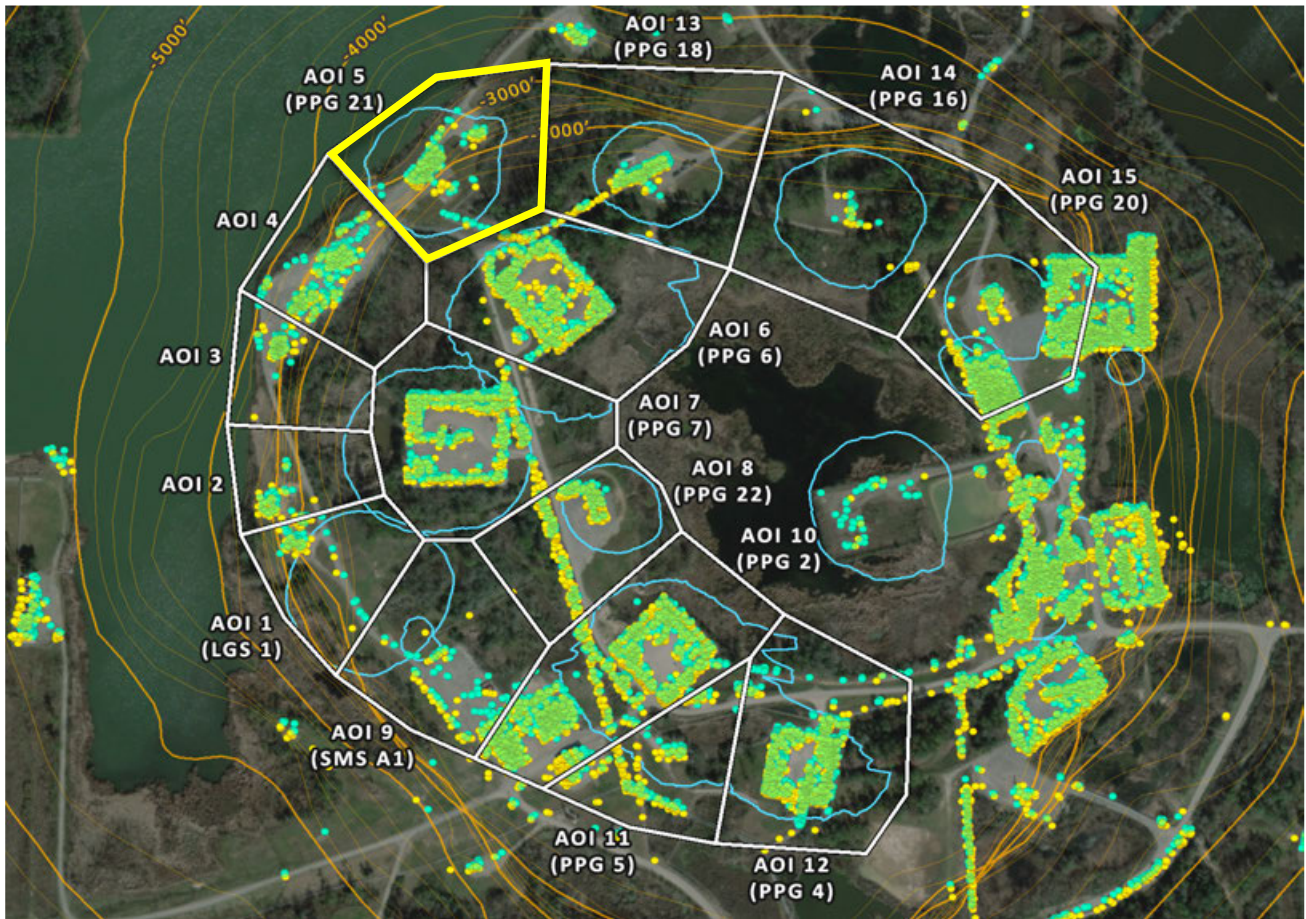
TSX-A (9/29/2025) Point Count: **124**



	Nonlinear Trend	Linear Trend
Velocity:	-0.66 in/yr	-0.61 in/yr
Acceleration:	-0.03 in/yr ²	0.00 in/yr ²

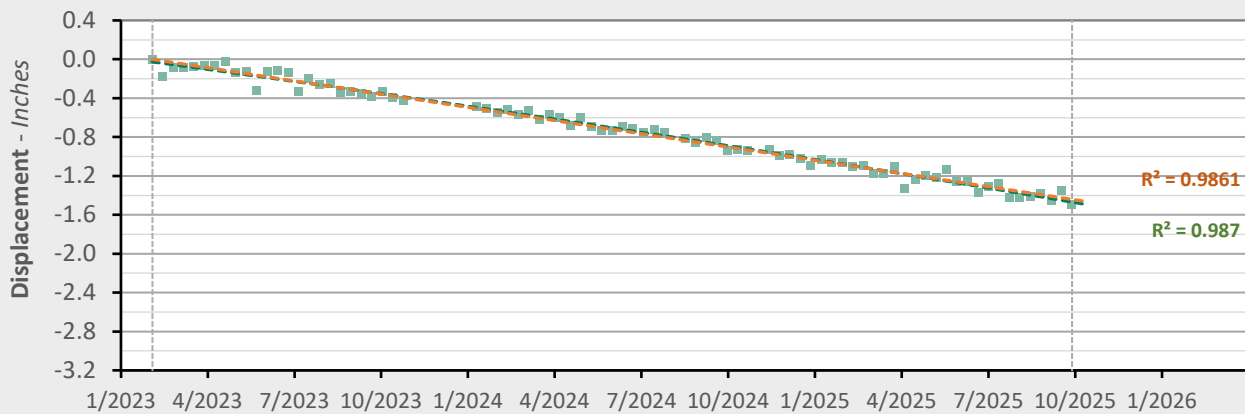


AOI 5 (PPG 21) - Location Map

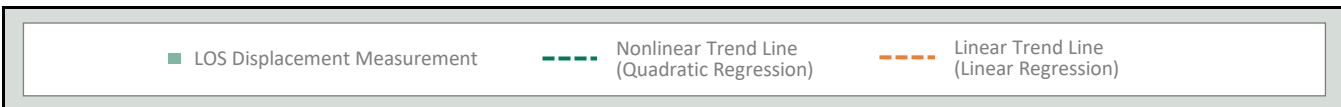


AOI 5 (PPG 21) - Displacement Time Series

TSX-A (9/29/2025) Point Count: **111**



	Nonlinear Trend	Linear Trend
Velocity:	-0.61 in/yr	-0.54 in/yr
Acceleration:	-0.05 in/yr ²	0.00 in/yr ²

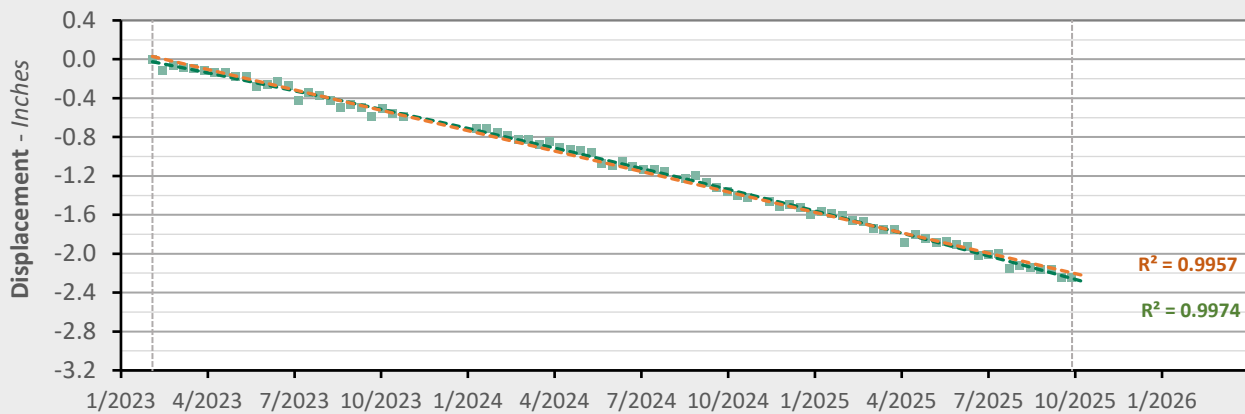


AOI 6 (PPG 6) - Location Map

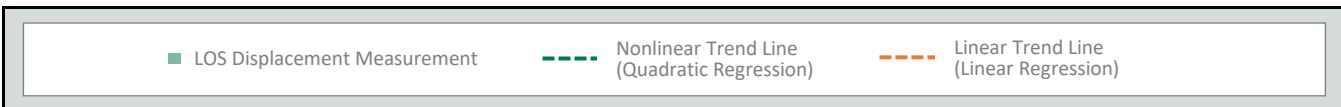


AOI 6 (PPG 6) - Displacement Time Series

TSX-A (9/29/2025) Point Count: 408



	Nonlinear Trend	Linear Trend
Velocity:	-0.98 in/yr	-0.84 in/yr
Acceleration:	-0.10 in/yr ²	0.00 in/yr ²

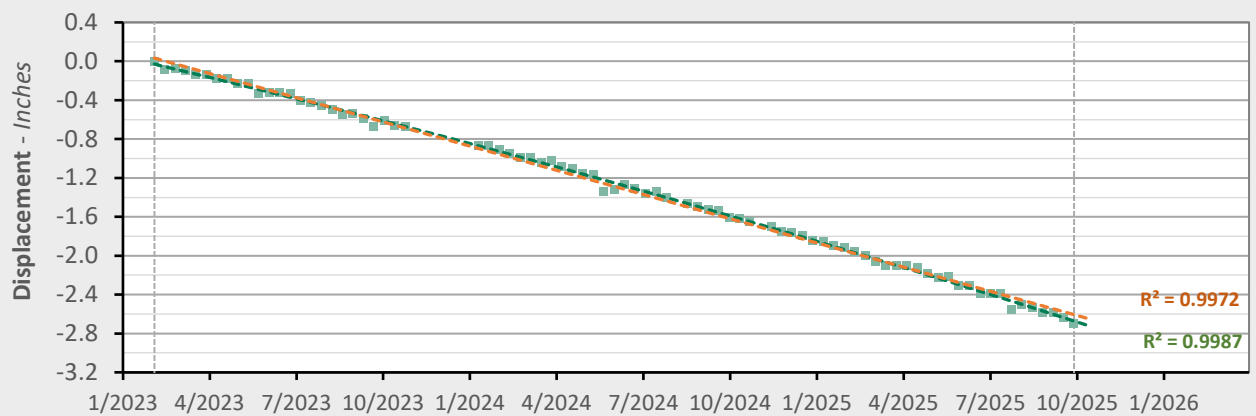


AOI 7 (PPG 7) - Location Map

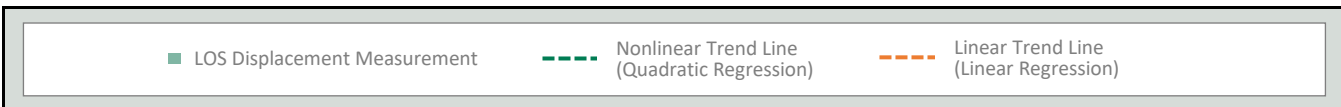


AOI 7 (PPG 7) - Displacement Time Series

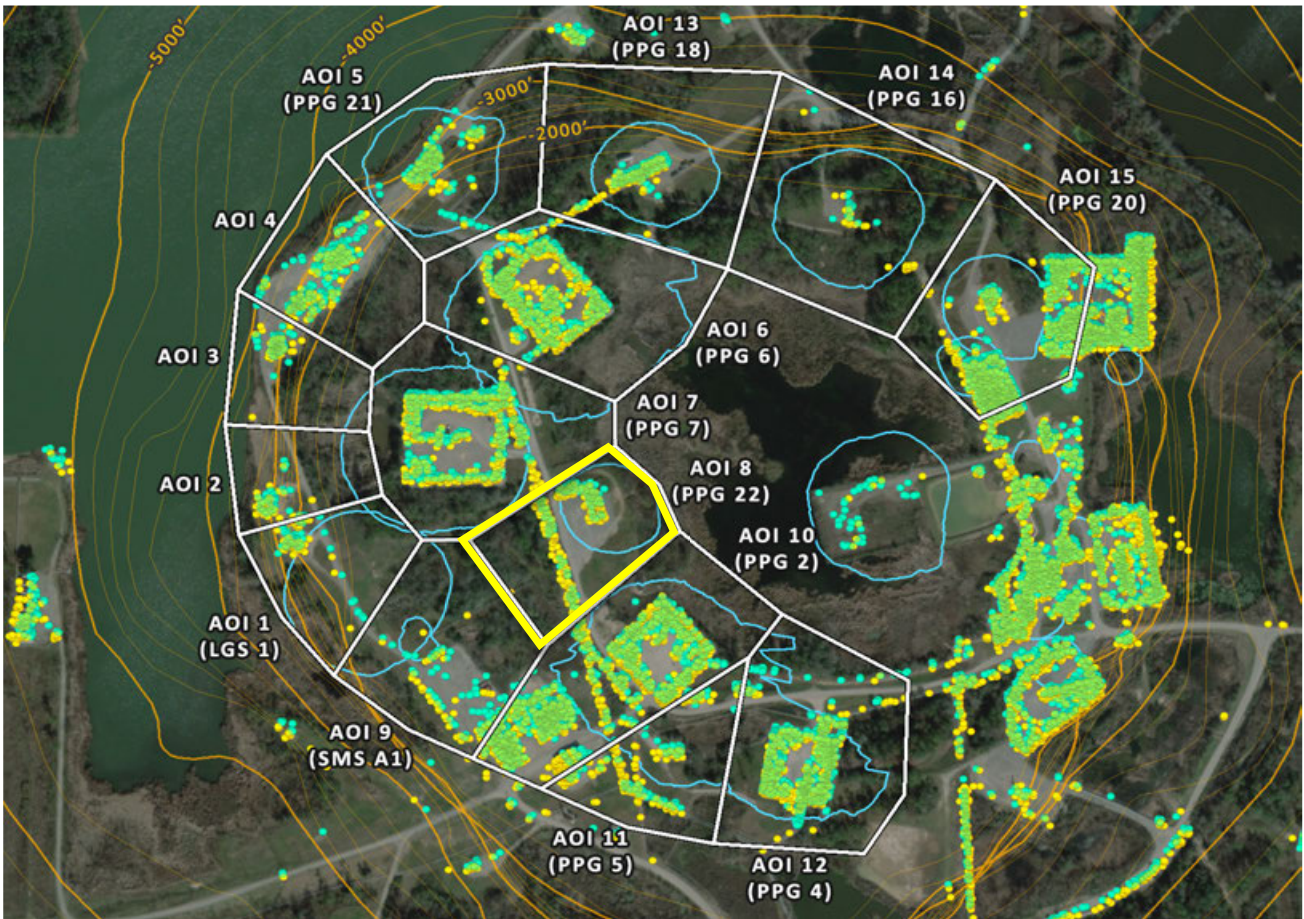
TSX-A (9/29/2025) Point Count: **371**



	Nonlinear Trend	Linear Trend
Velocity:	-1.15 in/yr	-1.00 in/yr
Acceleration:	-0.11 in/yr ²	0.00 in/yr ²

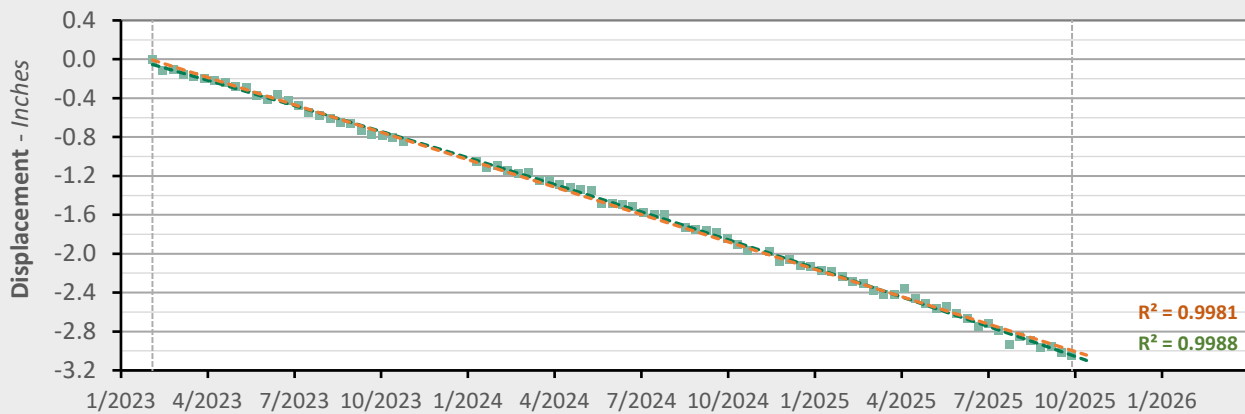


AOI 8 (PPG 22) - Location Map

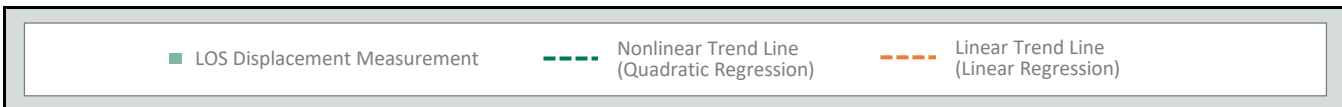


AOI 8 (PPG 22) - Displacement Time Series

TSX-A (9/29/2025) Point Count: **188**



	Nonlinear Trend	Linear Trend
Velocity:	-1.24 in/yr	-1.13 in/yr
Acceleration:	-0.09 in/yr ²	0.00 in/yr ²

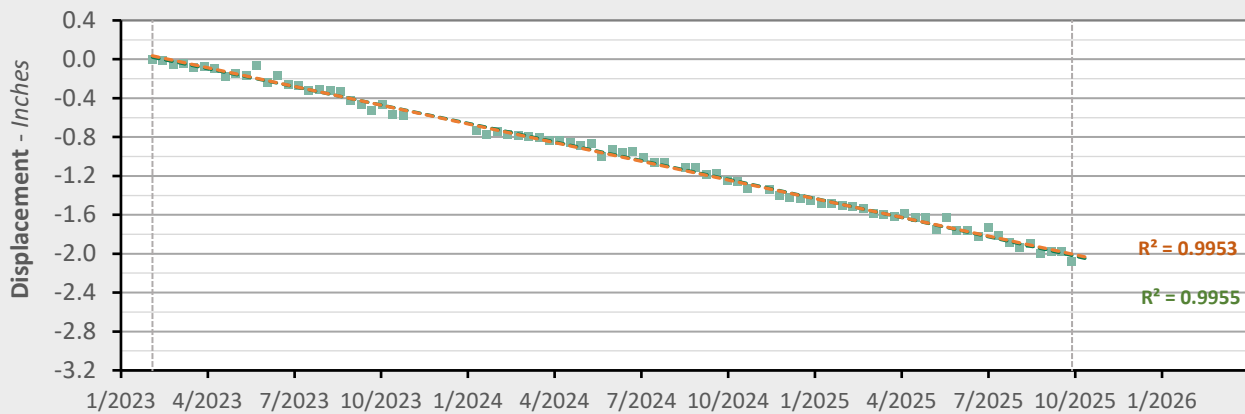


AOI 9 (PPG A1) - Location Map

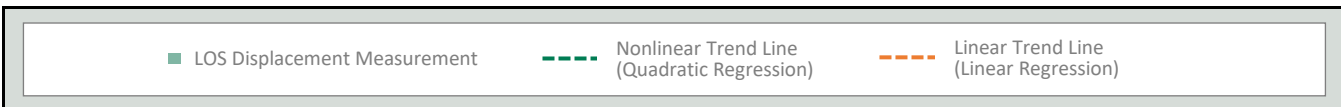


AOI 9 (SMS A1) - Displacement Time Series

TSX-A (9/29/2025) Point Count: 50



	Nonlinear Trend	Linear Trend
Velocity:	-0.80 in/yr	-0.77 in/yr
Acceleration:	-0.02 in/yr ²	0.00 in/yr ²

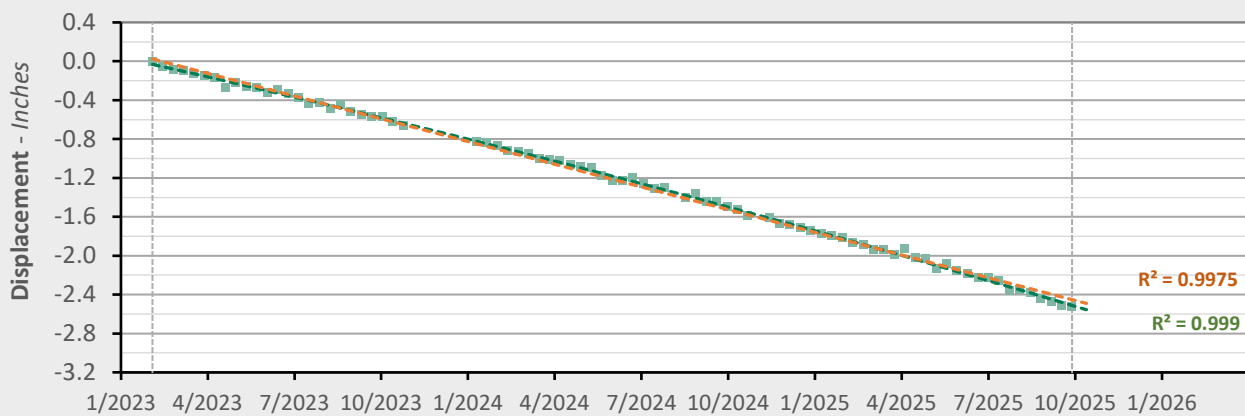


AOI 10 (PPG 2) - Location Map

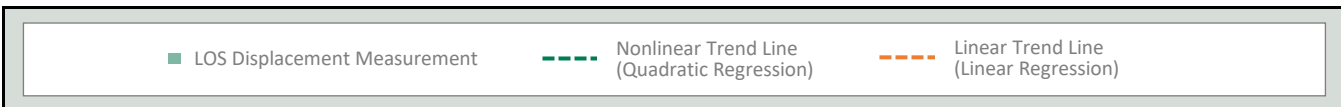


AOI 10 (PPG 2) - Displacement Time Series

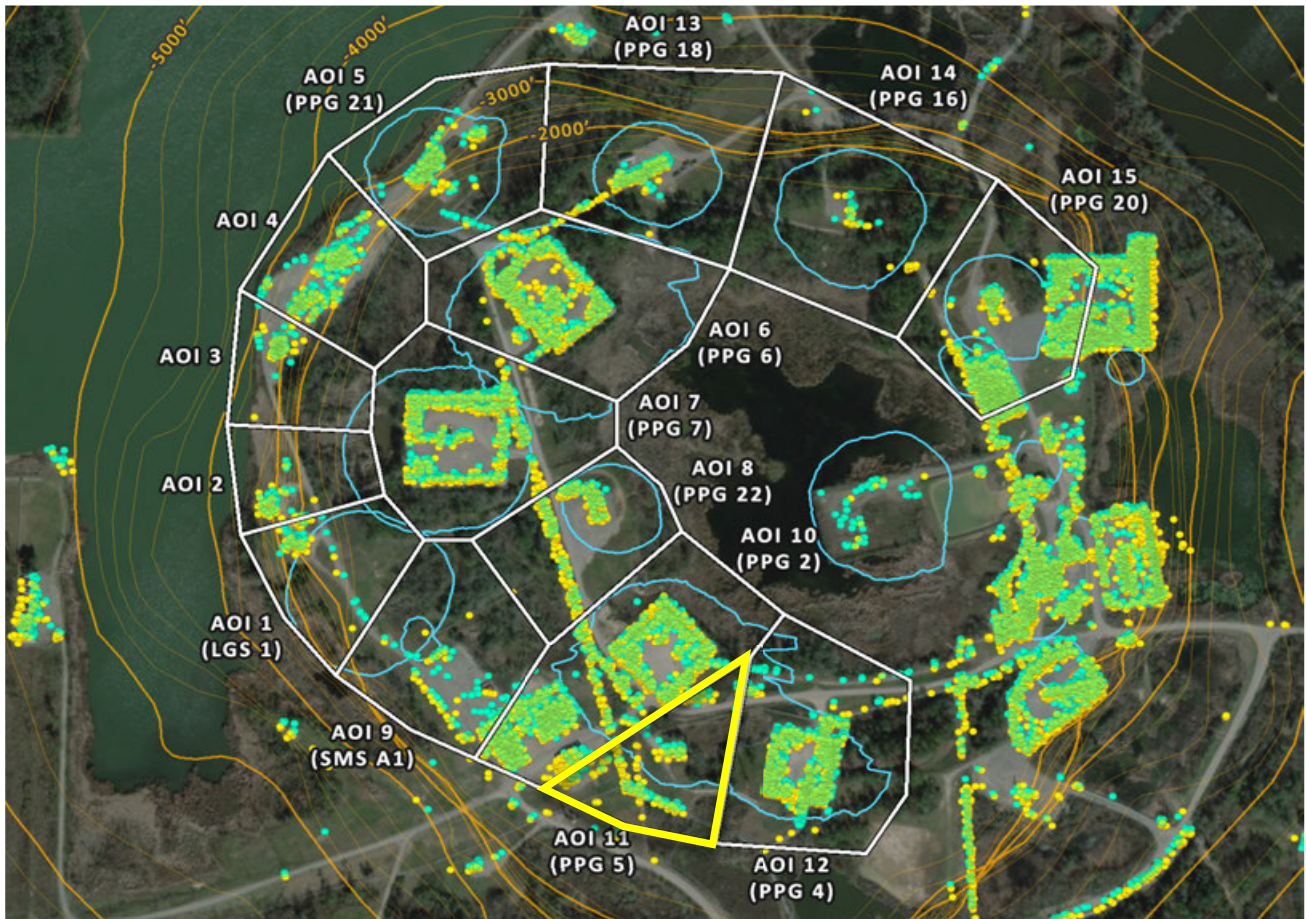
TSX-A (9/29/2025) Point Count: **813**



	Nonlinear Trend	Linear Trend
Velocity:	-1.07 in/yr	-0.93 in/yr
Acceleration:	-0.10 in/yr ²	0.00 in/yr ²

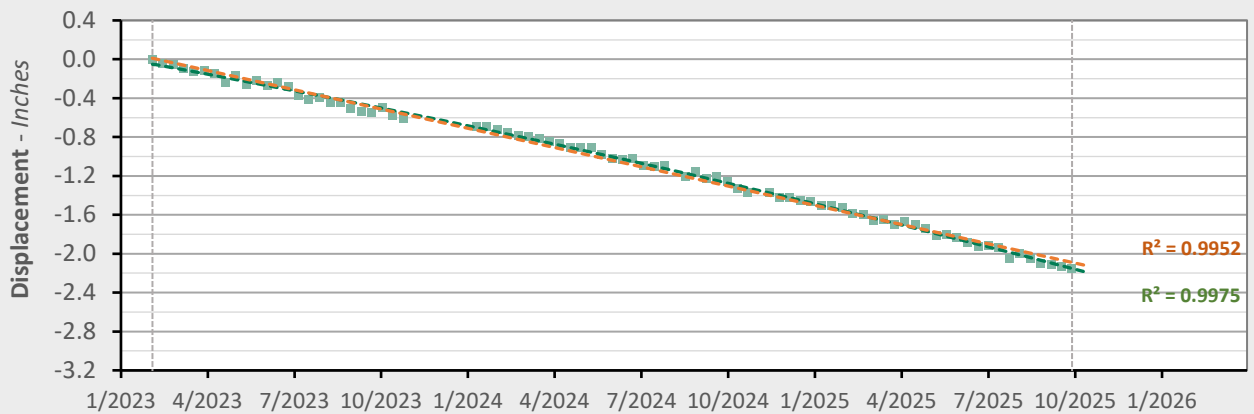


AOI 11 (PPG 5) - Location Map

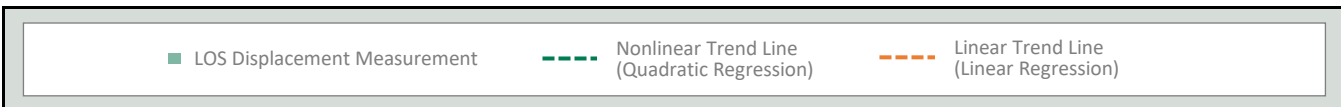


AOI 11 (PPG 5) - Displacement Time Series

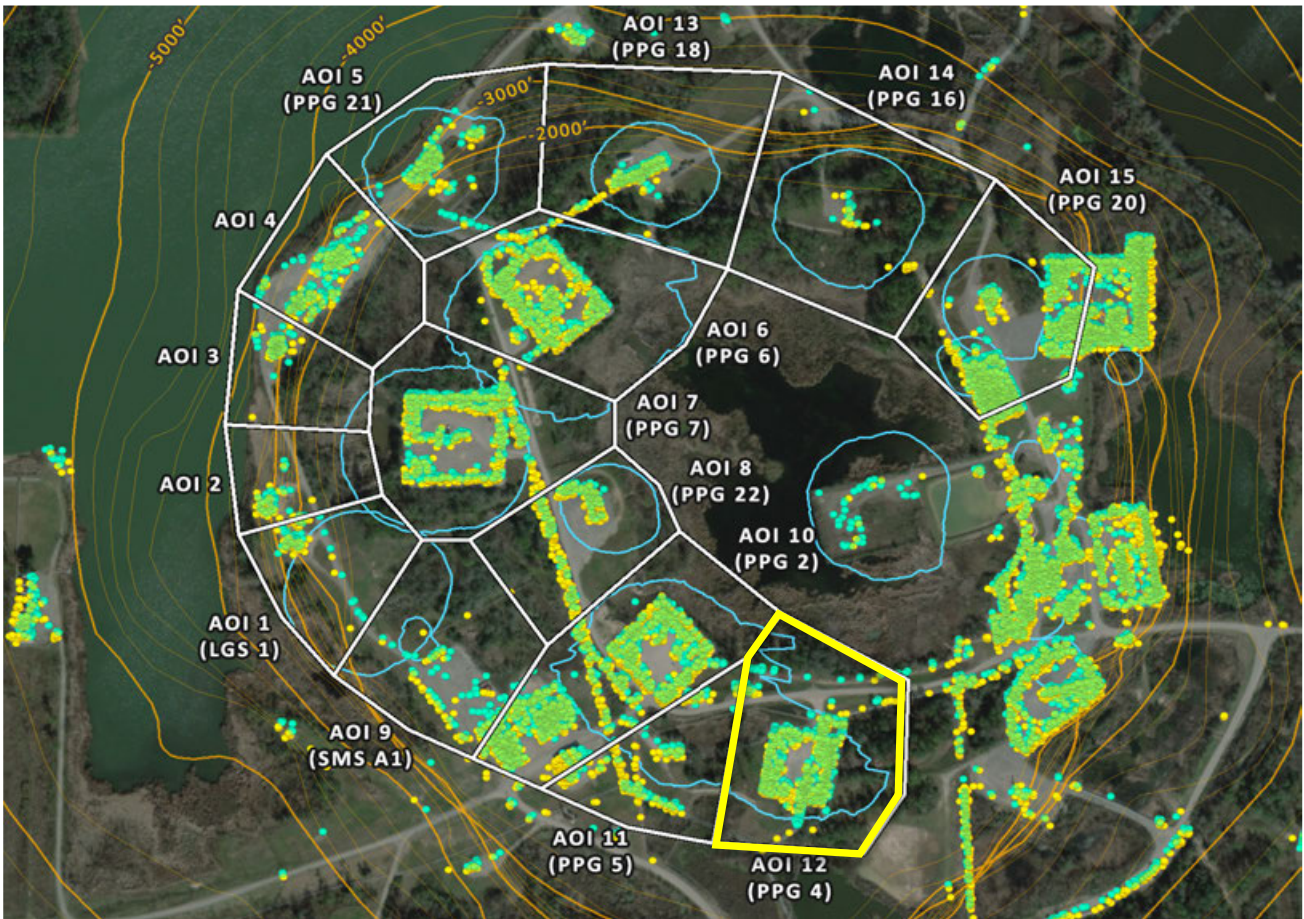
TSX-A (9/29/2025) Point Count: 154



	Nonlinear Trend	Linear Trend
Velocity:	-0.94 in/yr	-0.79 in/yr
Acceleration:	-0.11 in/yr ²	0.00 in/yr ²

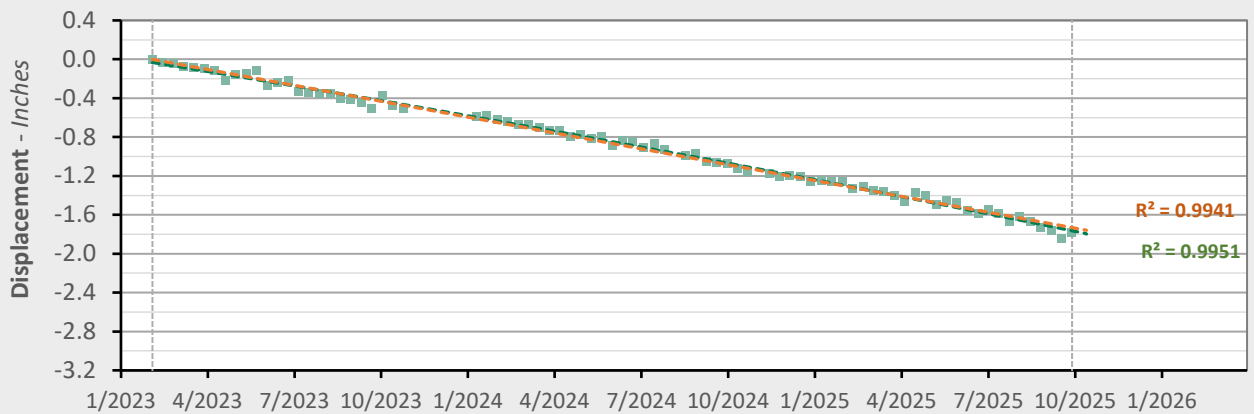


AOI 12 (PPG 4) - Location Map

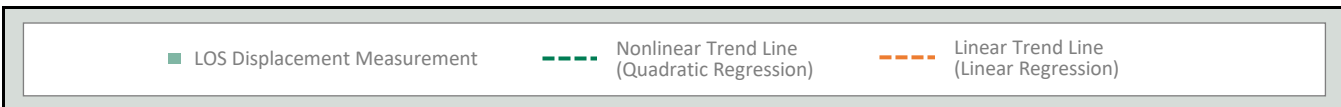


AOI 12 (PPG 4) - Displacement Time Series

TSX-A (9/29/2025) Point Count: 326



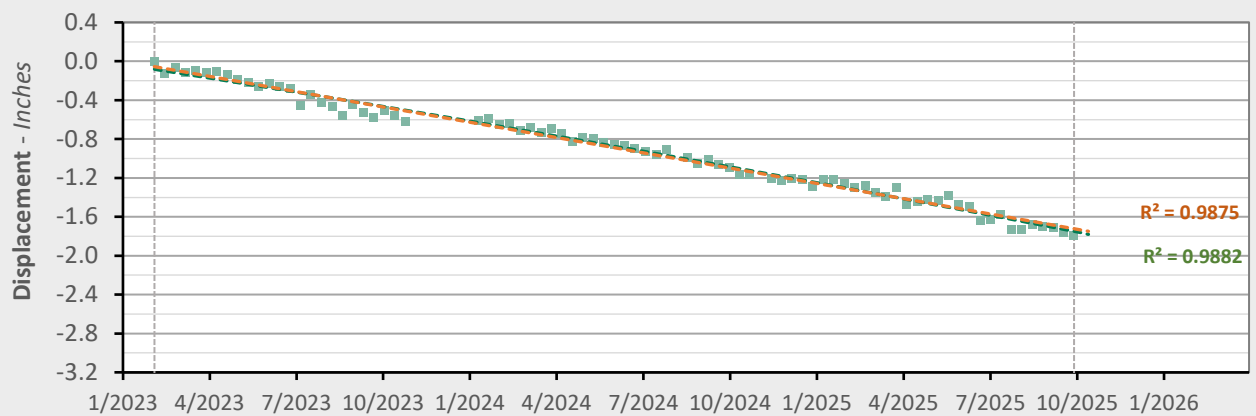
	Nonlinear Trend	Linear Trend
Velocity:	-0.73 in/yr	-0.65 in/yr
Acceleration:	-0.06 in/yr ²	0.00 in/yr ²



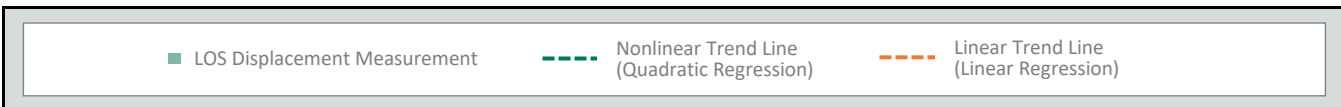
AOI 13 (PPG 18) - Location Map



AOI 13 (PPG 18) - Displacement Time Series TSX-A (9/29/2025) Point Count: 93



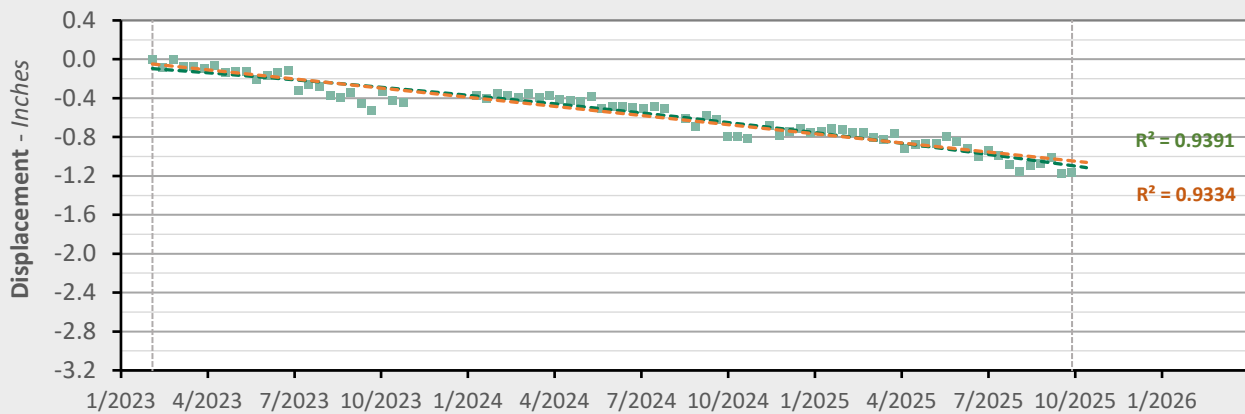
	Nonlinear Trend	Linear Trend
Velocity:	-0.69 in/yr	-0.63 in/yr
Acceleration:	-0.05 in/yr ²	0.00 in/yr ²



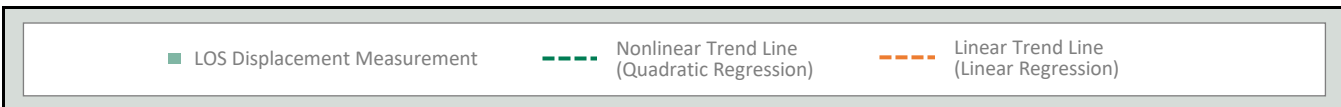
AOI 14 (PPG 16) - Location Map



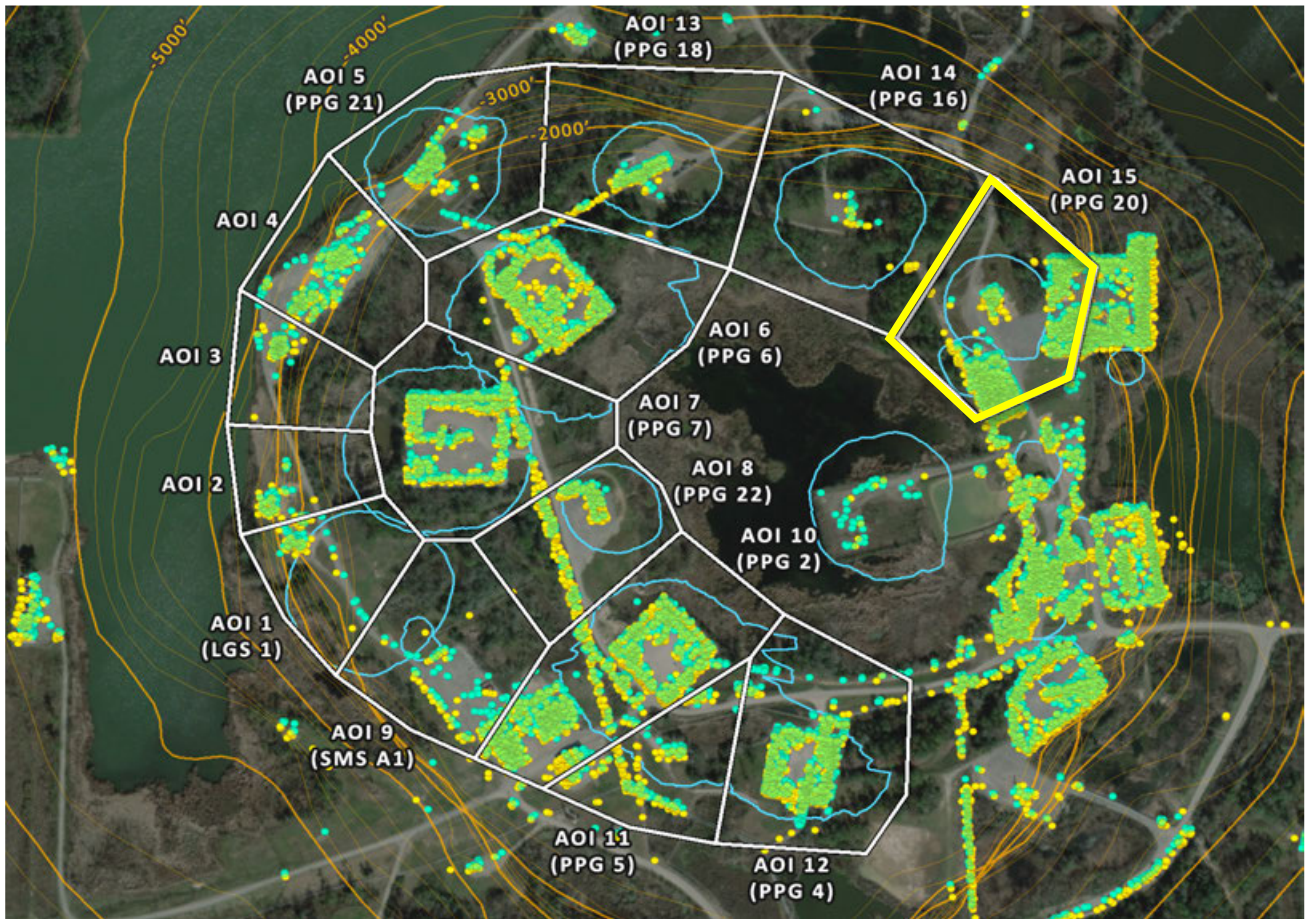
AOI 14 (PPG 16) - Displacement Time Series TSX-A (9/29/2025) Point Count: 22



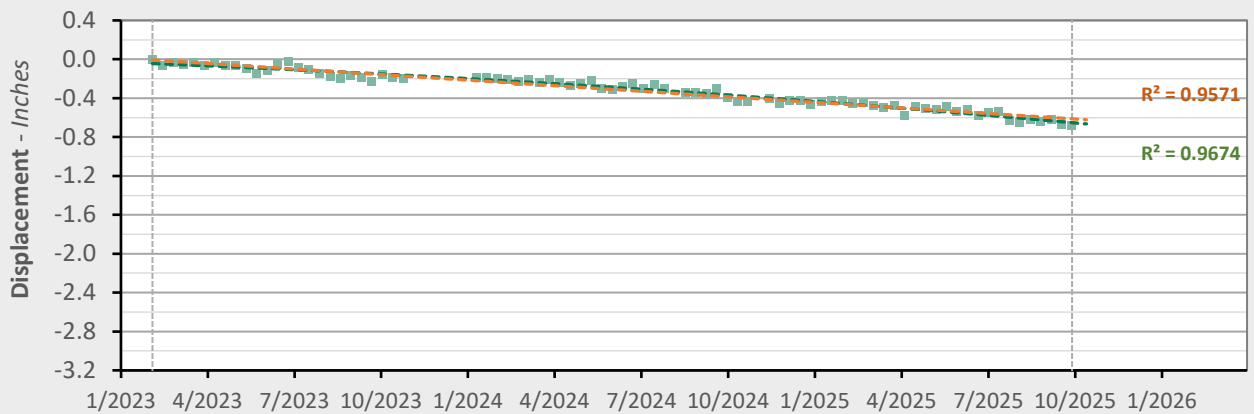
	Nonlinear Trend	Linear Trend
Velocity:	-0.49 in/yr	-0.38 in/yr
Acceleration:	-0.09 in/yr ²	0.00 in/yr ²



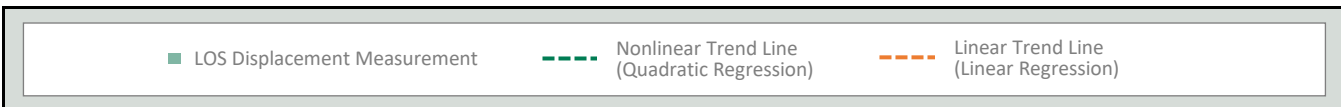
AOI 15 (PPG 20) - Location Map



AOI 15 (PPG 20) - Displacement Time Series TSX-A (9/29/2025) Point Count: 526



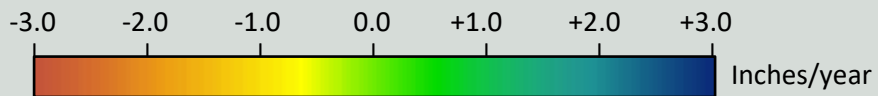
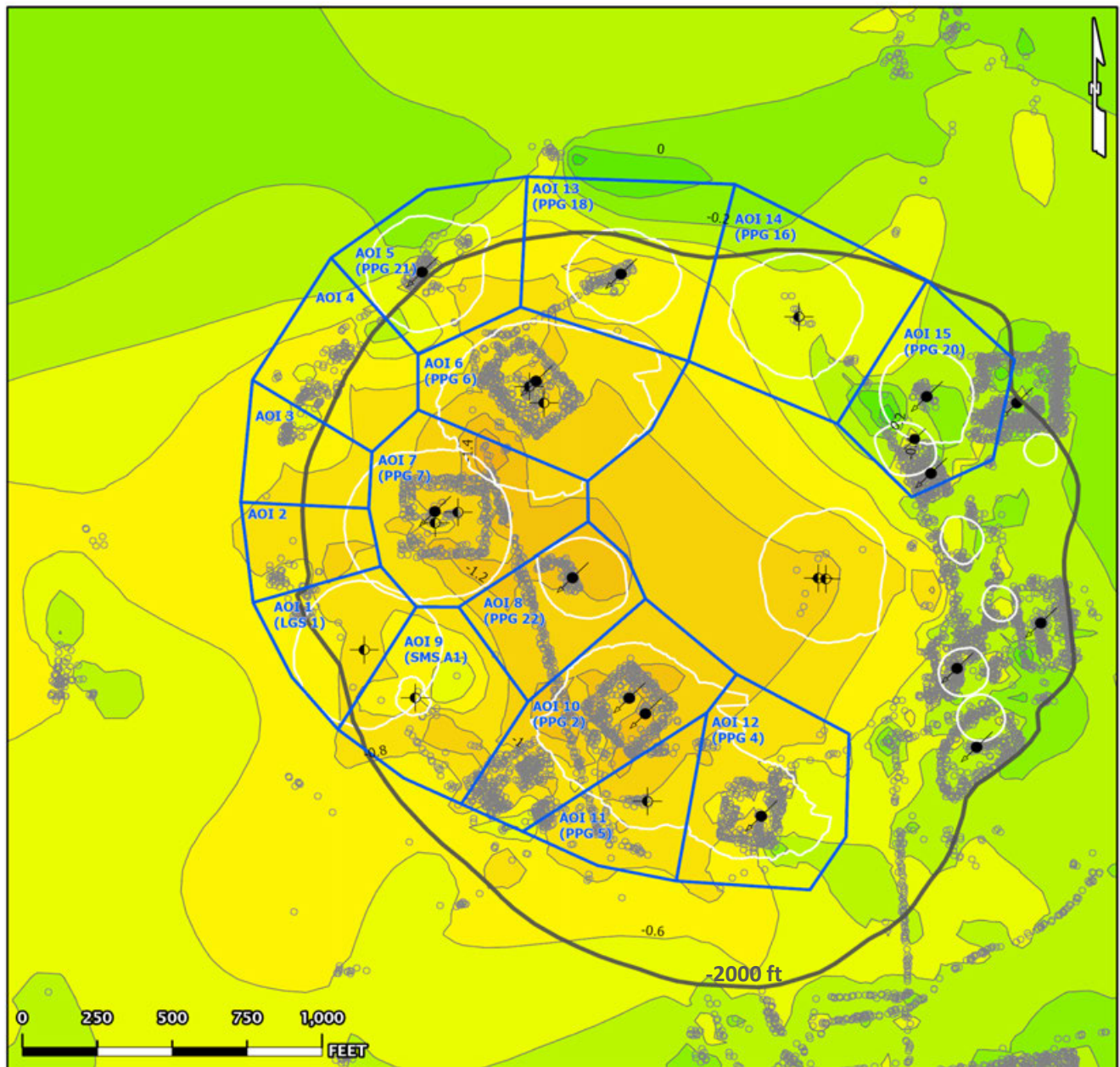
	Nonlinear Trend	Linear Trend
Velocity:	-0.32 in/yr	-0.23 in/yr
Acceleration:	-0.07 in/yr ²	0.00 in/yr ²



TSX-A Data (02/04/2023 - 09/29/2025)

Nonlinear Velocity Contours

As of date: 09/29/2025

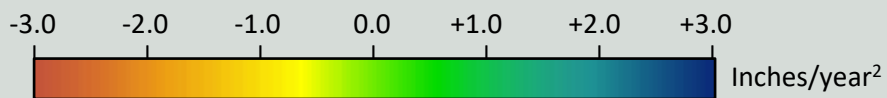
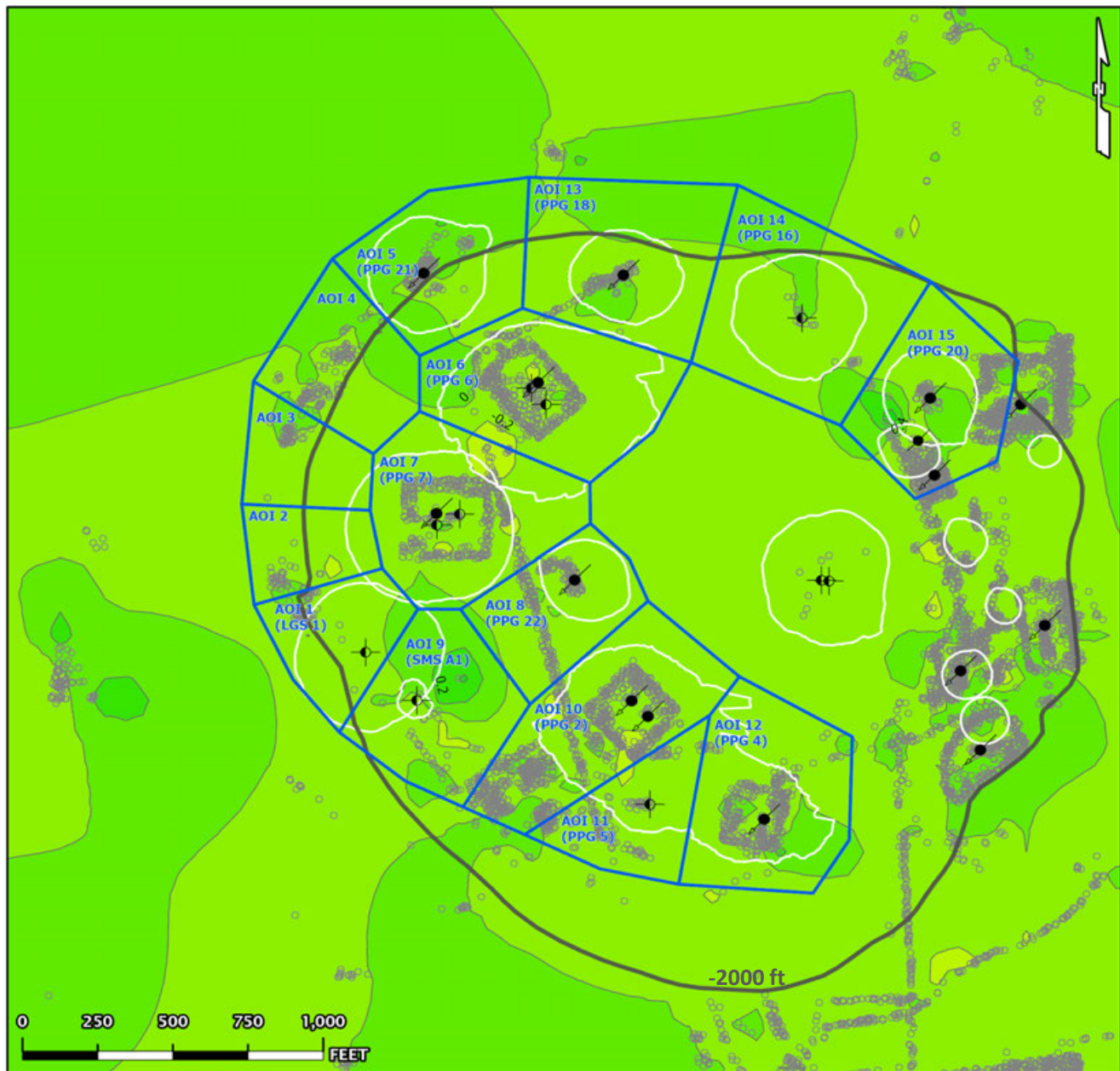


- AOI Boundary
 - InSAR LOS Measurement Point
 - Contour (0.2)
 - Historical Cavern Extent
 - Top of Dome (-2000 ft Contour)
- Cavern Well Surface Locations
- 09 - Active - Injection
 - 29 - Dry and Plugged

TSX-A Data (02/04/2023 - 09/29/2025)

Nonlinear Acceleration Contours

Date range: 02/04/2023 - 09/29/2025

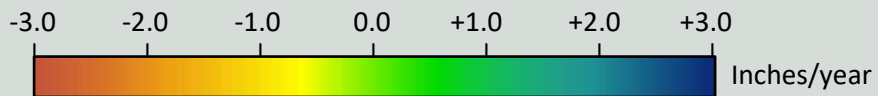
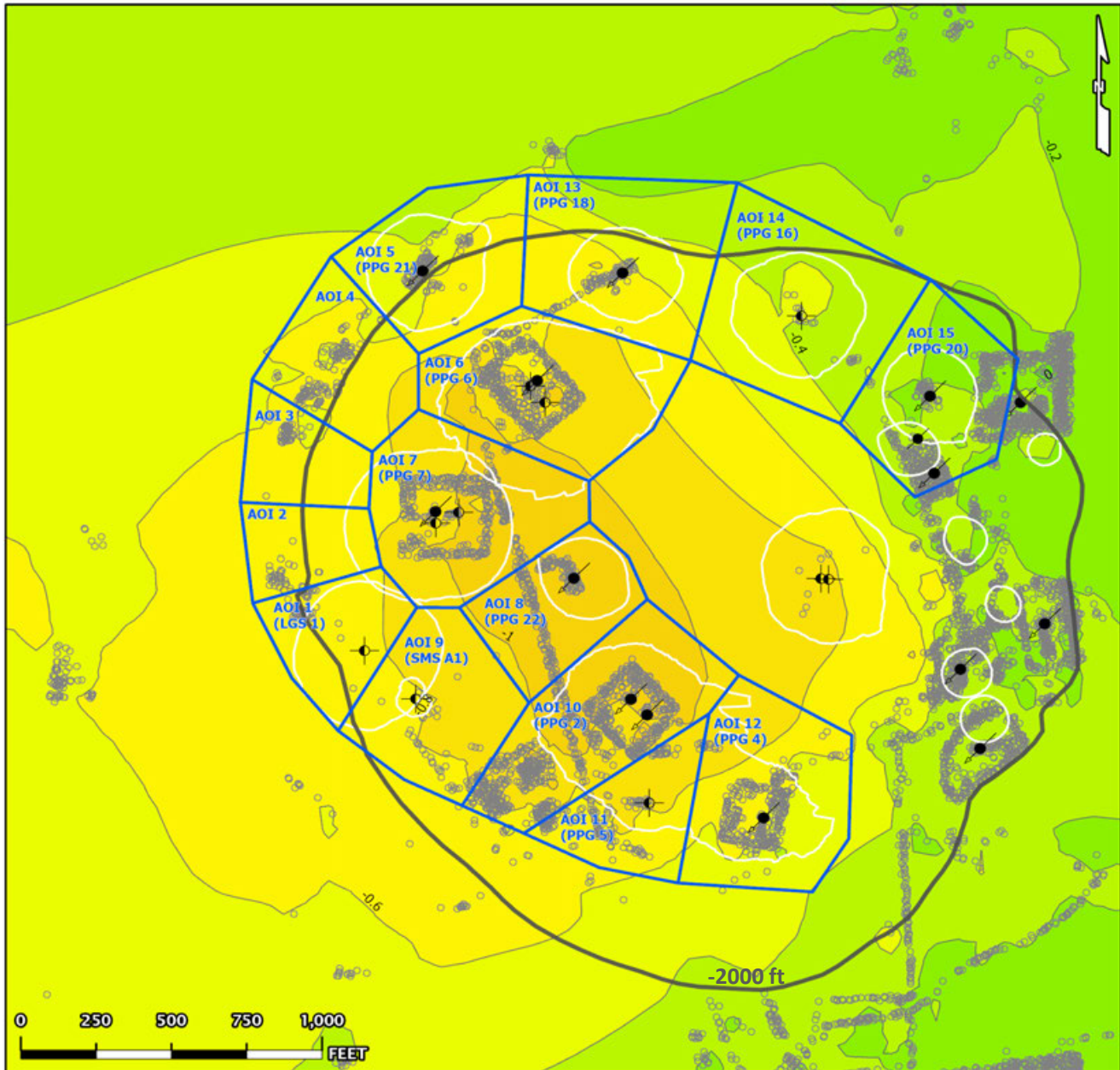


- AOI Boundary
 - InSAR LOS Measurement Point
 - Contour (0.2)
 - Historical Cavern Extent
 - Top of Dome (-2000 ft Contour)
- Cavern Well Surface Locations
- 09 - Active - Injection
 - 29 - Dry and Plugged

TSX-A Data (02/04/2023 - 09/29/2025)

Linear Velocity Contours

Date range: 02/04/2023 - 09/29/2025

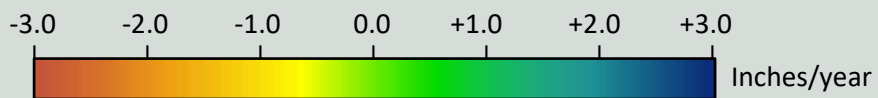
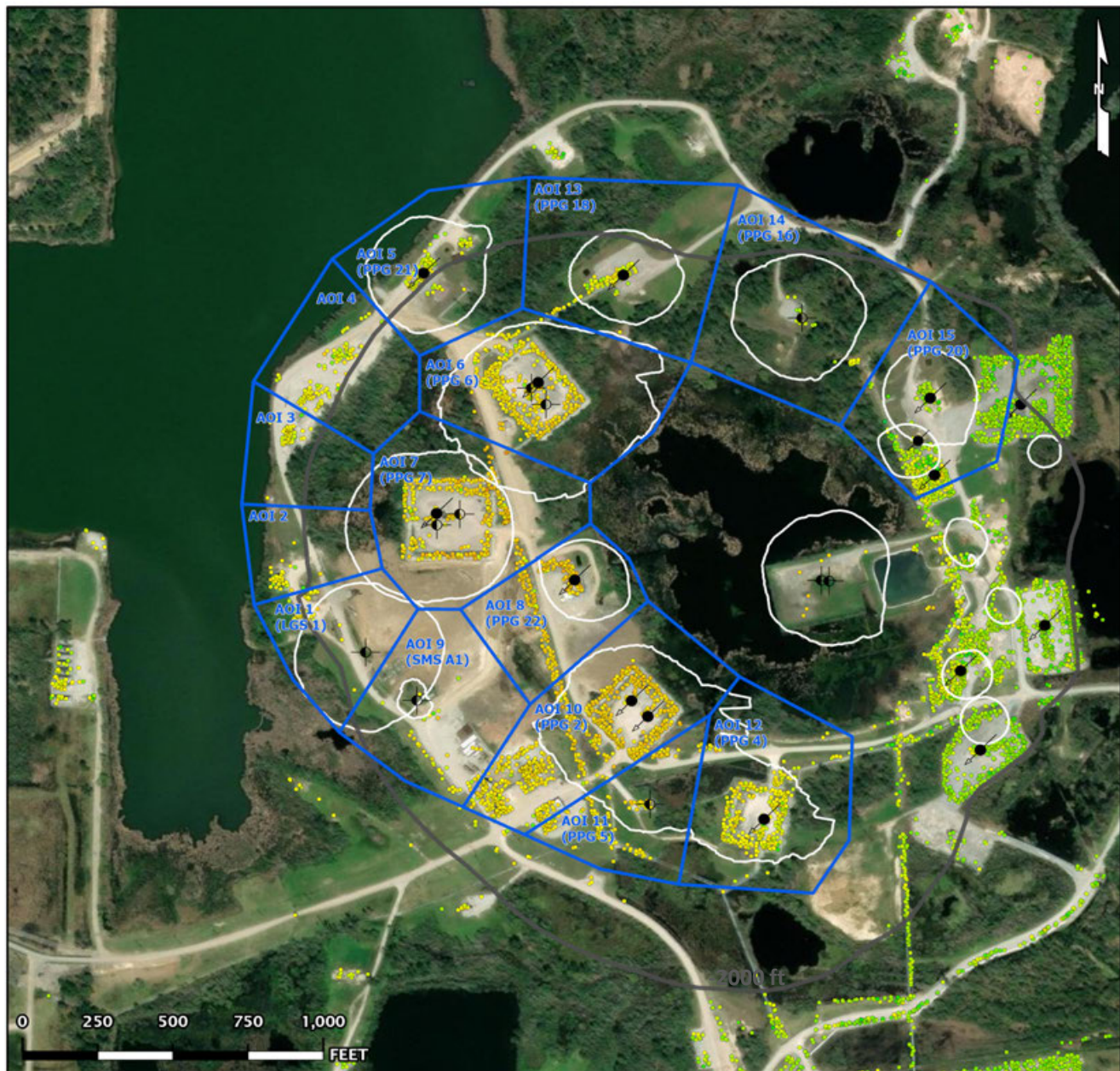


- AOI Boundary
 - InSAR LOS Measurement Point
 - Contour (0.2)
 - Historical Cavern Extent
 - Top of Dome (-2000 ft Contour)
- Cavern Well Surface Locations
- 09 - Active - Injection
 - 29 - Dry and Plugged

TSX-A Data (02/04/2023 - 09/29/2025)

Nonlinear Velocity Data Points

As of date: 09/29/2025

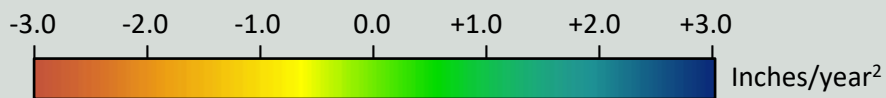


- AOI Boundary
 - InSAR LOS Measurement Point
 - Historical Cavern Extent
 - Top of Dome (-2000 ft Contour)
- Cavern Well Surface Locations
- 09 - Active - Injection
 - 29 - Dry and Plugged

TSX-A Data (02/04/2023 - 09/29/2025)

Nonlinear Acceleration Data Points

Date range: 02/04/2023 - 09/29/2025

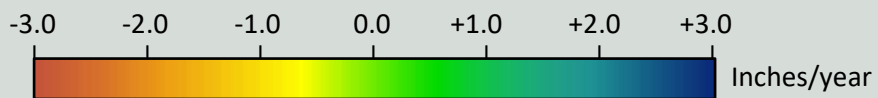


- AOI Boundary
 - InSAR LOS Measurement Point
 - Historical Cavern Extent
 - Top of Dome (-2000 ft Contour)
- Cavern Well Surface Locations
- 09 - Active - Injection
 - 29 - Dry and Plugged

TSX-A Data (02/04/2023 - 09/29/2025)

Linear Velocity Data Points

Date range: 02/04/2023 - 09/29/2025



- AOI Boundary
 - InSAR LOS Measurement Point
 - Historical Cavern Extent
 - Top of Dome (-2000 ft Contour)
- Cavern Well Surface Locations
- 09 - Active - Injection
 - 29 - Dry and Plugged

ATTACHMENT C

TSX/PAZ InSAR report - September 29, 2025



TSX/PAZ Satellite Update

Continuous InSAR Monitoring of
Ground Displacement At Westlake
Caverns and Western Dome Flank

Sulphur Mines Salt Dome

Prepared for:
Westlake Chemical

Prepared by:
Lonquist Field Service, LLC
8591 United Plaza Blvd., Suite 280
Baton Rouge, LA 70809

Dataset
Satellite Source
TerraSAR-X - PAZ Constellation
Most Recent Image Date
Monday, September 29, 2025

Analysis Report Date:
October 15, 2025

Dataset Information	
Satellite Source	TerraSAR-X - PAZ Constellation - Descending
Revisit Frequency	4 and 7 days
Most Recent Image Date	Monday, September 29, 2025
Dataset Image Count	169
Dataset Time Range	January 24, 2023 - September 29, 2025
Dataset Length	2.68 Years
Satellite Line-of-Sight (LOS)	37° East of Vertical (Viewing site from the East)

Analysis Methodology

Time Series Charts
Trend lines were calculated for the averaged displacement values within each AOI. Both a nonlinear (quadratic) and linear regression were applied to each AOI point group to identify rates of change in LOS displacement. These trends are displayed in the Time Series section of this report.

Contour Maps
A nonlinear (quadratic) and linear trend was also calculated for each individual measurement point across the analysis region. Nonlinear trend values for each point were used to generate Velocity and Acceleration contour maps to convey the spatial distribution of the calculated movement. The linear trend values for each point (which lack an acceleration component) were used to generate an additional Velocity contour map. Maps depicting the individual data points colored by these trend values are also included in the last section of the report.

Negative velocity values indicate subsidence or westward movement and positive velocity indicates uplift or eastward movement. Negative acceleration values indicate increasing rates of subsidence, increasing westward movement, or slowing eastward movement and positive acceleration values indicate slowing rates of subsidence, slowing westward movement, or increasing eastward movement.

Observations

To-date there have been no acute deviations from established subsidence trends in the areas investigated.

The time series charts show broadly consistent near-linear trends among the analysis AOIs. Acceleration values for the quadratic (non-linear) trend fit are negative in most AOIs (increasing negative displacement rates) but minor overall. This is mostly due to a recent below-trend dip associated with historically observed seasonal fluctuation. The dip is slightly greater in some areas than in past years, but appears to be returning to trend.

The contour maps show the greatest negative displacement centered around the eastern central portion of the dome where the combination of subsidence and western horizontal movement (toward dome center) are expected to produce the greatest rate of movement away from the satellite's line of sight from the east.



Date Signed: October 15, 2025
Austin, Texas

Nathaniel L. Byars, P.E.
Principal Engineer
Louisiana License No. 40697

InSAR Data Sources

InSAR Data

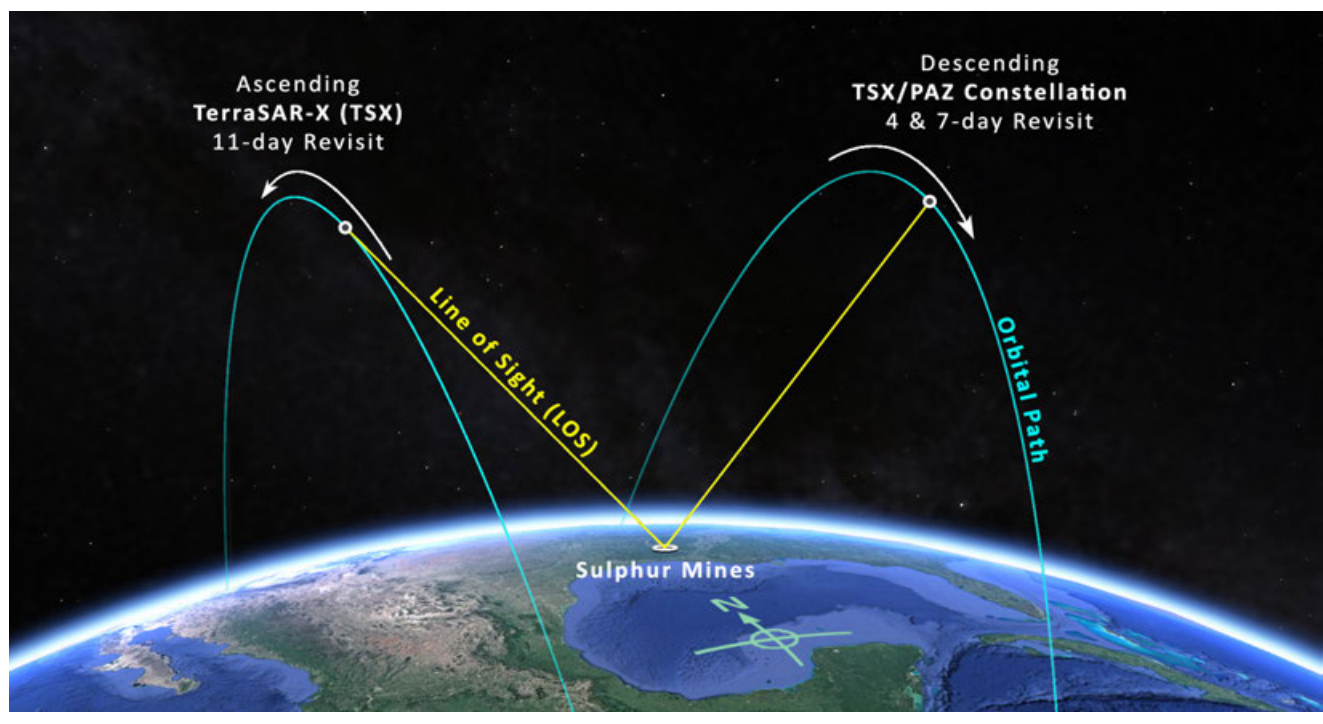
Interferometric Synthetic Aperture Radar (InSAR) is the most well established method to continually evaluate small, normally undetectable, ground movement over a large area. Radar imagery collected via satellites over successive orbital passes is used to identify and define measurement points on the ground. Objects or ground features providing a stable reflection of radar energy such as buildings, roads, and infrastructure produce the highest quality measurement points. InSAR analysis identifies the change in distance between the satellite and each measurement point over time relative to a stable reference point within the imaged area.

Satellite Sources

Two InSAR datasets are being used to evaluate subsidence over the Sulphur Mines Salt Dome. These datasets provide Line-of-Sight (LOS) displacement measurements from both ascending and descending orbits. An ascending orbit denotes the satellite's longitudinal course from south to north as it passes over the site, while a descending orbit denotes the satellite is moving from north to south.

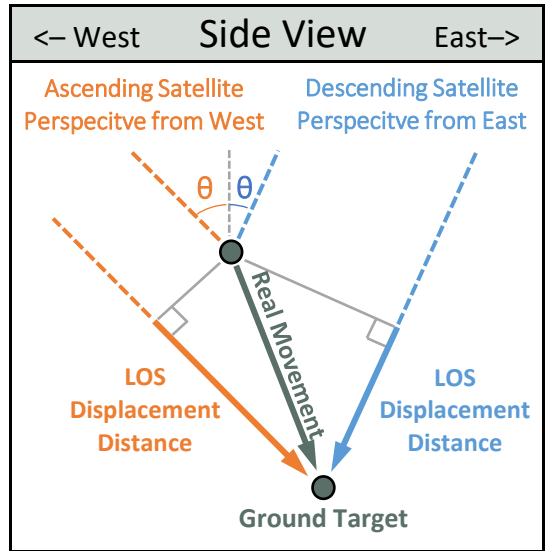
The first dataset comes from the high-resolution TerraSAR-X satellite on an ascending orbit track ("TSX-A") that captures data from the west of the site on an 11-day frequency. The second comes from a pair of high-resolution satellites that include the TerraSAR-X satellite and the PAZ satellite ("TSX/PAZ Constellation") which share the same descending orbit track and capture data from east of the site, each with an 11-day frequency. Their orbits are offset with the PAZ satellite passing over the site 4 days after the TSX satellite. Prior to May 2024, the ascending data was captured from a low-resolution Sentinel-1 satellite at a similar viewing angle to the TSX orbit. The transition to the ascending TSX track was made to increase data accuracy and measurement point density once a suitable data history had been gathered for trend analysis. The image below depicts the orbital paths of the current satellites in relation to the Sulphur Mines Salt Dome.

Satellite Orbital Diagram



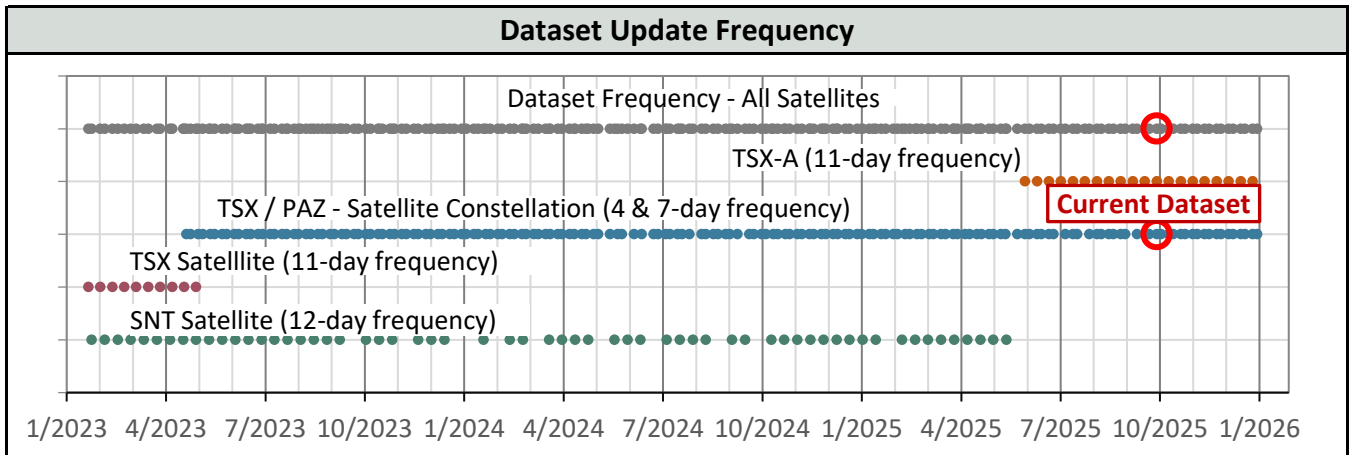
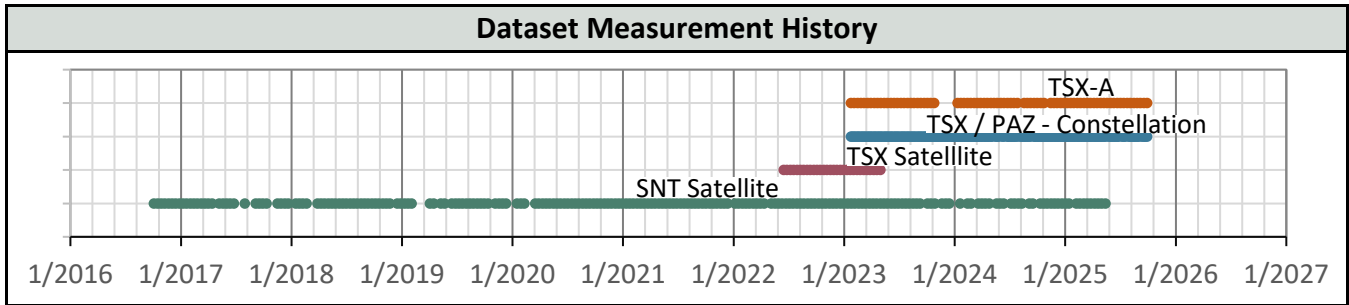
InSAR Line-of-Site (LOS) Data

LOS displacement measurements refer to a change in distance between the satellite sensor and the ground target. Measurement positions on the west side of the Sulphur Dome are known to be experiencing some eastward movement toward the dome center due to the geometry of the subsidence basin. The InSAR satellites view the site from eastward and westward positions so LOS measurements are understood to convey a movement distance that is not purely vertical. The diagram to the right illustrates the geometric relationship between the theoretical Real movement of a ground target and LOS displacement measurements from two different satellite viewing directions.

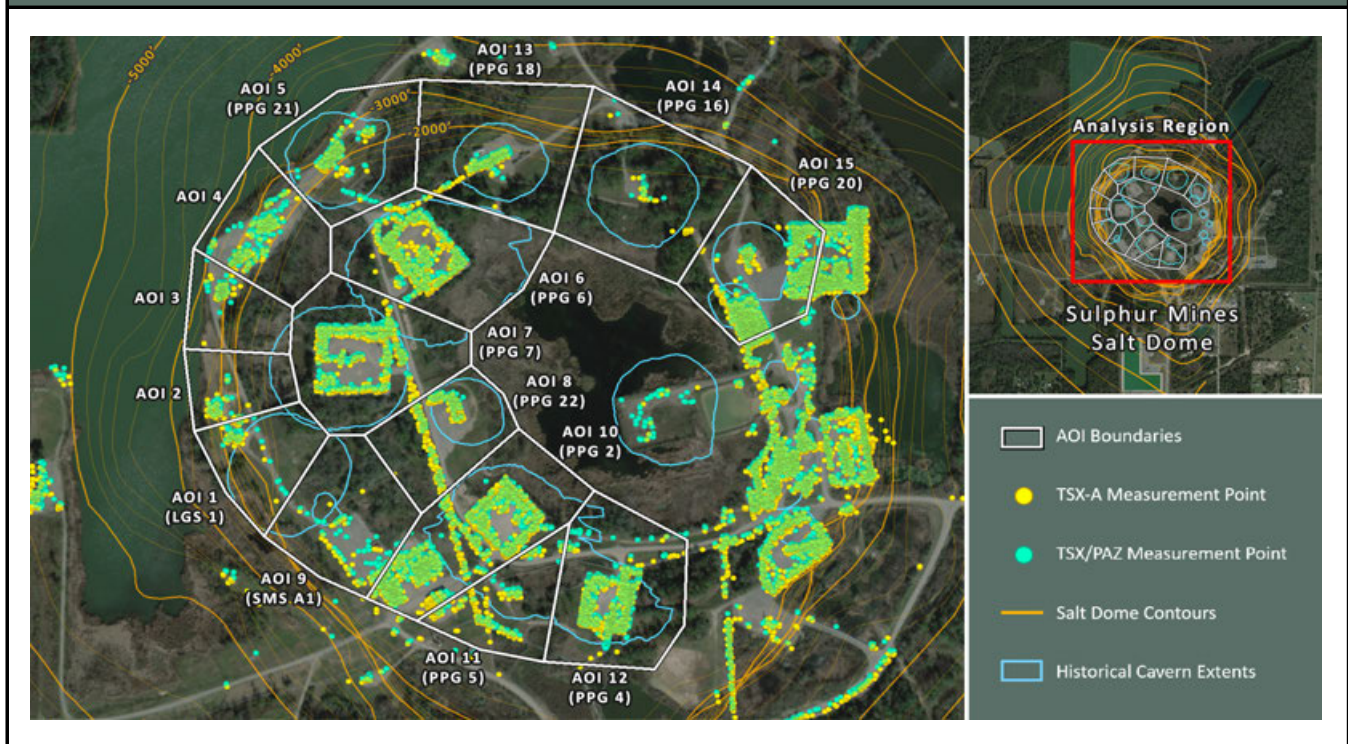


Satellite Properties & Image Frequency

Satellite and Data Properties	SNT	TSX-A	TSX/PAZ Constellation
Band (Wavelength)	C-band (2.32 in)	X-band (1.22 in)	X-band (1.22 in)
Track	T136	T52	T67 & T120
Pixel resolution	65 x 16 ft	3 x 3 ft	3 x 3 ft
Revisit frequency	12 days	11 days	4 & 7 days
Orbit (LOS Angle, θ)	Ascending (42°)	Ascending (44°)	Descending (37°)
Data Start Date	10/4/2016	2/4/2023	1/24/2023
Measurement error range	± 0.20 in	± 0.06 in	± 0.07 in



AOI Boundaries & InSAR Measurement Points

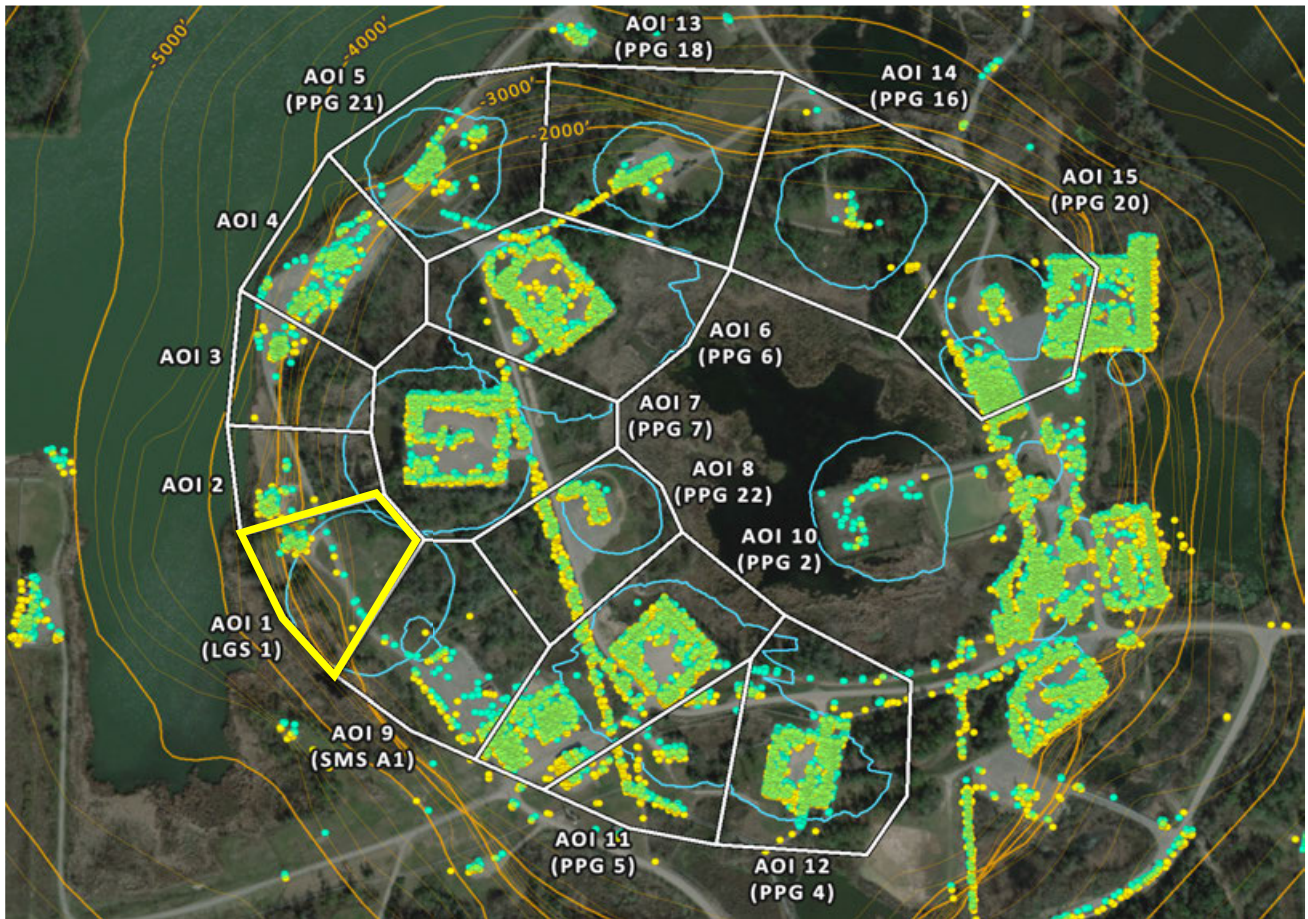


Subsidence Monitoring Areas of Interest (AOIs)

To visually convey and evaluate trend consistency for the displacement time series of each ground target, measurement points were grouped and their displacement values were averaged. The point groups are referred to as Areas of Interest (AOIs) in this analysis and their boundaries are depicted on the above map. The below table lists the trend values calculated in each AOI for the dataset evaluated in this report.

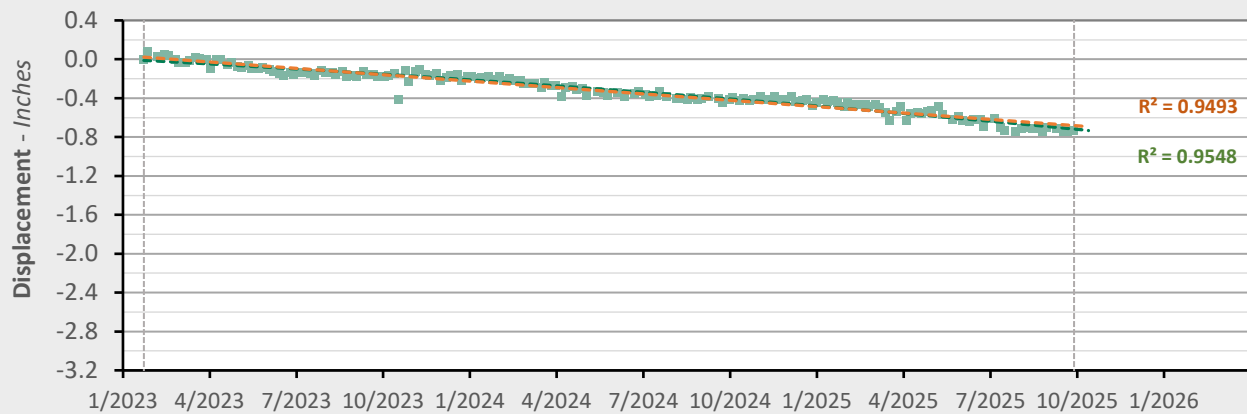
AOI Name	TSX/PAZ (9/29/2025)	LOS Velocity (in/yr)		LOS Acceleration (in/yr ²)	
	Point Count	Nonlinear	Linear	Nonlinear	Linear
AOI 1 (LGS 1)	59	-0.34	-0.26	-0.06	0.00
AOI 2	40	-0.29	-0.25	-0.03	0.00
AOI 3	65	-0.45	-0.40	-0.04	0.00
AOI 4	218	-0.31	-0.25	-0.04	0.00
AOI 5 (PPG 21)	120	-0.41	-0.34	-0.06	0.00
AOI 6 (PPG 6)	383	-0.72	-0.59	-0.10	0.00
AOI 7 (PPG 7)	368	-0.59	-0.47	-0.09	0.00
AOI 8 (PPG 22)	121	-0.80	-0.76	-0.03	0.00
AOI 9 (SMS A1)	73	-0.34	-0.38	+0.03	0.00
AOI 10 (PPG 2)	815	-0.72	-0.64	-0.06	0.00
AOI 11 (PPG 5)	125	-0.73	-0.63	-0.08	0.00
AOI 12 (PPG 4)	525	-1.02	-0.91	-0.08	0.00
AOI 13 (PPG 18)	108	-0.50	-0.52	+0.01	0.00
AOI 14 (PPG 16)	18	-0.73	-0.88	+0.11	0.00
AOI 15 (PPG 20)	687	-1.16	-1.04	-0.09	0.00

AOI 1 (LGS 1) - Location Map

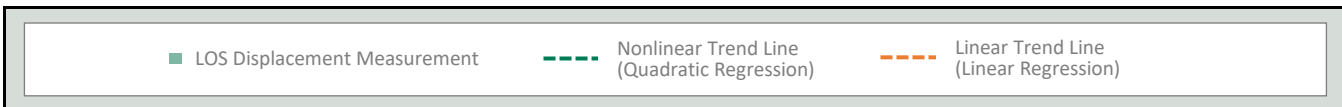


AOI 1 (LGS 1) - Displacement Time Series

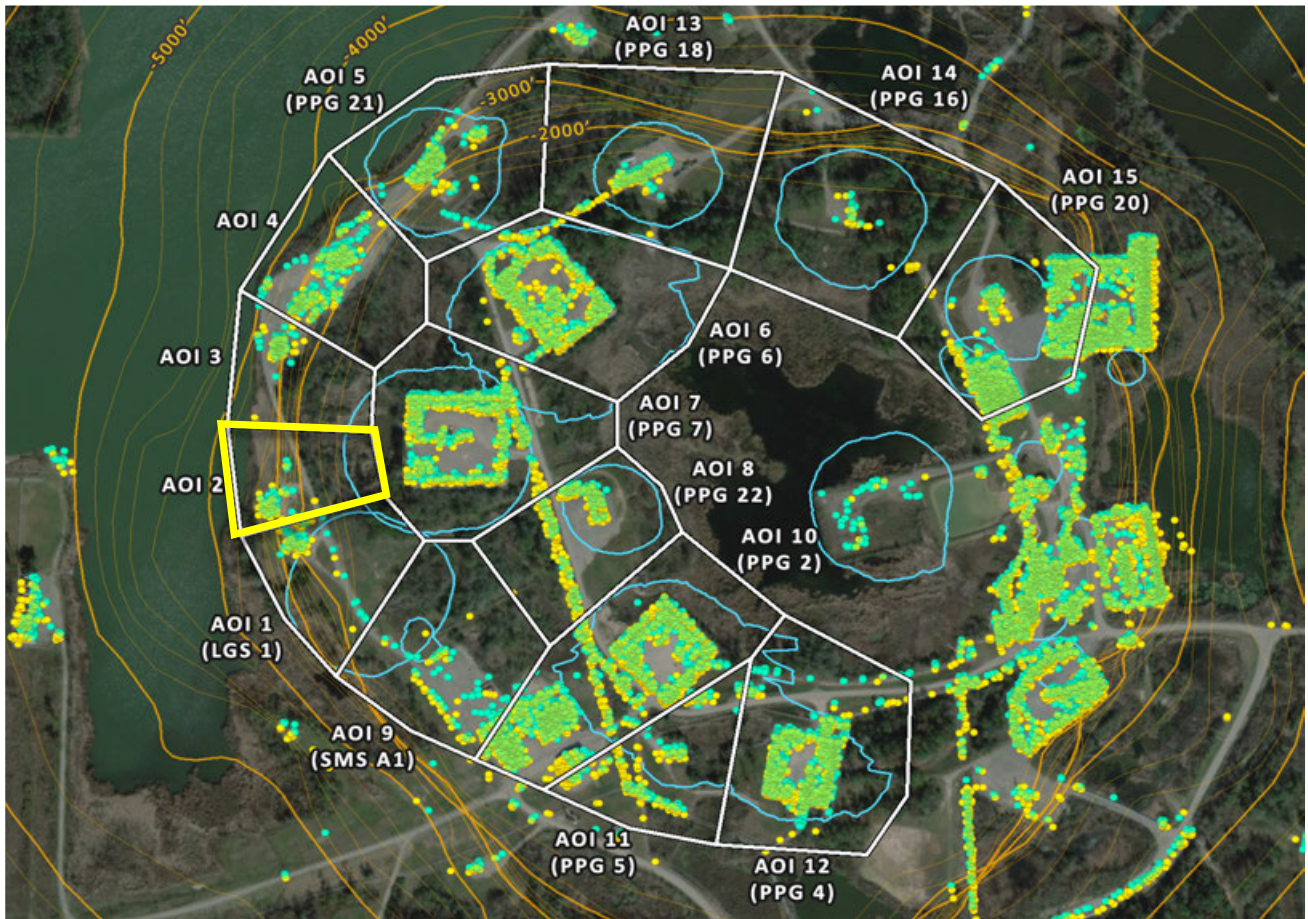
TSX/PAZ (9/29/2025) Point Count: 59



	Nonlinear Trend	Linear Trend
Velocity:	-0.34 in/yr	-0.26 in/yr
Acceleration:	-0.06 in/yr ²	0.00 in/yr ²

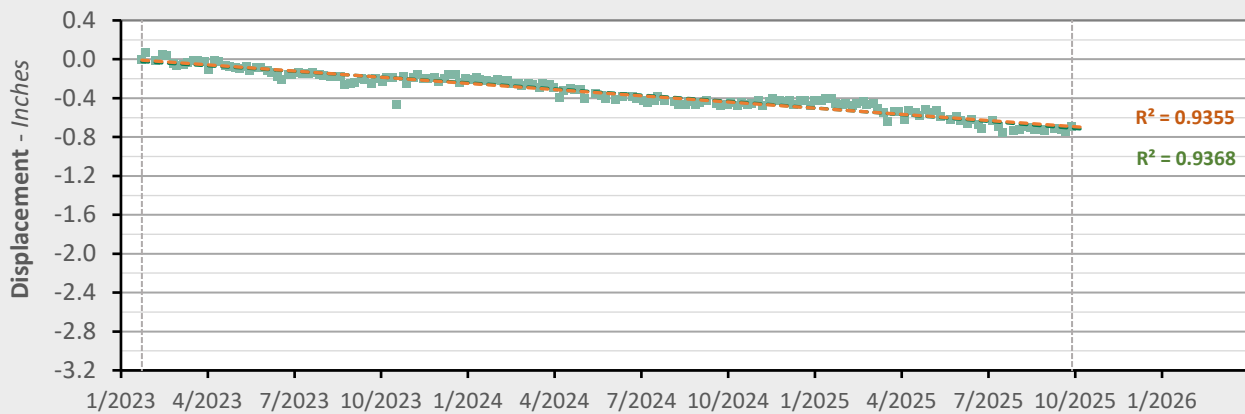


AOI 2 - Location Map

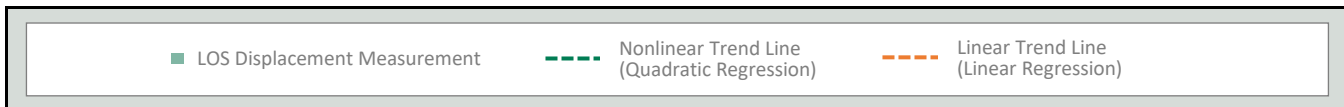


AOI 2 - Displacement Time Series

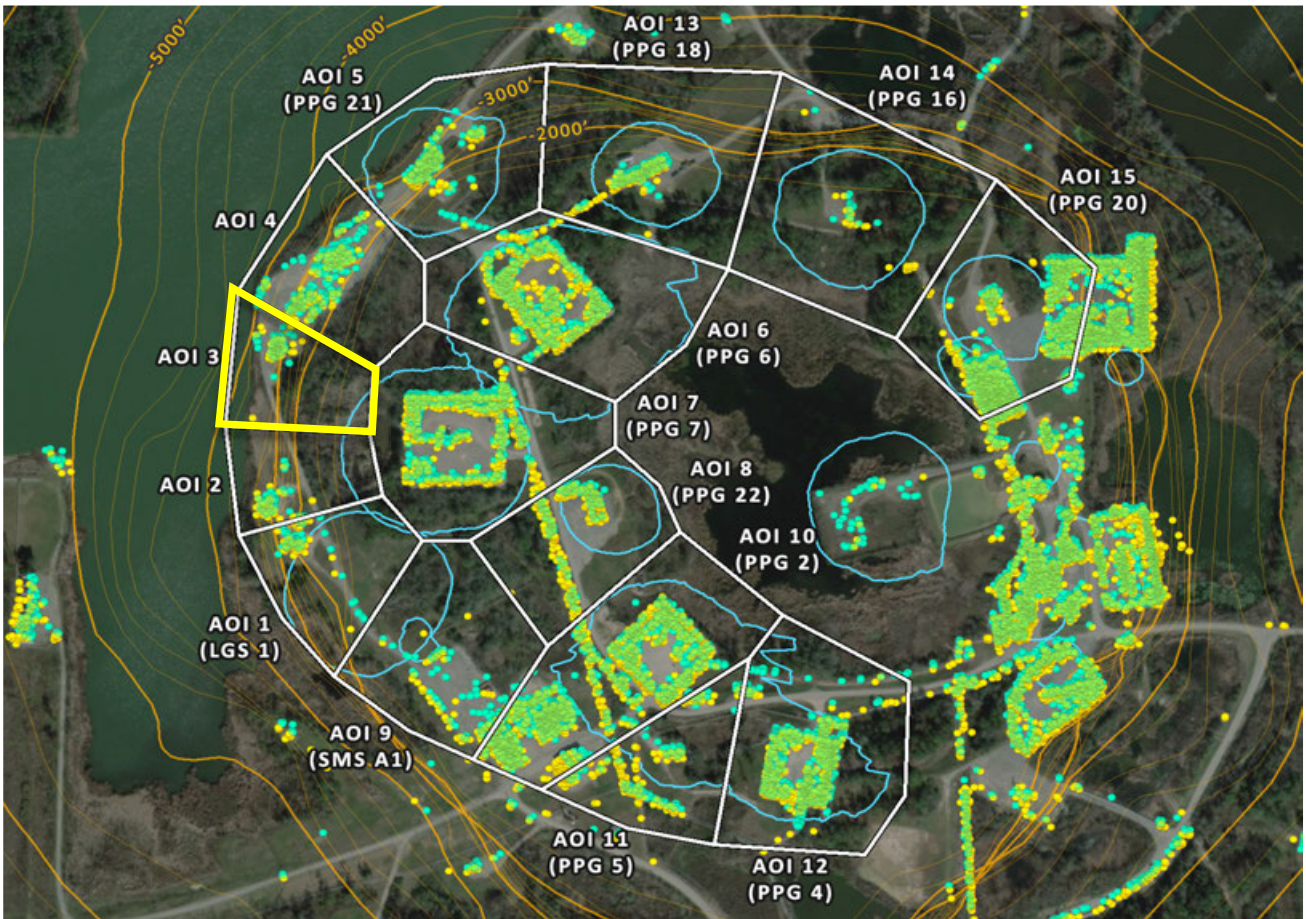
TSX/PAZ (9/29/2025) Point Count: 40



	Nonlinear Trend	Linear Trend
Velocity:	-0.29 in/yr	-0.25 in/yr
Acceleration:	-0.03 in/yr ²	0.00 in/yr ²

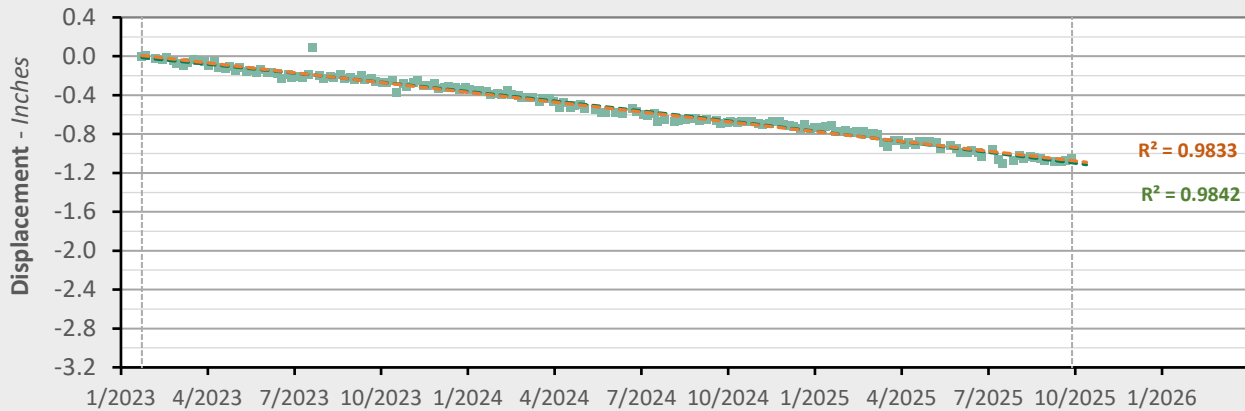


AOI 3 - Location Map

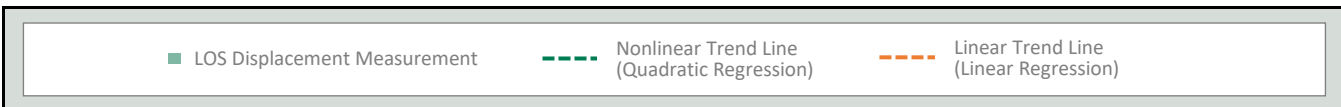


AOI 3 - Displacement Time Series

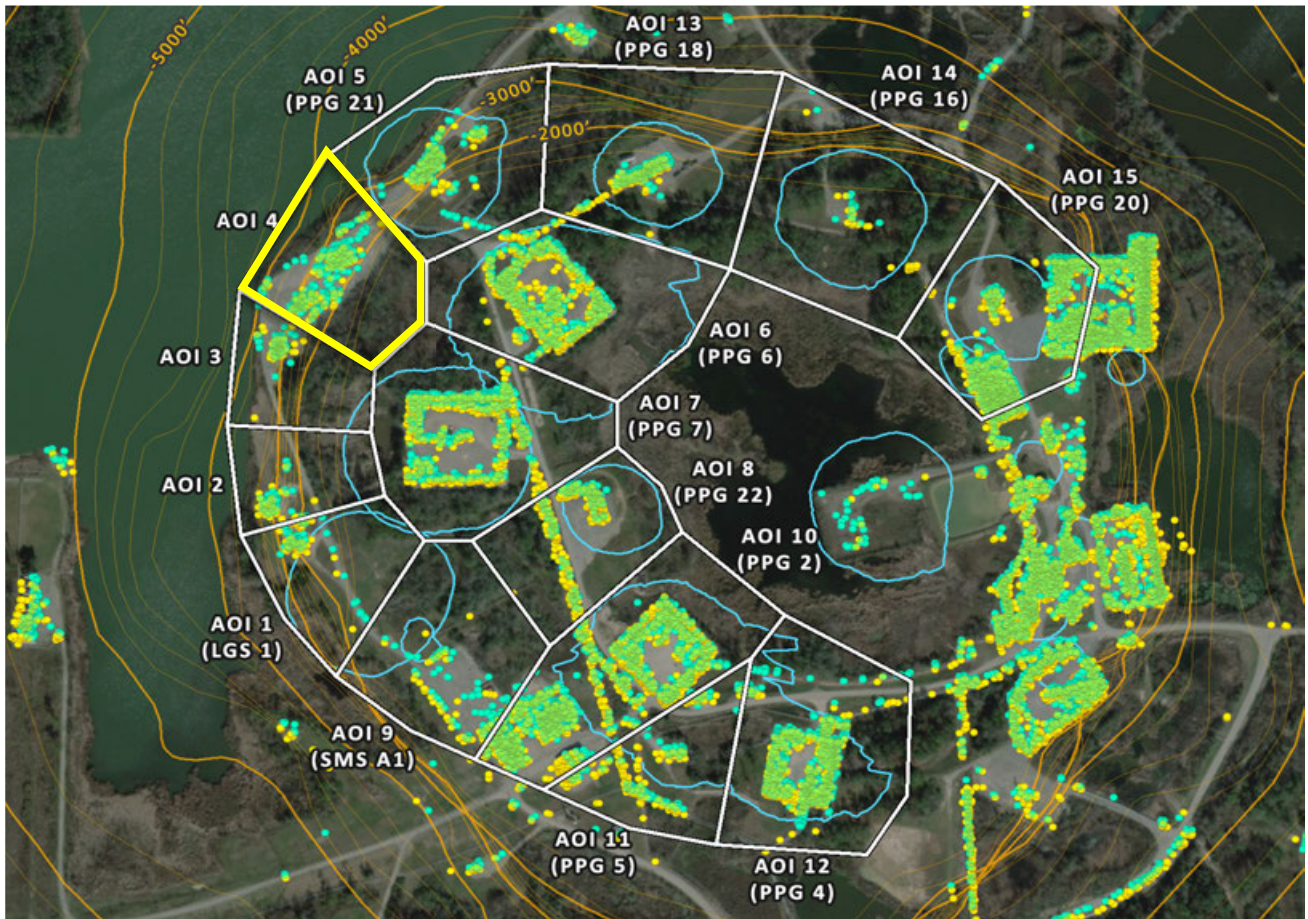
TSX/PAZ (9/29/2025) Point Count: 65



	Nonlinear Trend	Linear Trend
Velocity:	-0.45 in/yr	-0.40 in/yr
Acceleration:	-0.04 in/yr ²	0.00 in/yr ²

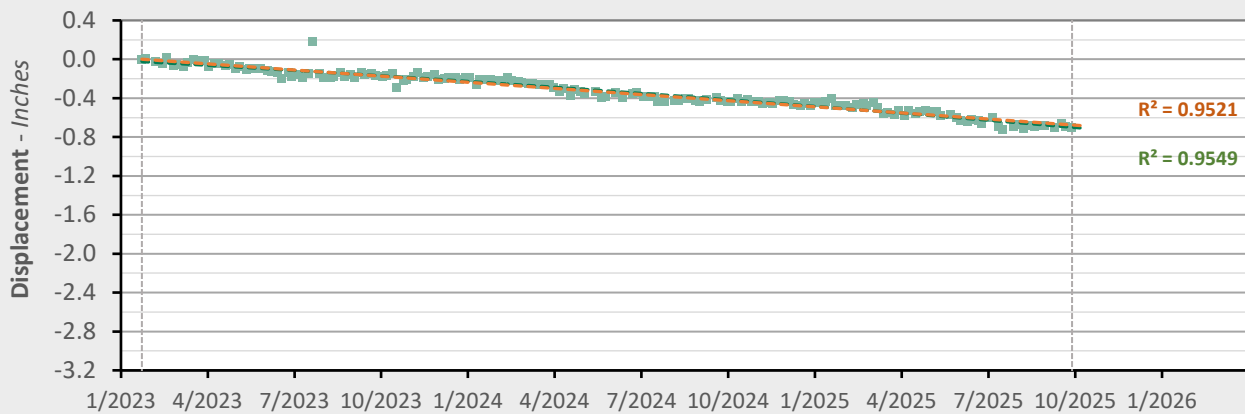


AOI 4 - Location Map

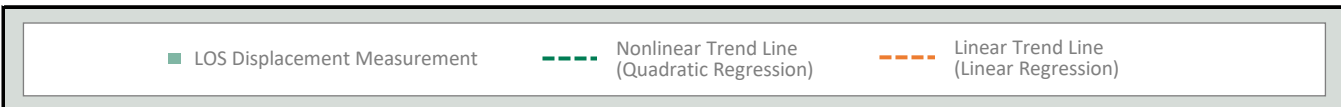


AOI 4 - Displacement Time Series

TSX/PAZ (9/29/2025) Point Count: 218



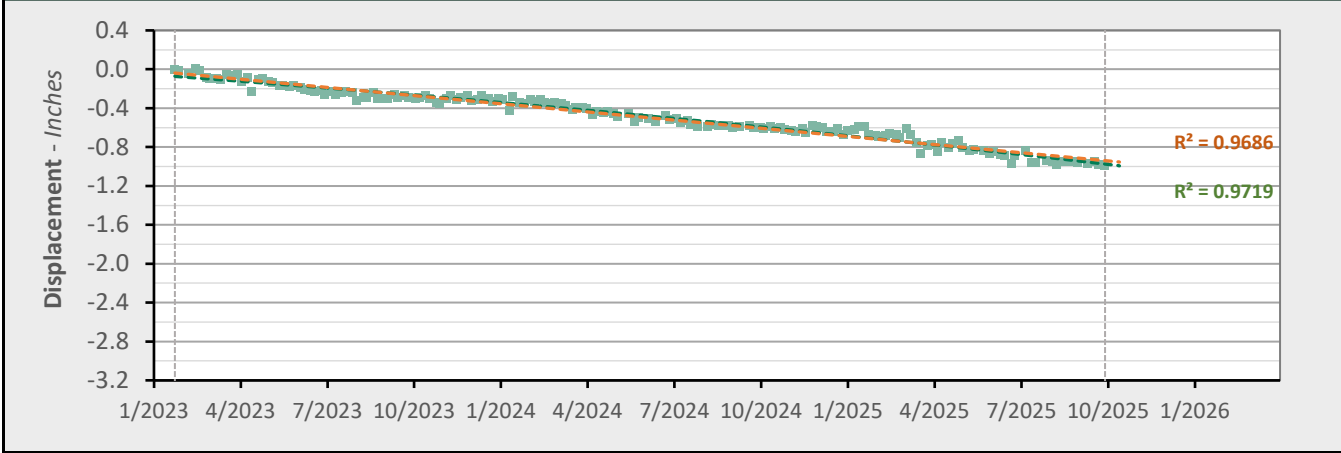
	Nonlinear Trend	Linear Trend
Velocity:	-0.31 in/yr	-0.25 in/yr
Acceleration:	-0.04 in/yr ²	0.00 in/yr ²



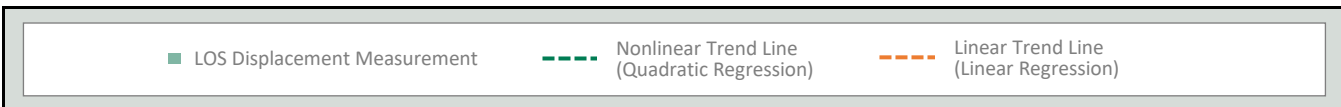
AOI 5 (PPG 21) - Location Map



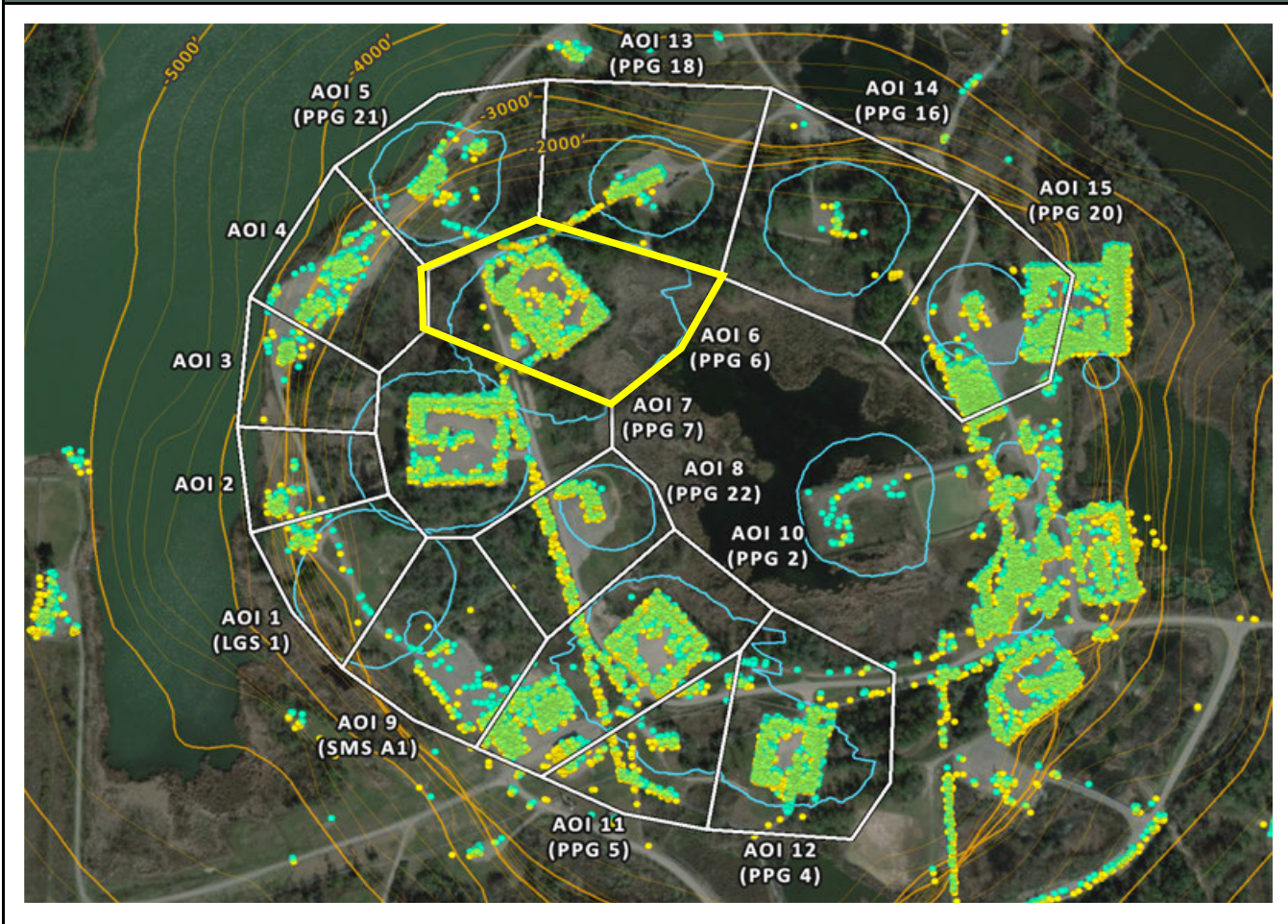
AOI 5 (PPG 21) - Displacement Time Series TSX/PAZ (9/29/2025) Point Count: 120



	Nonlinear Trend	Linear Trend
Velocity:	-0.41 in/yr	-0.34 in/yr
Acceleration:	-0.06 in/yr ²	0.00 in/yr ²

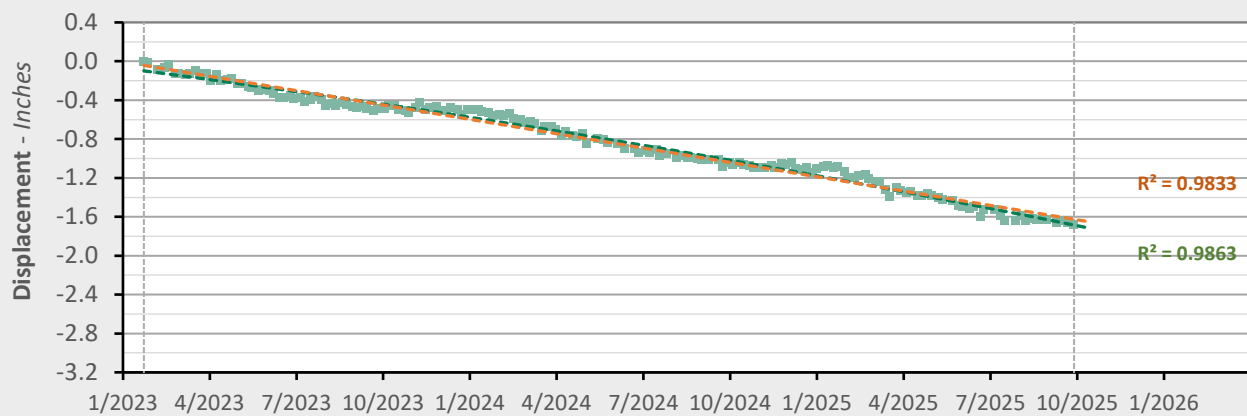


AOI 6 (PPG 6) - Location Map

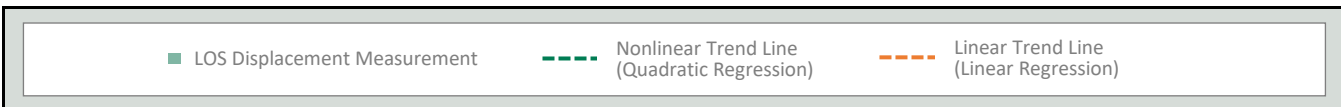


AOI 6 (PPG 6) - Displacement Time Series

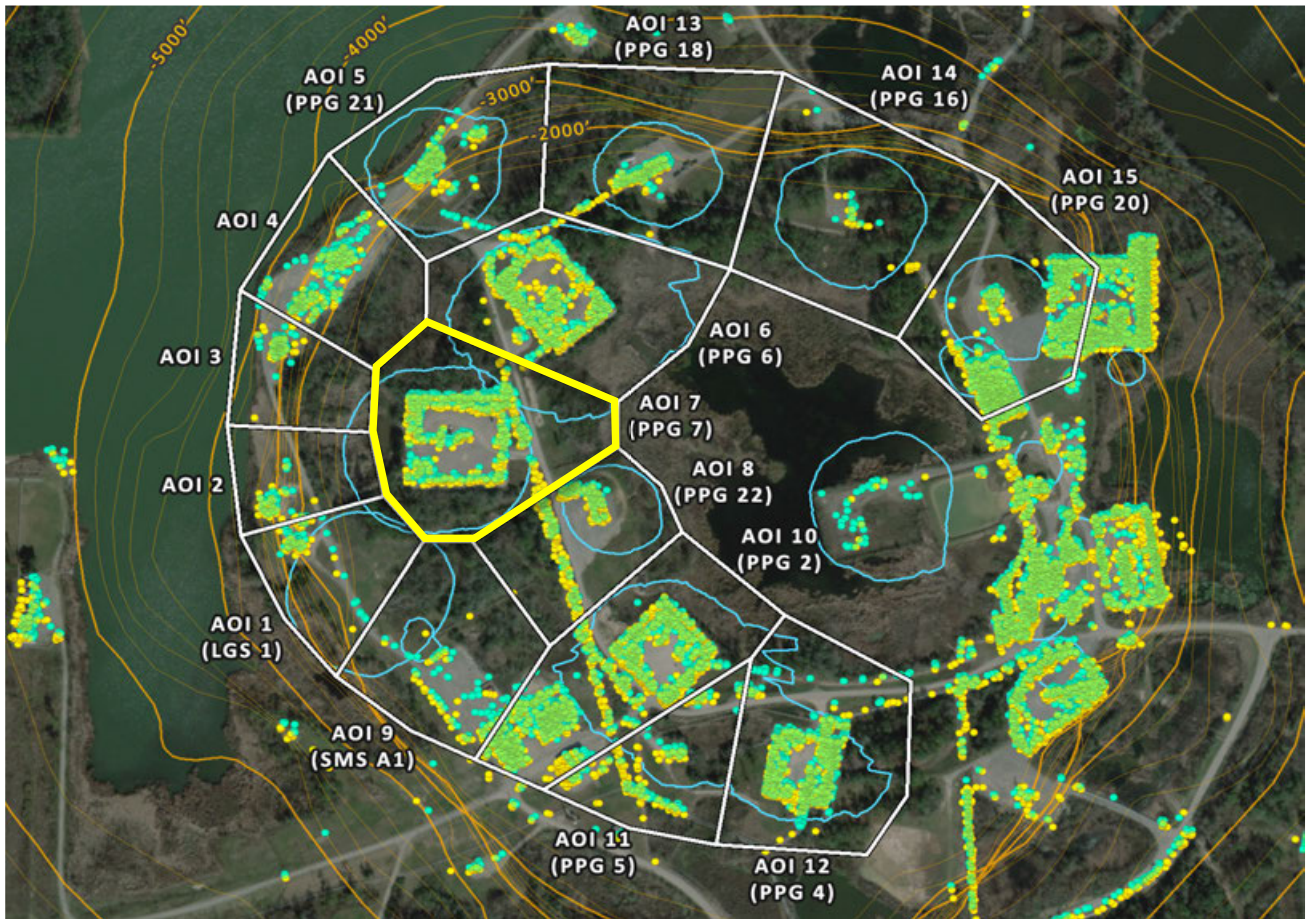
TSX/PAZ (9/29/2025) Point Count: **383**



	Nonlinear Trend	Linear Trend
Velocity:	-0.72 in/yr	-0.59 in/yr
Acceleration:	-0.10 in/yr ²	0.00 in/yr ²

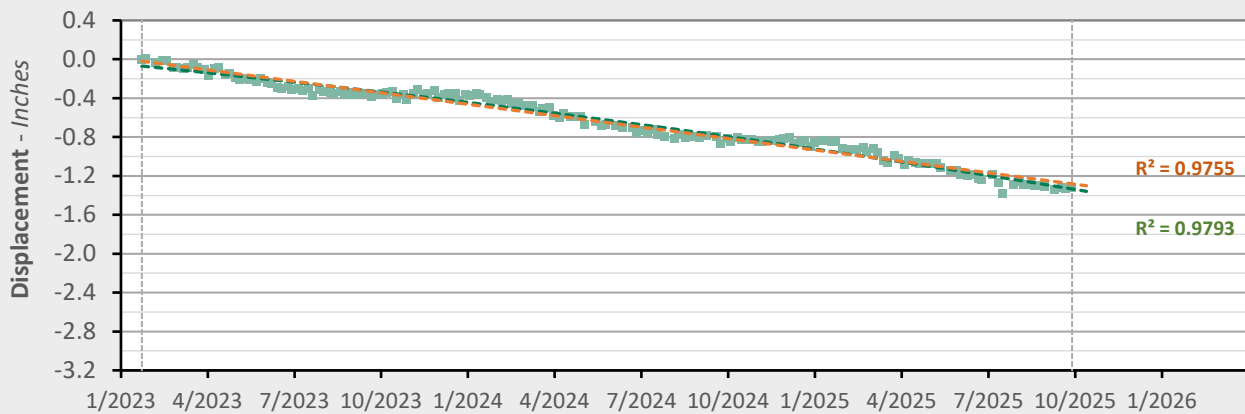


AOI 7 (PPG 7) - Location Map

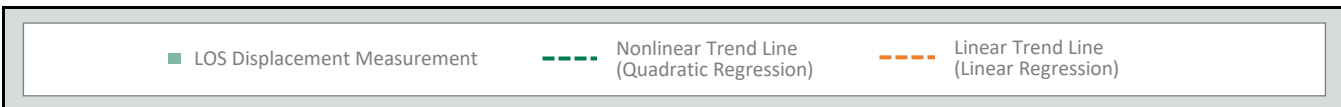


AOI 7 (PPG 7) - Displacement Time Series

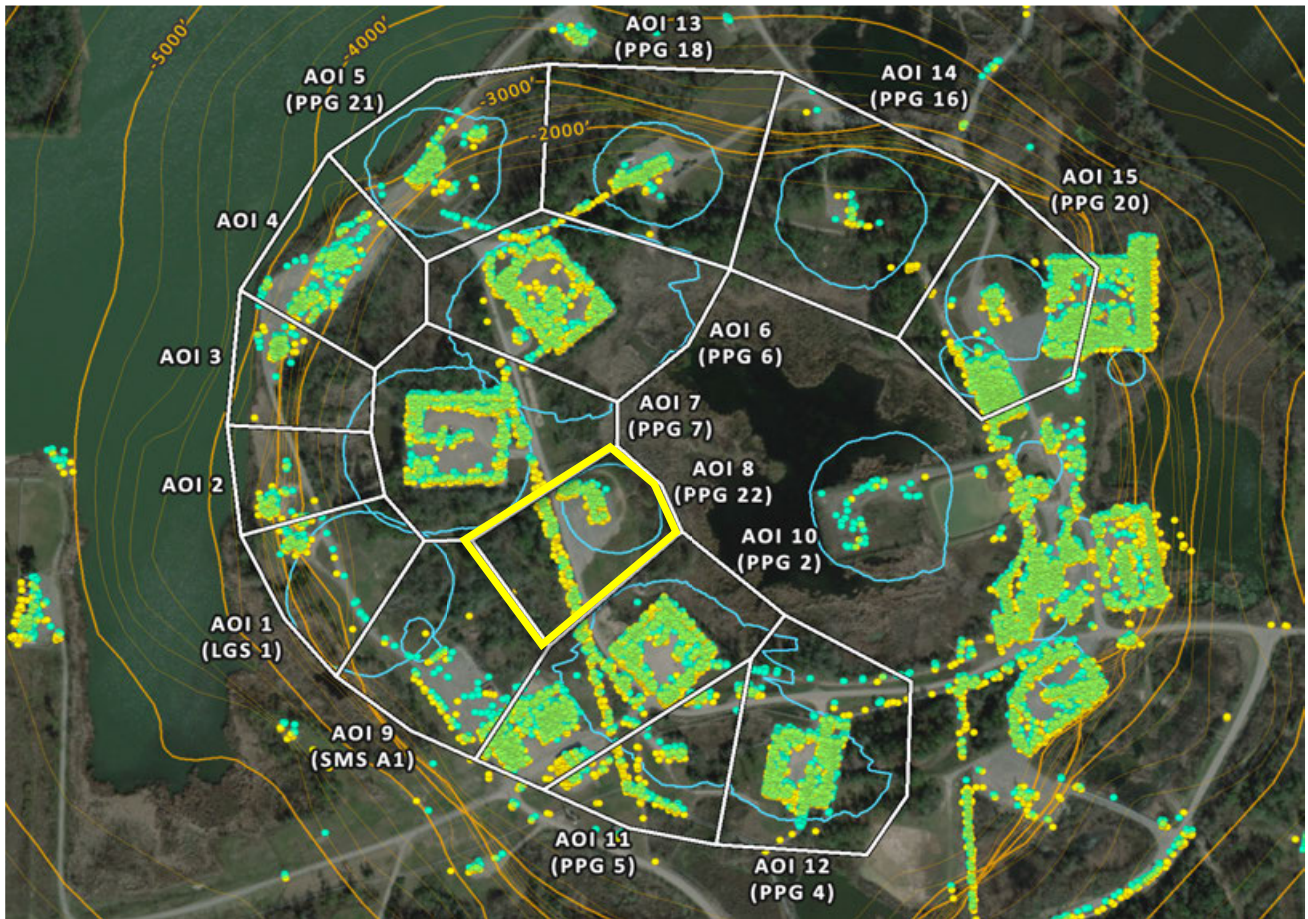
TSX/PAZ (9/29/2025) Point Count: 368



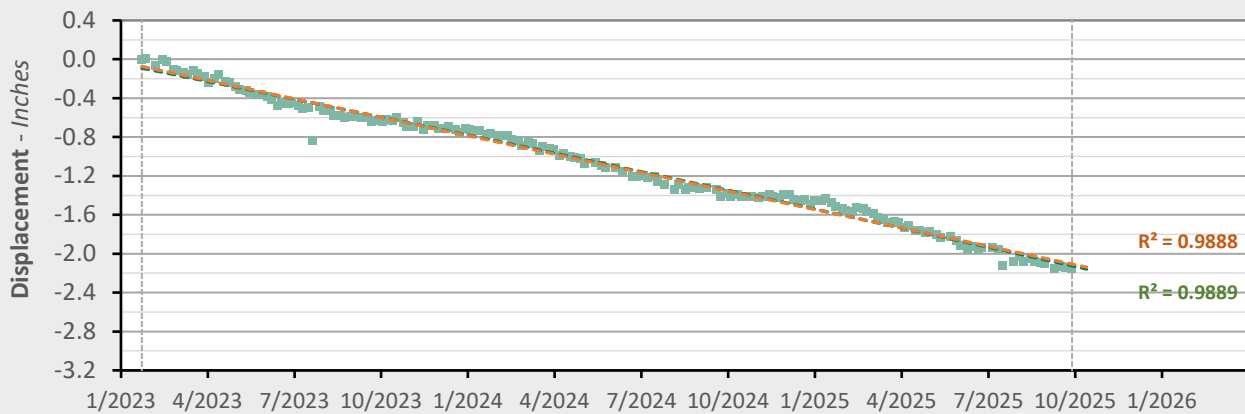
	Nonlinear Trend	Linear Trend
Velocity:	-0.59 in/yr	-0.47 in/yr
Acceleration:	-0.09 in/yr ²	0.00 in/yr ²



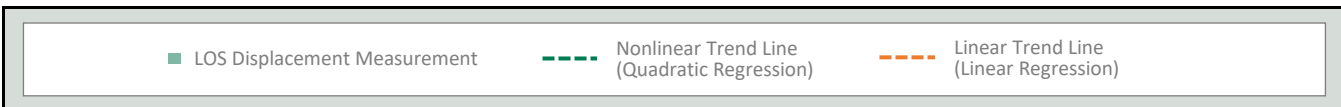
AOI 8 (PPG 22) - Location Map



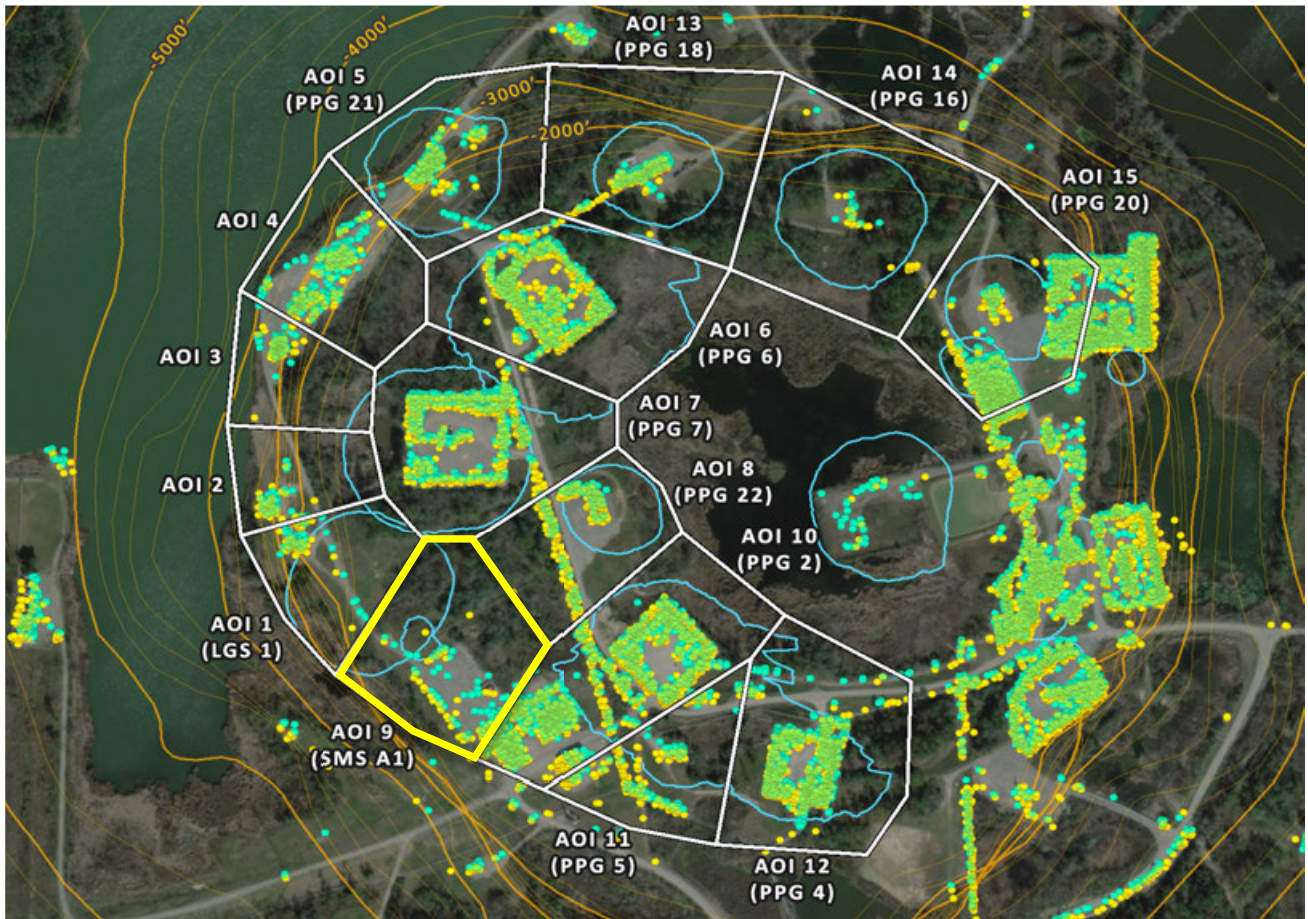
AOI 8 (PPG 22) - Displacement Time Series TSX/PAZ (9/29/2025) Point Count: 121



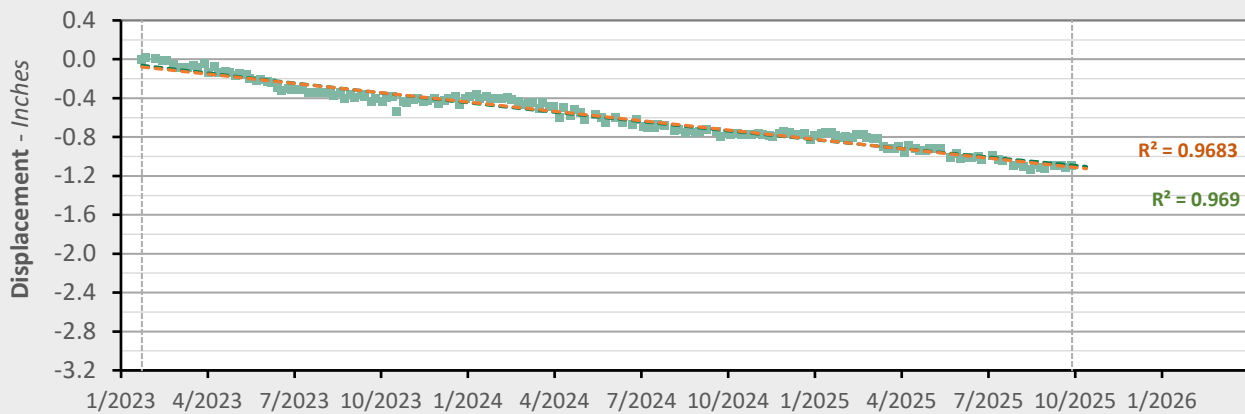
	Nonlinear Trend	Linear Trend
Velocity:	-0.80 in/yr	-0.76 in/yr
Acceleration:	-0.03 in/yr ²	0.00 in/yr ²



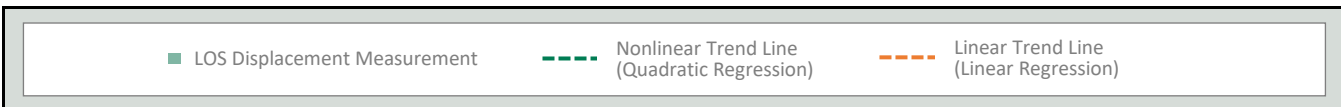
AOI 9 (PPG A1) - Location Map



AOI 9 (SMS A1) - Displacement Time Series TSX/PAZ (9/29/2025) Point Count: 73



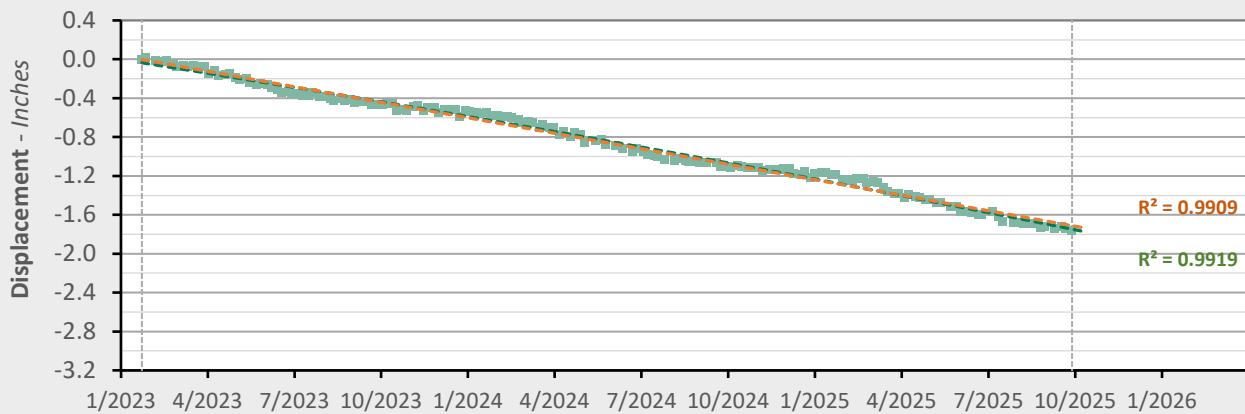
	Nonlinear Trend	Linear Trend
Velocity:	-0.34 in/yr	-0.38 in/yr
Acceleration:	+0.03 in/yr ²	0.00 in/yr ²



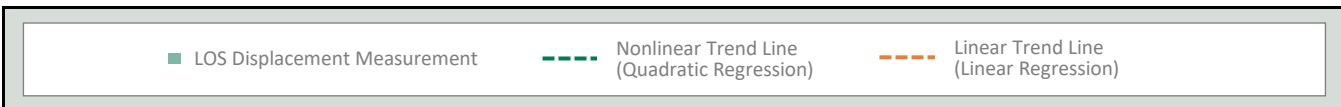
AOI 10 (PPG 2) - Location Map



AOI 10 (PPG 2) - Displacement Time Series TSX/PAZ (9/29/2025) Point Count: 815



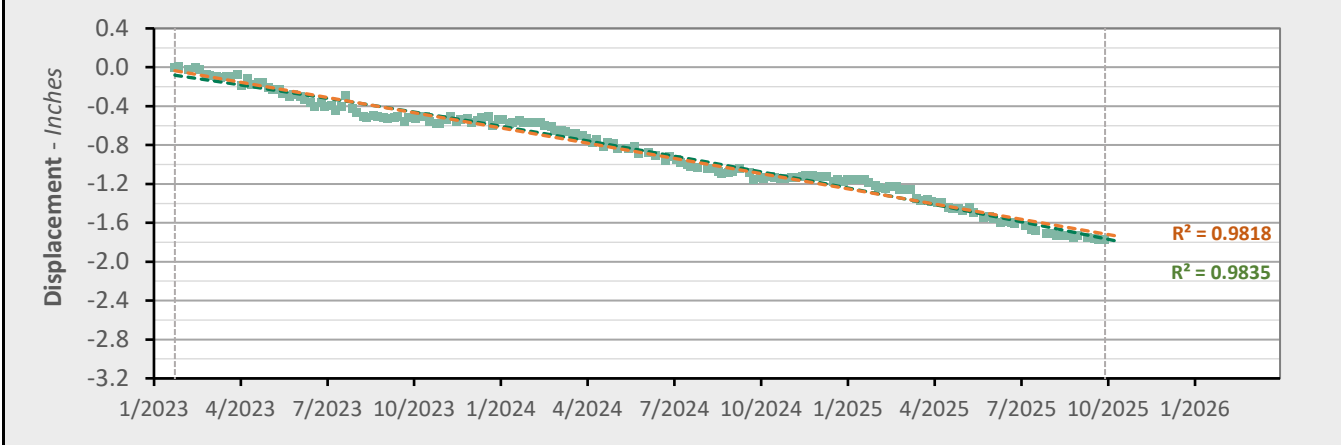
	Nonlinear Trend	Linear Trend
Velocity:	-0.72 in/yr	-0.64 in/yr
Acceleration:	-0.06 in/yr ²	0.00 in/yr ²



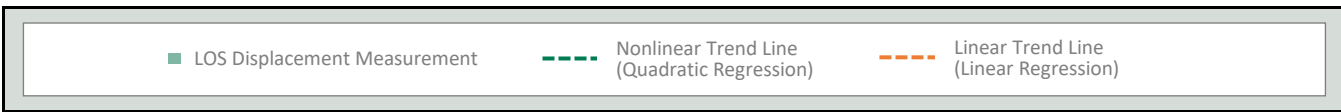
AOI 11 (PPG 5) - Location Map



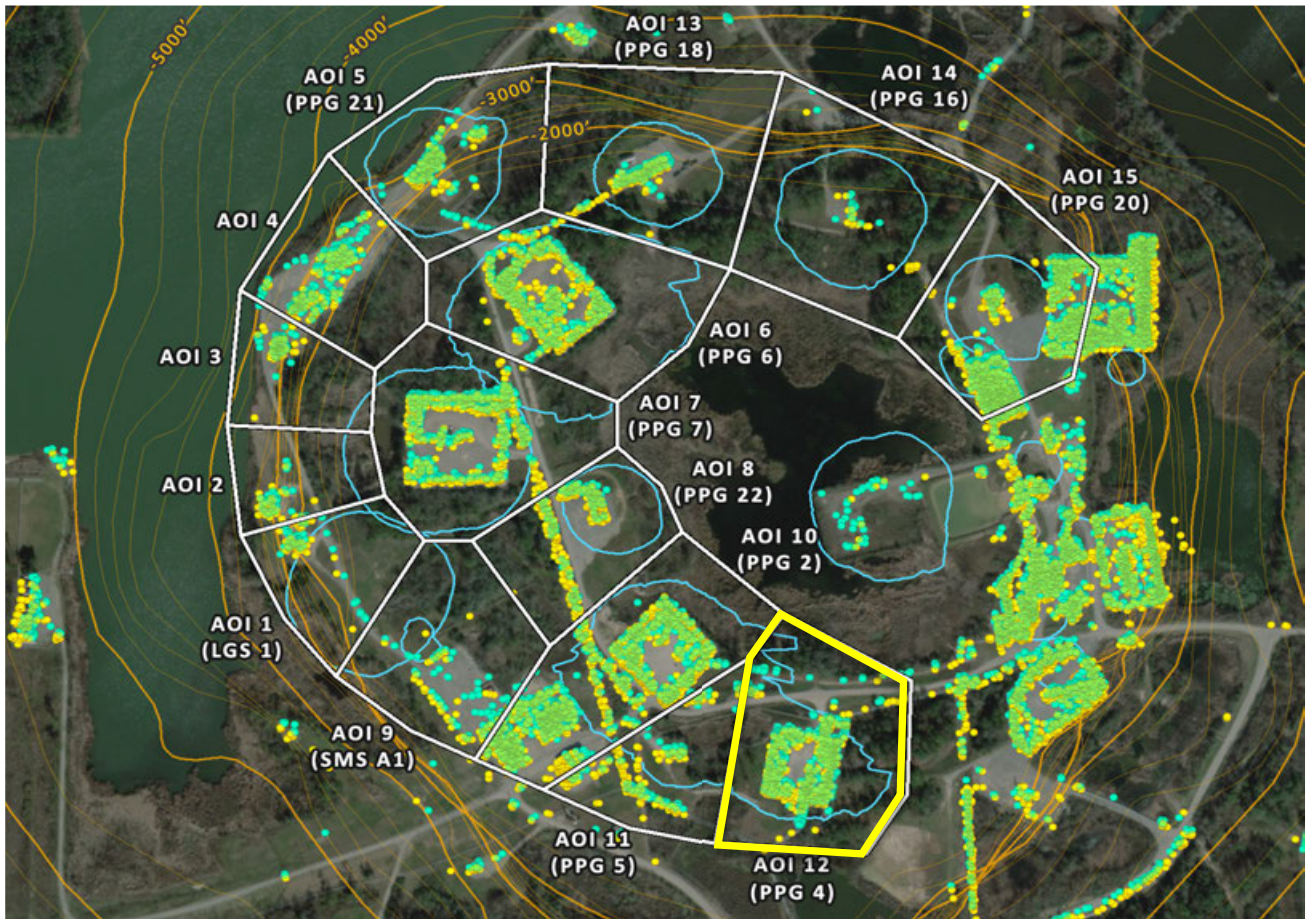
AOI 11 (PPG 5) - Displacement Time Series TSX/PAZ (9/29/2025) Point Count: 125



	Nonlinear Trend	Linear Trend
Velocity:	-0.73 in/yr	-0.63 in/yr
Acceleration:	-0.08 in/yr ²	0.00 in/yr ²



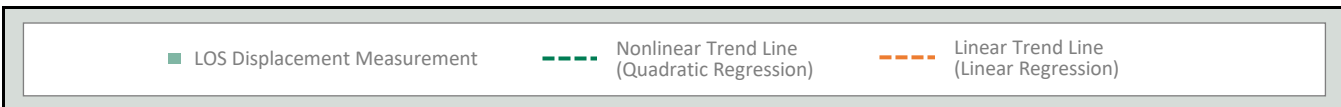
AOI 12 (PPG 4) - Location Map



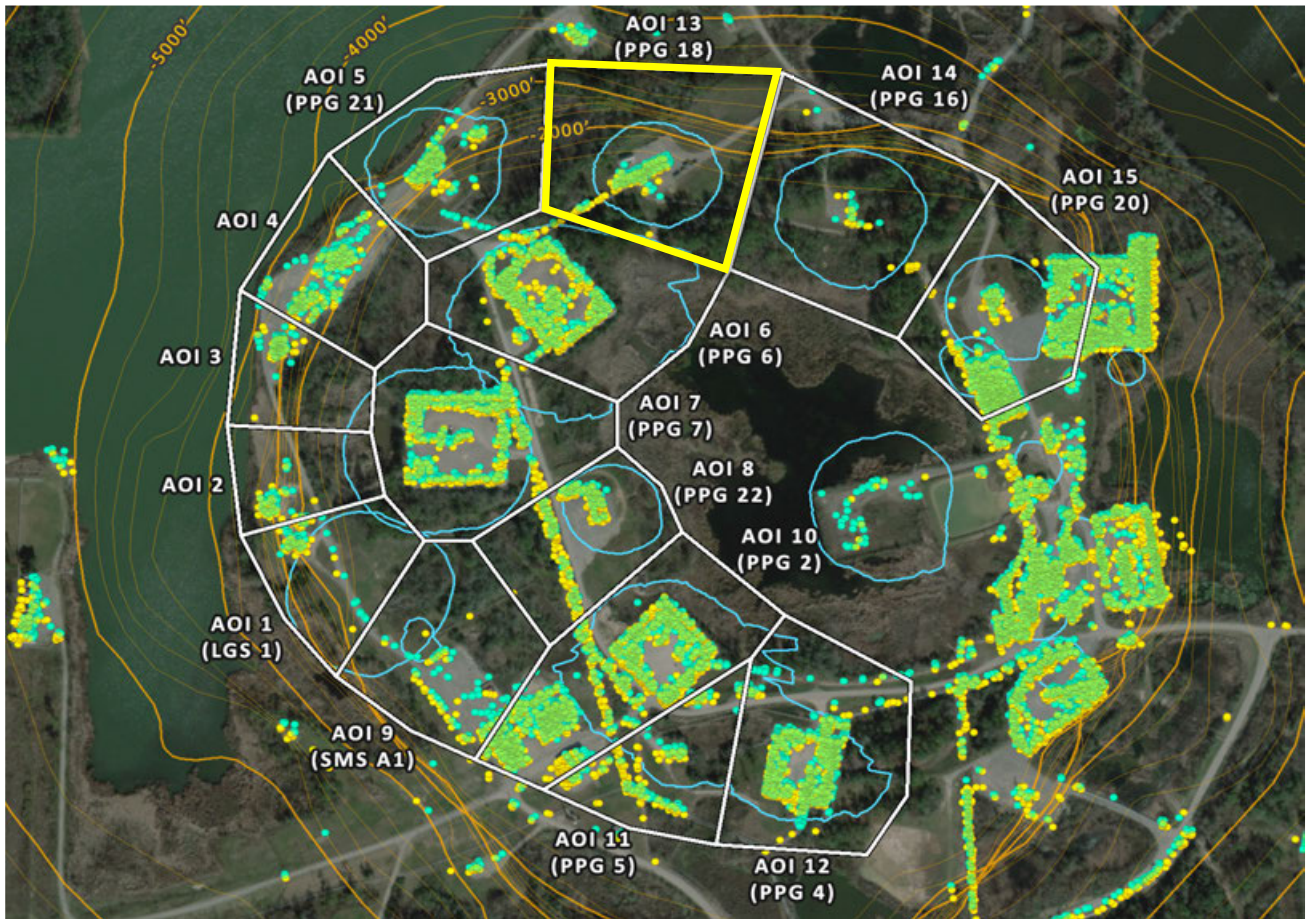
AOI 12 (PPG 4) - Displacement Time Series TSX/PAZ (9/29/2025) Point Count: 525



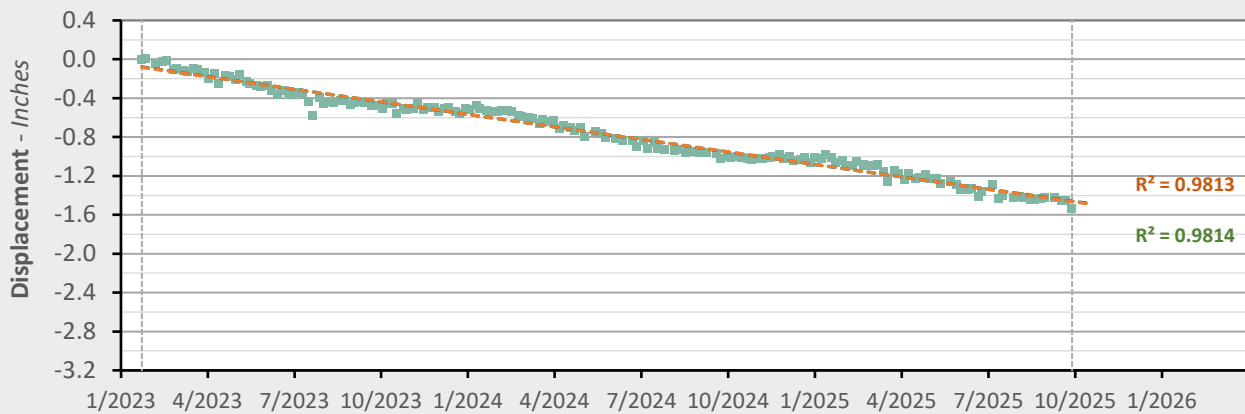
	Nonlinear Trend	Linear Trend
Velocity:	-1.02 in/yr	-0.91 in/yr
Acceleration:	-0.08 in/yr ²	0.00 in/yr ²



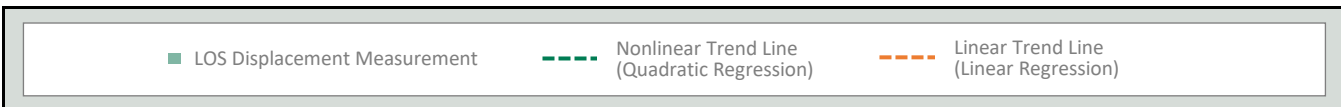
AOI 13 (PPG 18) - Location Map



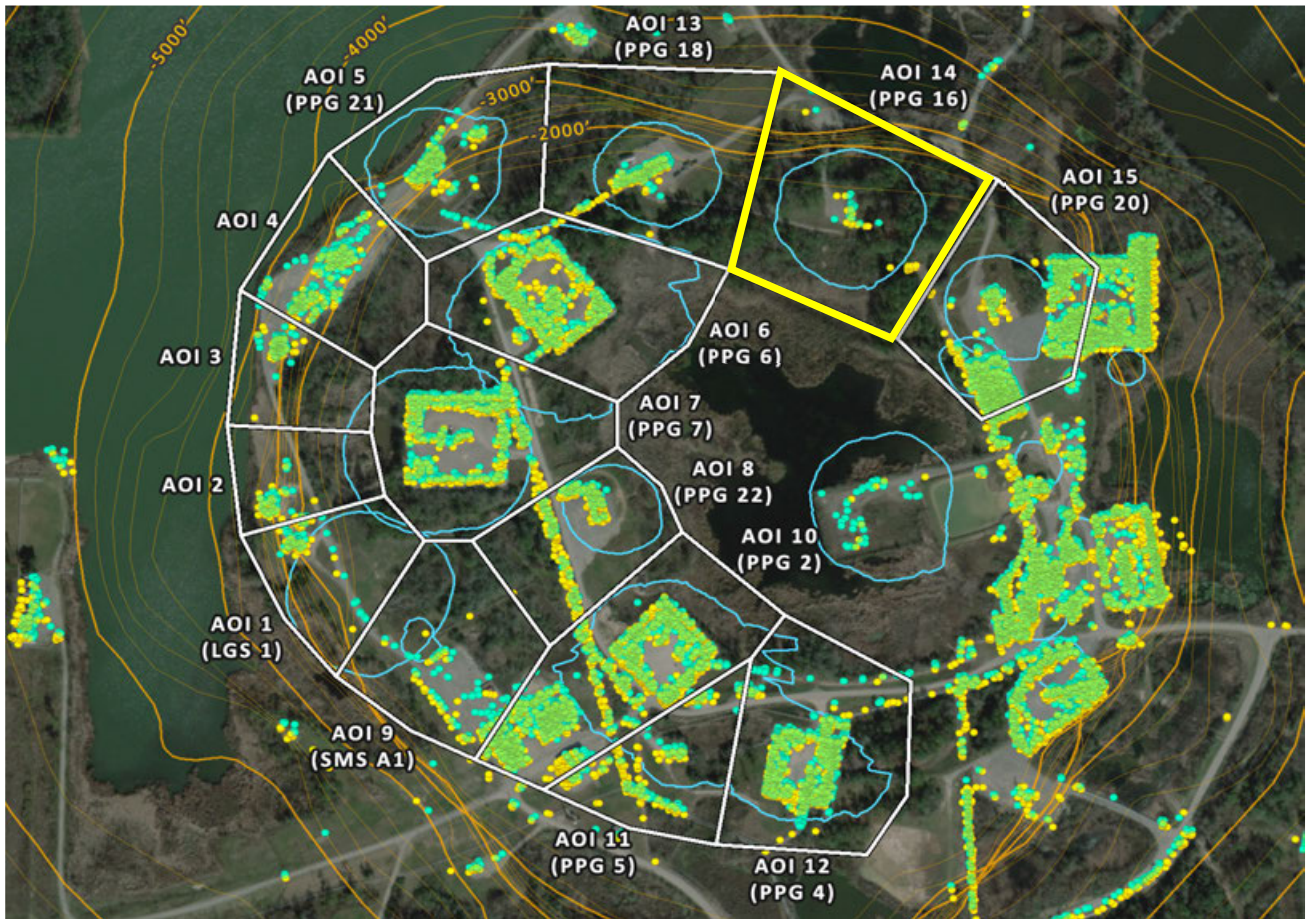
AOI 13 (PPG 18) - Displacement Time Series TSX/PAZ (9/29/2025) Point Count: 108



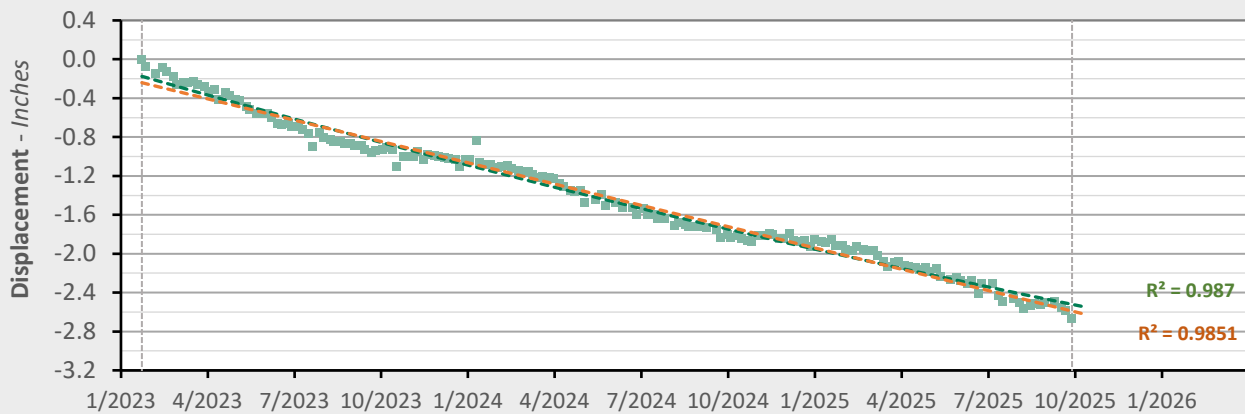
	Nonlinear Trend	Linear Trend
Velocity:	-0.50 in/yr	-0.52 in/yr
Acceleration:	+0.01 in/yr ²	0.00 in/yr ²



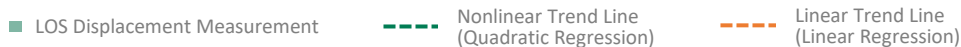
AOI 14 (PPG 16) - Location Map



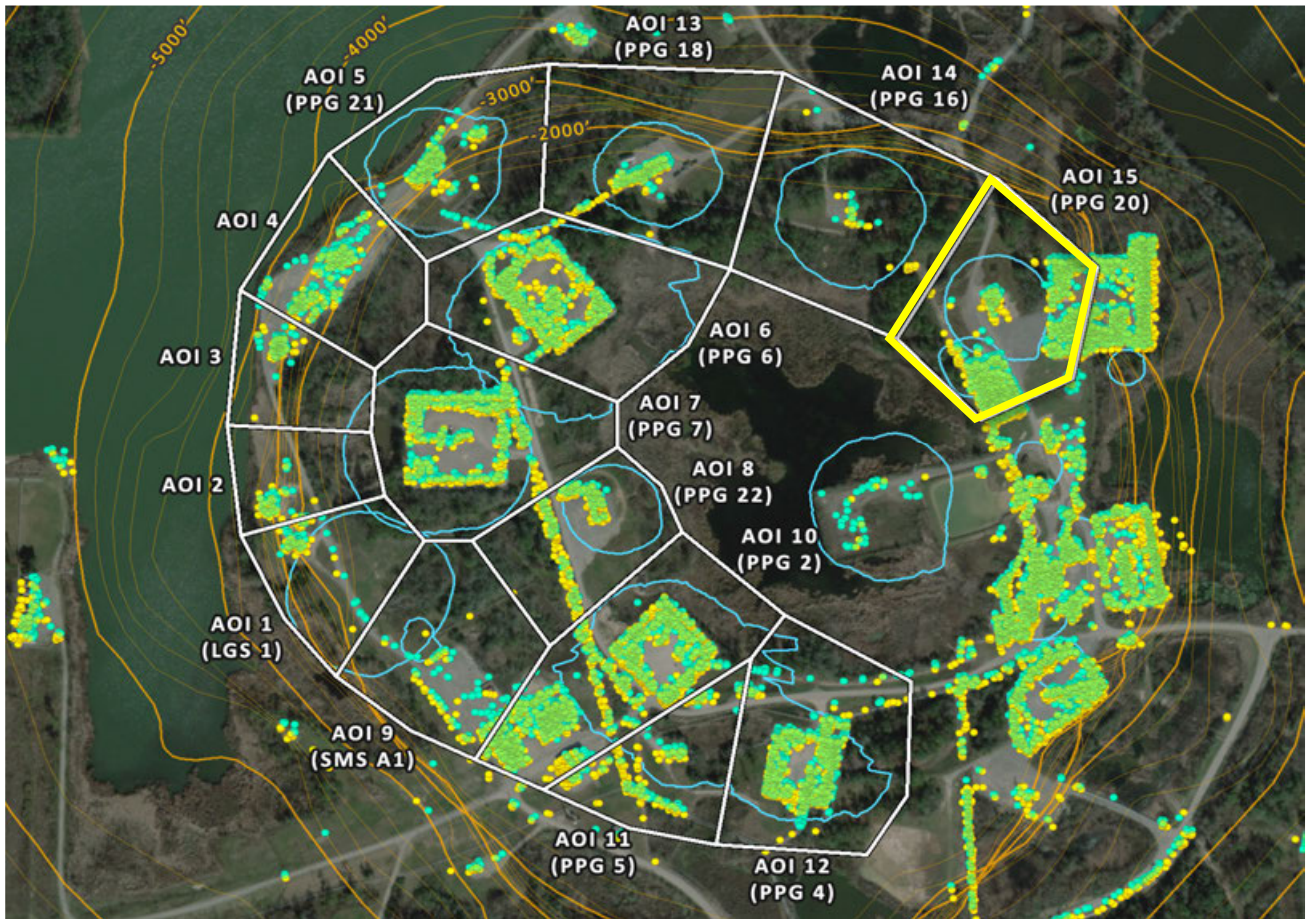
AOI 14 (PPG 16) - Displacement Time Series TSX/PAZ (9/29/2025) Point Count: 18



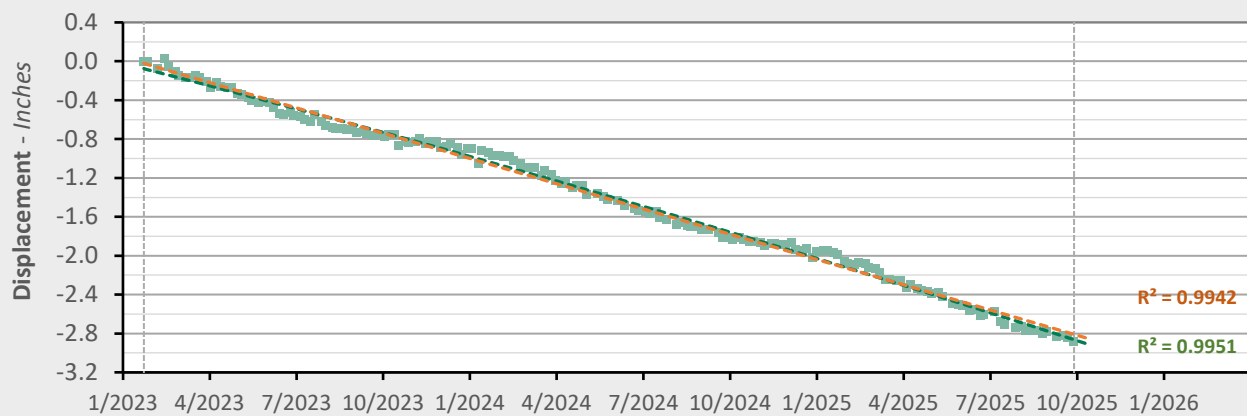
	Nonlinear Trend	Linear Trend
Velocity:	-0.73 in/yr	-0.88 in/yr
Acceleration:	+0.11 in/yr ²	0.00 in/yr ²



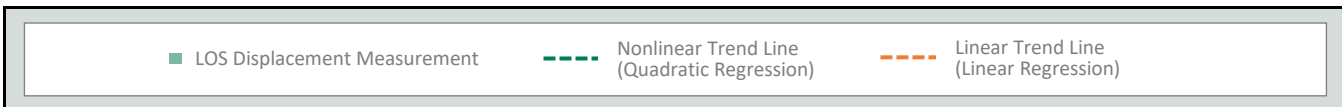
AOI 15 (PPG 20) - Location Map



AOI 15 (PPG 20) - Displacement Time Series TSX/PAZ (9/29/2025) Point Count: 687



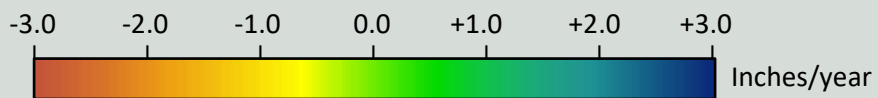
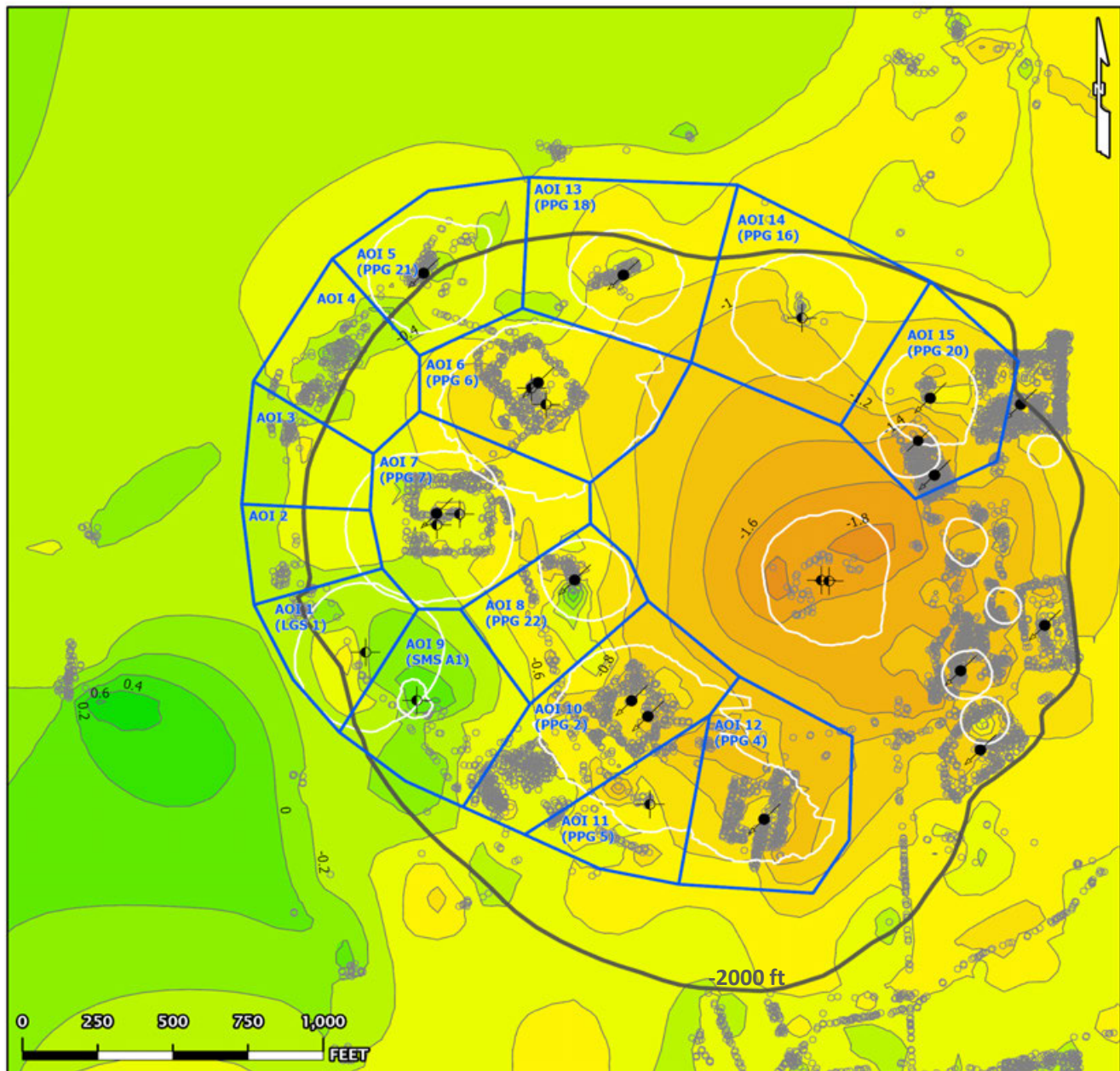
	Nonlinear Trend	Linear Trend
Velocity:	-1.16 in/yr	-1.04 in/yr
Acceleration:	-0.09 in/yr ²	0.00 in/yr ²



TSX/PAZ Data (01/24/2023 - 09/29/2025)

Nonlinear Velocity Contours

As of date: 09/29/2025

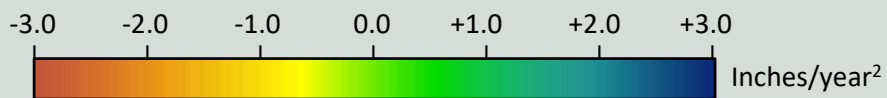
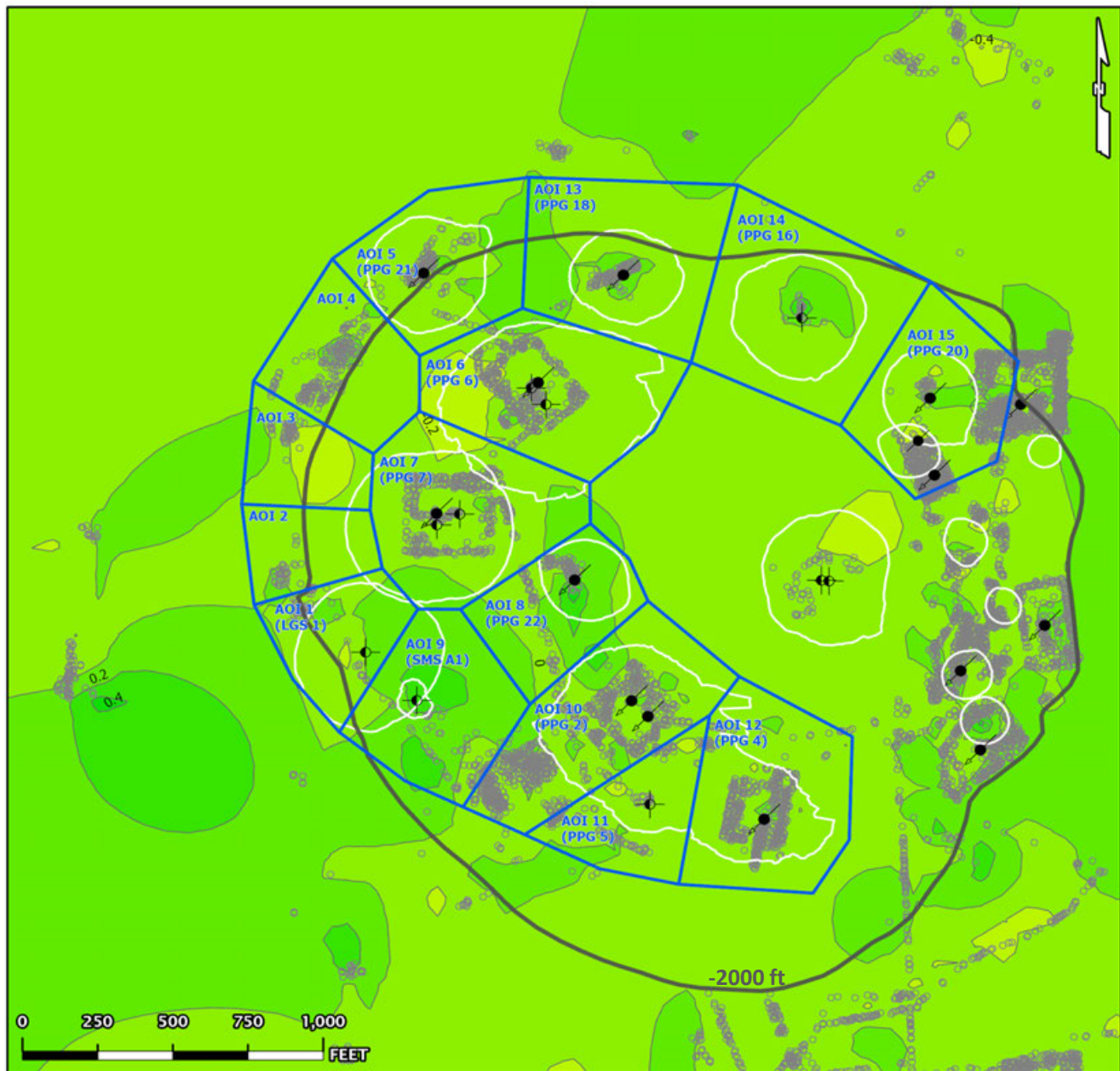


- AOI Boundary
 - InSAR LOS Measurement Point
 - Contour (0.2)
 - Historical Cavern Extent
 - Top of Dome (-2000 ft Contour)
- Cavern Well Surface Locations
- 09 - Active - Injection
 - 29 - Dry and Plugged

TSX/PAZ Data (01/24/2023 - 09/29/2025)

Nonlinear Acceleration Contours

Date range: 01/24/2023 - 09/29/2025

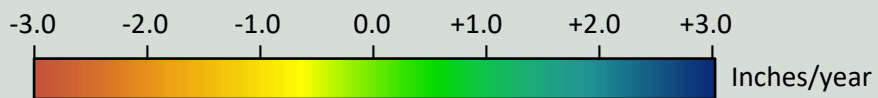
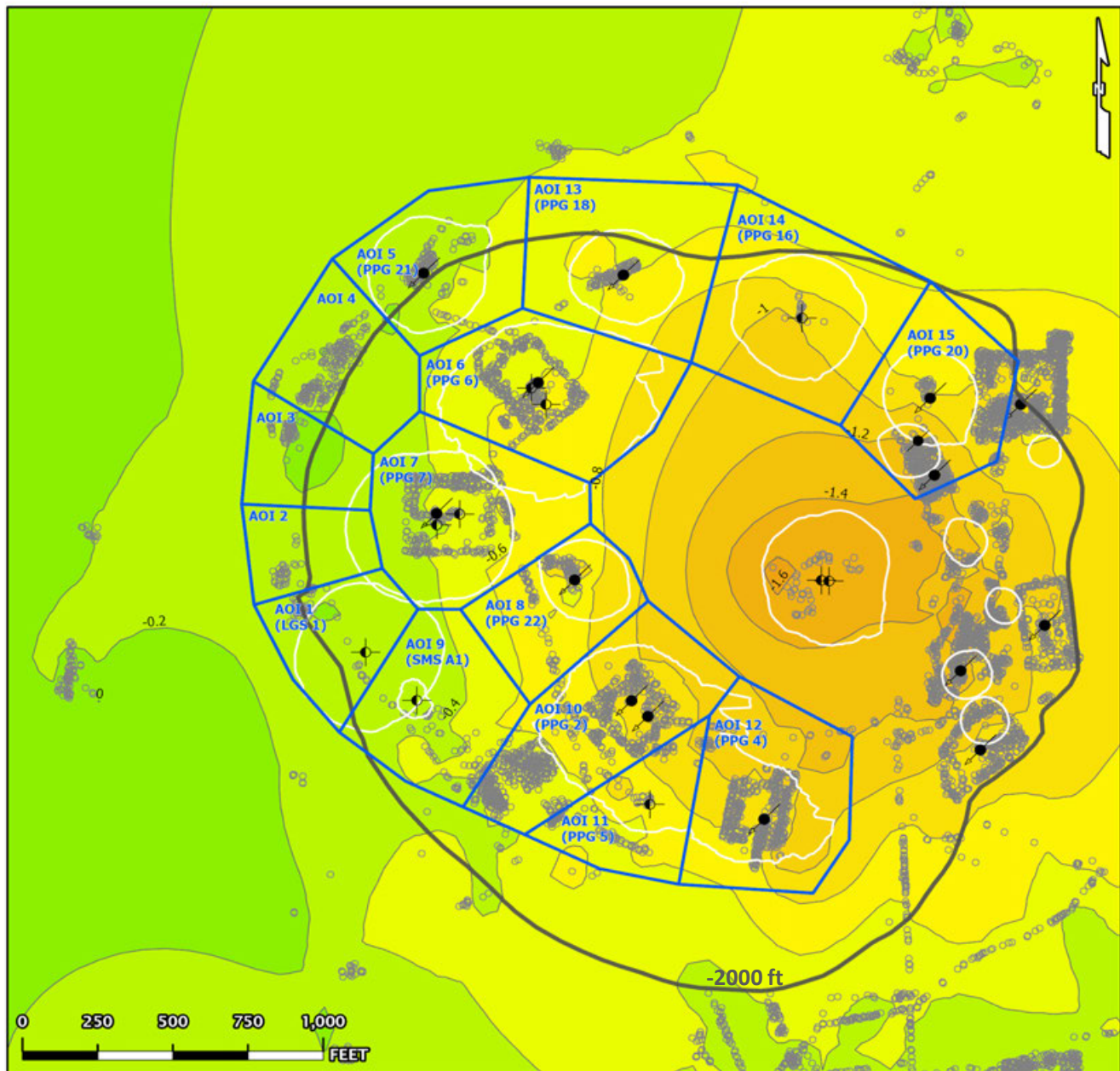


- AOI Boundary
 - InSAR LOS Measurement Point
 - Contour (0.2)
 - Historical Cavern Extent
 - Top of Dome (-2000 ft Contour)
- Cavern Well Surface Locations
- 09 - Active - Injection
 - 29 - Dry and Plugged

TSX/PAZ Data (01/24/2023 - 09/29/2025)

Linear Velocity Contours

Date range: 01/24/2023 - 09/29/2025

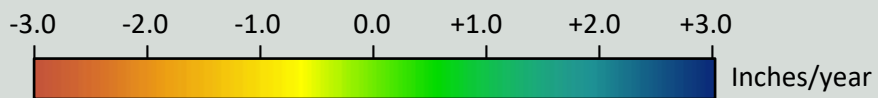


- AOI Boundary
 - InSAR LOS Measurement Point
 - Contour (0.2)
 - Historical Cavern Extent
 - Top of Dome (-2000 ft Contour)
- Cavern Well Surface Locations
- 09 - Active - Injection
 - 29 - Dry and Plugged

TSX/PAZ Data (01/24/2023 - 09/29/2025)

Nonlinear Velocity Data Points

As of date: 09/29/2025

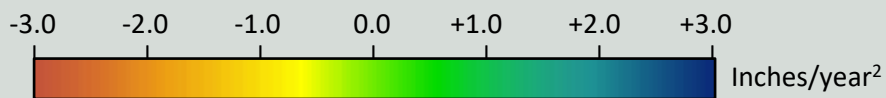


- AOI Boundary
 - Historical Cavern Extent
 - Top of Dome (-2000 ft Contour)
 - InSAR LOS Measurement Point
- Cavern Well Surface Locations
- 09 - Active - Injection
 - 29 - Dry and Plugged

TSX/PAZ Data (01/24/2023 - 09/29/2025)

Nonlinear Acceleration Data Points

Date range: 01/24/2023 - 09/29/2025

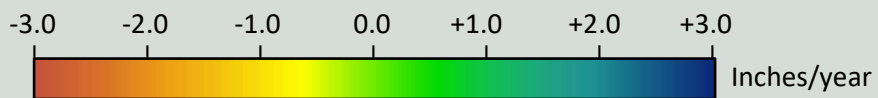


- AOI Boundary
 - InSAR LOS Measurement Point
 - Historical Cavern Extent
 - Top of Dome (-2000 ft Contour)
- Cavern Well Surface Locations
- 09 - Active - Injection
 - 29 - Dry and Plugged

TSX/PAZ Data (01/24/2023 - 09/29/2025)

Linear Velocity Data Points

Date range: 01/24/2023 - 09/29/2025



- AOI Boundary
 - Historical Cavern Extent
 - Top of Dome (-2000 ft Contour)
 - InSAR LOS Measurement Point
- Cavern Well Surface Locations
- 09 - Active - Injection
 - 29 - Dry and Plugged

ATTACHMENT D

Vertical & East-West 2D InSAR report - September 29, 2025



Vertical & E-W 2D Update

Continuous InSAR Monitoring of
Ground Displacement At Westlake
Caverns and Western Dome Flank

Sulphur Mines Salt Dome

Prepared for:
Westlake Chemical

Prepared by:
Lonquist Field Service, LLC
8591 United Plaza Blvd., Suite 280
Baton Rouge, LA 70809

Dataset
Satellite Source
TSX-Ascending and TSX/PAZ-Descending
Most Recent Image Date
Monday, September 29, 2025

Analysis Report Date:
October 15, 2025

Dataset Information	
Satellite Source	TSX-Ascending and TSX/PAZ-Descending
Update Frequency	11 days
Most Recent Image Date	Monday, September 29, 2025
Dataset Image Count	163
Dataset Time Range	February 4, 2023 - September 29, 2025
Dataset Length	2.65 Years
Measurement Directions	Vertical and East-West

Analysis Methodology

Time Series Charts
Trend lines were calculated for the averaged vertical and east-west displacement values within each AOI. Both a nonlinear (quadratic) and linear regression were applied to each AOI point group to identify rates of change in 2D displacement. These trends are displayed in the Time Series section of this report.

Contour Maps
A nonlinear (quadratic) and linear trend was also calculated for each individual measurement point across the analysis region. Nonlinear trend values for each point were used to generate Velocity and Acceleration contour maps to convey the spatial distribution of the calculated movement. The linear trend values for each point (which lack an acceleration component) were used to generate an additional Velocity contour map. Maps depicting the individual data points colored by these trend values are also included following the

Rate Interpretation
For the vertical data, positive velocity values indicate uplift and negative velocity values indicate subsidence. Positive acceleration values indicate increasing rates of uplift or slowing rates of subsidence, while negative acceleration values indicate slowing rates of uplift or increasing rates of subsidence. For the east-west data, positive velocity values indicate eastward horizontal movement and negative velocity values indicate westward horizontal movement. Positive acceleration values indicate increasing rates of eastward movement or decreasing rates of westward movement, while negative acceleration values indicate increasing rates of westward movement or decreasing rates of eastward movement.

Observations

To-date there have been no acute deviations from established subsidence trends in the areas investigated.

The calculated vertical displacement values indicate that subsidence is occurring with near-linear trends in all AOIs, with the greatest rates occurring in the central portions of the dome. Minor positive and negative vertical acceleration is broadly balanced among the AOIs.

The calculated east-west displacement values generally indicate near-linear horizontal movement toward the dome center with the greatest rates of eastward movement occurring in the western AOIs and the greatest rates of westward movement occurring in the easternmost AOIs. Minor negative (westward) acceleration is present in most of the nonlinear AOI trends due to a recent seasonal below-trend dip noted in the TSX/PAZ data.



Date Signed: October 15, 2025
Austin, Texas

Nathaniel L. Byars, P.E.
Principal Engineer
Louisiana License No. 40697

InSAR Data Sources

InSAR Data

Interferometric Synthetic Aperture Radar (InSAR) is the most well established method to continually evaluate small, normally undetectable, ground movement over a large area. Radar imagery collected via satellites over successive orbital passes is used to identify and define measurement points on the ground. Objects or ground features providing a stable reflection of radar energy such as buildings, roads, and infrastructure produce the highest quality measurement points. InSAR analysis identifies the change in distance between the satellite and each measurement point over time relative to a stable reference point within the imaged area.

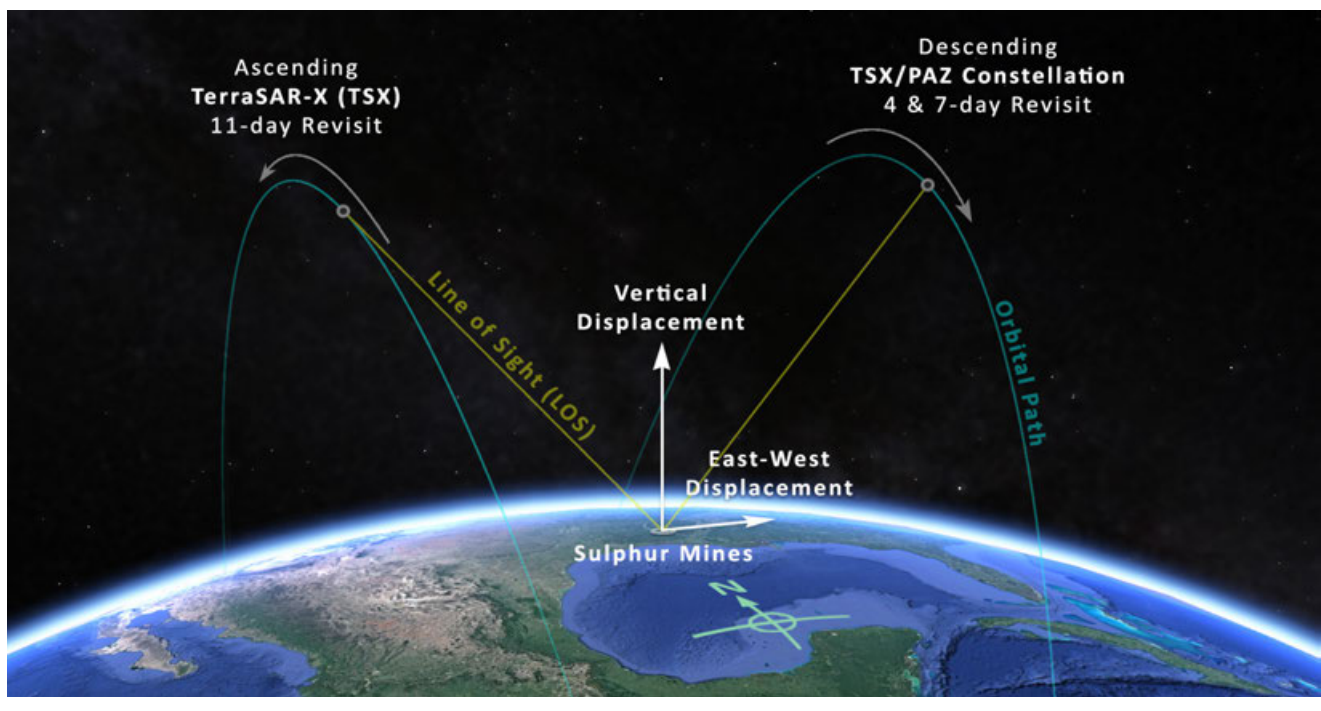
Satellite Sources

Two InSAR datasets are being used to evaluate subsidence over the Sulphur Mines Salt Dome. These datasets provide Line-of-Sight (LOS) displacement measurements from both ascending and descending orbits. An ascending orbit denotes the satellite's longitudinal course from south to north as it passes over the site, while a descending orbit denotes the satellite is moving from north to south.

The first dataset comes from the high-resolution TerraSAR-X satellite on an ascending orbit track ("TSX-A") that captures data from the west of the site on an 11-day frequency. The second comes from a pair of high-resolution satellites that include the TerraSAR-X satellite and the PAZ satellite ("TSX/PAZ Constellation") which share the same descending orbit track and capture data from east of the site, each with an 11-day frequency. Their orbits are offset with the PAZ satellite passing over the site 4 days after the TSX satellite.

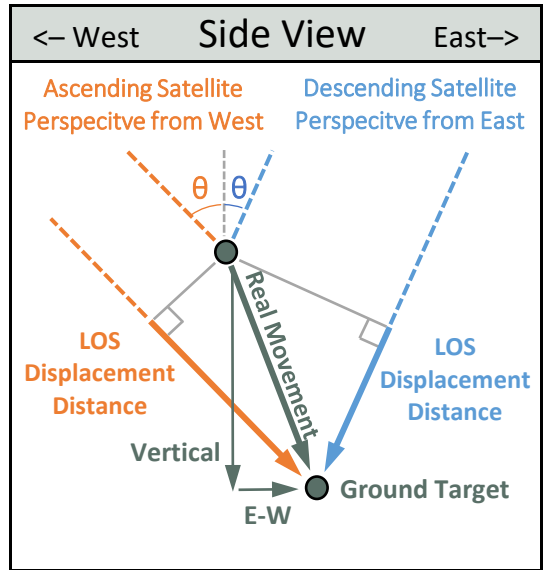
Each instance of data capture in either the TSX-A or TSX/PAZ constellation is used to generate two-dimensional ("2D") displacement values in the vertical and east-west directions for each measurement point within the 2D data grid. The image below depicts the orbital paths of the current satellites in relation to the Sulphur Mines Salt Dome as well as the 2D components of the calculated displacement. Prior to May 2024, the ascending data for the 2D calculations was captured from a low-resolution Sentinel-1 satellite at a similar viewing angle to the TSX orbit.

Satellite Orbital Diagram



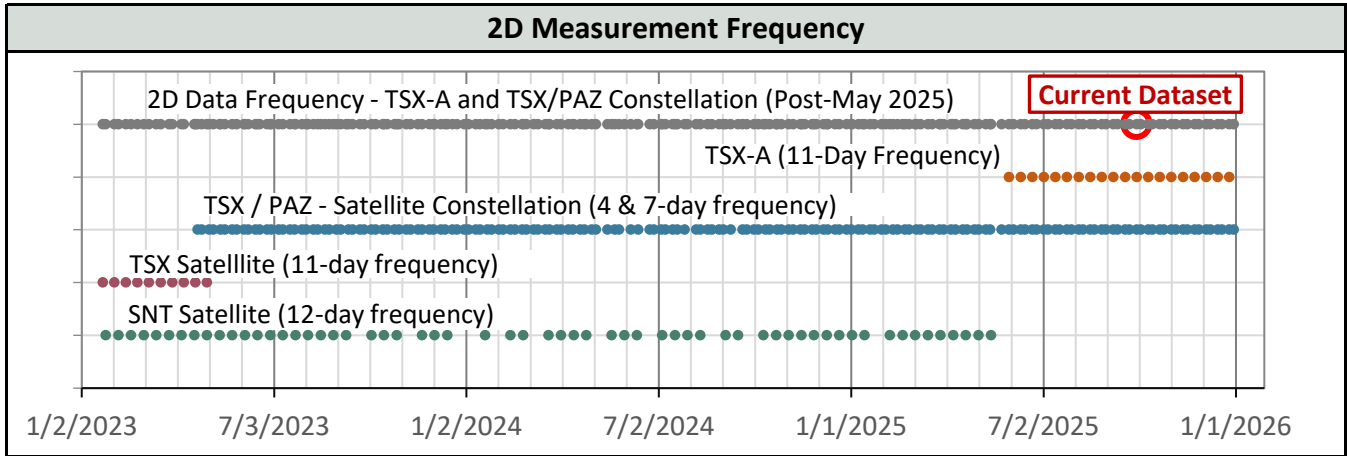
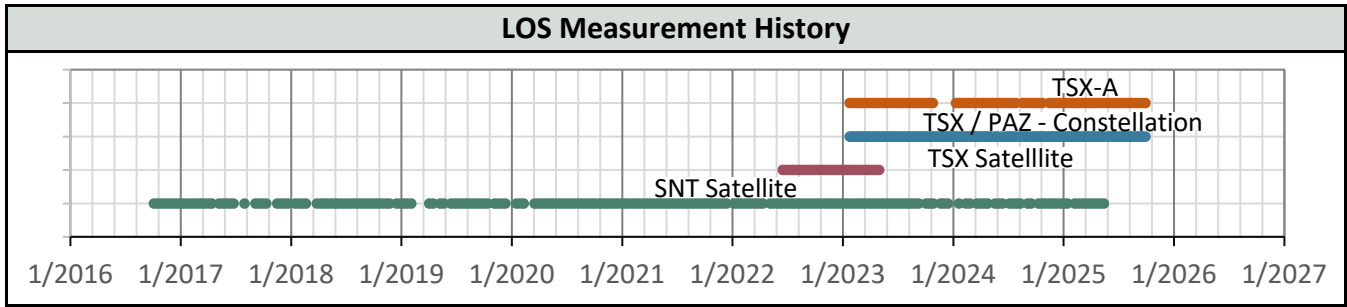
InSAR 2D Vertical and East-West Data

LOS (line-of-sight) displacement measurements, which refer to a change in distance between the satellite sensor and the ground target, are used to triangulate the real movement along the 2D plane defined by the satellite positions and the ground target. The diagram to the right illustrates the geometric relationship between the Real Movement of a ground target, the LOS displacement measurements from two different satellite viewing directions, and the resulting vertical and east-west components of calculated 2D displacement. Ground targets are not consistent between LOS datasets so these calculations are performed on averaged LOS data within 33-ft square cells. One 2D measurement point is generated within each cell where data from both LOS sources are present.

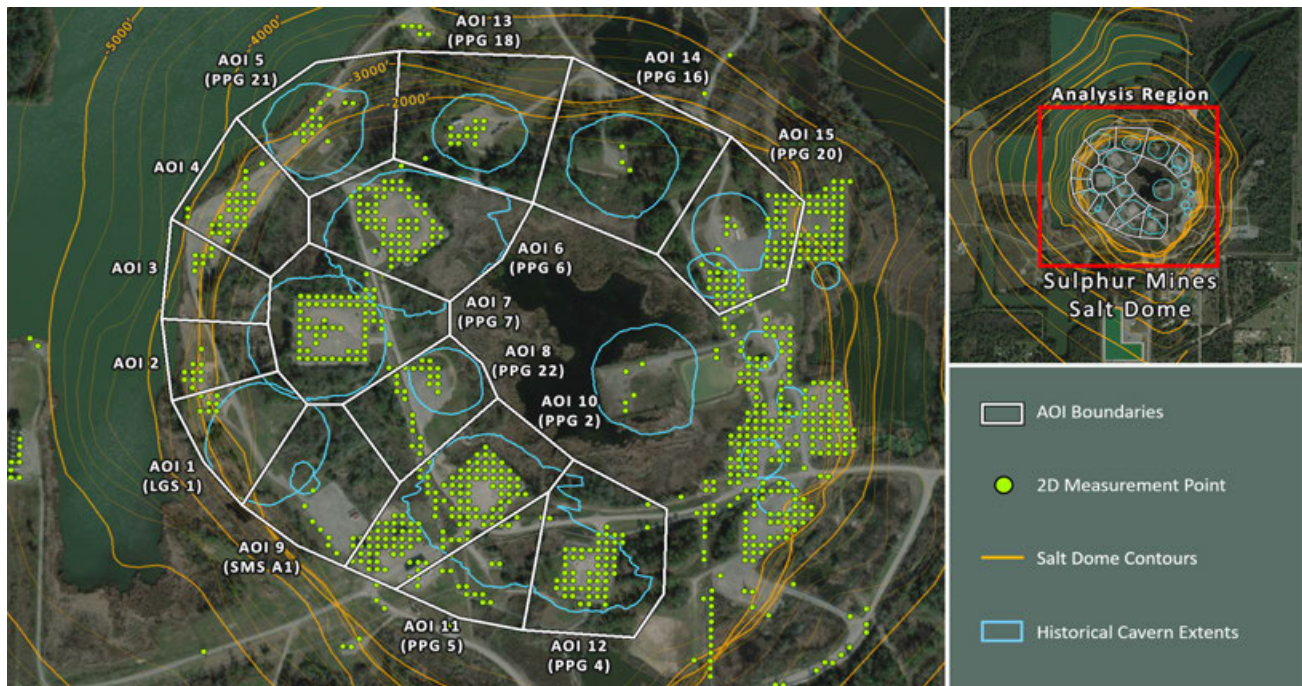


Satellite Properties & Image Frequency

Satellite and Data Properties	TSX-A	TSX/PAZ Constellation
Band (Wavelength)	X-band (1.22 in)	X-band (1.22 in)
Track	T52	T67 & T120
Pixel resolution	3 x 3 ft	3 x 3 ft
Revisit frequency	11 days	4 & 7 days
Orbit (LOS Angle, θ)	Ascending (44°)	Descending (37°)
Data Start Date	2/4/2023	1/24/2023
Measurement error range	± 0.06 in	± 0.07 in



AOI Boundaries & 2D InSAR Measurement Points

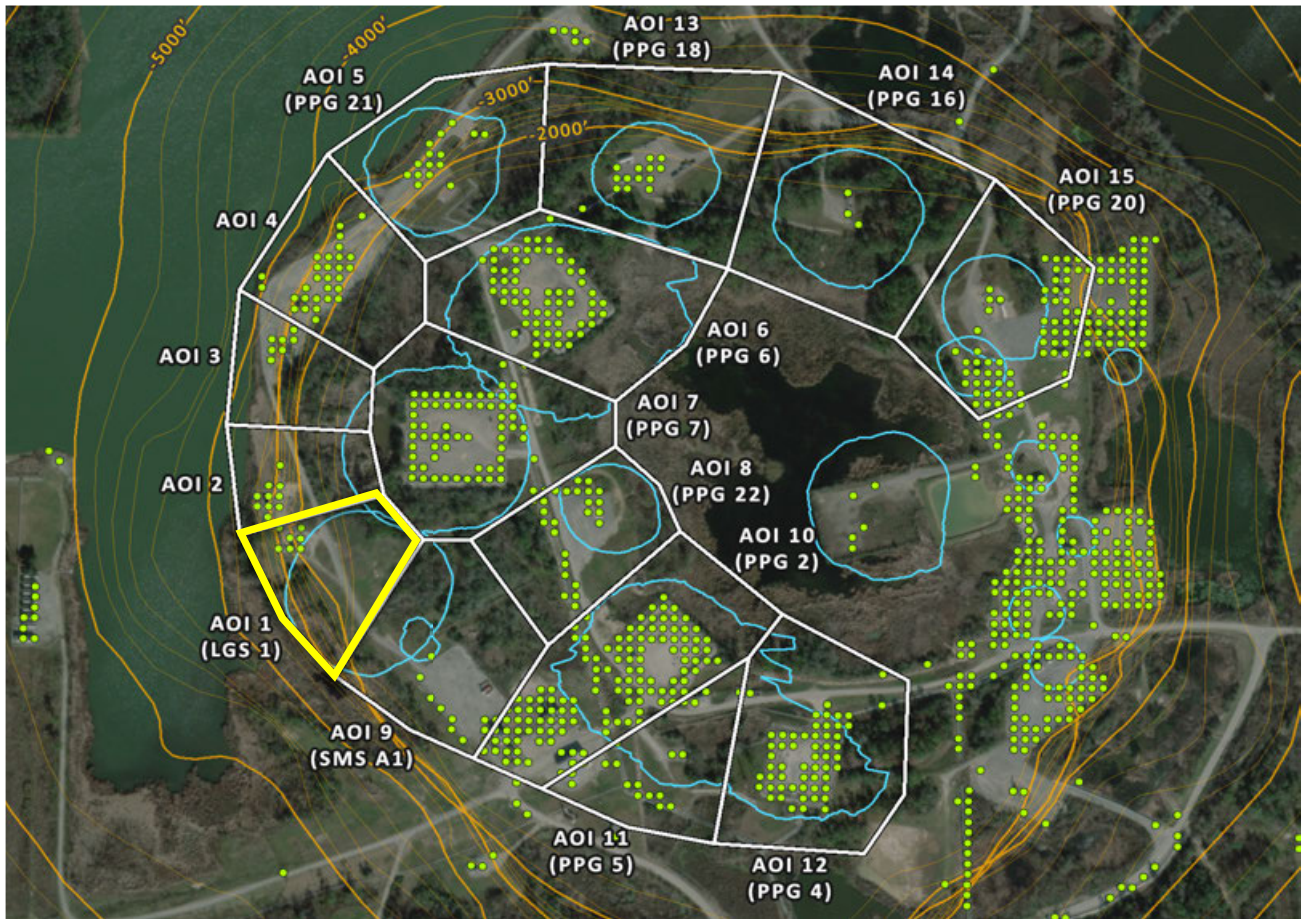


Subsidence Monitoring Areas of Interest (AOIs)

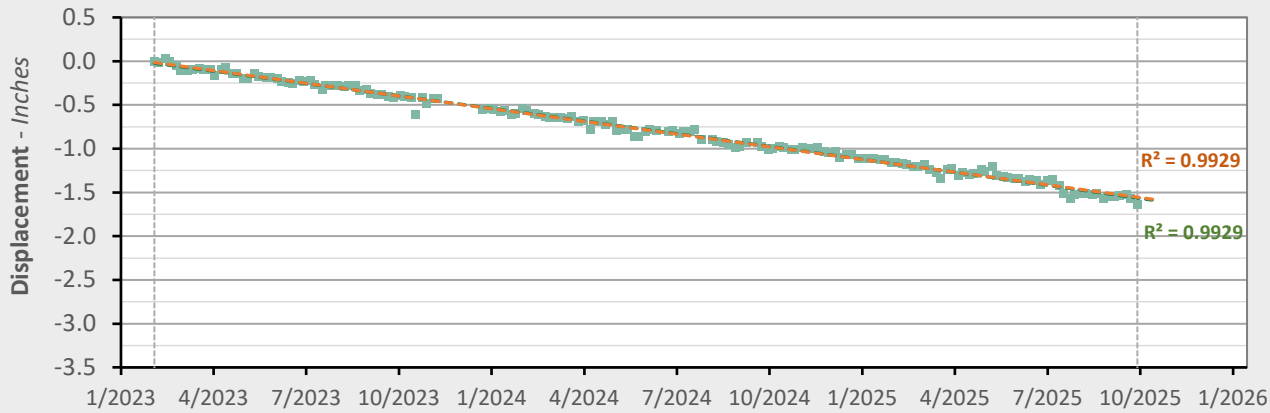
To visually convey and evaluate trend consistency for the Vertical displacement time series of each ground target, measurement points were grouped and their displacement values were averaged. The point groups are referred to as Areas of Interest (AOIs) in this analysis and their boundaries are depicted on the above map. The below table lists the Vertical trend values calculated in each AOI for the dataset evaluated in this report.

AOI Name	Vertical (9/29/2025)	Vertical Velocity (in/yr)		Vertical Acceleration (in/yr ²)	
	Point Count	Nonlinear	Linear	Nonlinear	Linear
AOI 1 (LGS 1)	9	-0.60	-0.58	-0.01	0.00
AOI 2	10	-0.55	-0.59	+0.03	0.00
AOI 3	7	-0.54	-0.55	+0.00	0.00
AOI 4	29	-0.57	-0.55	-0.02	0.00
AOI 5 (PPG 21)	15	-0.59	-0.55	-0.03	0.00
AOI 6 (PPG 6)	65	-1.04	-0.91	-0.10	0.00
AOI 7 (PPG 7)	62	-1.05	-0.94	-0.09	0.00
AOI 8 (PPG 22)	25	-1.24	-1.19	-0.04	0.00
AOI 9 (SMS A1)	12	-0.56	-0.74	+0.13	0.00
AOI 10 (PPG 2)	124	-1.14	-1.04	-0.07	0.00
AOI 11 (PPG 5)	19	-1.06	-0.93	-0.09	0.00
AOI 12 (PPG 4)	56	-1.11	-1.04	-0.05	0.00
AOI 13 (PPG 18)	13	-0.69	-0.75	+0.04	0.00
AOI 14 (PPG 16)	3	-0.86	-0.87	+0.01	0.00
AOI 15 (PPG 20)	61	-0.94	-0.83	-0.08	0.00

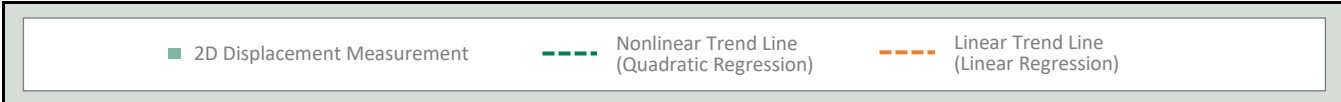
AOI 1 (LGS 1) - Location Map



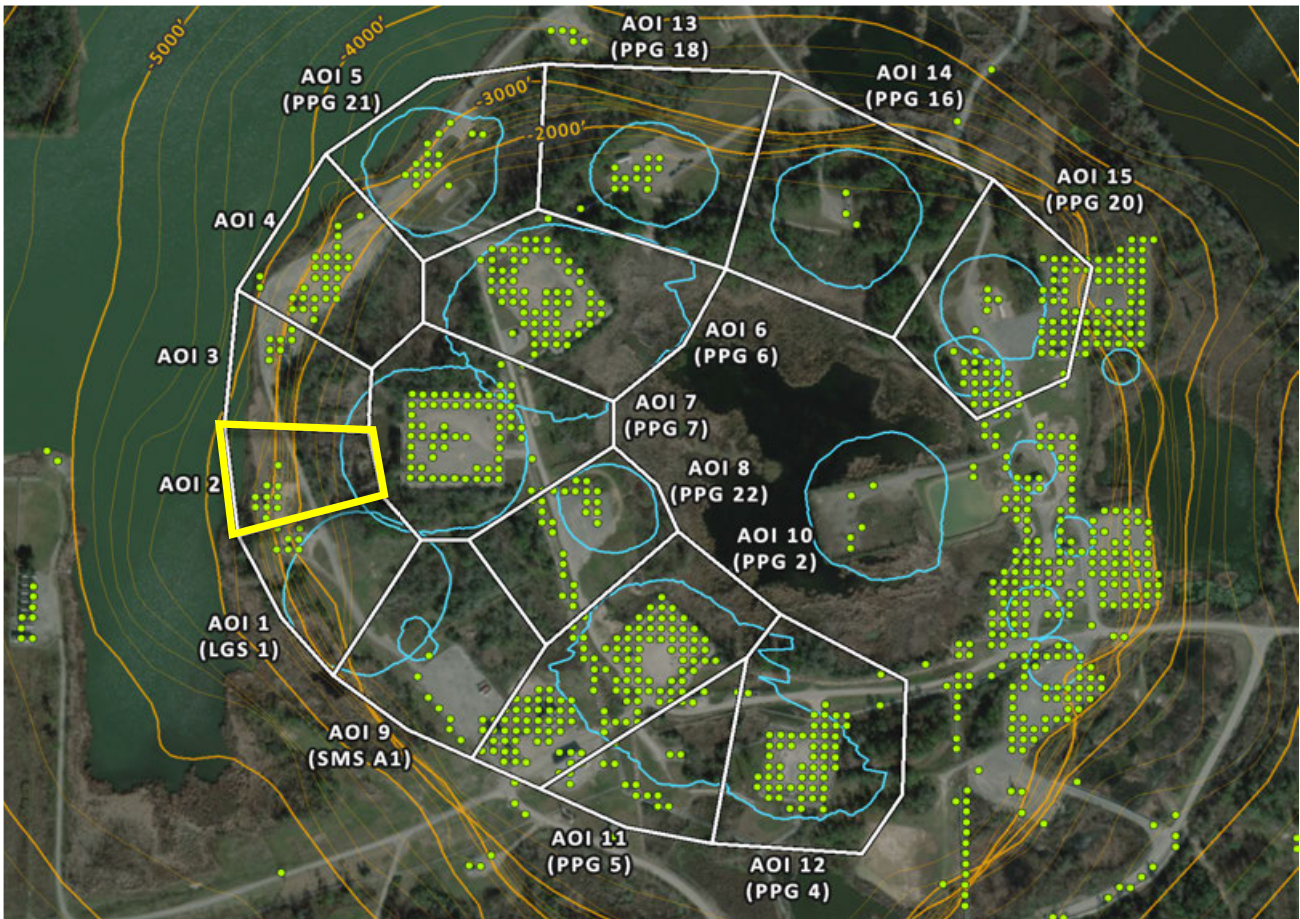
AOI 1 (LGS 1) - Vertical Time Series Vertical (9/29/2025) Point Count: 9



	Nonlinear Trend	Linear Trend
Velocity:	-0.60 in/yr	-0.58 in/yr
Acceleration:	-0.01 in/yr ²	0.00 in/yr ²

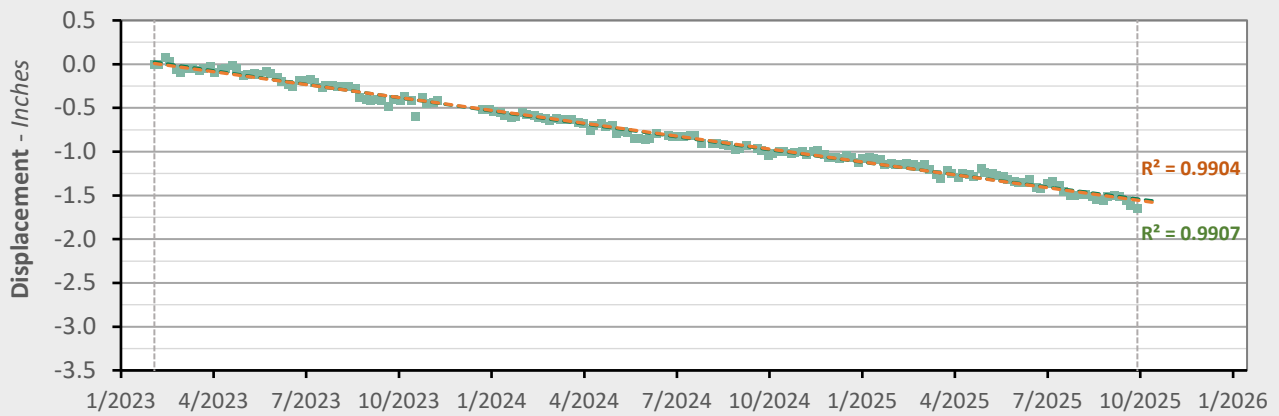


AOI 2 - Location Map

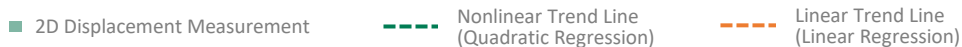


AOI 2 - Vertical Time Series

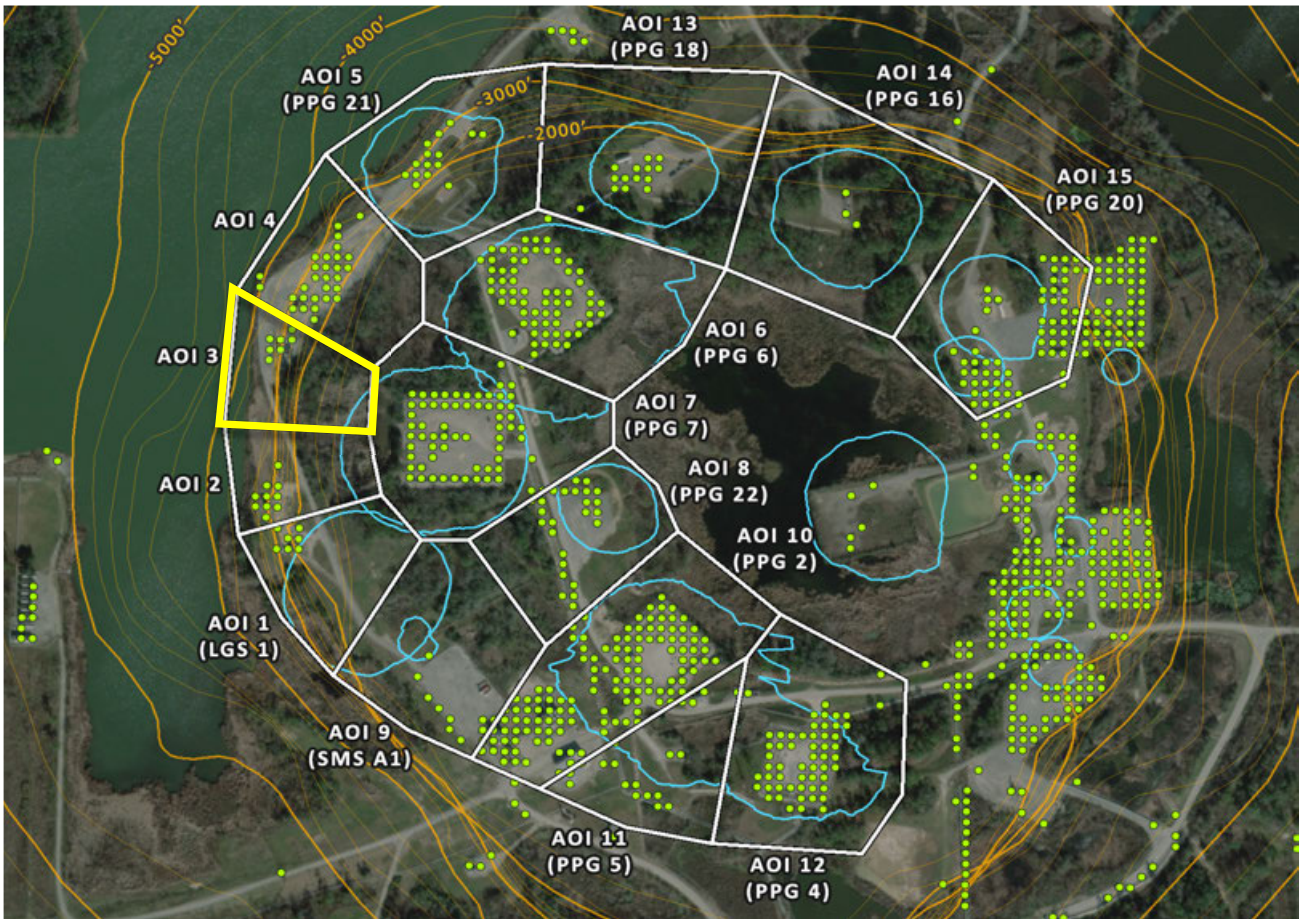
Vertical (9/29/2025) Point Count: **10**



	Nonlinear Trend	Linear Trend
Velocity:	-0.55 in/yr	-0.59 in/yr
Acceleration:	+0.03 in/yr ²	0.00 in/yr ²

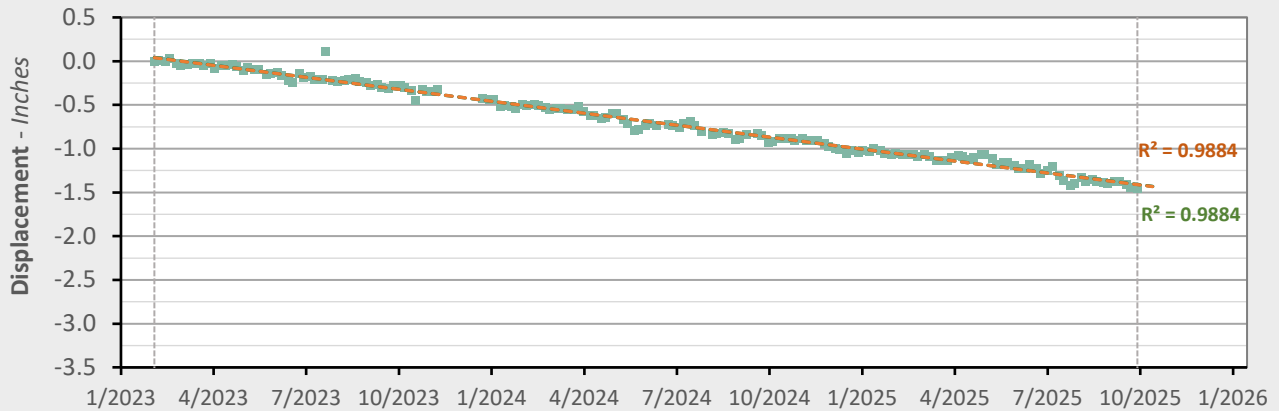


AOI 3 - Location Map

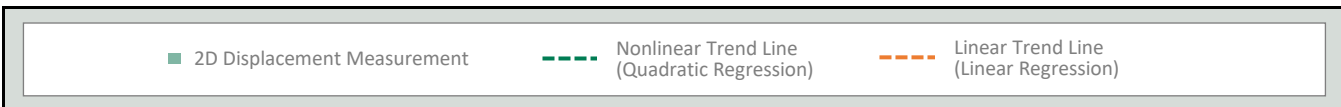


AOI 3 - Vertical Time Series

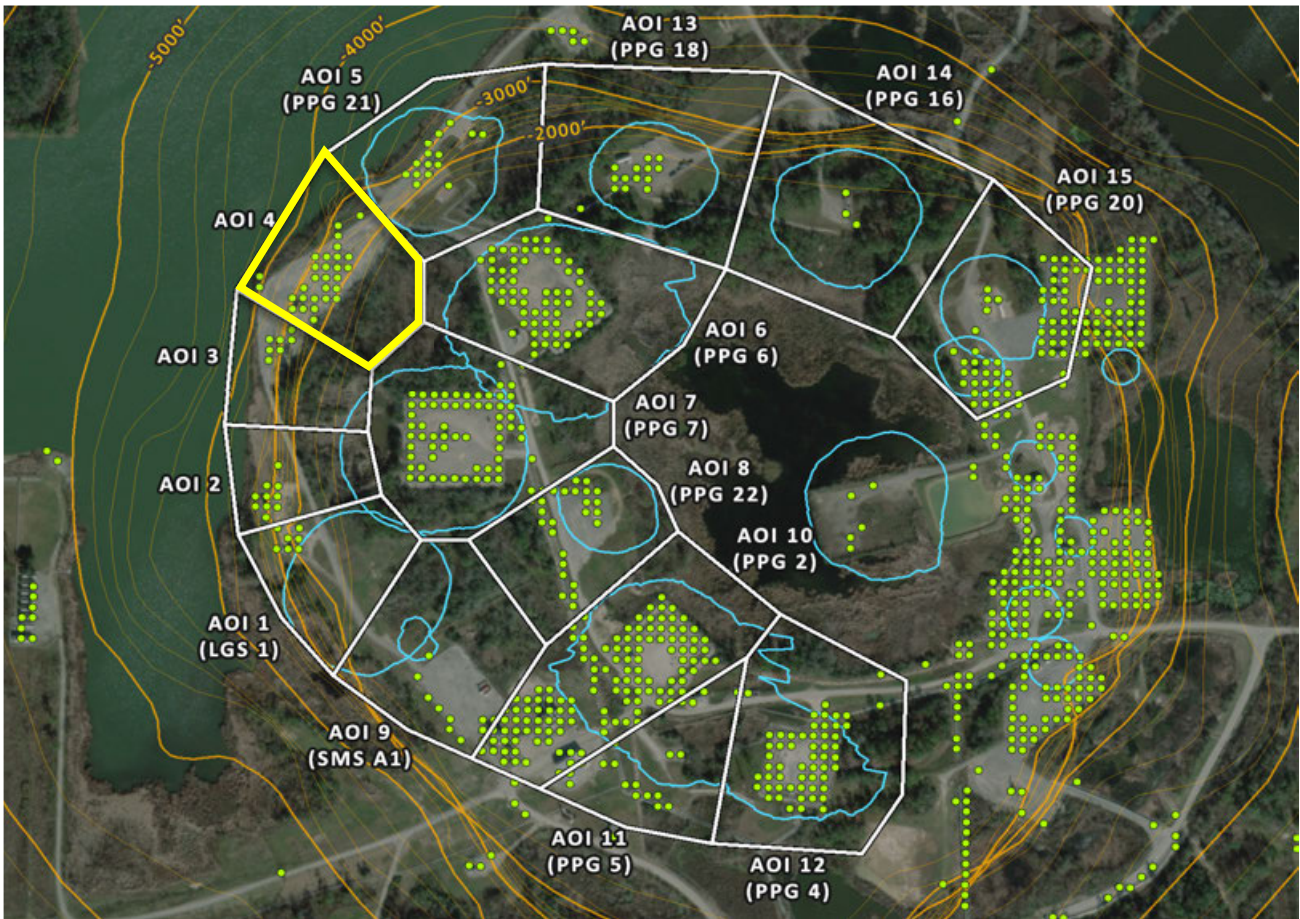
Vertical (9/29/2025) Point Count: **7**



	Nonlinear Trend	Linear Trend
Velocity:	-0.54 in/yr	-0.55 in/yr
Acceleration:	+0.00 in/yr ²	0.00 in/yr ²

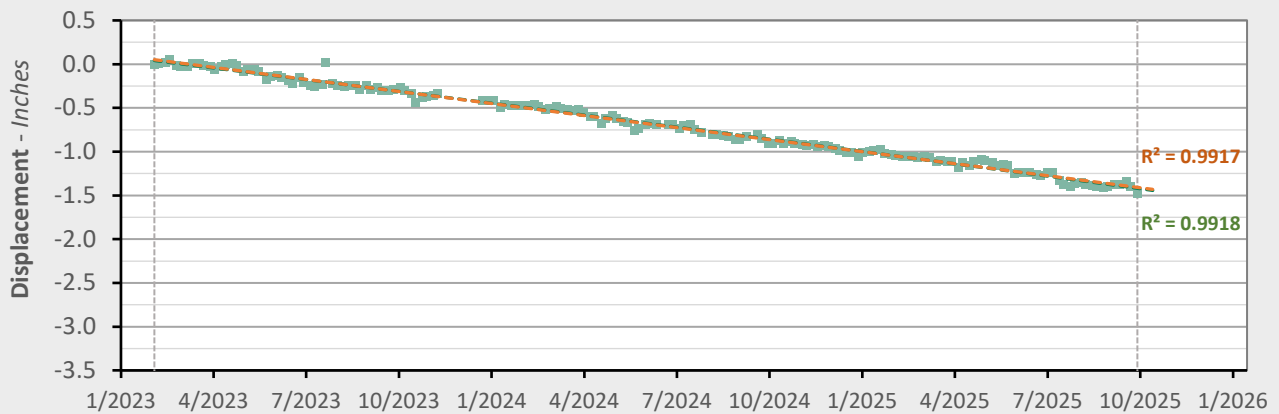


AOI 4 - Location Map

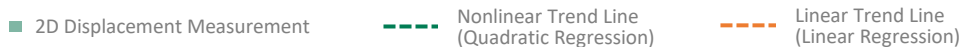


AOI 4 - Vertical Time Series

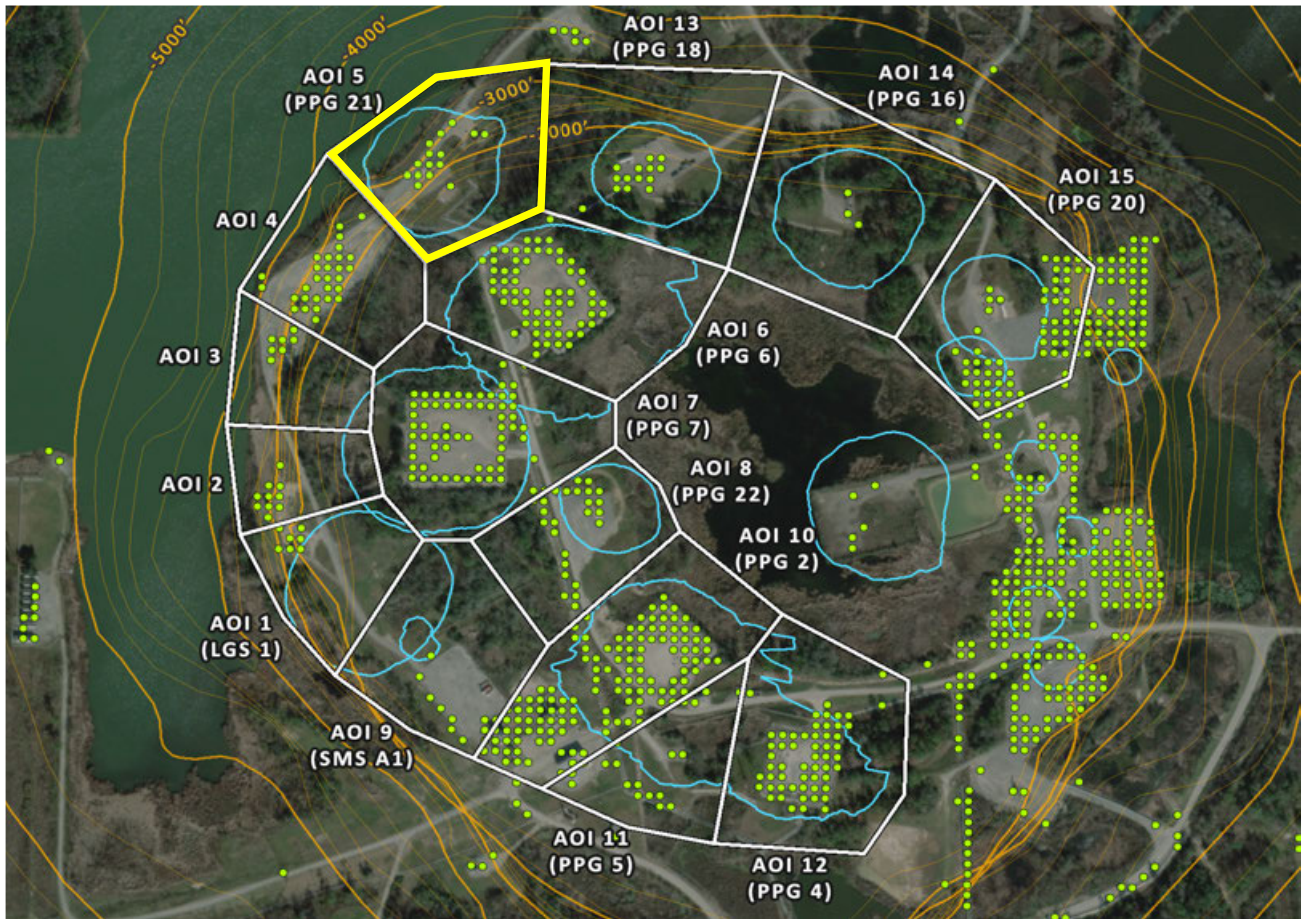
Vertical (9/29/2025) Point Count: 29



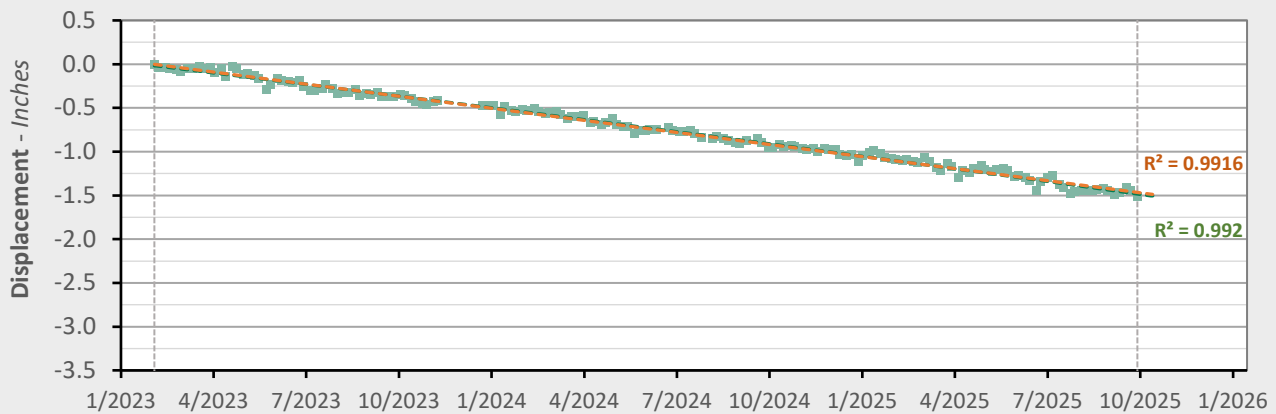
	Nonlinear Trend	Linear Trend
Velocity:	-0.57 in/yr	-0.55 in/yr
Acceleration:	-0.02 in/yr ²	0.00 in/yr ²



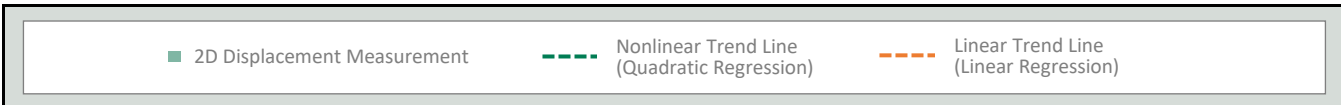
AOI 5 (PPG 21) - Location Map



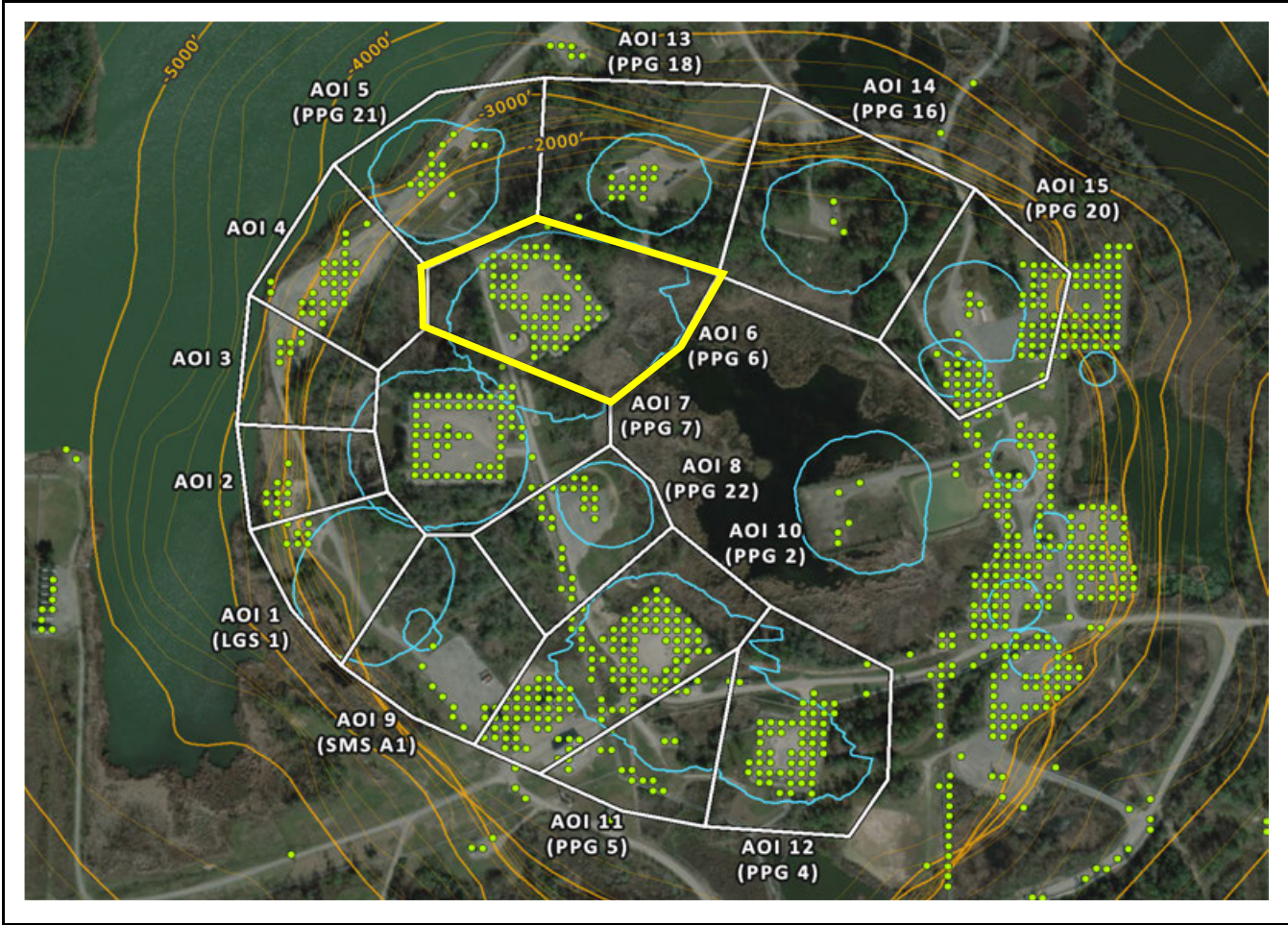
AOI 5 (PPG 21) - Vertical Time Series Vertical (9/29/2025) Point Count: 15



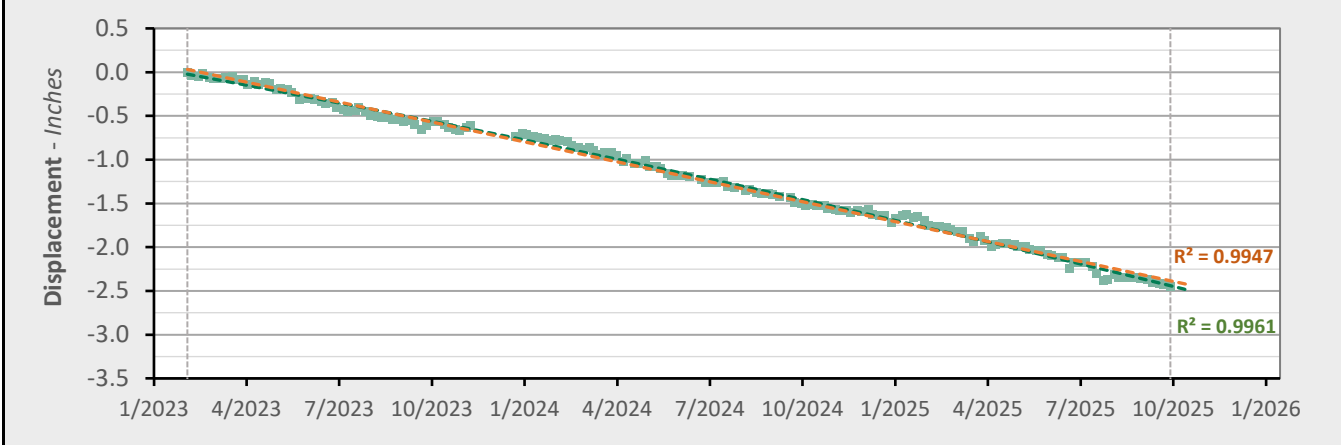
	Nonlinear Trend	Linear Trend
Velocity:	-0.59 in/yr	-0.55 in/yr
Acceleration:	-0.03 in/yr ²	0.00 in/yr ²



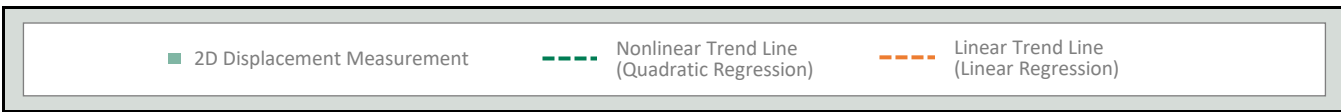
AOI 6 (PPG 6) - Location Map



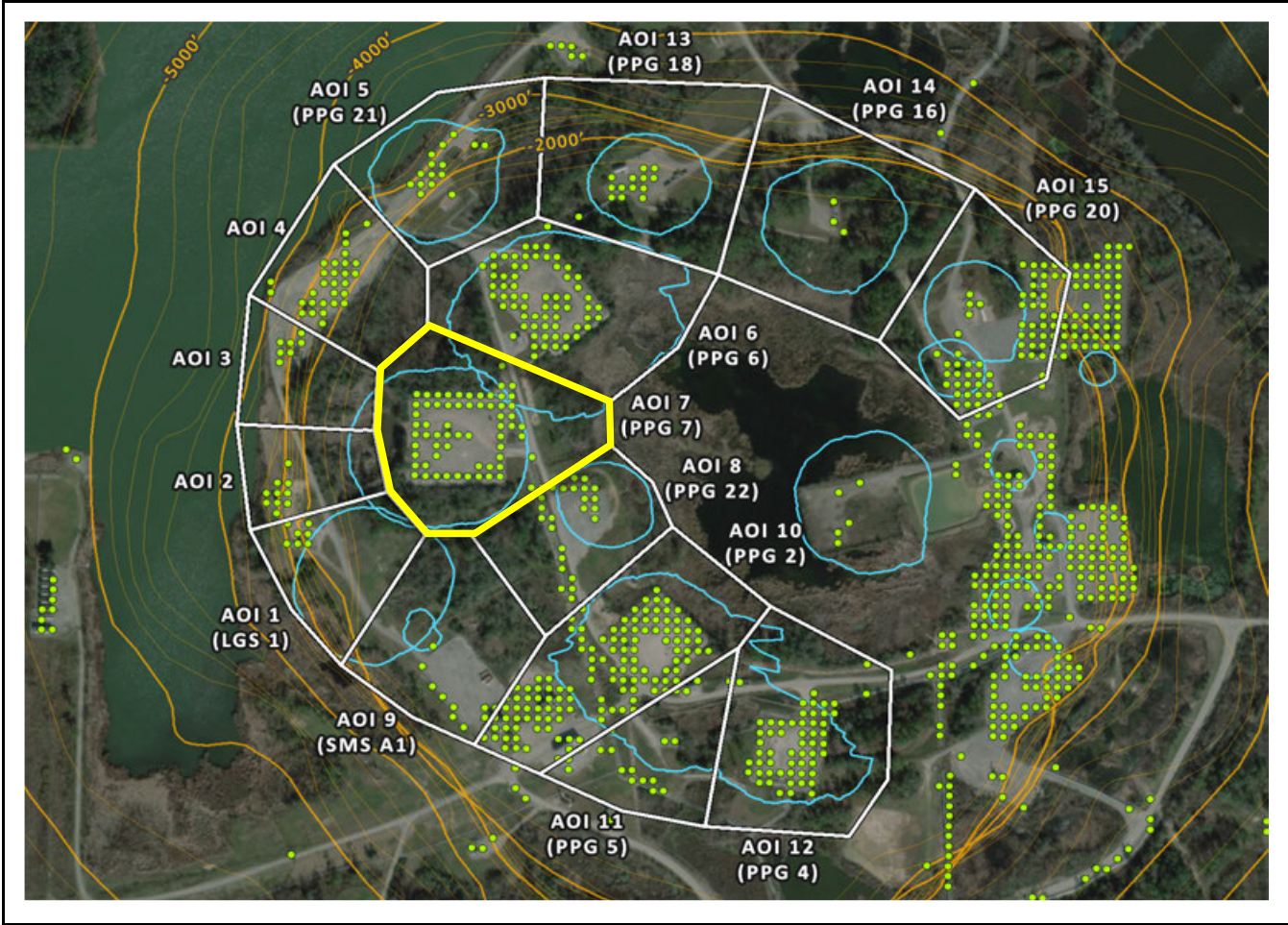
AOI 6 (PPG 6) - Vertical Time Series Vertical (9/29/2025) Point Count: 65



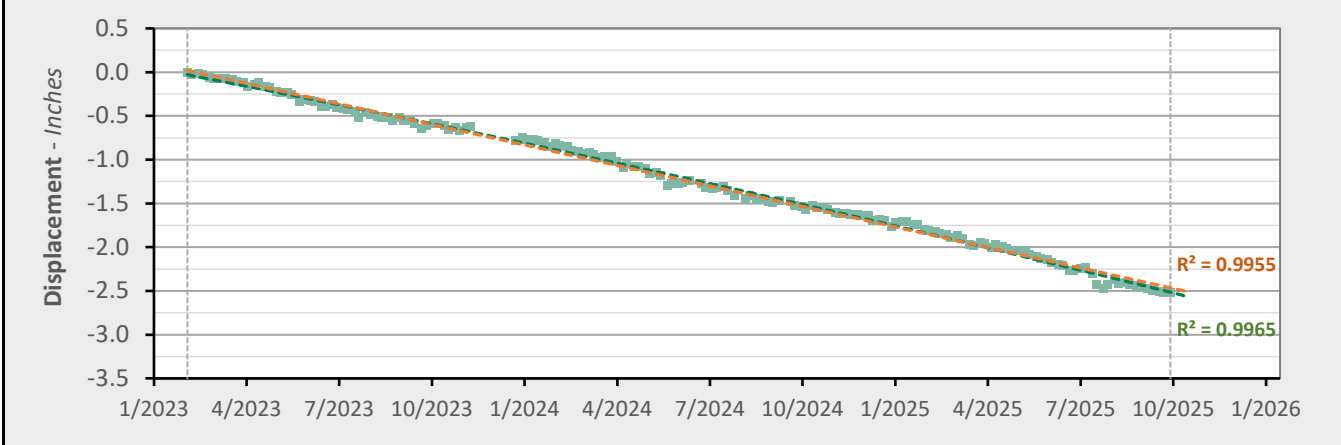
	Nonlinear Trend	Linear Trend
Velocity:	-1.04 in/yr	-0.91 in/yr
Acceleration:	-0.10 in/yr ²	0.00 in/yr ²



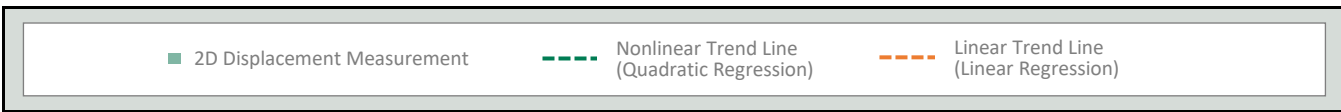
AOI 7 (PPG 7) - Location Map



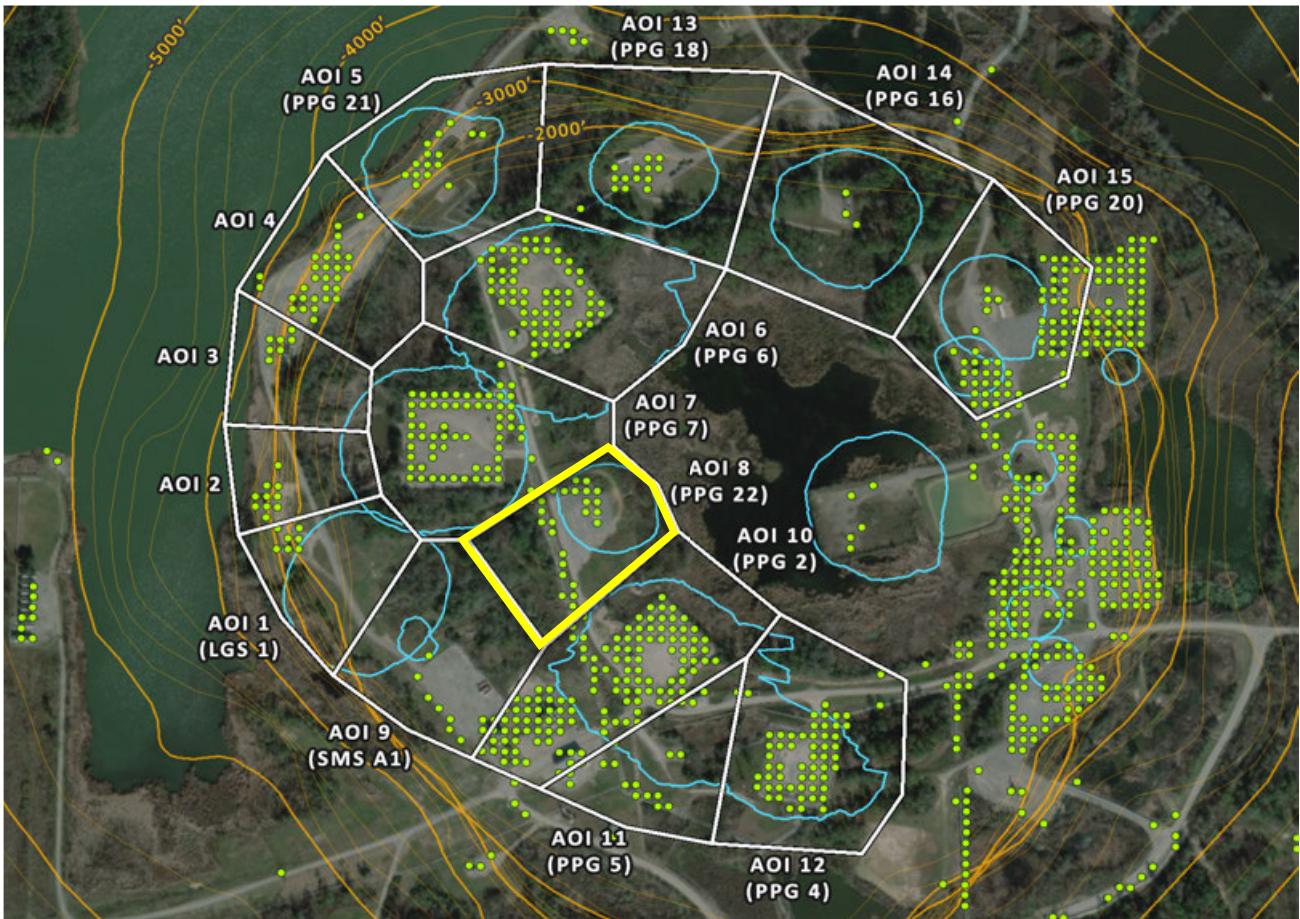
AOI 7 (PPG 7) - Vertical Time Series Vertical (9/29/2025) Point Count: 62



	Nonlinear Trend	Linear Trend
Velocity:	-1.05 in/yr	-0.94 in/yr
Acceleration:	-0.09 in/yr ²	0.00 in/yr ²

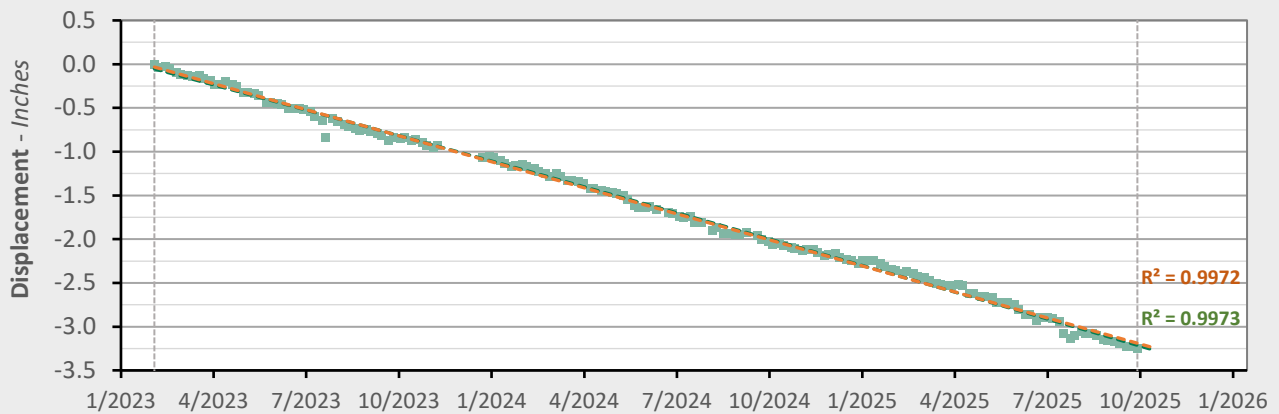


AOI 8 (PPG 22) - Location Map

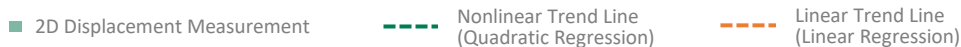


AOI 8 (PPG 22) - Vertical Time Series

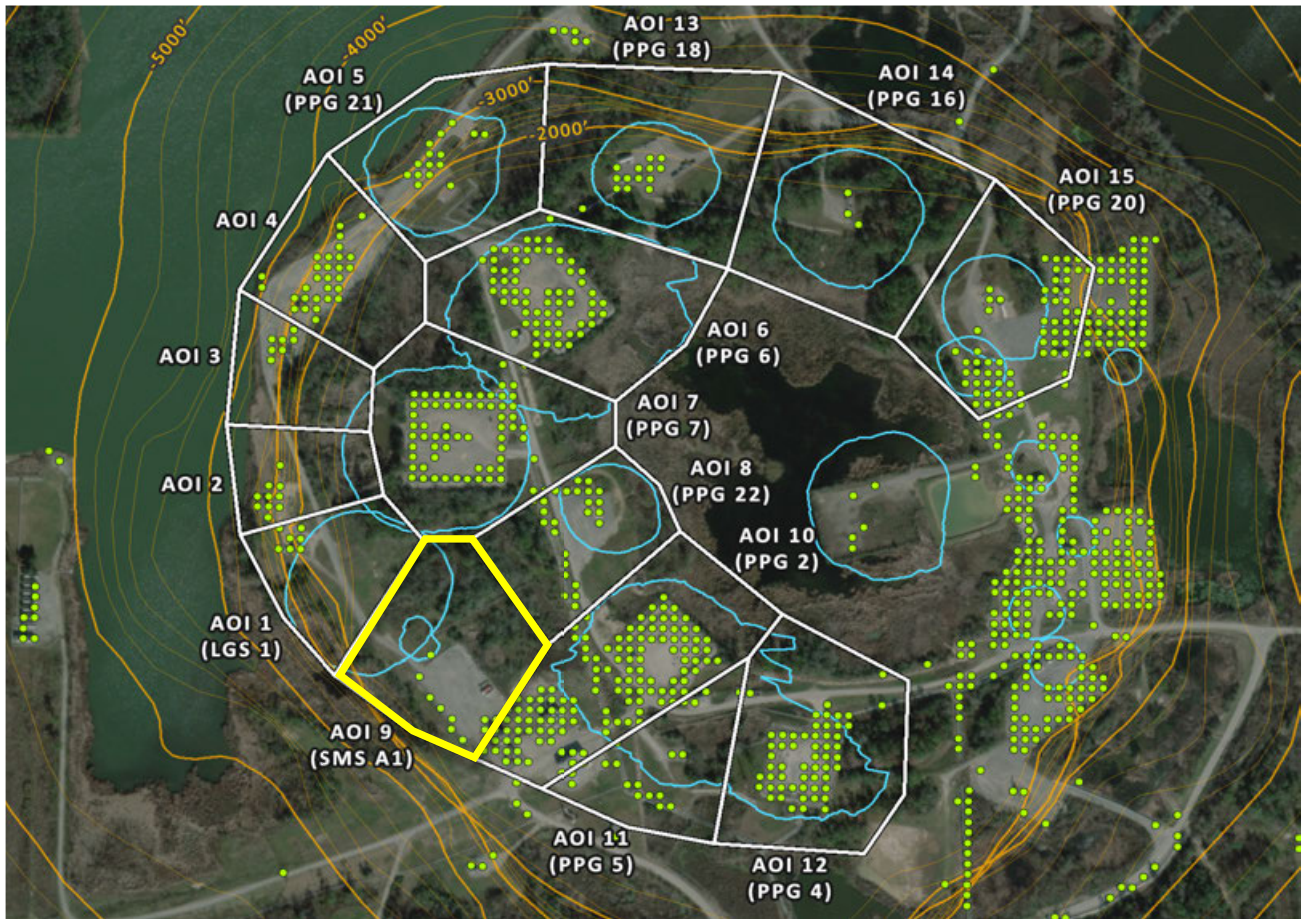
Vertical (9/29/2025) Point Count: 25



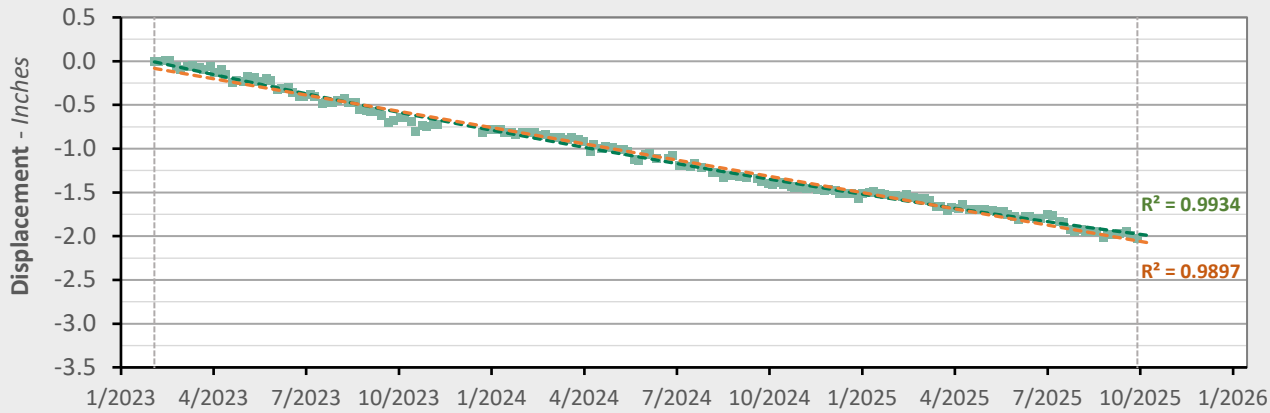
	Nonlinear Trend	Linear Trend
Velocity:	-1.24 in/yr	-1.19 in/yr
Acceleration:	-0.04 in/yr ²	0.00 in/yr ²



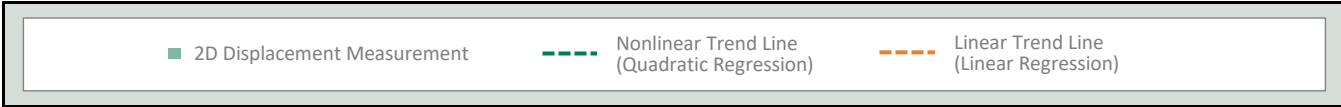
AOI 9 (PPG A1) - Location Map



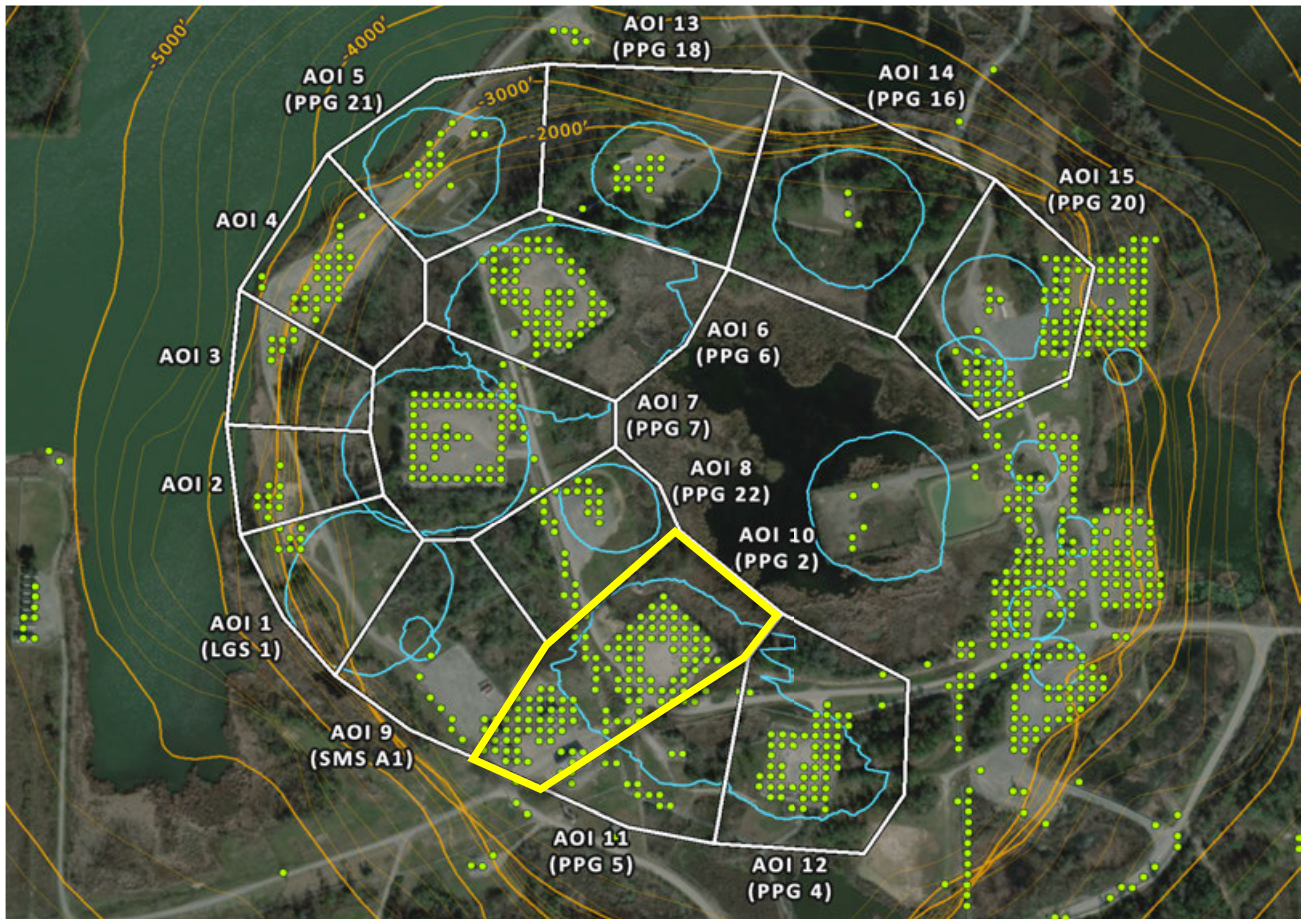
AOI 9 (SMS A1) - Vertical Time Series Vertical (9/29/2025) Point Count: 12



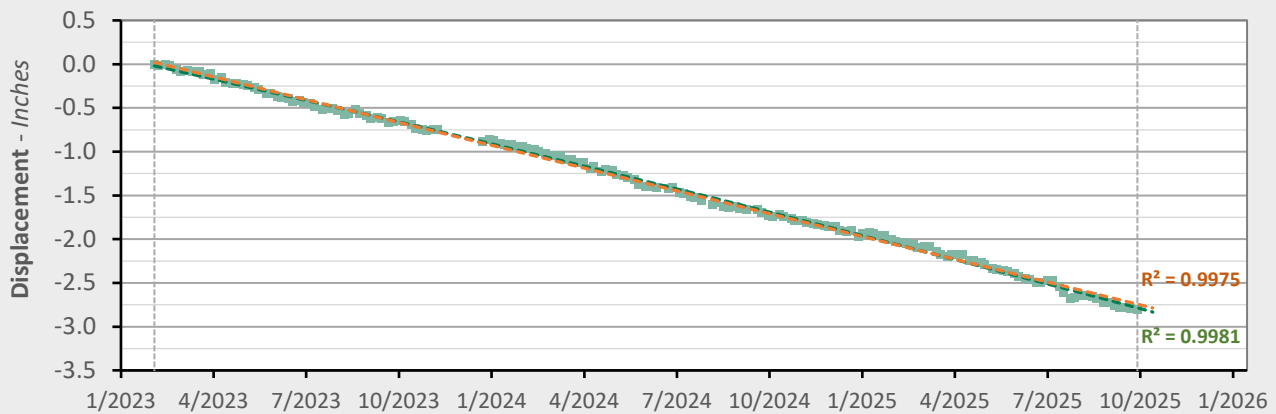
	Nonlinear Trend	Linear Trend
Velocity:	-0.56 in/yr	-0.74 in/yr
Acceleration:	+0.13 in/yr ²	0.00 in/yr ²



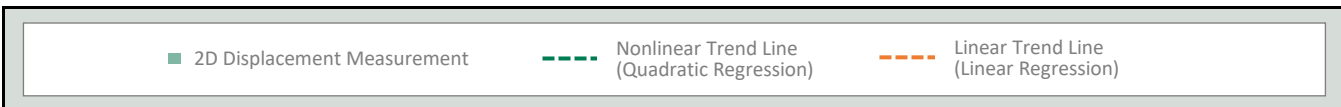
AOI 10 (PPG 2) - Location Map



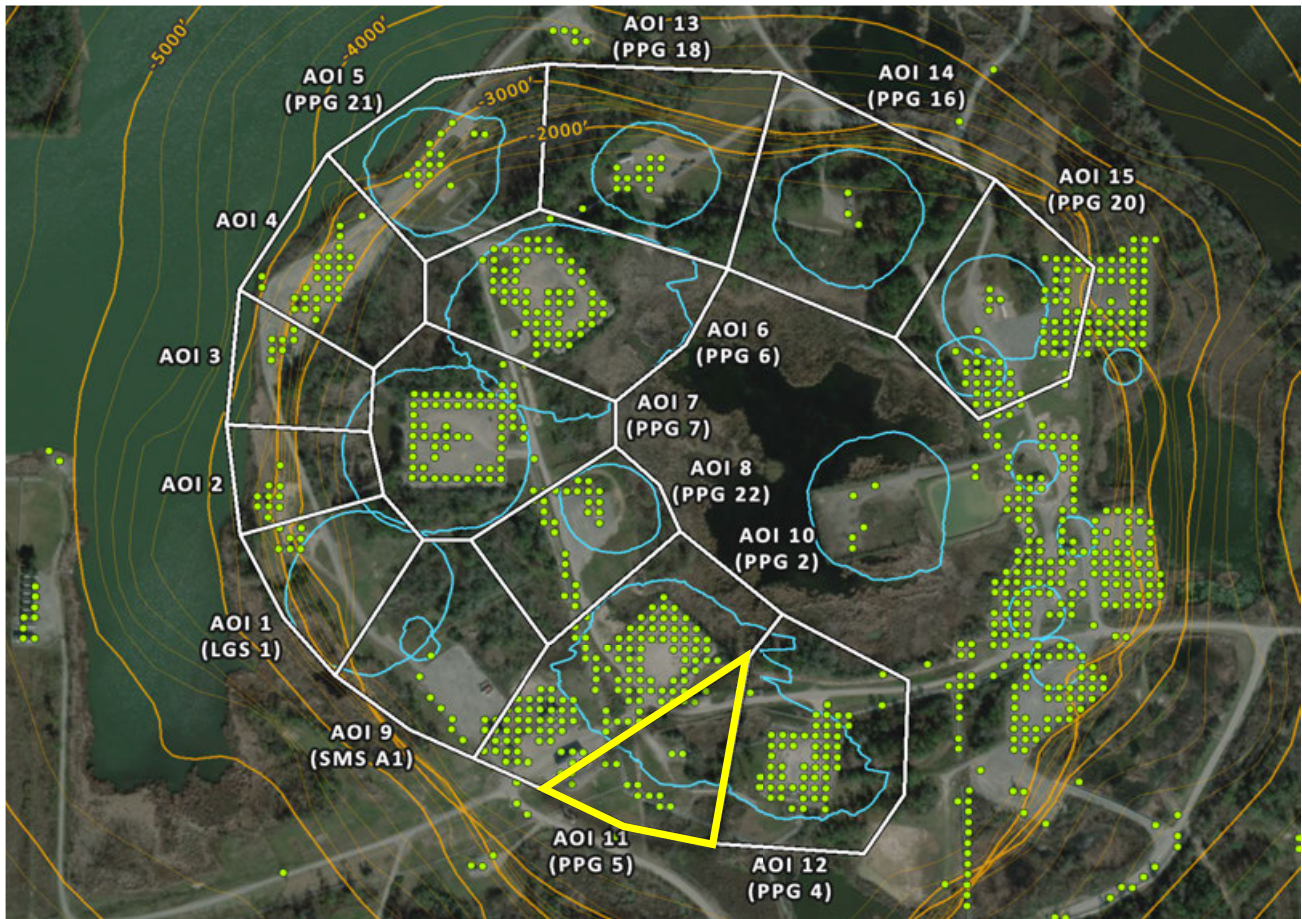
AOI 10 (PPG 2) - Vertical Time Series Vertical (9/29/2025) Point Count: 124



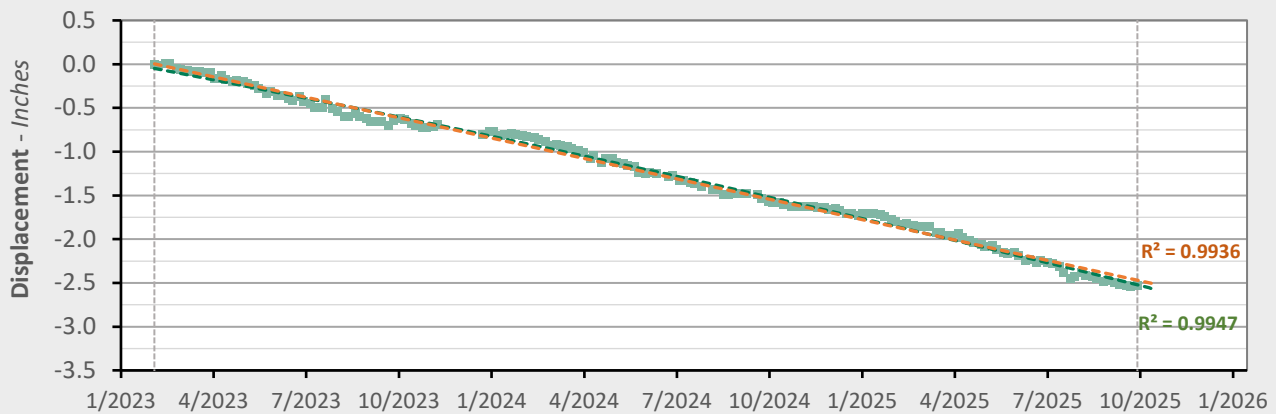
	Nonlinear Trend	Linear Trend
Velocity:	-1.14 in/yr	-1.04 in/yr
Acceleration:	-0.07 in/yr ²	0.00 in/yr ²



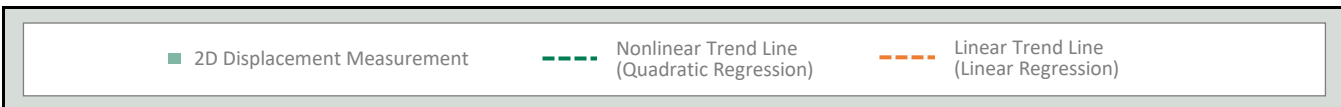
AOI 11 (PPG 5) - Location Map



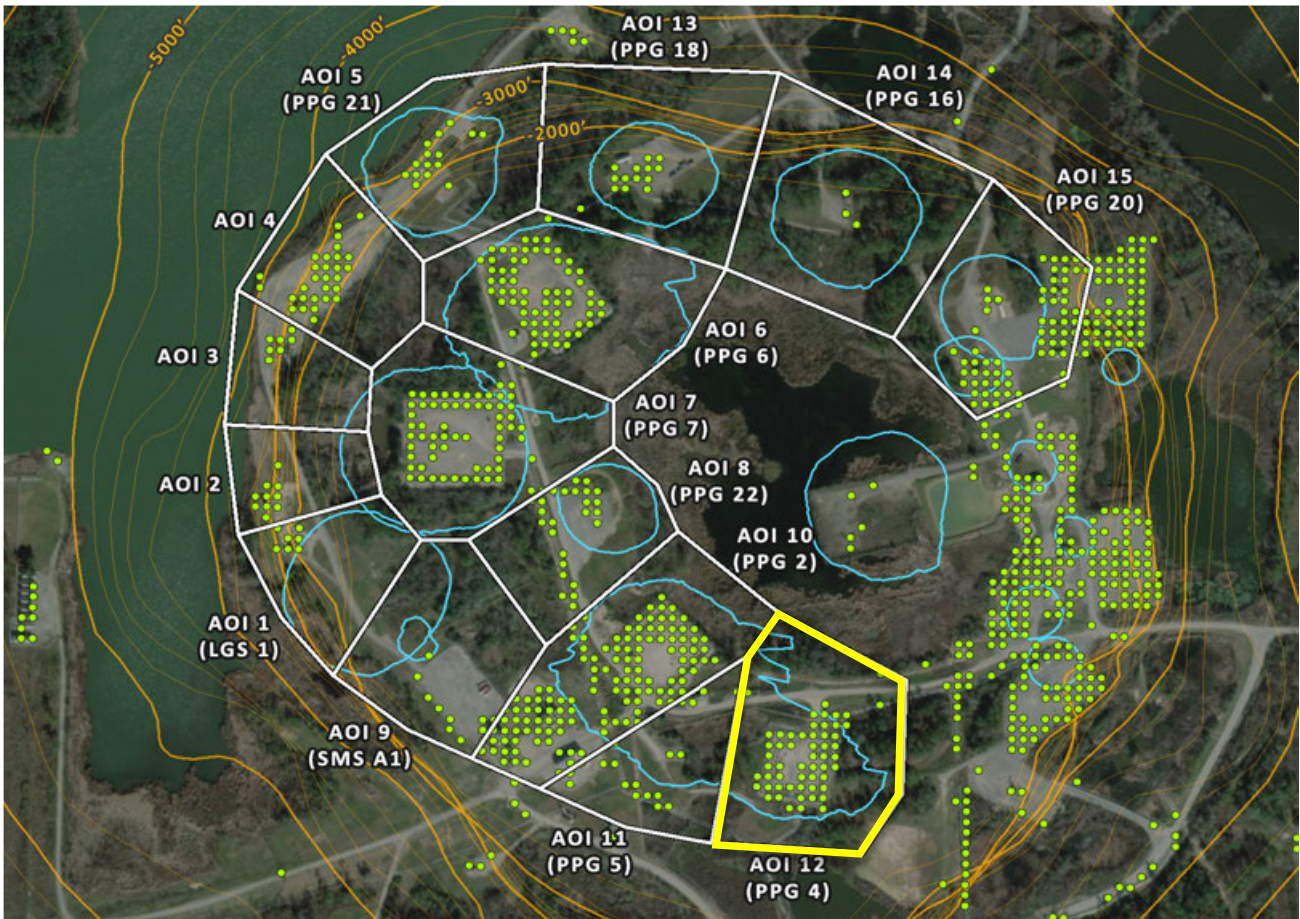
AOI 11 (PPG 5) - Vertical Time Series Vertical (9/29/2025) Point Count: 19



	Nonlinear Trend	Linear Trend
Velocity:	-1.06 in/yr	-0.93 in/yr
Acceleration:	-0.09 in/yr ²	0.00 in/yr ²

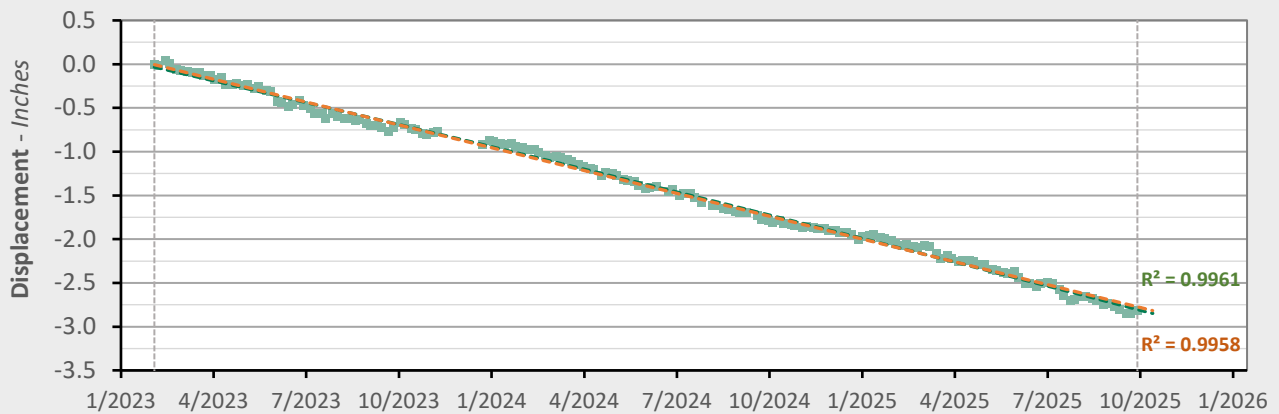


AOI 12 (PPG 4) - Location Map

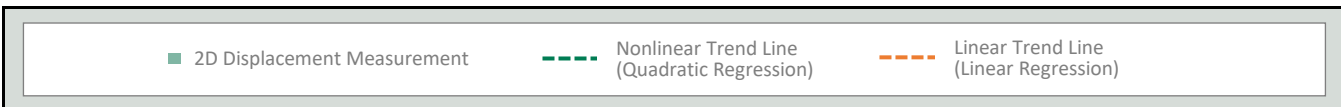


AOI 12 (PPG 4) - Vertical Time Series

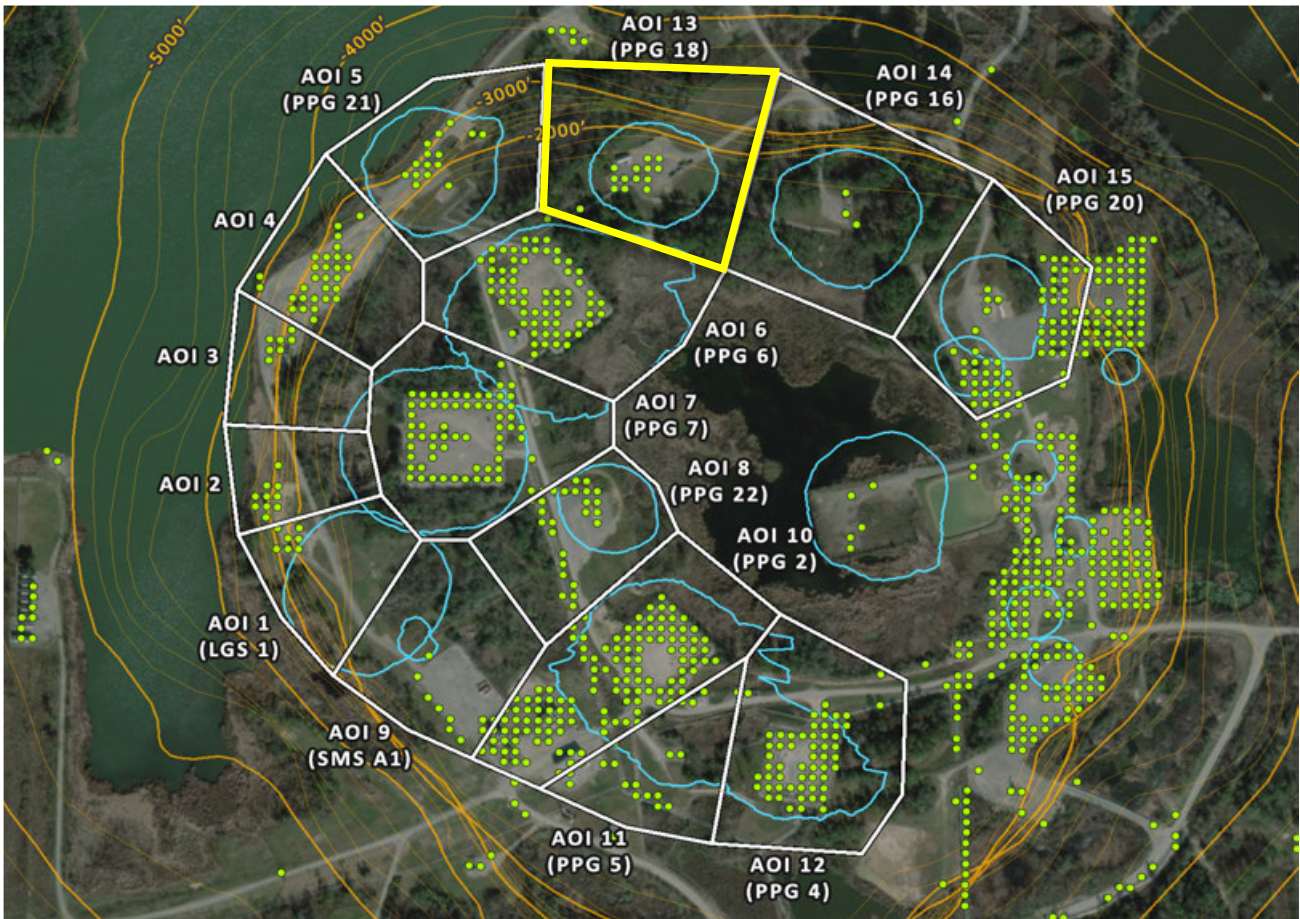
Vertical (9/29/2025) Point Count: 56



	Nonlinear Trend	Linear Trend
Velocity:	-1.11 in/yr	-1.04 in/yr
Acceleration:	-0.05 in/yr ²	0.00 in/yr ²

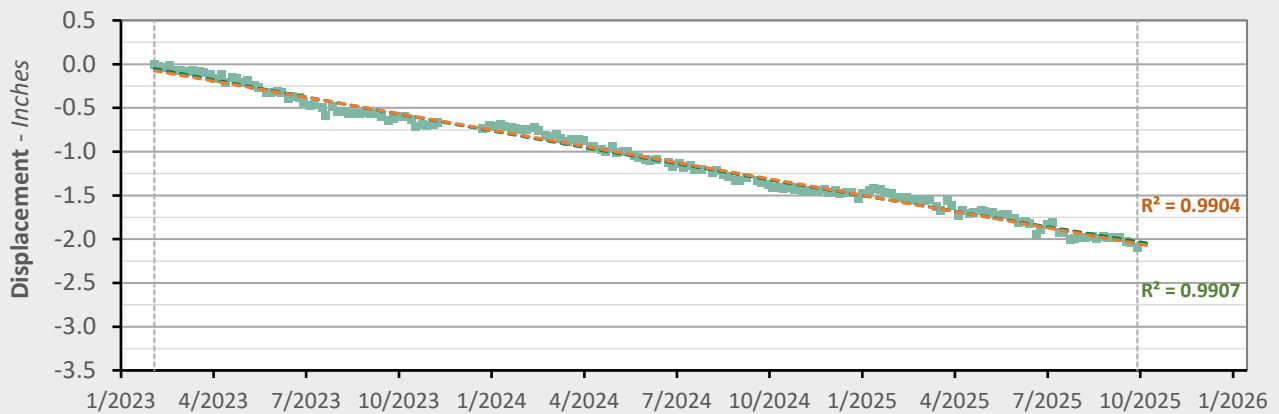


AOI 13 (PPG 18) - Location Map

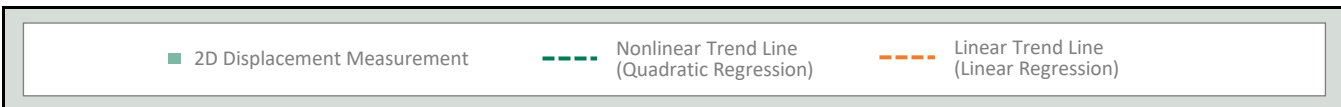


AOI 13 (PPG 18) - Vertical Time Series

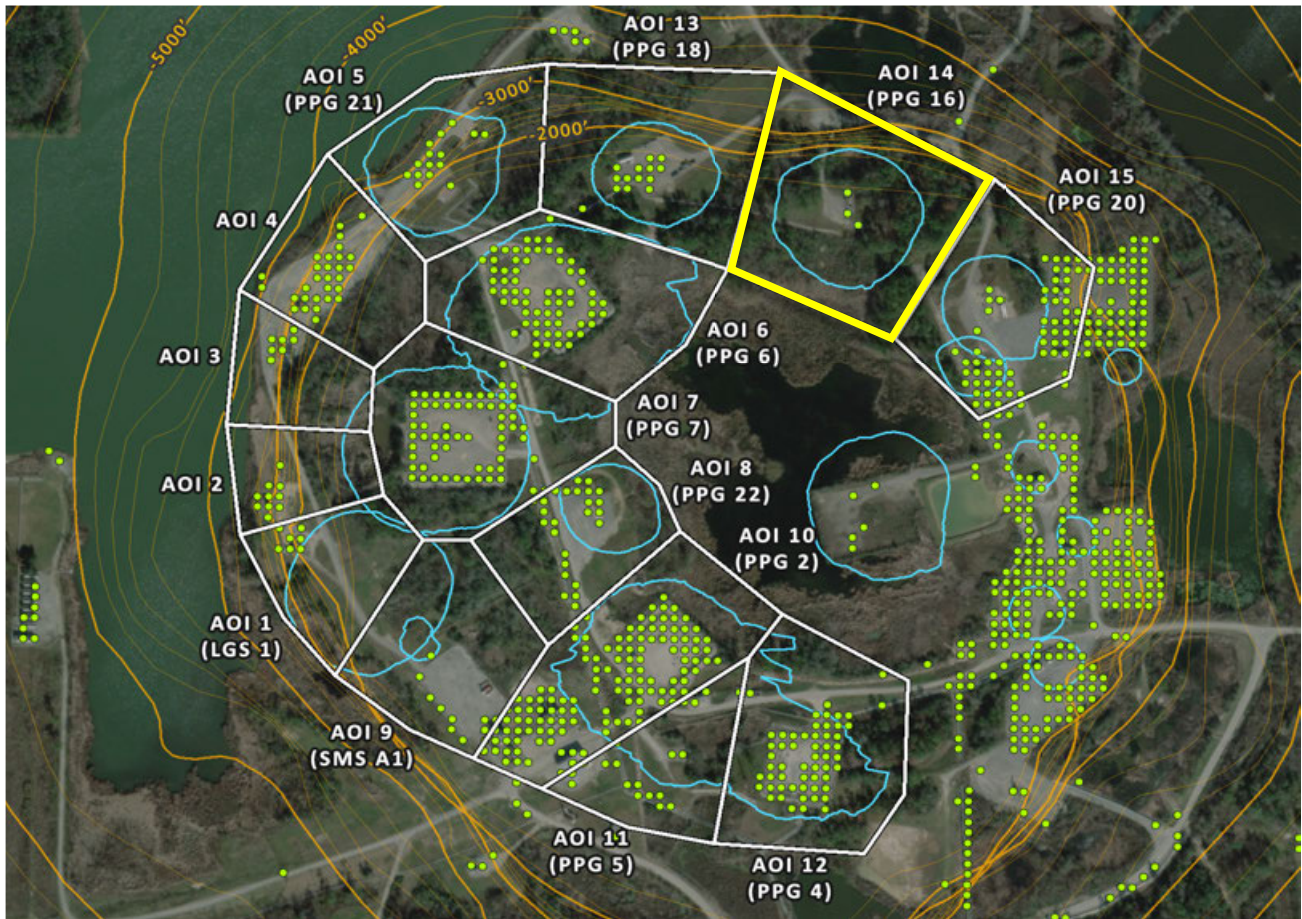
Vertical (9/29/2025) Point Count: **13**



	Nonlinear Trend	Linear Trend
Velocity:	-0.69 in/yr	-0.75 in/yr
Acceleration:	+0.04 in/yr ²	0.00 in/yr ²



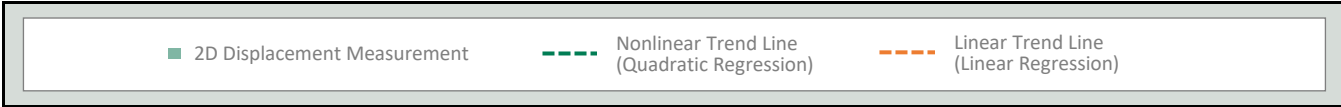
AOI 14 (PPG 16) - Location Map



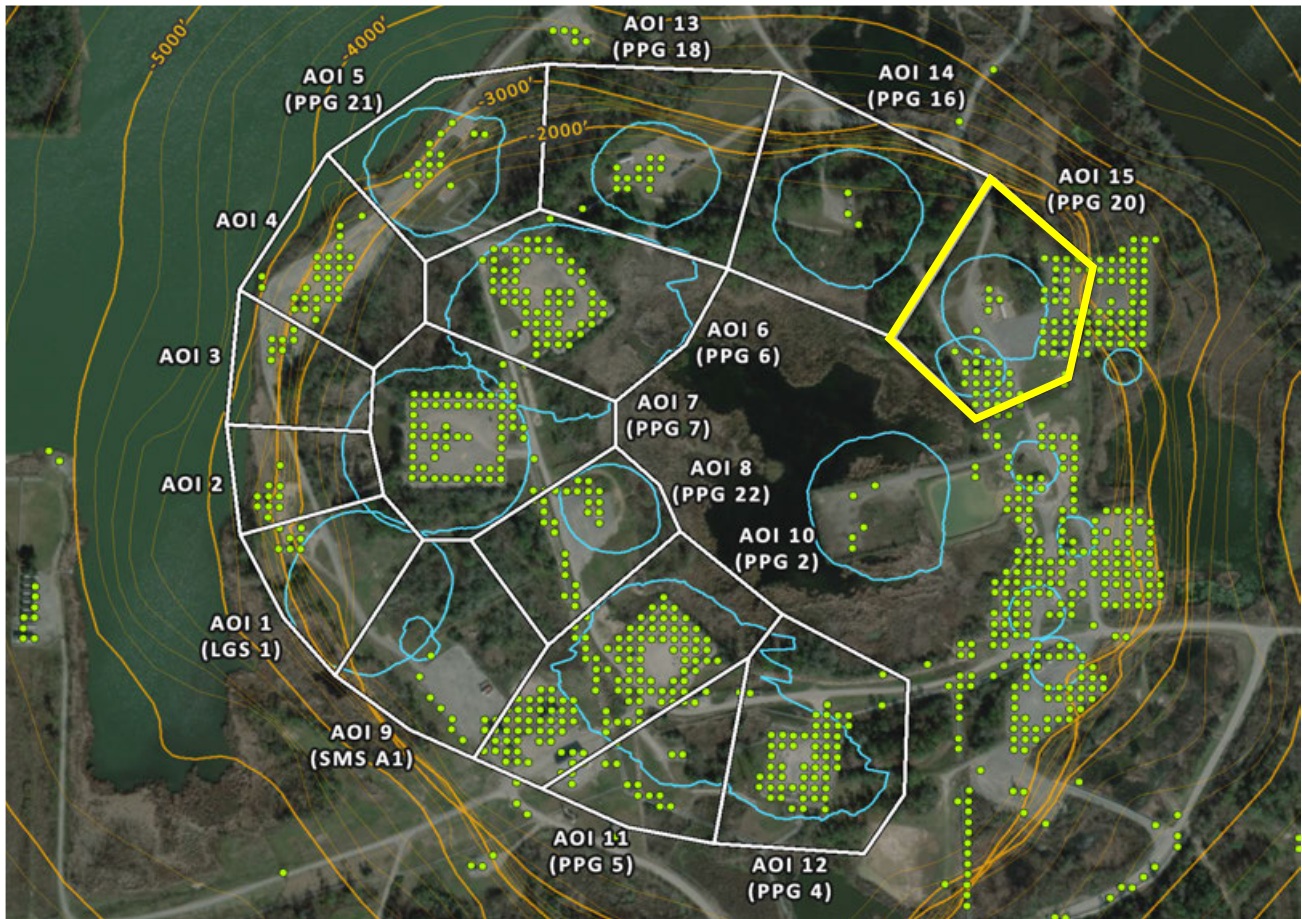
AOI 14 (PPG 16) - Vertical Time Series Vertical (9/29/2025) Point Count: 3



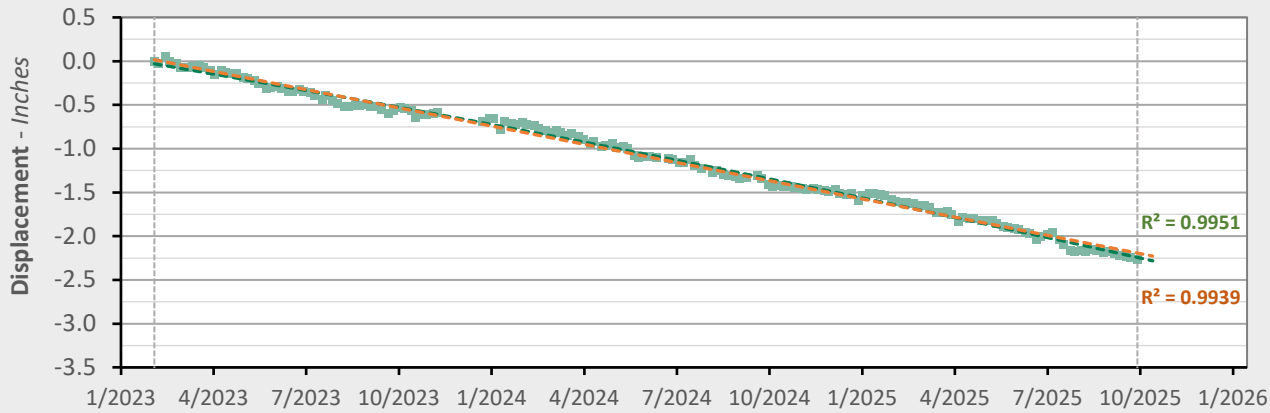
	Nonlinear Trend	Linear Trend
Velocity:	-0.86 in/yr	-0.87 in/yr
Acceleration:	+0.01 in/yr ²	0.00 in/yr ²



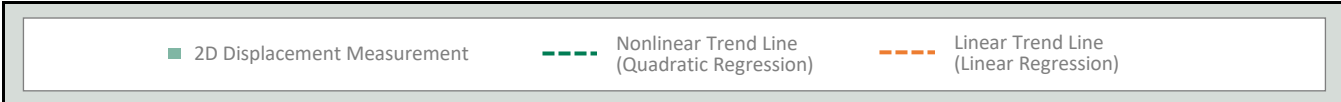
AOI 15 (PPG 20) - Location Map



AOI 15 (PPG 20) - Vertical Time Series Vertical (9/29/2025) Point Count: 61



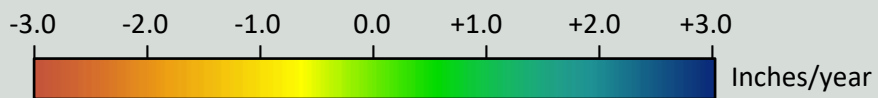
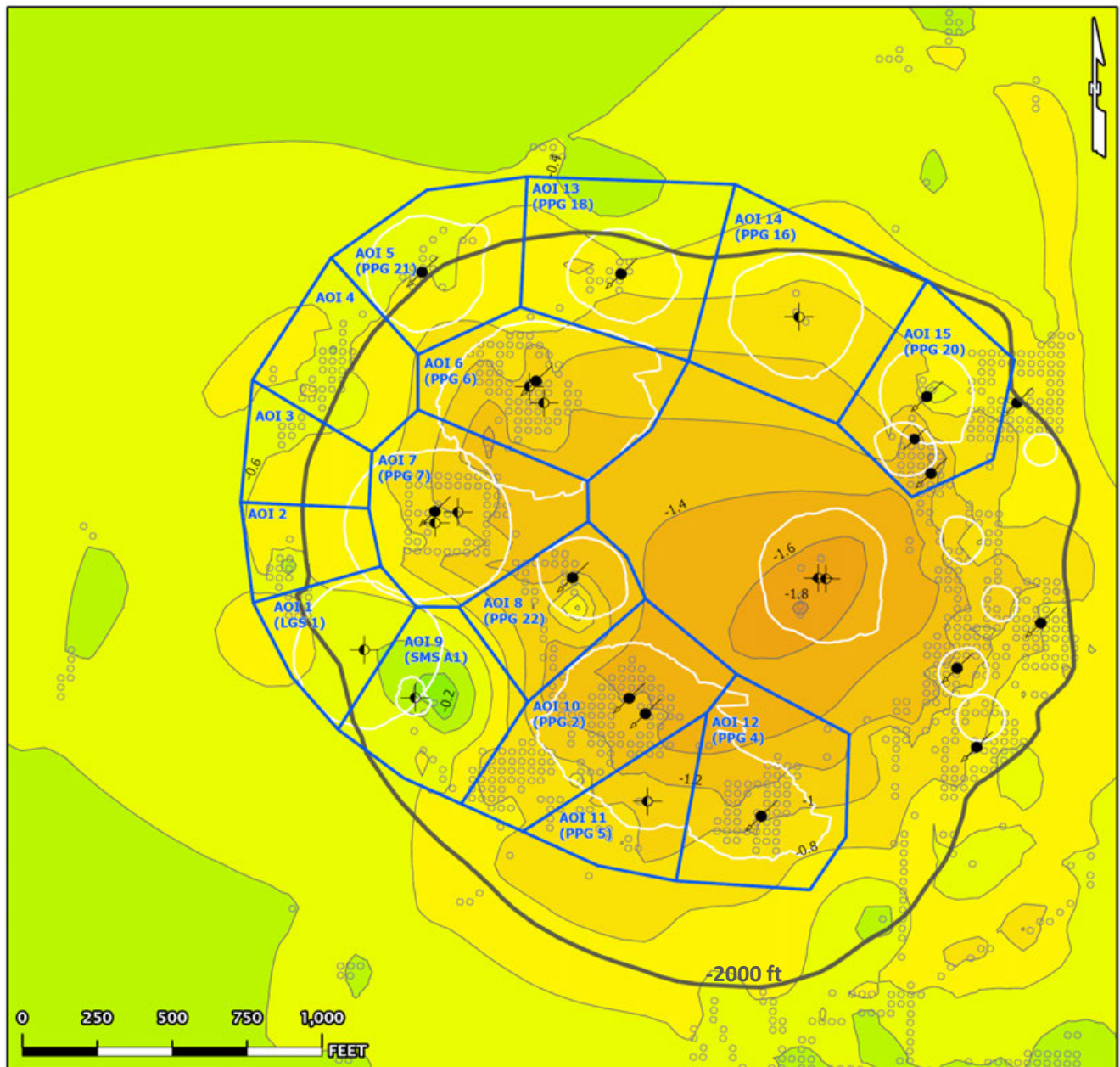
	Nonlinear Trend	Linear Trend
Velocity:	-0.94 in/yr	-0.83 in/yr
Acceleration:	-0.08 in/yr ²	0.00 in/yr ²



Vertical Data (02/04/2023 - 09/29/2025)

Nonlinear Velocity Contours

As of date: 09/29/2025

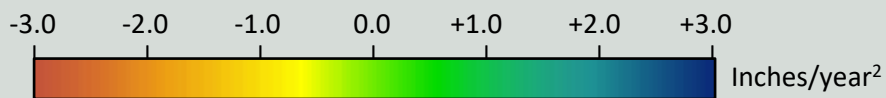
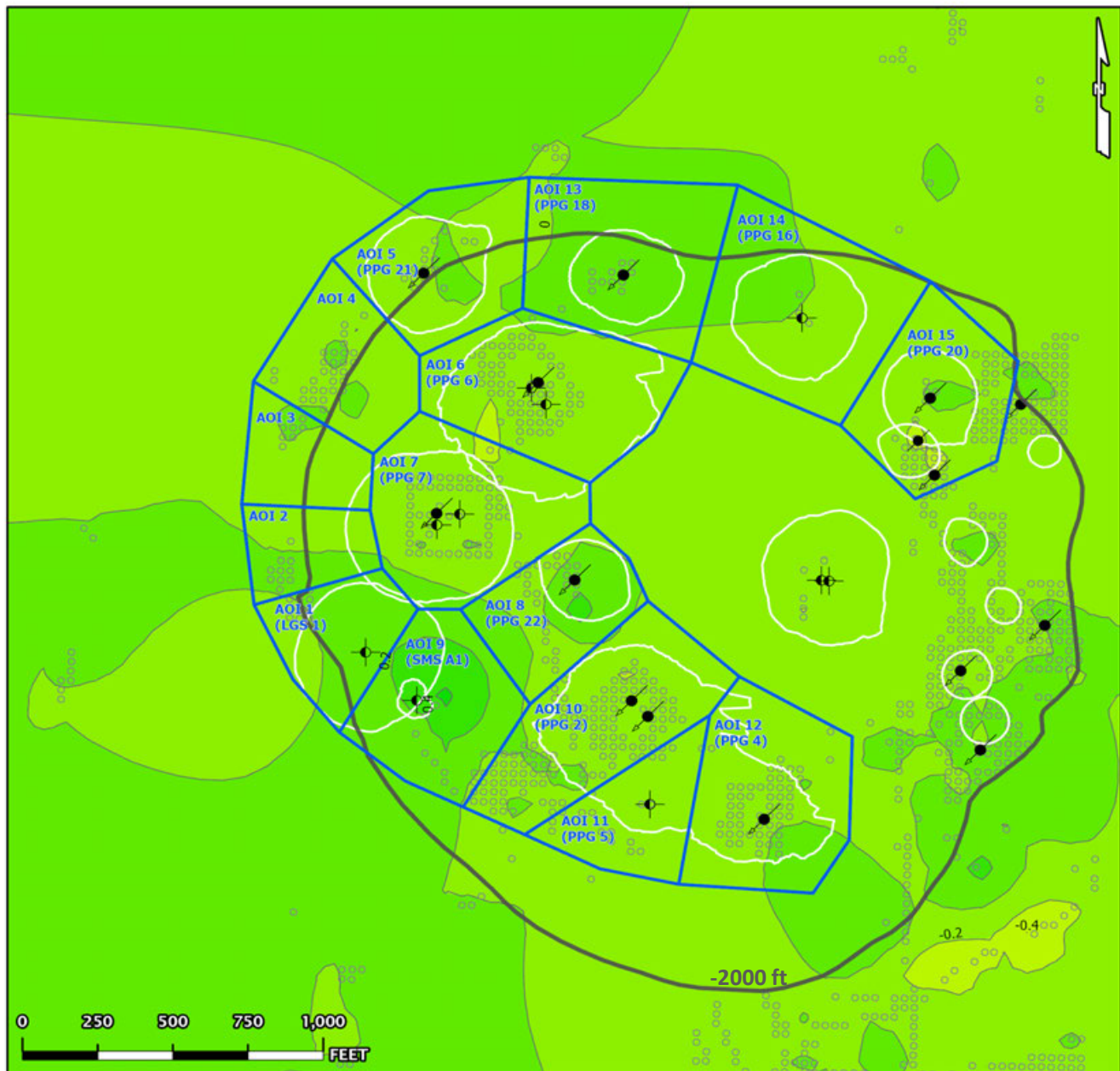


- AOI Boundary
 - InSAR LOS Measurement Point
 - Contour (0.2)
 - Historical Cavern Extent
 - Top of Dome (-2000 ft Contour)
- Cavern Well Surface Locations
- 09 - Active - Injection
 - 29 - Dry and Plugged

Vertical Data (02/04/2023 - 09/29/2025)

Nonlinear Acceleration Contours

Date range: 02/04/2023 - 09/29/2025

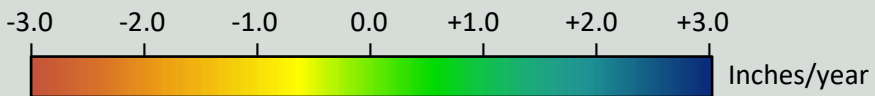
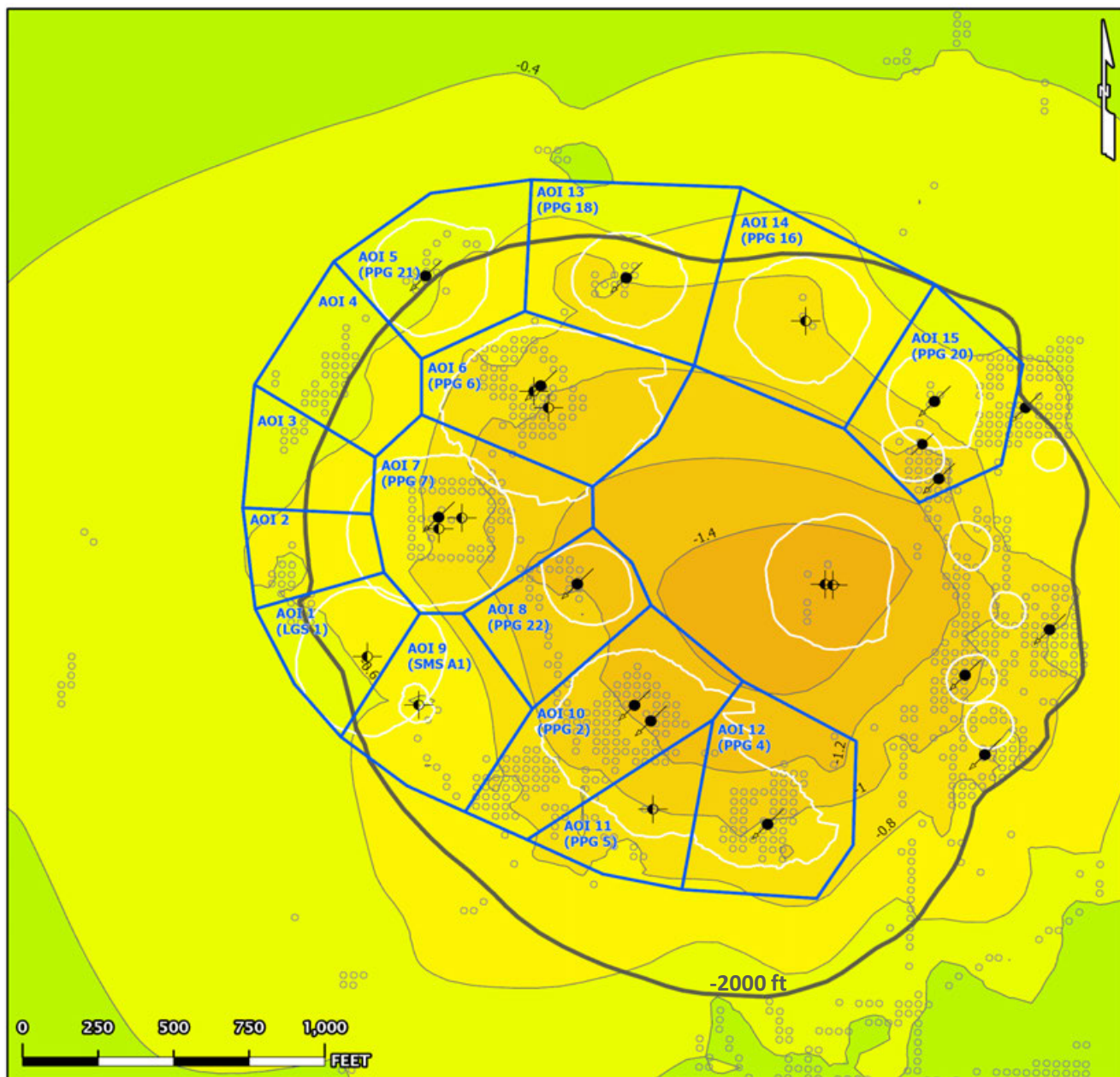


- AOI Boundary
 - InSAR LOS Measurement Point
 - Contour (0.2)
 - Historical Cavern Extent
 - Top of Dome (-2000 ft Contour)
- Cavern Well Surface Locations
- 09 - Active - Injection
 - 29 - Dry and Plugged

Vertical Data (02/04/2023 - 09/29/2025)

Linear Velocity Contours

Date range: 02/04/2023 - 09/29/2025

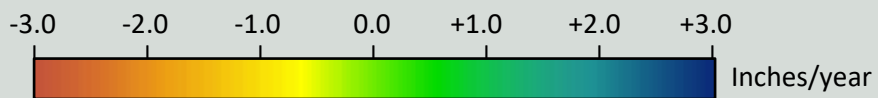


- AOI Boundary
 - Historical Cavern Extent
 - Top of Dome (-2000 ft Contour)
 - InSAR LOS Measurement Point
 - Contour (0.2)
- Cavern Well Surface Locations
- 09 - Active - Injection
 - 29 - Dry and Plugged

Vertical Data (02/04/2023 - 09/29/2025)

Nonlinear Velocity Data Points

As of date: 09/29/2025

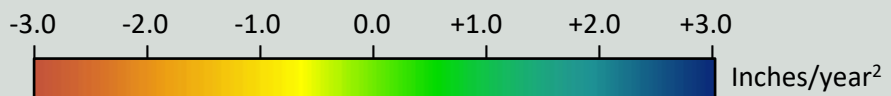


- AOI Boundary
 - InSAR LOS Measurement Point
 - Historical Cavern Extent
 - Top of Dome (-2000 ft Contour)
- Cavern Well Surface Locations
- 09 - Active - Injection
 - 29 - Dry and Plugged

Vertical Data (02/04/2023 - 09/29/2025)

Nonlinear Acceleration Data Points

Date range: 02/04/2023 - 09/29/2025

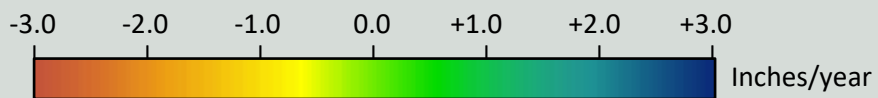
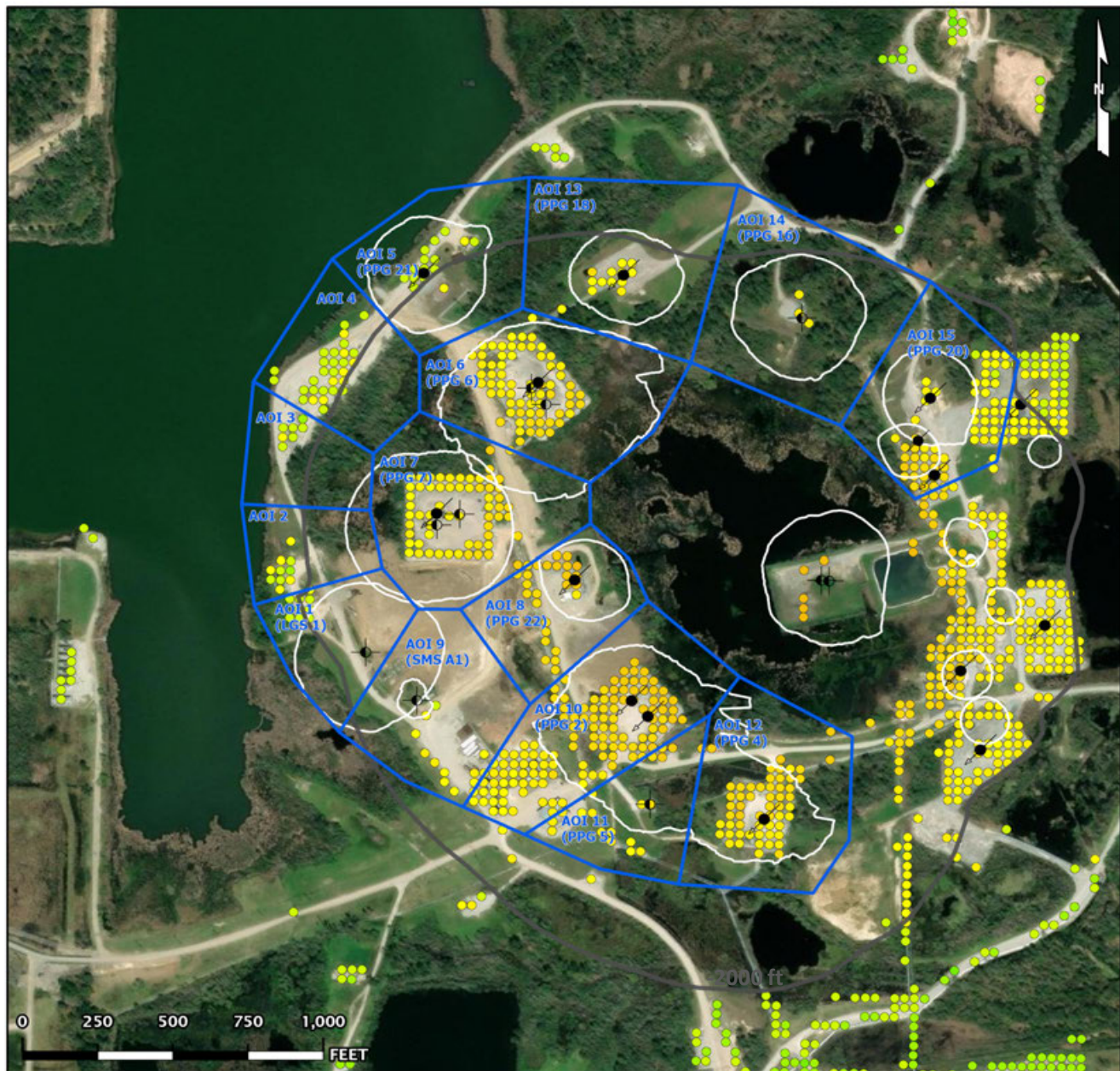


- AOI Boundary
 - InSAR LOS Measurement Point
 - Historical Cavern Extent
 - Top of Dome (-2000 ft Contour)
- Cavern Well Surface Locations
- 09 - Active - Injection
 - 29 - Dry and Plugged

Vertical Data (02/04/2023 - 09/29/2025)

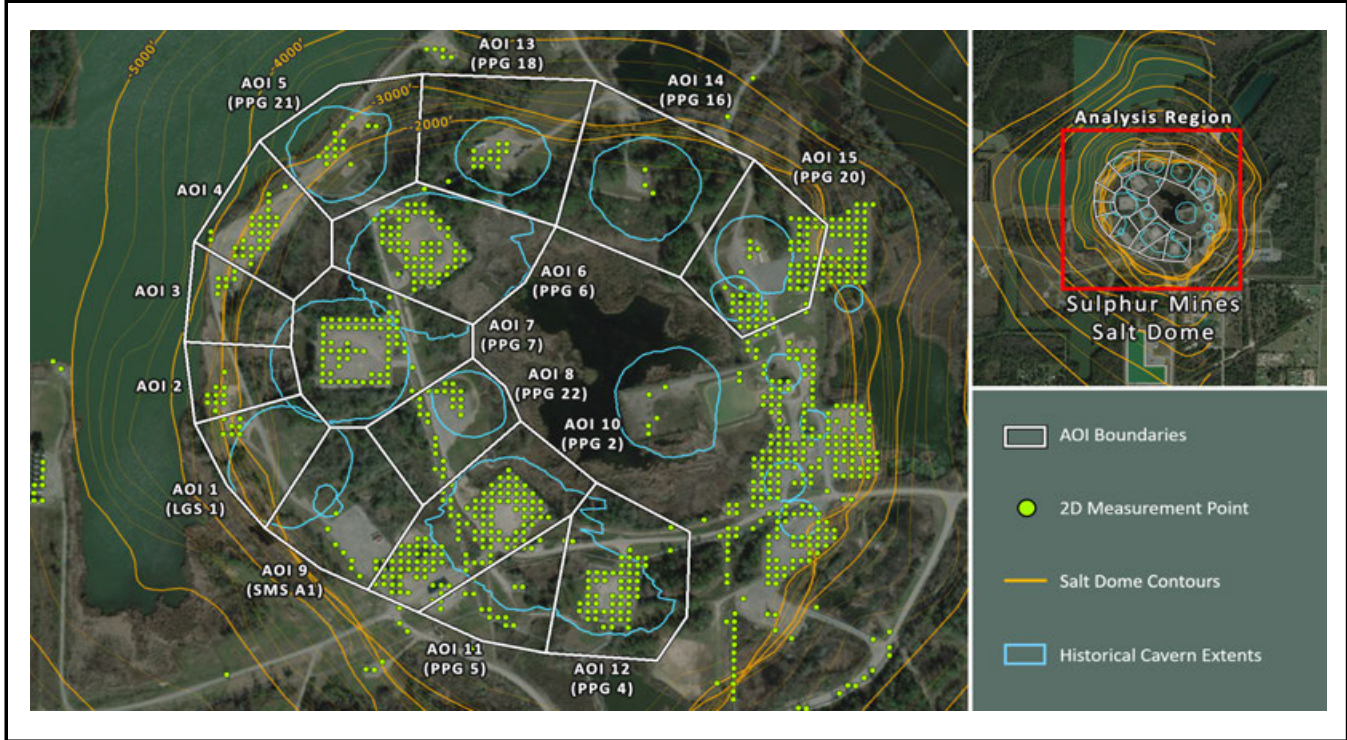
Linear Velocity Data Points

Date range: 02/04/2023 - 09/29/2025



- AOI Boundary
 - InSAR LOS Measurement Point
 - Historical Cavern Extent
 - Top of Dome (-2000 ft Contour)
- Cavern Well Surface Locations
- 09 - Active - Injection
 - 29 - Dry and Plugged

AOI Boundaries & 2D InSAR Measurement Points

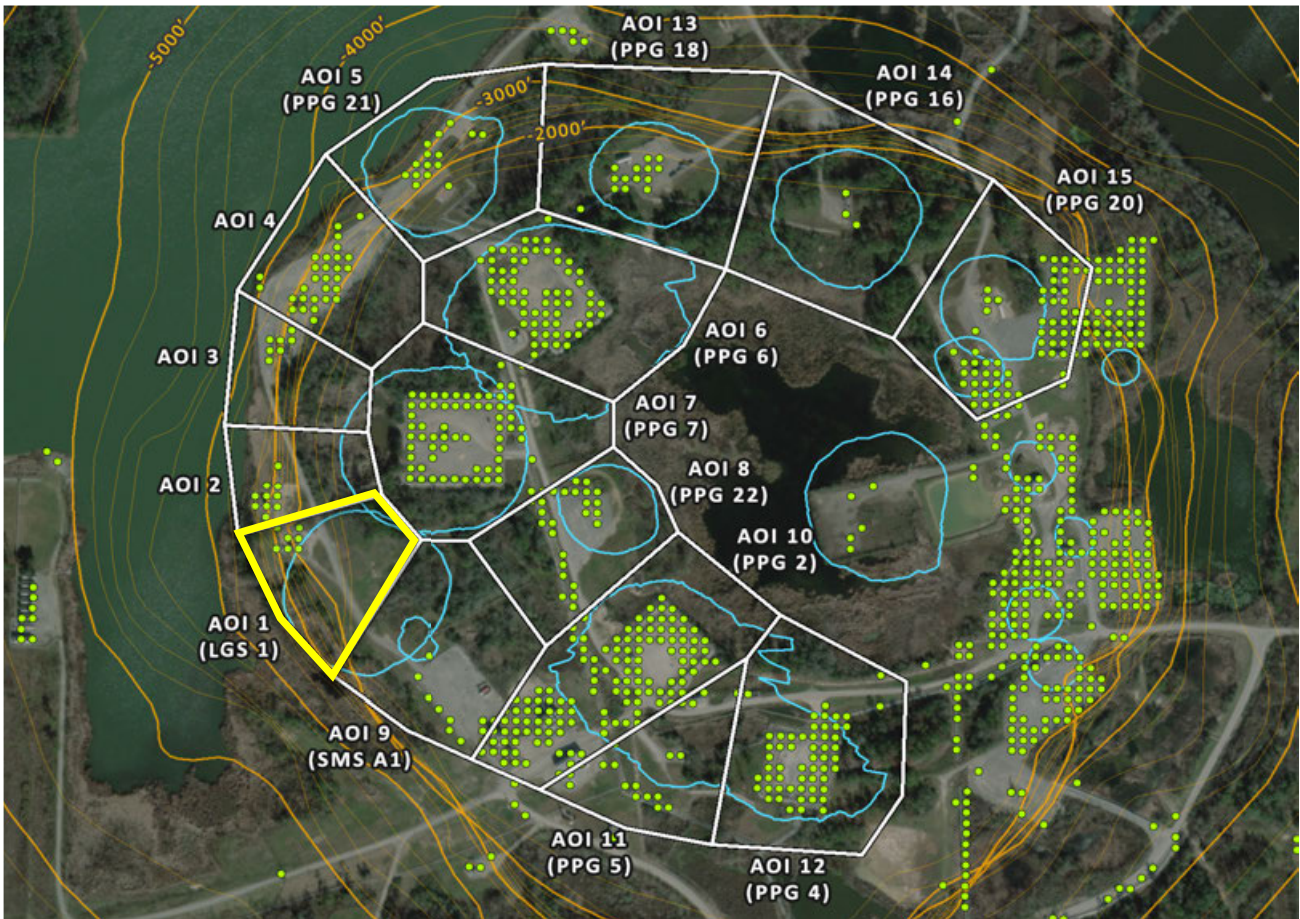


Subsidence Monitoring Areas of Interest (AOIs)

To visually convey and evaluate trend consistency for the East-West displacement time series of each ground target, measurement points were grouped and their displacement values were averaged. The point groups are referred to as Areas of Interest (AOIs) in this analysis and their boundaries are depicted on the above map. The below table lists the East-West trend values calculated in each AOI for the dataset evaluated in this report.

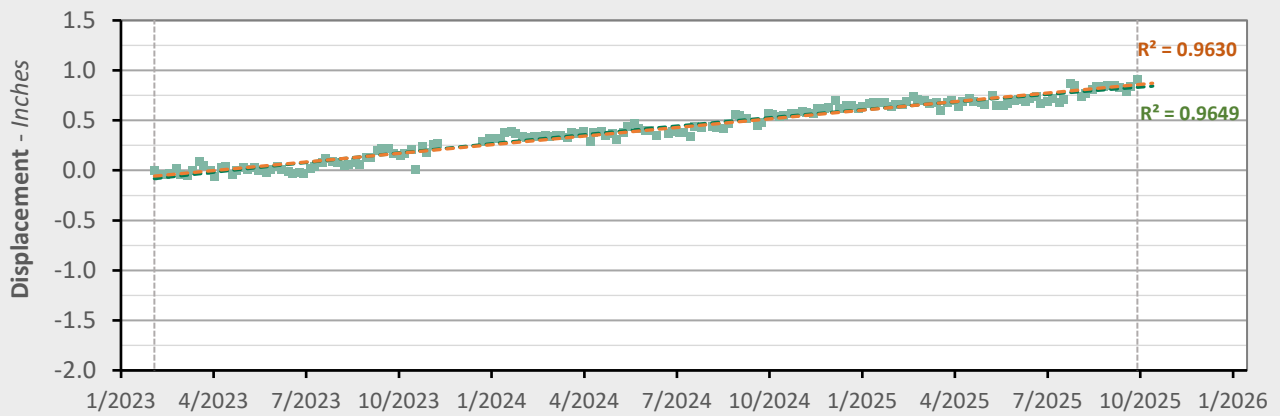
AOI Name	East-West (9/29/2025)	East-West Velocity (in/yr)		East-West Acceleration (in/yr ²)	
	Point Count	Nonlinear	Linear	Nonlinear	Linear
AOI 1 (LGS 1)	9	+0.29	+0.35	-0.04	0.00
AOI 2	10	+0.28	+0.38	-0.07	0.00
AOI 3	7	+0.19	+0.31	-0.09	0.00
AOI 4	29	+0.22	+0.32	-0.07	0.00
AOI 5 (PPG 21)	15	+0.09	+0.18	-0.06	0.00
AOI 6 (PPG 6)	65	+0.18	+0.25	-0.05	0.00
AOI 7 (PPG 7)	62	+0.43	+0.45	-0.02	0.00
AOI 8 (PPG 22)	25	+0.37	+0.38	-0.01	0.00
AOI 9 (SMS A1)	12	+0.38	+0.33	+0.04	0.00
AOI 10 (PPG 2)	124	+0.26	+0.26	-0.00	0.00
AOI 11 (PPG 5)	19	+0.13	+0.16	-0.02	0.00
AOI 12 (PPG 4)	56	-0.27	-0.17	-0.07	0.00
AOI 13 (PPG 18)	13	+0.13	+0.12	+0.01	0.00
AOI 14 (PPG 16)	3	-0.40	-0.26	-0.10	0.00
AOI 15 (PPG 20)	61	-0.64	-0.58	-0.05	0.00

AOI 1 (LGS 1) - Location Map

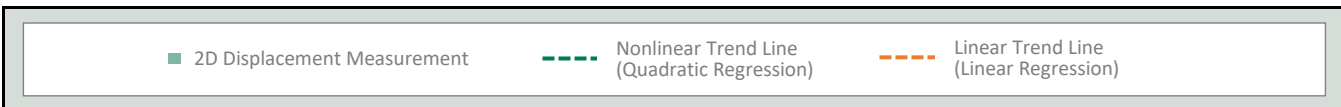


AOI 1 (LGS 1) - East-West Time Series

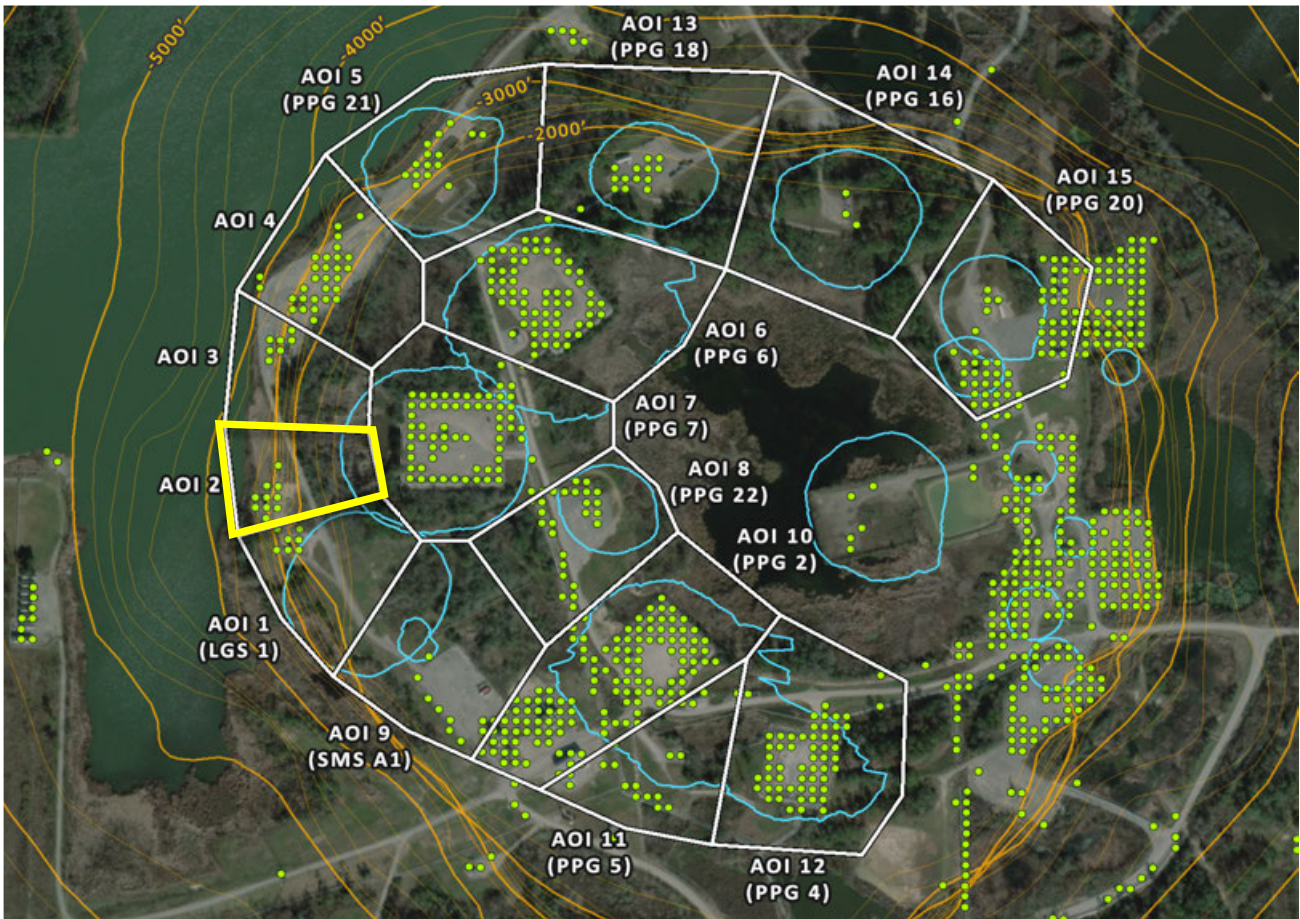
E-W (9/29/2025) Point Count: 9



	Nonlinear Trend	Linear Trend
Velocity:	+0.29 in/yr	+0.35 in/yr
Acceleration:	-0.04 in/yr ²	0.00 in/yr ²

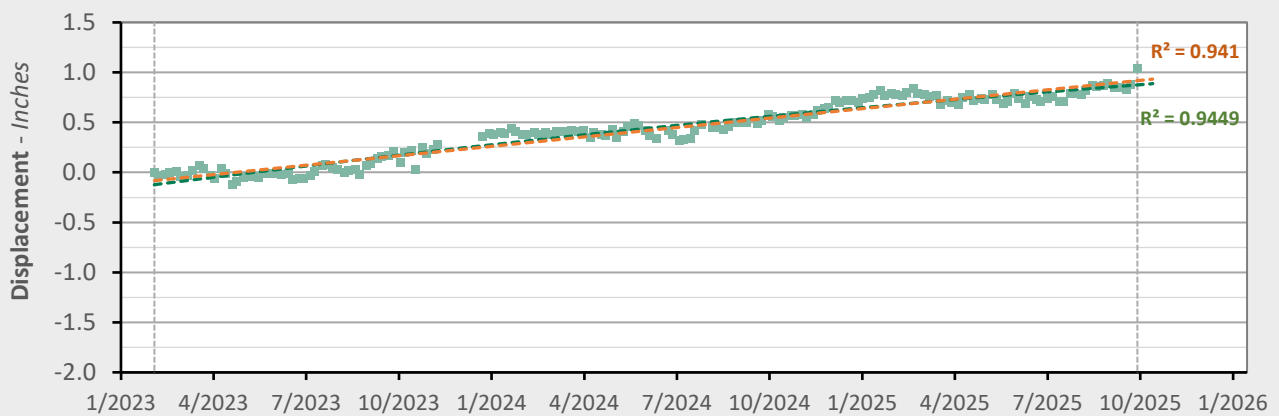


AOI 2 - Location Map

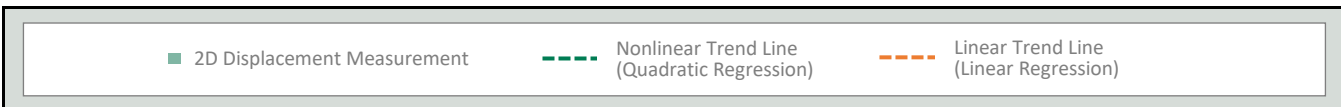


AOI 2 - East-West Time Series

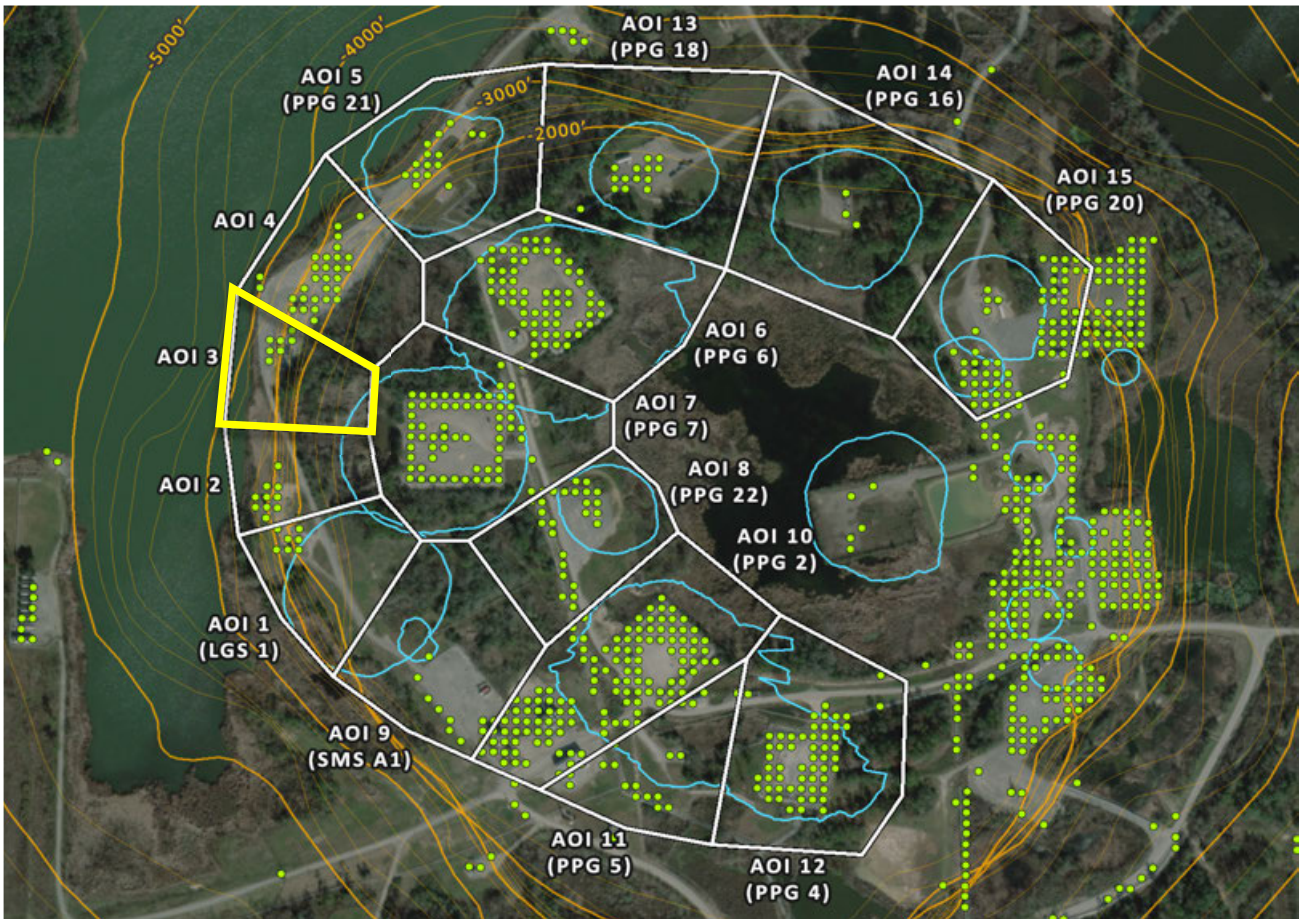
E-W (9/29/2025) Point Count: 10



	Nonlinear Trend	Linear Trend
Velocity:	+0.28 in/yr	+0.38 in/yr
Acceleration:	-0.07 in/yr ²	0.00 in/yr ²

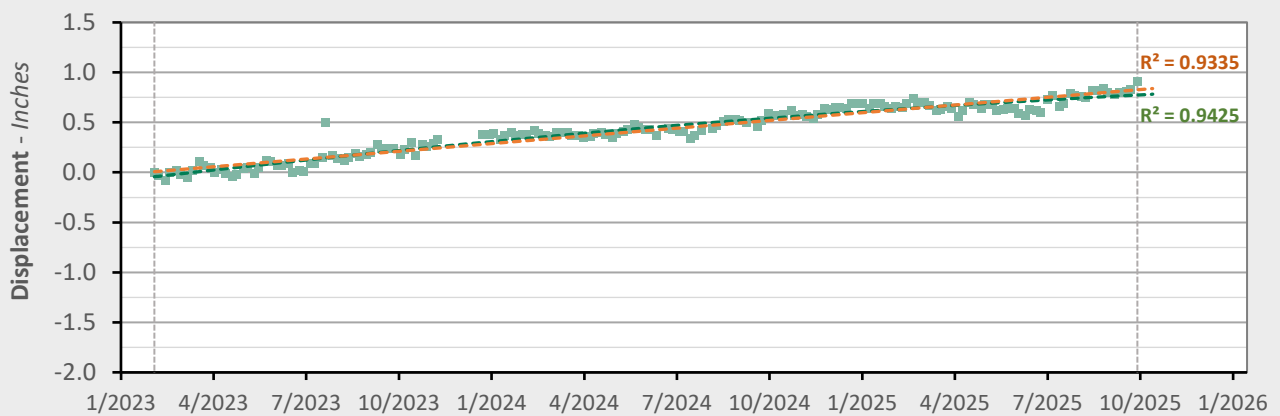


AOI 3 - Location Map

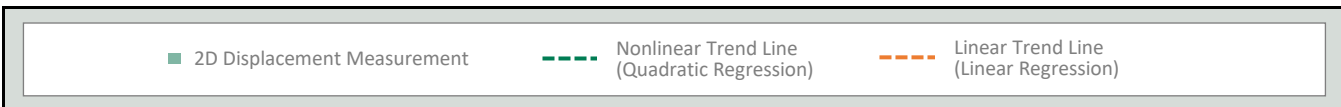


AOI 3 - East-West Time Series

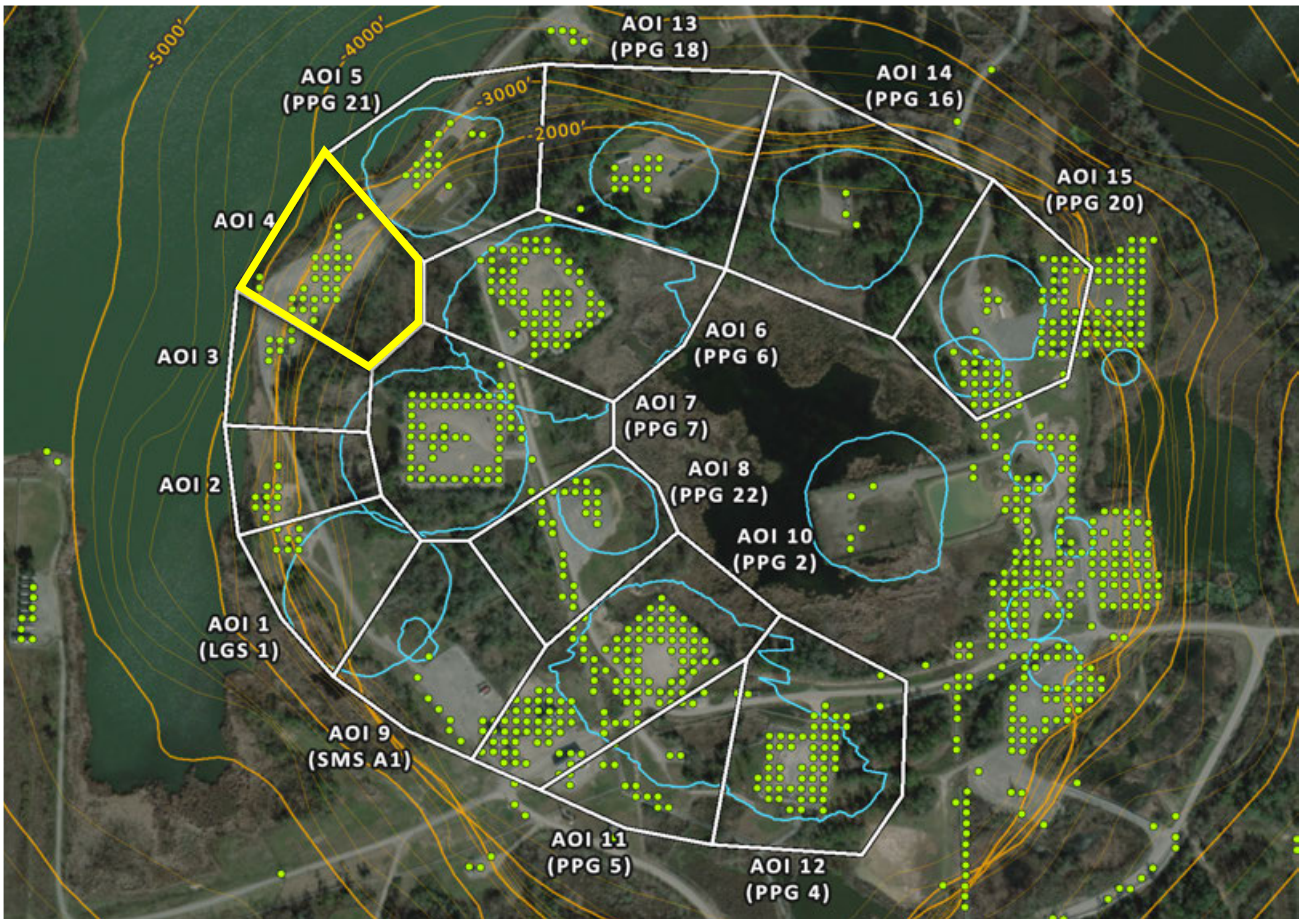
E-W (9/29/2025) Point Count: 7



	Nonlinear Trend	Linear Trend
Velocity:	+0.19 in/yr	+0.31 in/yr
Acceleration:	-0.09 in/yr ²	0.00 in/yr ²

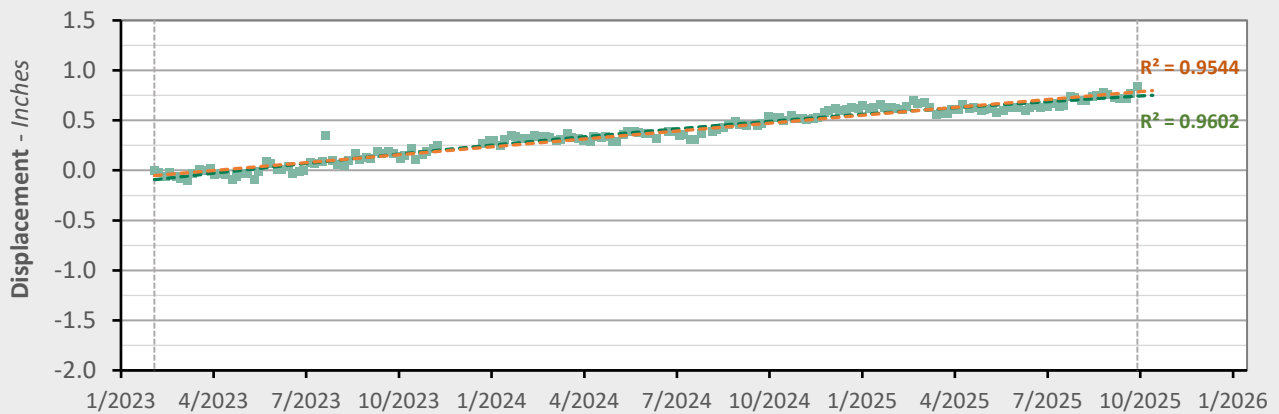


AOI 4 - Location Map

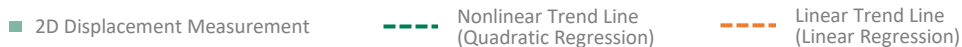


AOI 4 - East-West Time Series

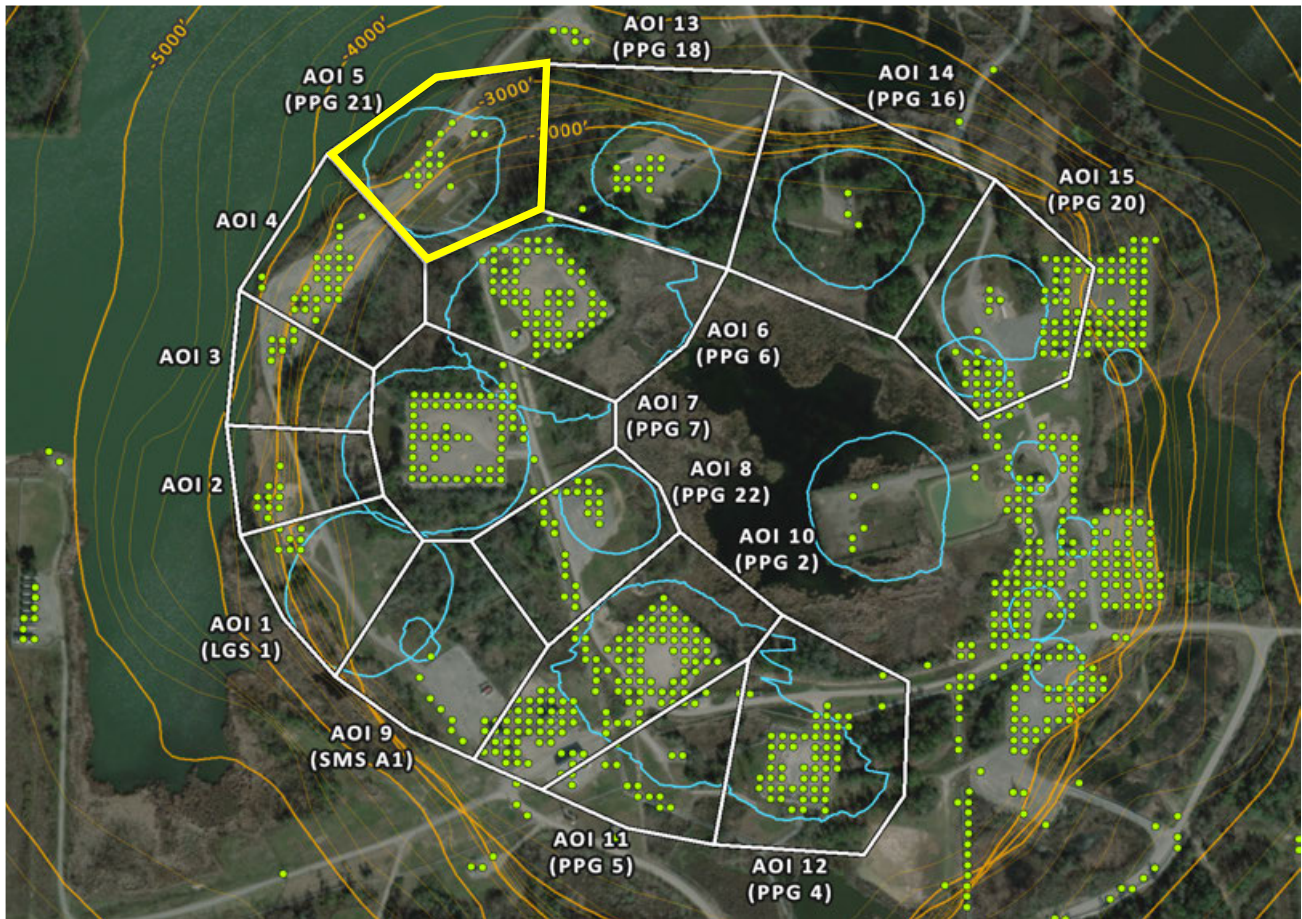
E-W (9/29/2025) Point Count: 29



	Nonlinear Trend	Linear Trend
Velocity:	+0.22 in/yr	+0.32 in/yr
Acceleration:	-0.07 in/yr ²	0.00 in/yr ²

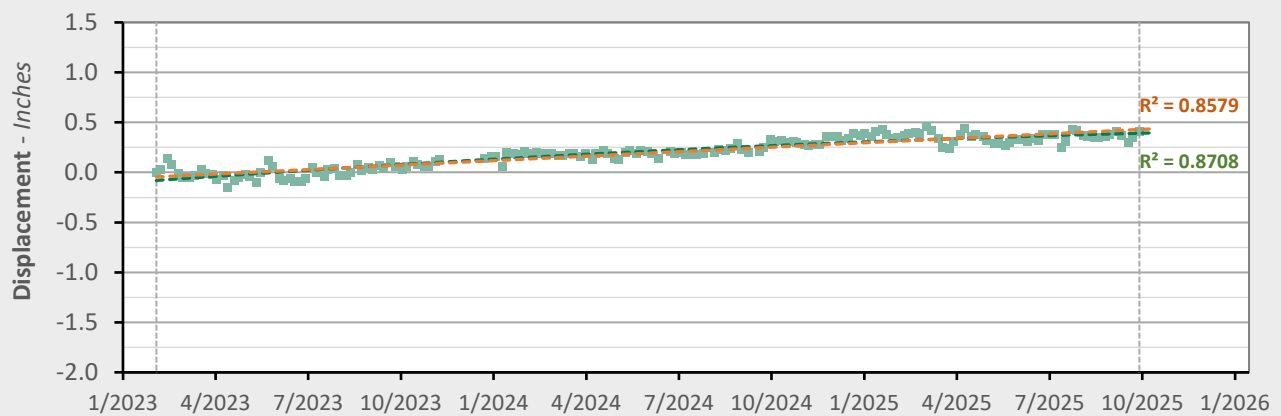


AOI 5 (PPG 21) - Location Map

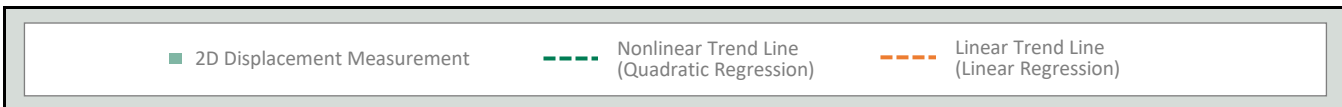


AOI 5 (PPG 21) - East-West Time Series

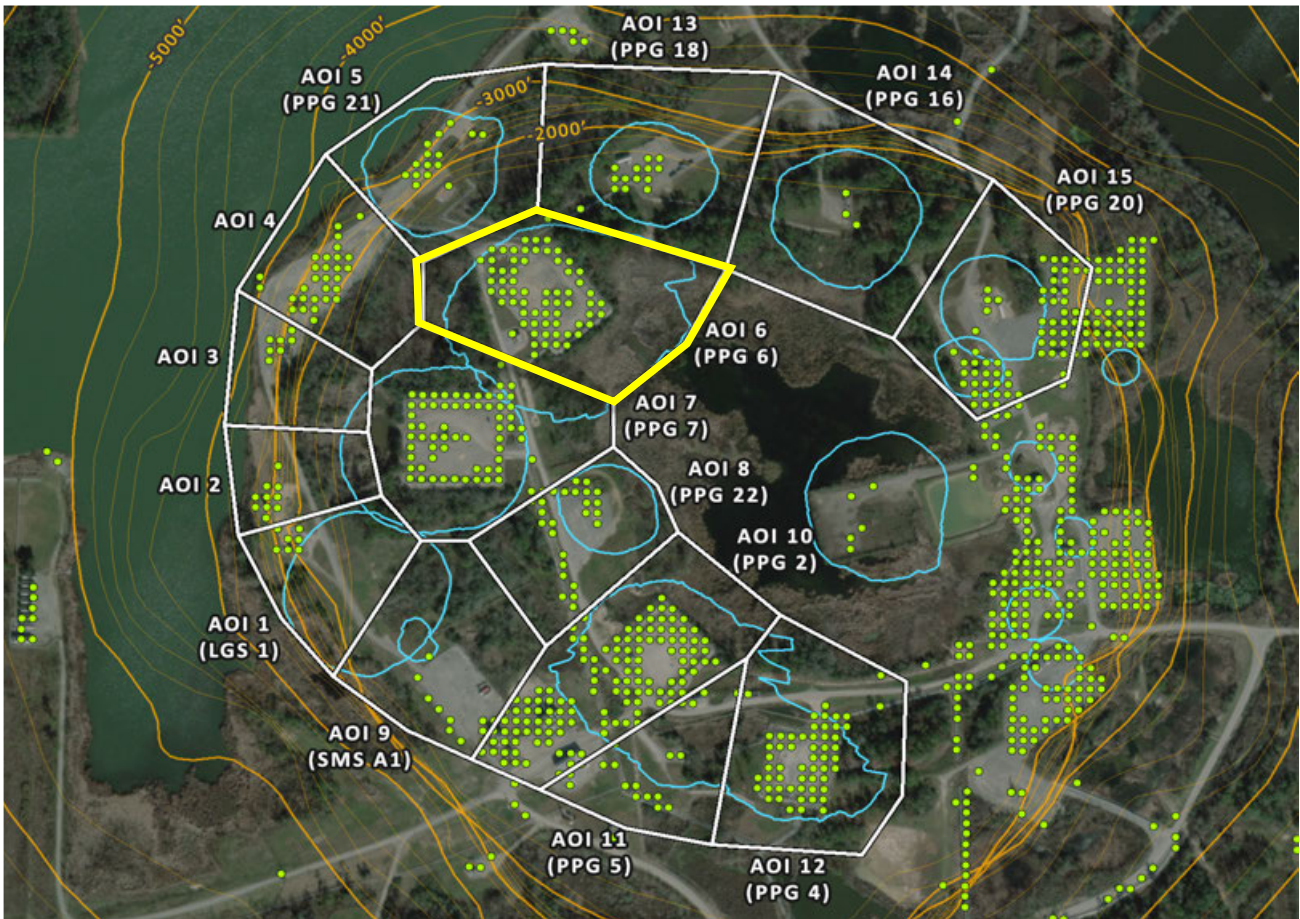
E-W (9/29/2025) Point Count: 15



	Nonlinear Trend	Linear Trend
Velocity:	+0.09 in/yr	+0.18 in/yr
Acceleration:	-0.06 in/yr ²	0.00 in/yr ²

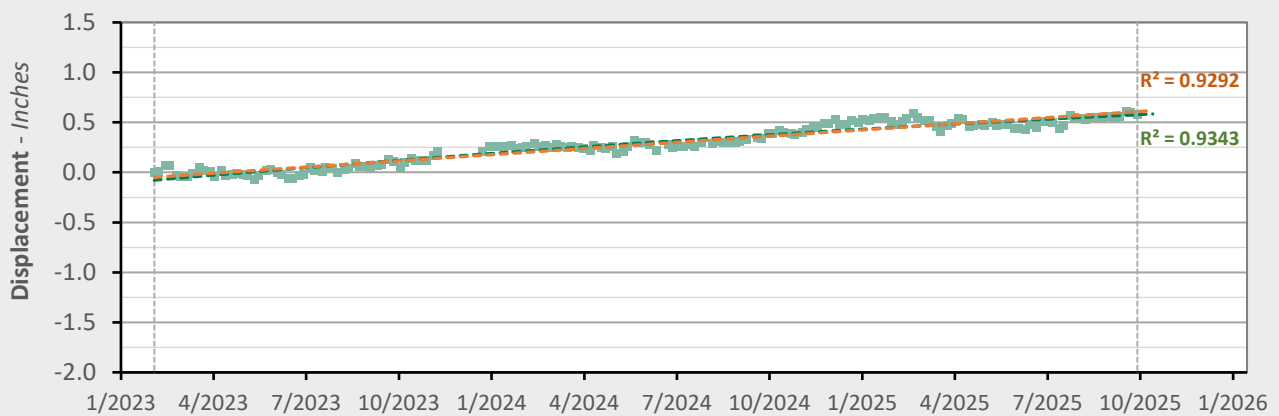


AOI 6 (PPG 6) - Location Map

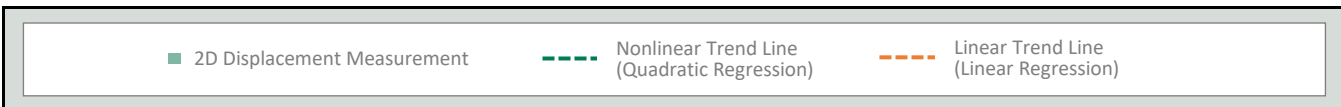


AOI 6 (PPG 6) - East-West Time Series

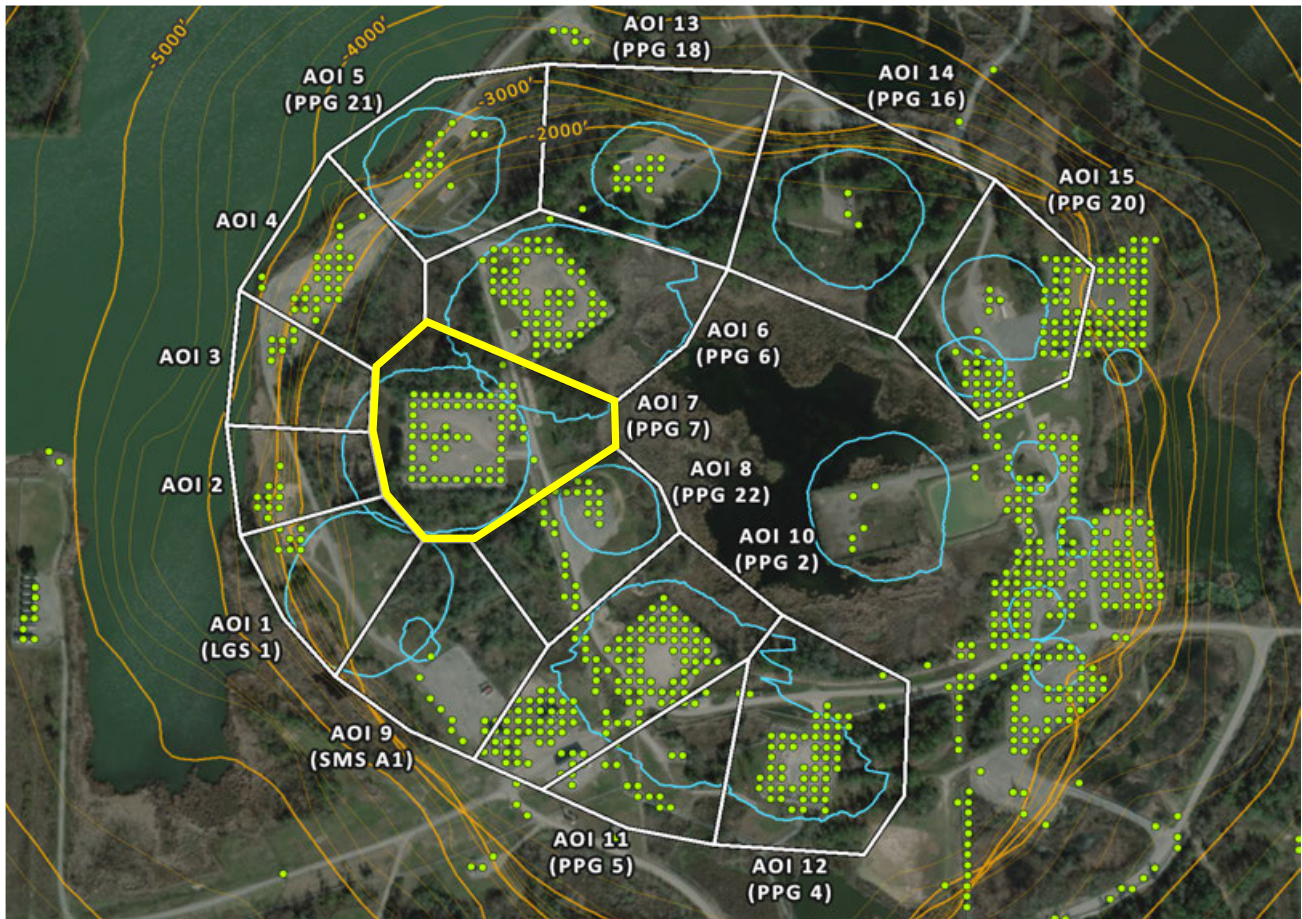
E-W (9/29/2025) Point Count: 65



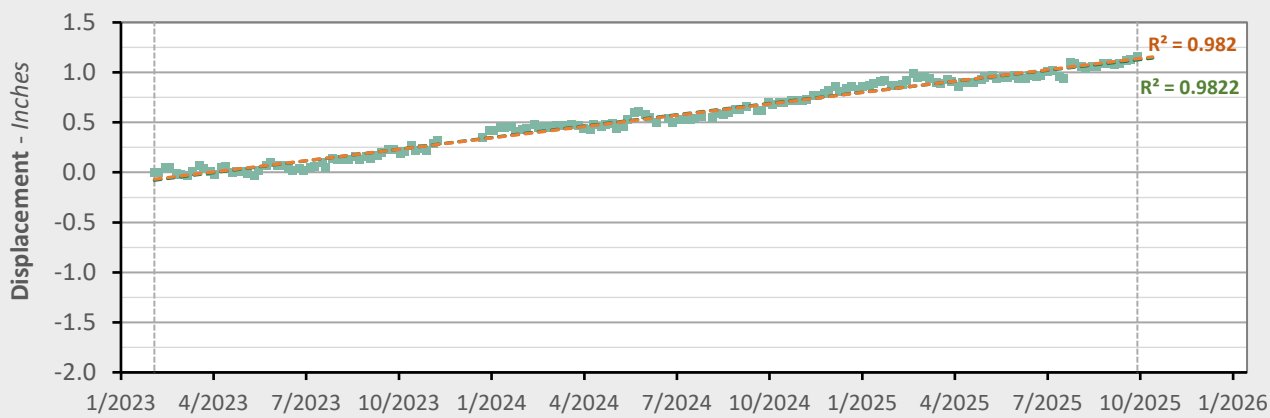
	Nonlinear Trend	Linear Trend
Velocity:	+0.18 in/yr	+0.25 in/yr
Acceleration:	-0.05 in/yr ²	0.00 in/yr ²



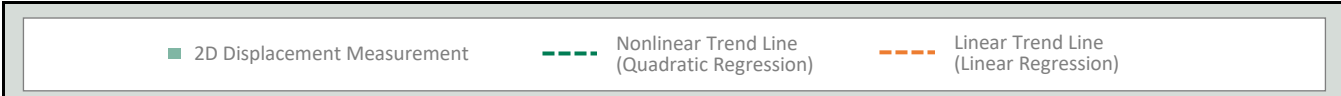
AOI 7 (PPG 7) - Location Map



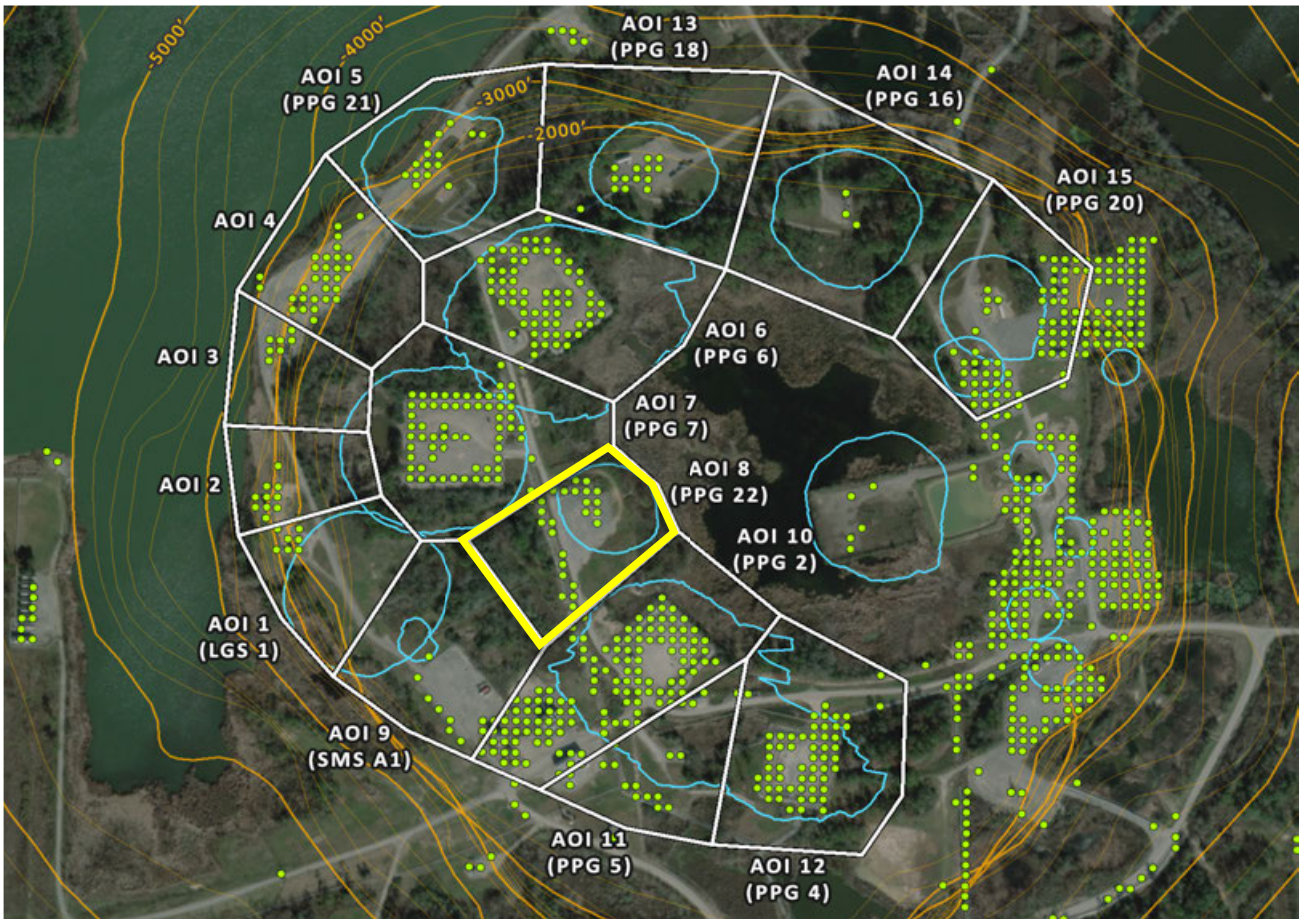
AOI 7 (PPG 7) - East-West Time Series E-W (9/29/2025) Point Count: 62



	Nonlinear Trend	Linear Trend
Velocity:	+0.43 in/yr	+0.45 in/yr
Acceleration:	-0.02 in/yr ²	0.00 in/yr ²

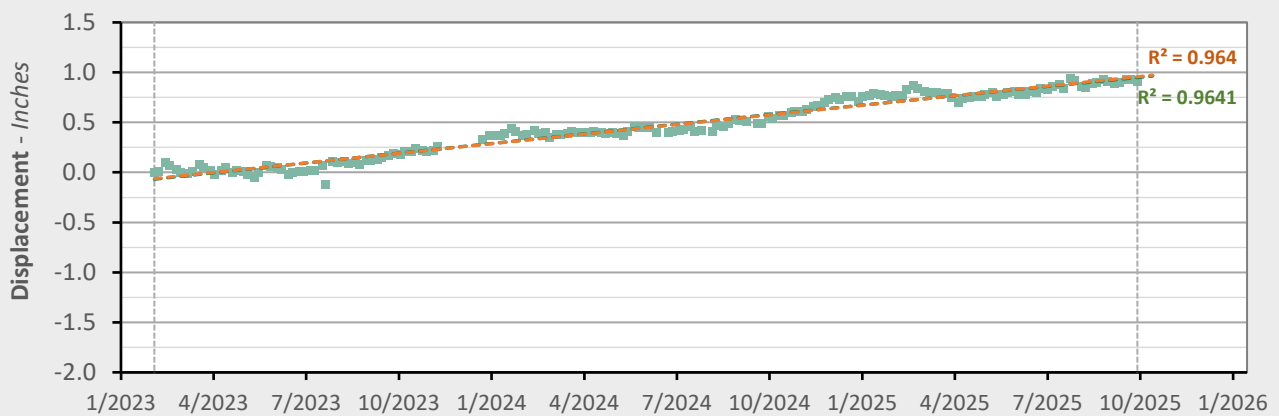


AOI 8 (PPG 22) - Location Map

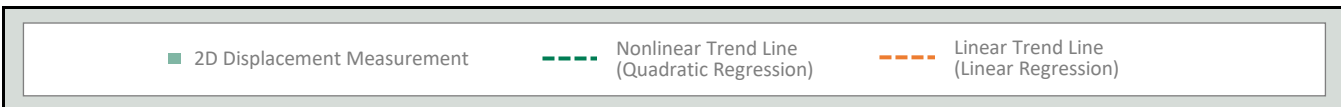


AOI 8 (PPG 22) - East-West Time Series

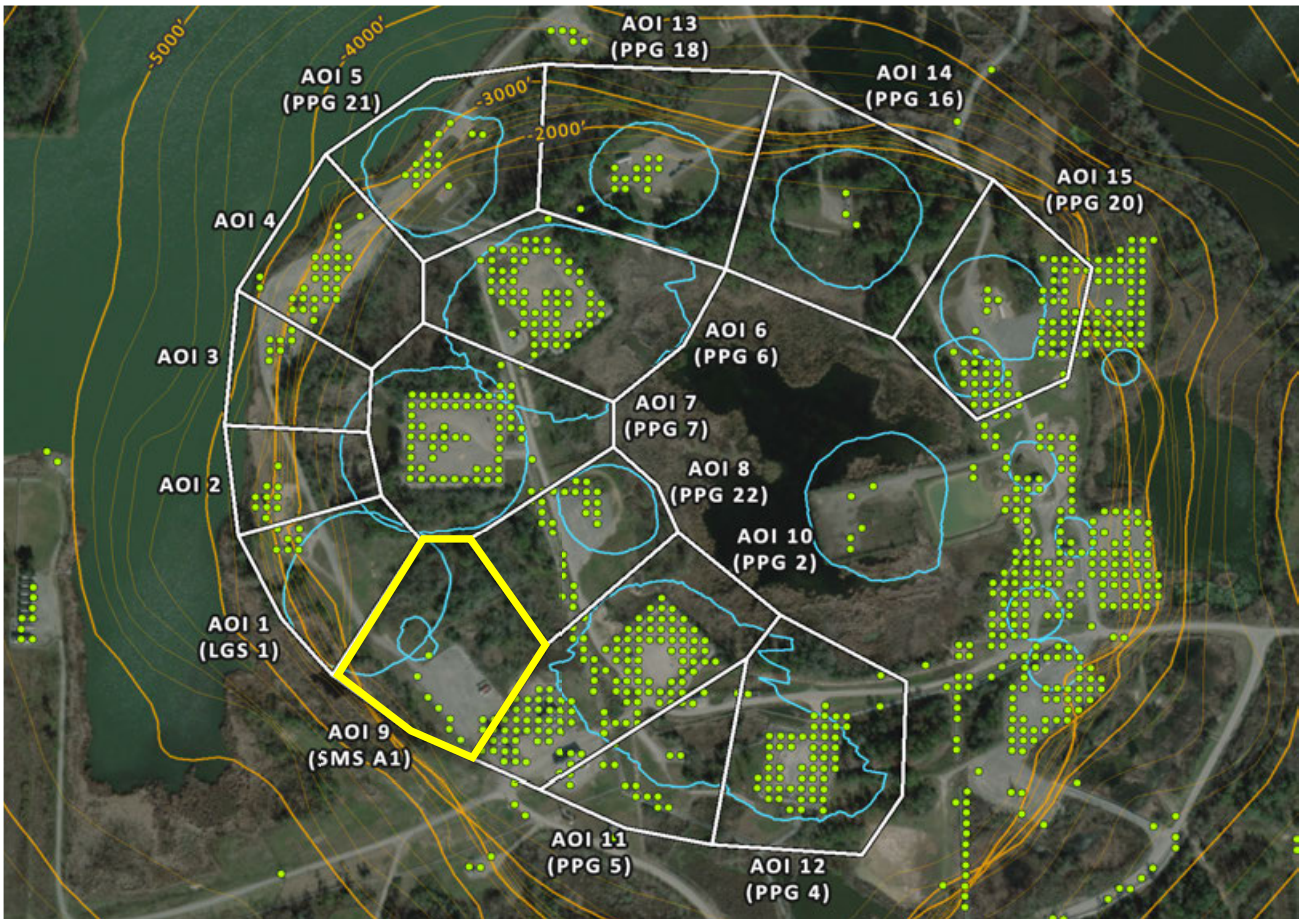
E-W (9/29/2025) Point Count: 25



	Nonlinear Trend	Linear Trend
Velocity:	+0.37 in/yr	+0.38 in/yr
Acceleration:	-0.01 in/yr ²	0.00 in/yr ²

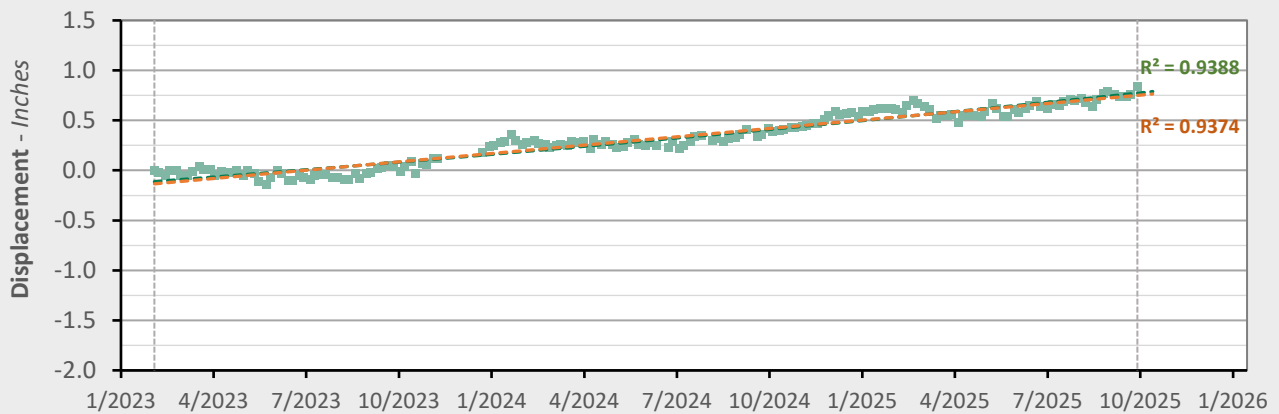


AOI 9 (PPG A1) - Location Map

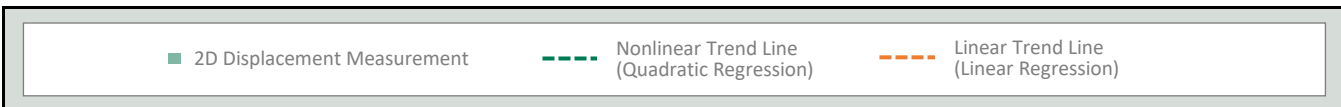


AOI 9 (SMS A1) - East-West Time Series

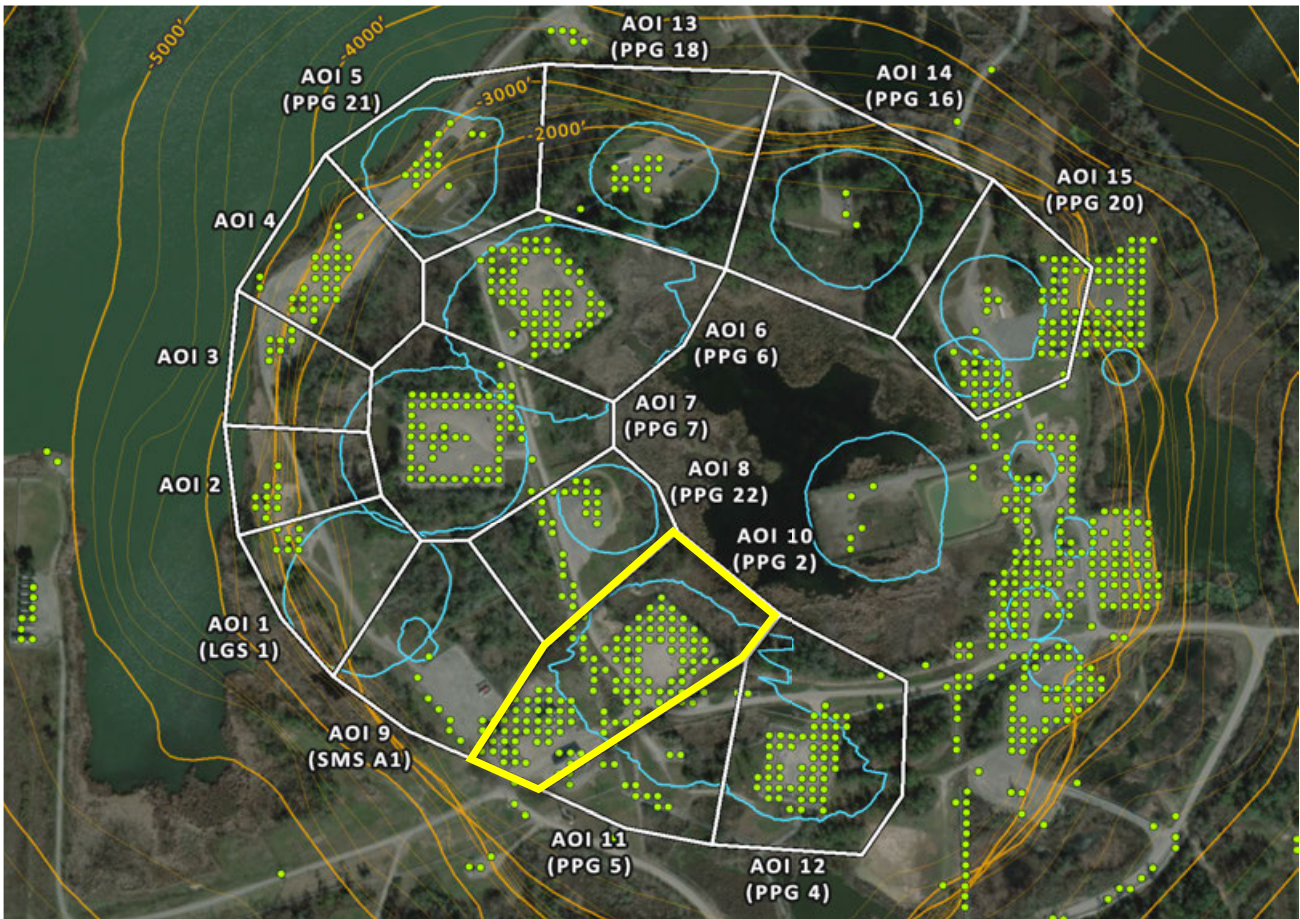
E-W (9/29/2025) Point Count: 12



	Nonlinear Trend	Linear Trend
Velocity:	+0.38 in/yr	+0.33 in/yr
Acceleration:	+0.04 in/yr ²	0.00 in/yr ²

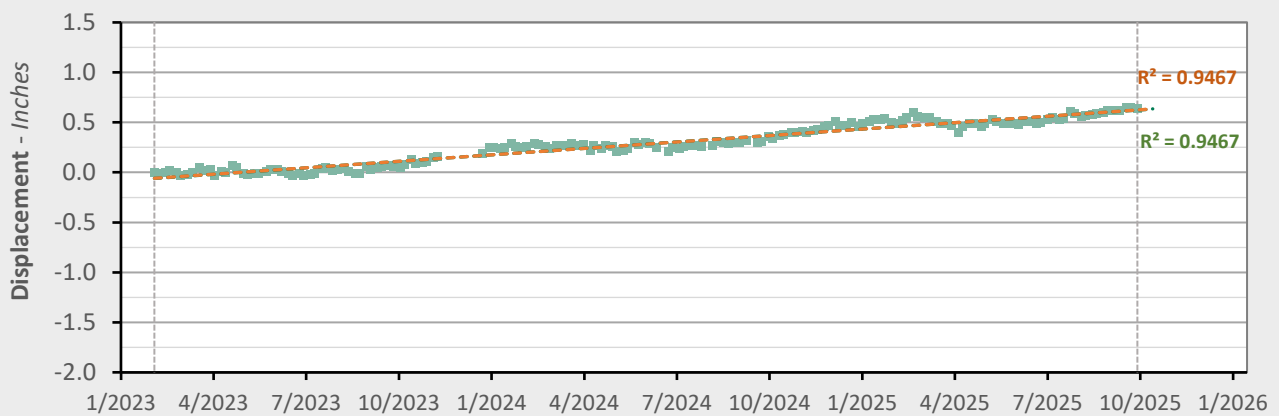


AOI 10 (PPG 2) - Location Map

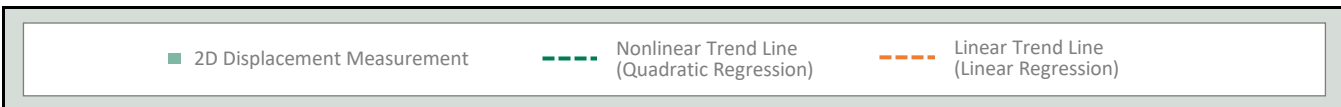


AOI 10 (PPG 2) - East-West Time Series

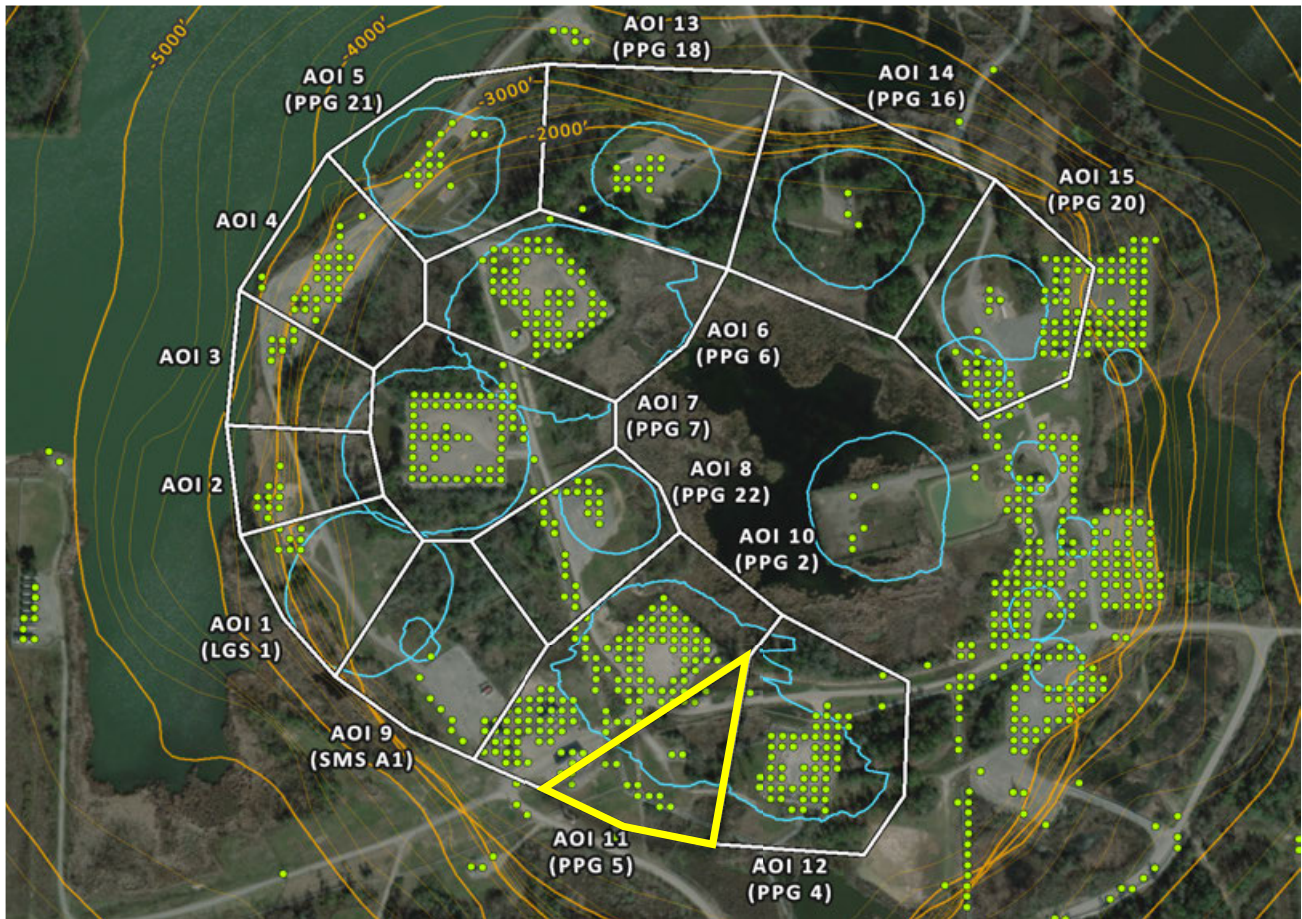
E-W (9/29/2025) Point Count: **124**



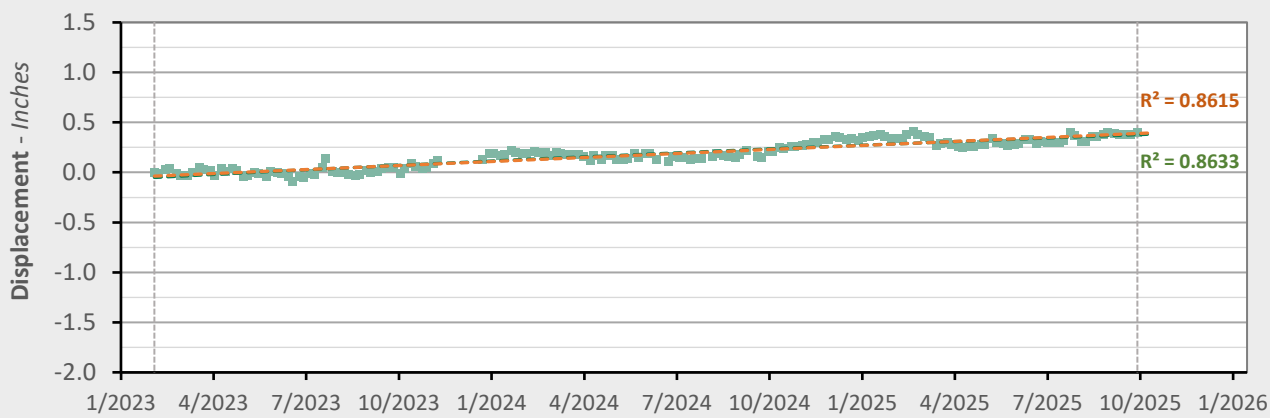
	Nonlinear Trend	Linear Trend
Velocity:	+0.26 in/yr	+0.26 in/yr
Acceleration:	-0.00 in/yr ²	0.00 in/yr ²



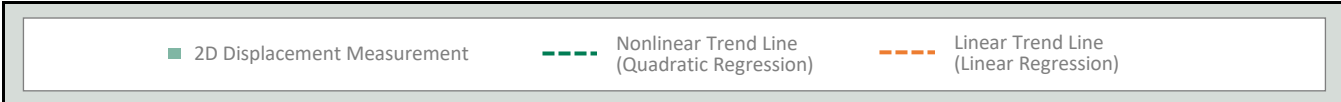
AOI 11 (PPG 5) - Location Map



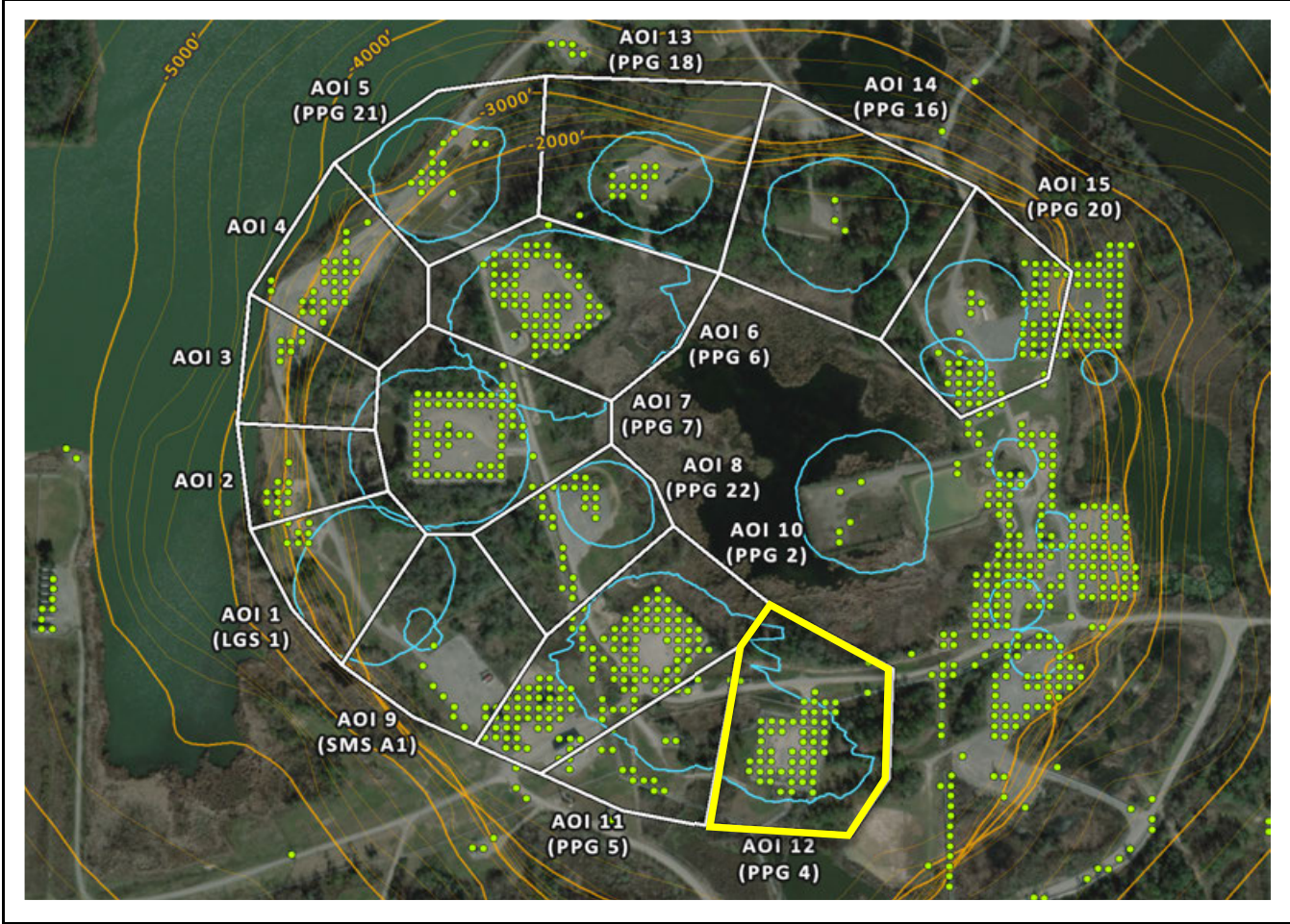
AOI 11 (PPG 5) - East-West Time Series E-W (9/29/2025) Point Count: 19



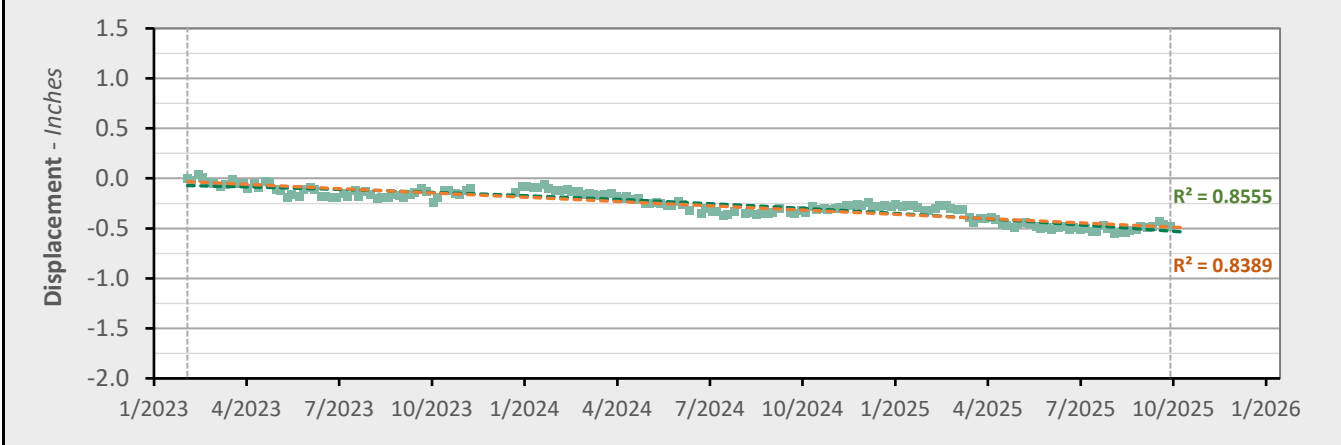
	Nonlinear Trend	Linear Trend
Velocity:	+0.13 in/yr	+0.16 in/yr
Acceleration:	-0.02 in/yr ²	0.00 in/yr ²



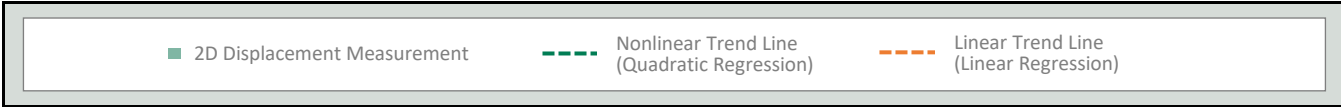
AOI 12 (PPG 4) - Location Map



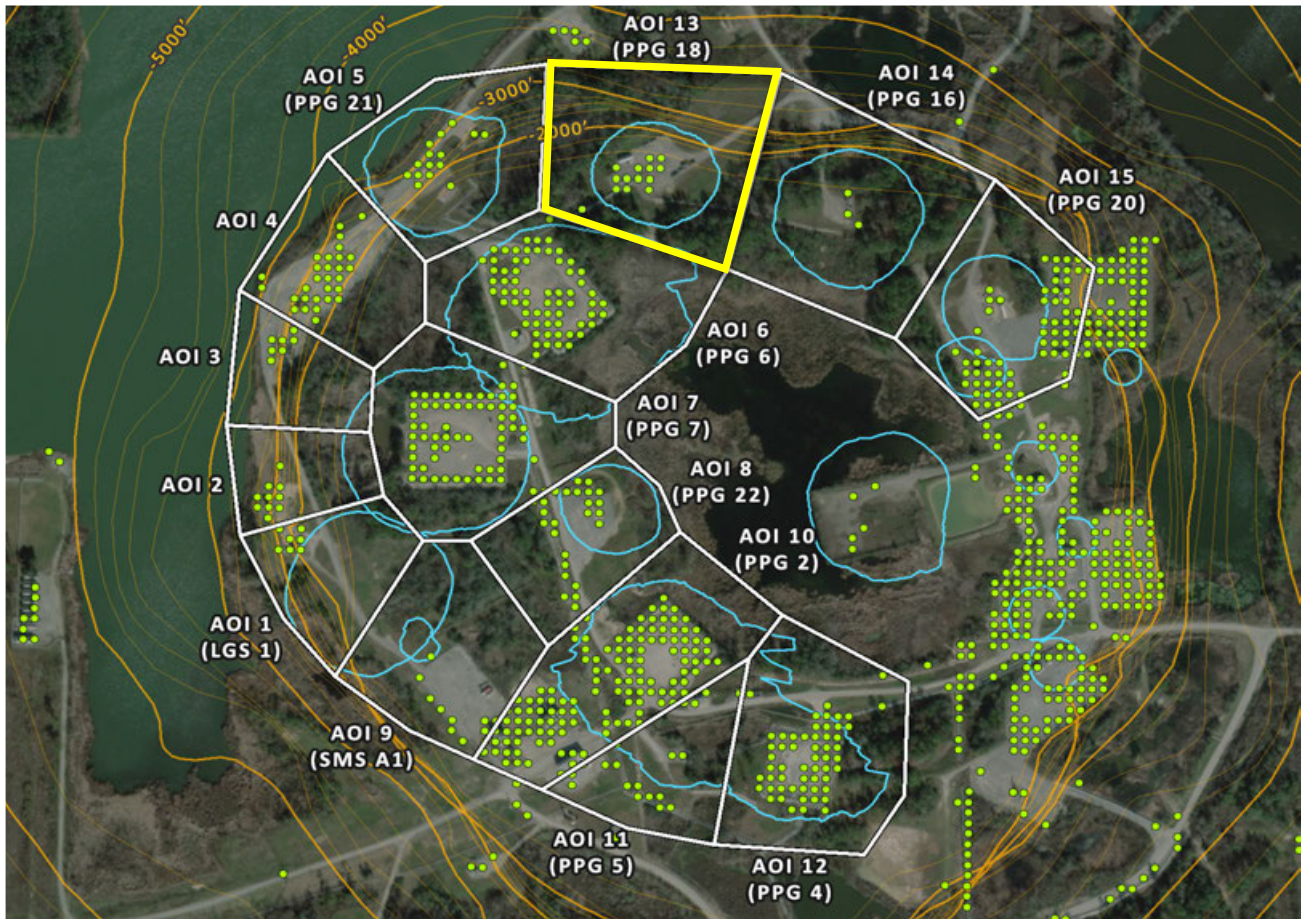
AOI 12 (PPG 4) - East-West Time Series E-W (9/29/2025) Point Count: 56



	Nonlinear Trend	Linear Trend
Velocity:	-0.27 in/yr	-0.17 in/yr
Acceleration:	-0.07 in/yr ²	0.00 in/yr ²

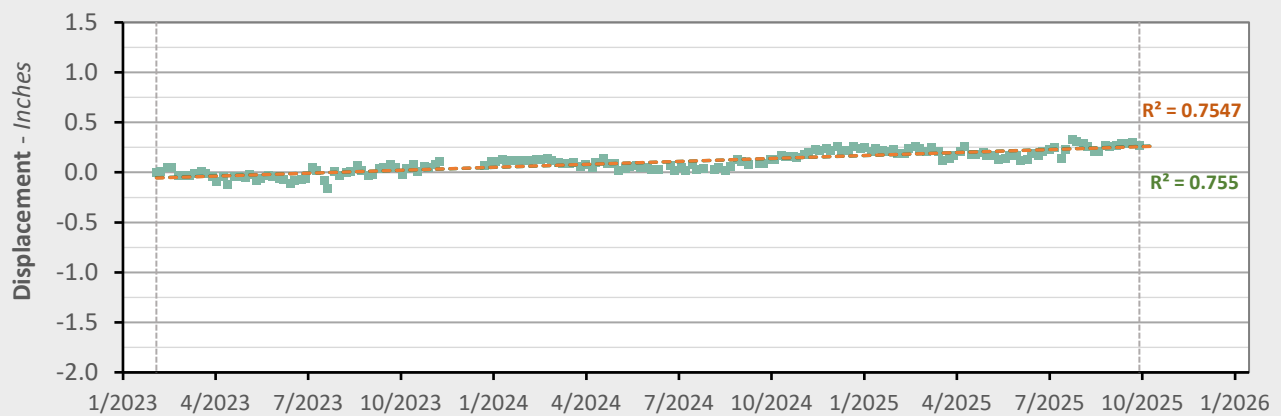


AOI 13 (PPG 18) - Location Map

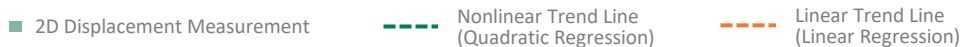


AOI 13 (PPG 18) - East-West Time Series

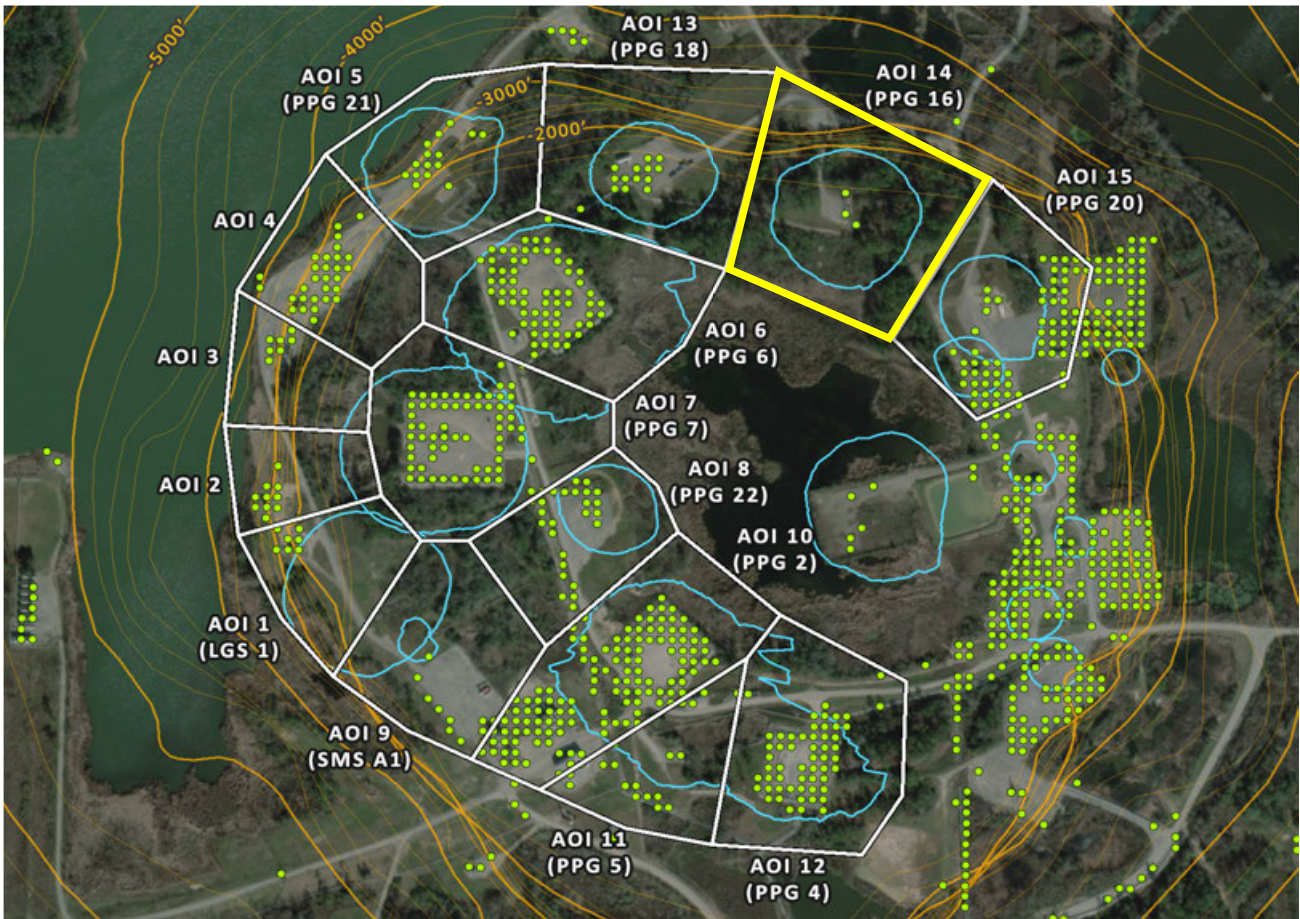
E-W (9/29/2025) Point Count: **13**



	Nonlinear Trend	Linear Trend
Velocity:	+0.13 in/yr	+0.12 in/yr
Acceleration:	+0.01 in/yr ²	0.00 in/yr ²

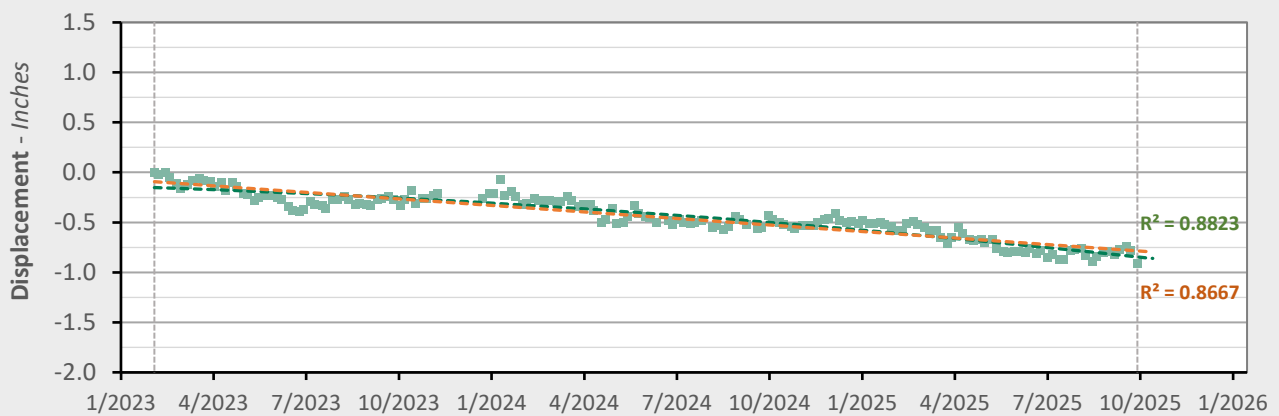


AOI 14 (PPG 16) - Location Map

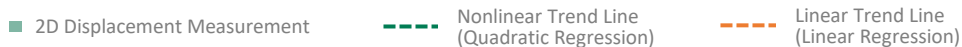


AOI 14 (PPG 16) - East-West Time Series

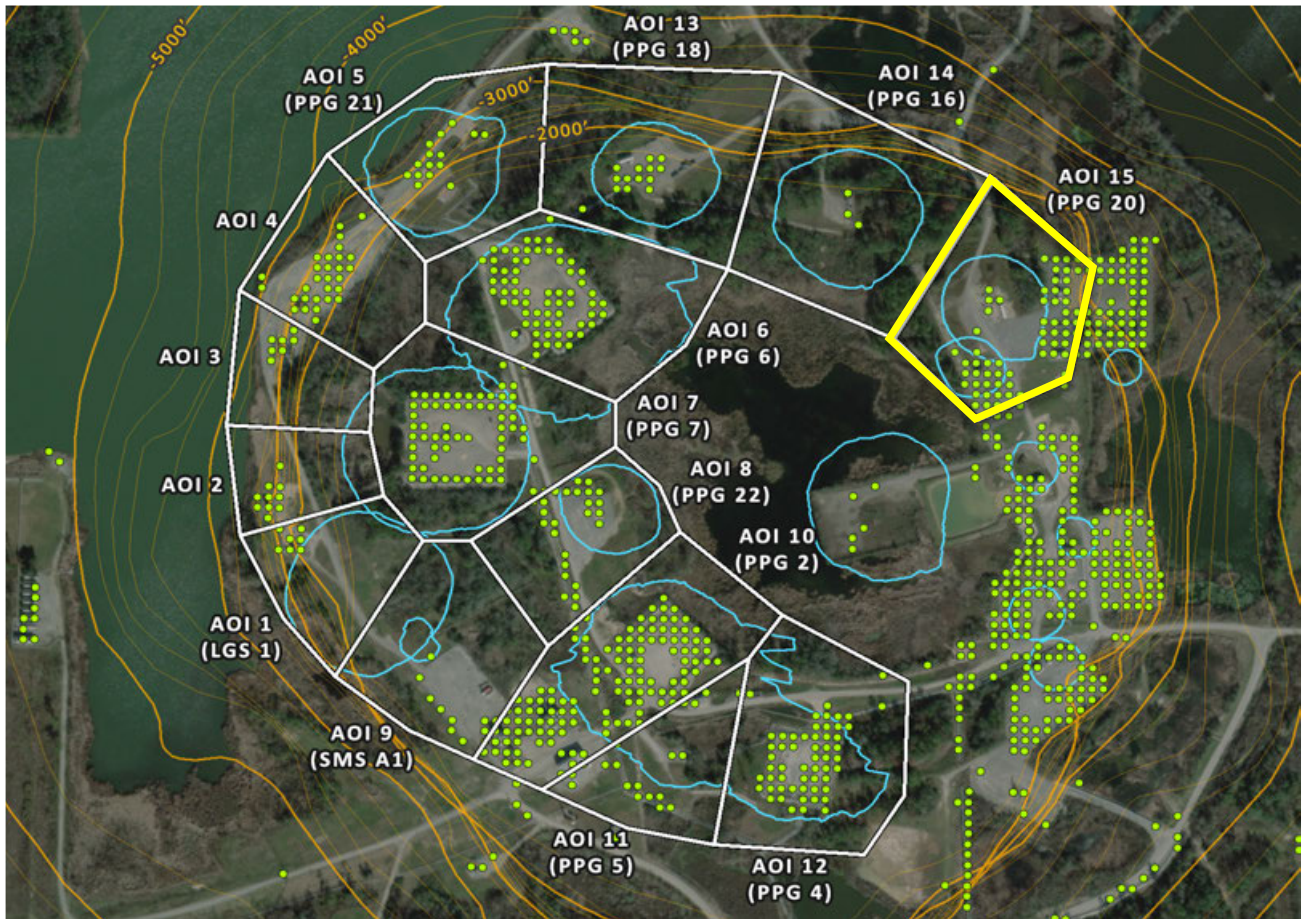
E-W (9/29/2025) Point Count: 3



	Nonlinear Trend	Linear Trend
Velocity:	-0.40 in/yr	-0.26 in/yr
Acceleration:	-0.10 in/yr ²	0.00 in/yr ²

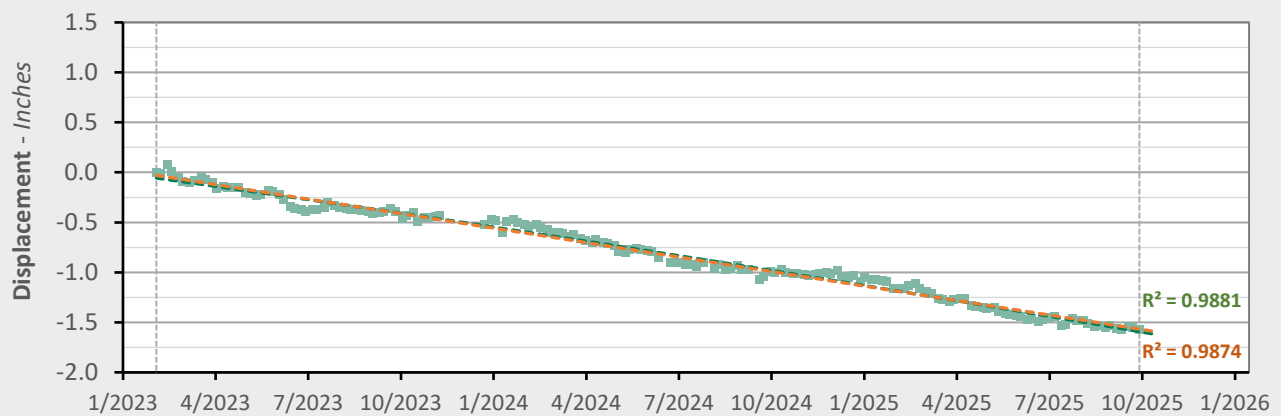


AOI 15 (PPG 20) - Location Map

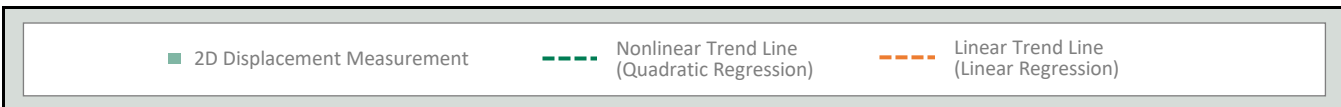


AOI 15 (PPG 20) - East-West Time Series

E-W (9/29/2025) Point Count: **61**



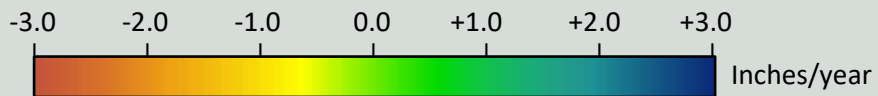
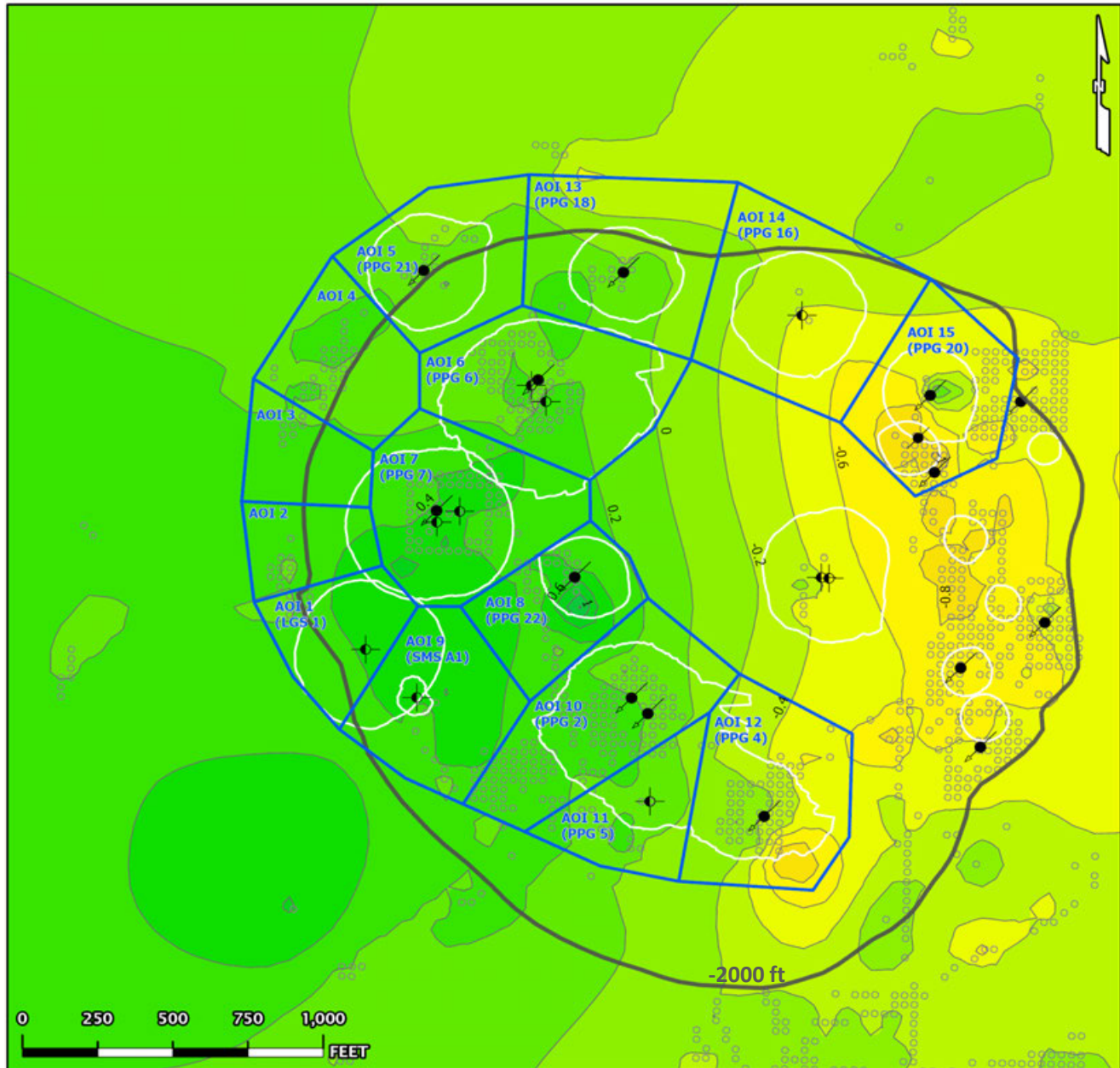
	Nonlinear Trend	Linear Trend
Velocity:	-0.64 in/yr	-0.58 in/yr
Acceleration:	-0.05 in/yr ²	0.00 in/yr ²



East-West Data (02/04/2023 - 09/29/2025)

Nonlinear Velocity Contours

As of date: 09/29/2025

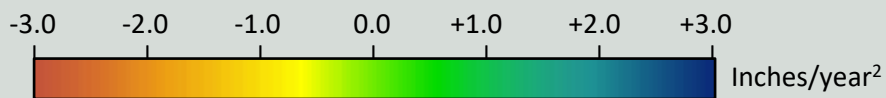
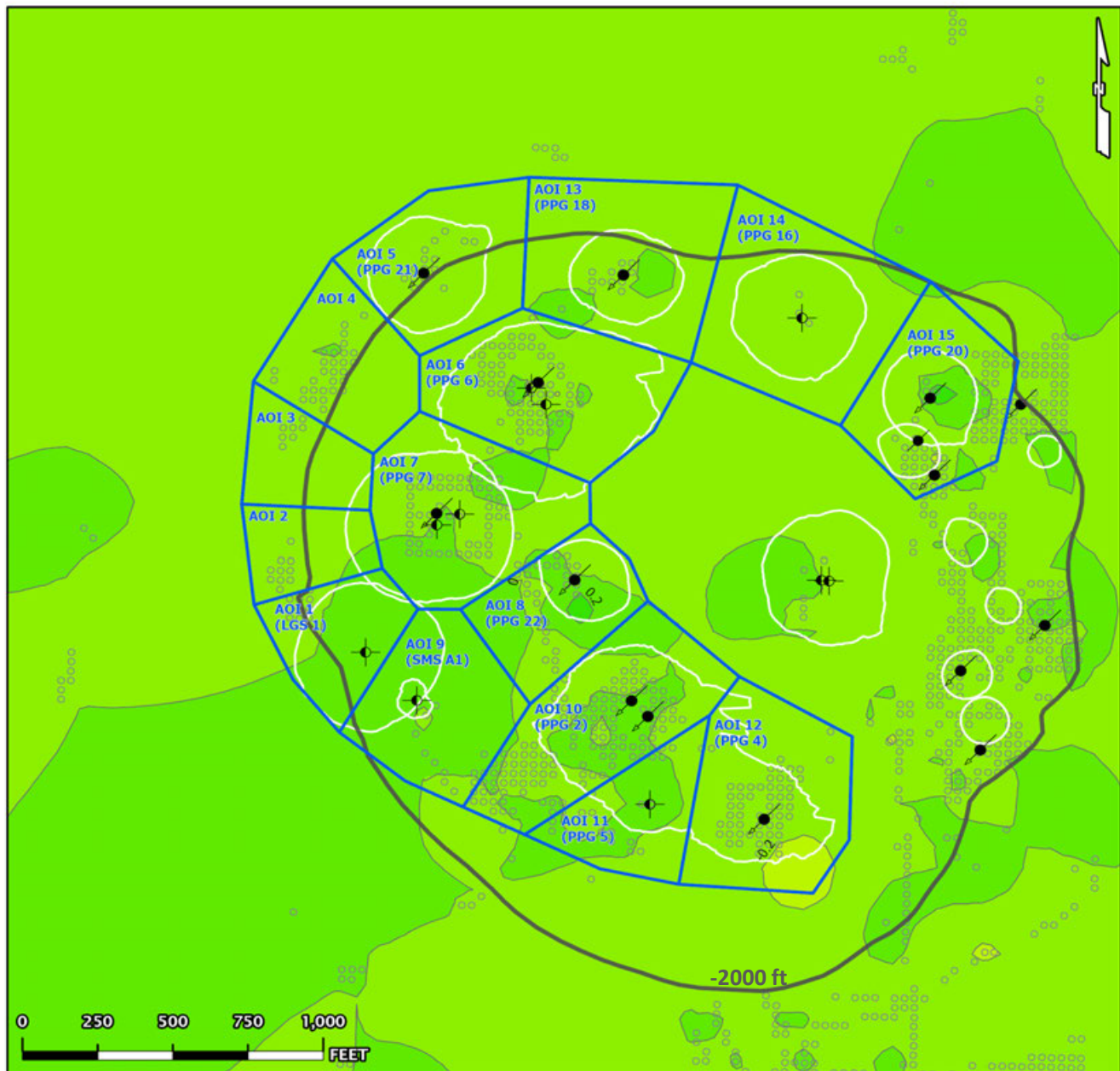


- AOI Boundary
 - InSAR LOS Measurement Point
 - Contour (0.2)
 - Historical Cavern Extent
 - Top of Dome (-2000 ft Contour)
- Cavern Well Surface Locations
- 09 - Active - Injection
 - 29 - Dry and Plugged

East-West Data (02/04/2023 - 09/29/2025)

Nonlinear Acceleration Contours

Date range: 02/04/2023 - 09/29/2025

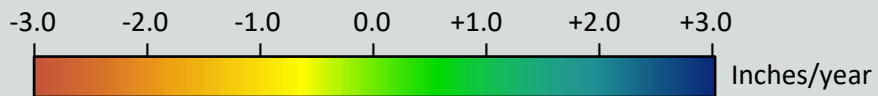
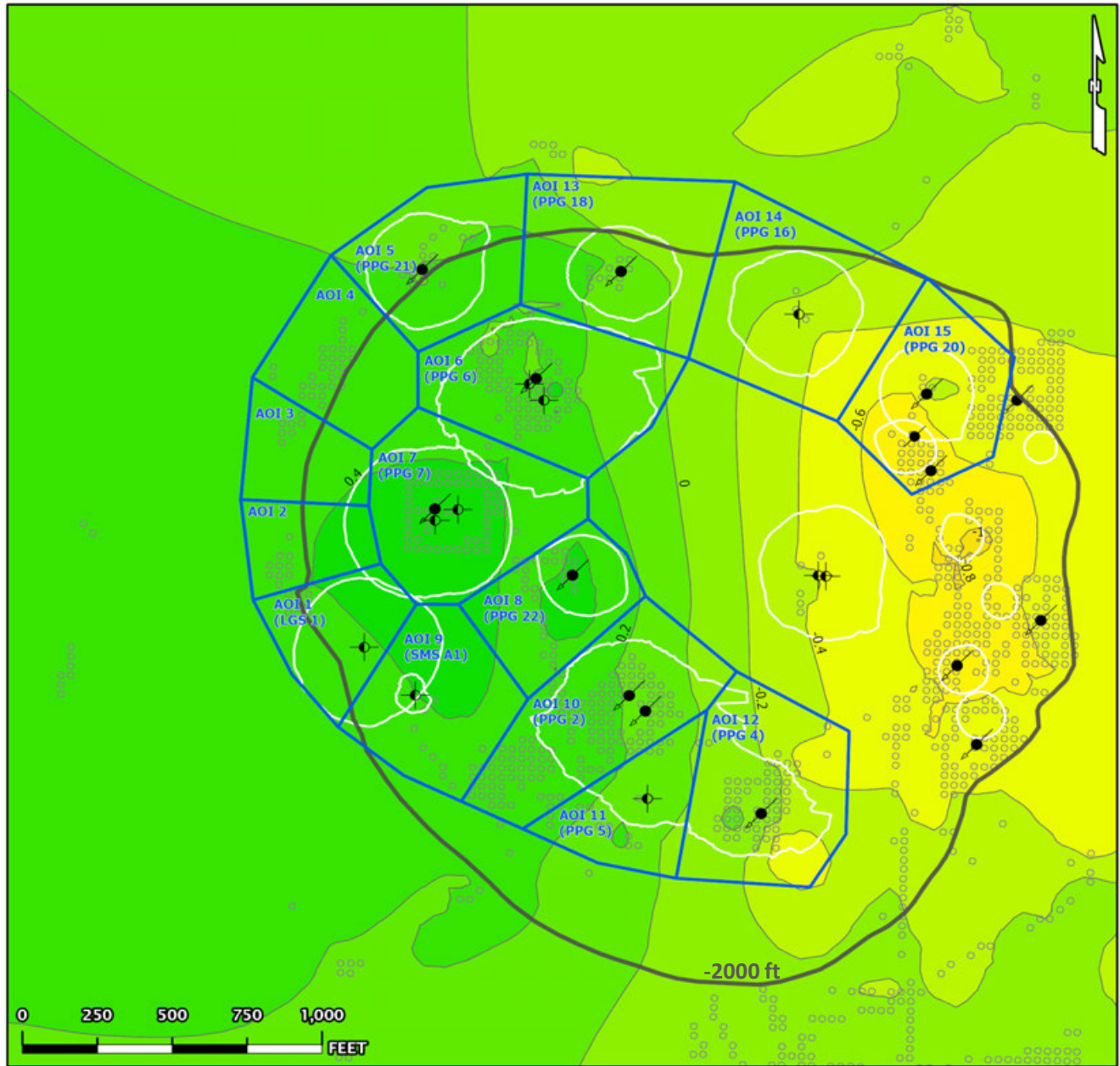


- AOI Boundary
- Historical Cavern Extent
- Top of Dome (-2000 ft Contour)
- InSAR LOS Measurement Point
- Contour (0.2)
- Cavern Well Surface Locations
- 09 - Active - Injection
- 29 - Dry and Plugged

East-West Data (02/04/2023 - 09/29/2025)

Linear Velocity Contours

Date range: 02/04/2023 - 09/29/2025

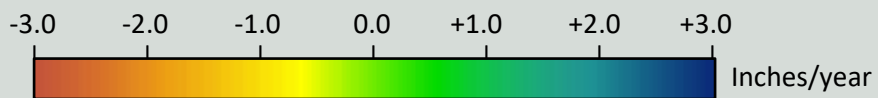


- AOI Boundary
 - InSAR LOS Measurement Point
 - Contour (0.2)
 - Historical Cavern Extent
 - Top of Dome (-2000 ft Contour)
- Cavern Well Surface Locations
- 09 - Active - Injection
 - 29 - Dry and Plugged

East-West Data (02/04/2023 - 09/29/2025)

Nonlinear Velocity Data Points

As of date: 09/29/2025

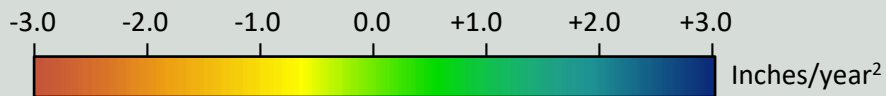
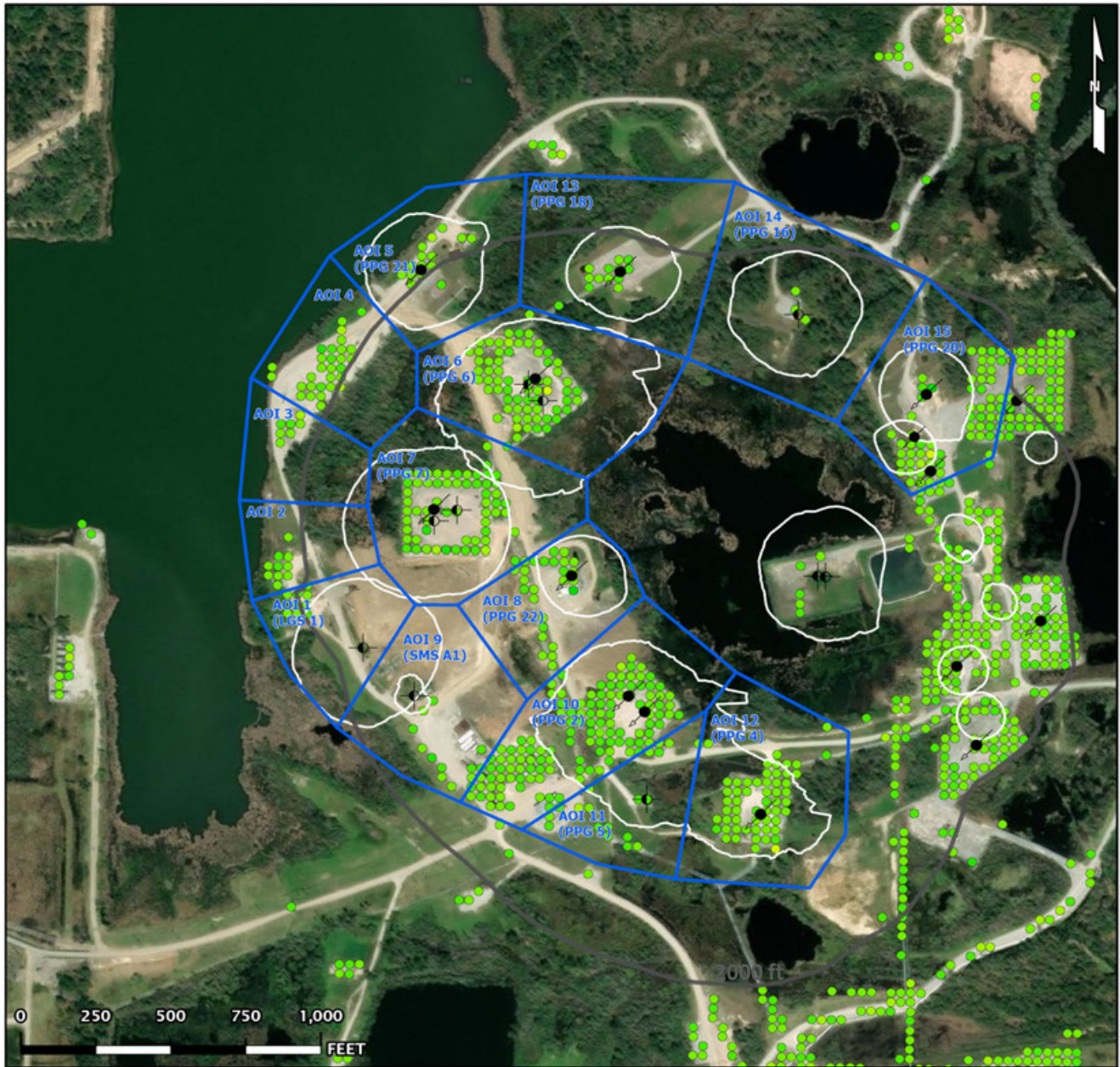


- AOI Boundary
 - Historical Cavern Extent
 - Top of Dome (-2000 ft Contour)
 - InSAR LOS Measurement Point
- Cavern Well Surface Locations
- 09 09 - Active - Injection
 - 29 29 - Dry and Plugged

East-West Data (02/04/2023 - 09/29/2025)

Nonlinear Acceleration Data Points

Date range: 02/04/2023 - 09/29/2025

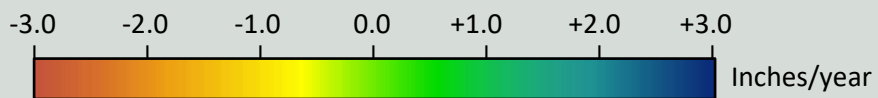
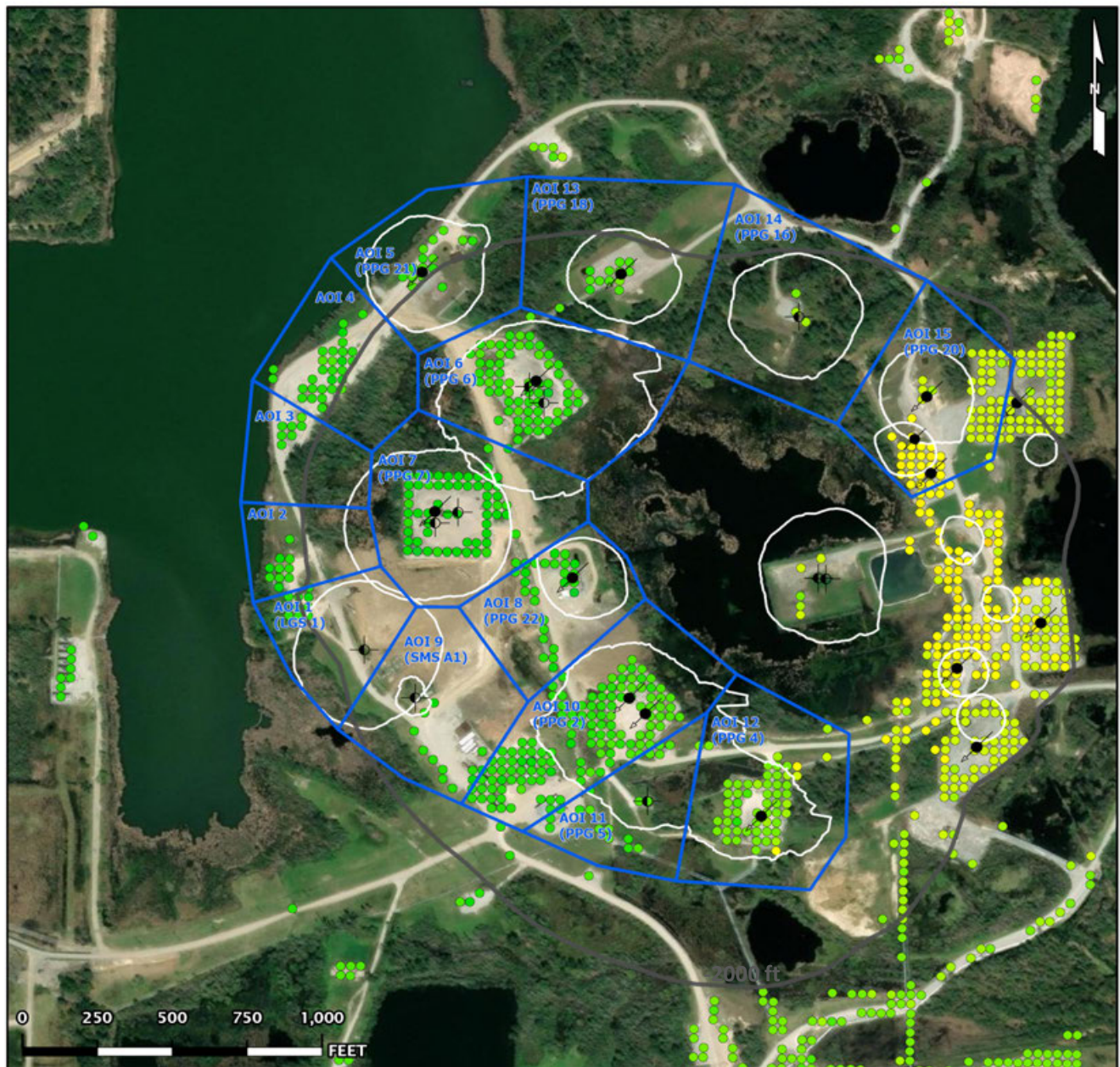


- AOI Boundary
 - InSAR LOS Measurement Point
 - Historical Cavern Extent
 - Top of Dome (-2000 ft Contour)
- Cavern Well Surface Locations
- 09 - Active - Injection
 - 29 - Dry and Plugged

East-West Data (02/04/2023 - 09/29/2025)

Linear Velocity Data Points

Date range: 02/04/2023 - 09/29/2025



- AOI Boundary
 - InSAR LOS Measurement Point
 - Historical Cavern Extent
 - Top of Dome (-2000 ft Contour)
- Cavern Well Surface Locations
- 09 - Active - Injection
 - 29 - Dry and Plugged